Role of the Intestinal Microbiota and metabolomic profile in Type 2 Diabetes: effects on risk factors for comorbidities associated with this pathology and insulin resistance of specific organs and tissues

Xingpeng Xiao

Universitat Autònoma de Barcelona

Role of the Intestinal Microbiota and metabolomic profile in Type 2 Diabetes: effects on risk factors for comorbidities associated with this pathology and insulin resistance of specific organs and tissues

Xingpeng Xiao

January 2023

ROLE OF THE INTESTINAL MICROBIOTA AND METABOLOMIC PROFILE IN TYPE 2 DIABETES: EFFECTS ON RISK FACTORS FOR COMORBIDITIES ASSOCIATED WITH THIS PATHOLOGY AND INSULIN RESISTANCE OF SPECIFIC ORGANS AND TISSUES

Doctoral thesis presented by

Xingpeng Xiao

to obtain the degree of

PhD from *Universitat Autònoma de Barcelona* (UAB)

Doctoral thesis completed in the Medical Molecular Imaging Research Group at Vall d'Hebron Research Institute (VHIR) under the supervision of **Dr. José Raúl Herance** and **Dra. Martina Palomino-Schätzlein**.

Doctoral study affiliated to the PhD program from the Department of Biochemistry and Molecular Biology of UAB under the tutoring of **Dr. Miguel Chillón Rodríguez**.

Universitat Autònoma de Barcelona, January 4th 2023

Dr. José Raúl Herance
(director)

Dra. Martina Palomino-Schätzlein
(director)

Dr. Miguel Chillón Rodríguez
(tutor)

Xingpeng Xiao
(PhD candidate)

Acknowledgements

First, I want to say thousands of thanks to my supervisor Dr. Raúl Herance. He gave me the valuable chance to come to Spain to pursue my Ph.D. degree. Without his help, I cannot successfully obtain the CSC scholarship. Especially, he asked VHIR and UAB to help me to get the internship chances and to give me living support within the law allowed. Without his help, I cannot finish the thesis, though it should be improved more. I still remember that he brings me to the glasses shop to test my vision and make a pair of glasses. He taught me how to write a paper and a thesis, and his rigorous scientific attitude is an example for me to learn now and in the future.

Next, I want to sincerely thank my supervisor Dra. Martina Palomino-Schätzlein. She gives me much help in metabolomics data analysis, which is very important for my thesis. With her guidance, I established a form for PCA, PLS, OPLS-DA, or PLS-DA models, and mastered these analyses. These days, she works a long time on my thesis. Thank you again.

Then, I want to thank our lab group. Dr. Julia Baguña Torres, Daniel García-Leon and Bruno Paun make many efforts in the translation and interpretation of PET/CT imaging data. Without their efforts, I cannot study tissue/organ-specific insulin resistance, which is the bone of my thesis. Further, Roso Mares and Carolina Aparicio spent much time in blood sample collection and process. Johanna Troya taught me some tips about using Graphpad software. Our group members are all very kind and friendly to me, and with them, I have a good time in Barcelona.

In addition, I want to thank members of my thesis follow-up commission: Dr. Diego Arango, Ibane Abasolo, and Patricia Bogdanov. They evaluate my Ph.D. study every academic year and give me much advice to improve my study. Dra. Patricia Bogdanov is very kind and friendly to me once we meet.

Thanks to Vall d'Hebron Research Institute (VHIR) to provide me with advanced experimental conditions and instruments. Many staffs are friendly and have a strong sense of responsibility. At the same time, I have made many friends in the Collserola

Building, and give my best wishes to them.

In particular, I would like to thank the China Scholarship Council, who awarded me the scholarship for covering my living costs for my PhD in Spain. Meanwhile, thanks to the Department of Education of the Chinese Embassy in Spain.

Finally, I want to thank my families, my girlfriend, and some friends. I am very missing my parents and brothers. My girlfriend gives me much support and encouragement, and she also gives me many tips about paper reading and thesis writing.

I would like to thank myself that never giving up during the hard time. Even though I met a lot of difficulties and problems, my heart says “don’t give up”. This belief allows me to overcome difficulties and supports me to the present.

Summary

Type 2 diabetes (T2DM) is a global epidemic with increasing incidence, accompanied by many comorbidities, such as cardiovascular (CV) disease, nonalcoholic fatty liver disease, and dementia, which lead to much death each year. Insulin resistance (IR), a pathological condition related to T2DM and above comorbidities, presents a high degree of heterogeneity in organs/tissues. Recently, alterations of gut microbiota (GM) are found to be associated with T2DM. However, the relationship between GM and tissue/organ-specific IR in T2DM is not clear, as well as the effects of age and gender on T2DM.

Therefore, a proof-of-concept clinical trial comprised of forty-six T2DM patients and twenty-one healthy volunteers was conducted. ^{1}H-NMR-based metabolomics was applied to identify plasma and fecal metabolites. Tissue/organ-specific IR in T2DM patients was assessed by two ^{18}F-FDG PET/CT scans, before and after a hyperinsulinemic-euglycemic clamp. GM was quantified in the patients and controls by next-generation sequencing. Biochemical analyses and anthropometric measurements were performed at the Department of Biochemistry and Endocrinology of the Vall d'Hebron University Hospital respectively.

Thus, T2DM patients showed higher IR, elevated cardiovascular risk factors reported by the atherogenic index of plasma, increased hepatic risk factors reported by the fatty liver index and NAFLD fibrosis score, and significant alterations in GM, plasma, and fecal metabolites against healthy controls. In addition, patients had a lower abundance of Firmicutes and Firmicutes/Bacteroidetes ratio than controls as well as a higher abundance of Proteobacteria. Accordingly, at a smaller level, a lower abundance of *Faecalibacterium prausnitzii* and a higher abundance of *Escherichia* was found in patients. Moreover, T2DM patients had a higher concentration of fecal malonate and plasma acetoacetate and lipids:CH_2CO as well as a lower concentration of fecal isovalerate, 2-hydroxyvalerate, and plasma LDL(CH_3), LDL(aliphatic chain),

VLDL(CH_3), phosphorylcholine, N-acetylated proteins and glutamine/glutamate ratio. Regarding associations, fecal malonate, plasma acetoacetate, and lipids:CH_2CO were positively associated with IR and some CV risk factors. On the other hand, fecal 2-hydroxyvalerate and plasma LDL(CH_3), LDL(aliphatic chain), phosphorylcholine, N-acetylated proteins, and glutamine/glutamate ratio were negatively associated with IR and some CV risk factors. Despite this, no specific bacteria were found to be significantly related to IR and CV risk factors unlike HbA1c and plasma insulin which had a significant association with GM profiles as well as feces and plasma metabolic profiles. *Faecalibacterium prausnitzii* was detected to be negatively associated with the NAFLD fibrosis score.

Further, some differences were found in T2DM patients caused by age and gender. Old-aged patients showed increased plasma troponin I levels, liver fibrosis scores, coronary artery calcium scores (CACs), and decreased glomerular filtration rate (GFR) compared with middle-aged patients. Additionally, old-aged patients presented a lower abundance of bacteria from Chromatiales and higher concentrations of fecal 2-hydroxyvalerate, β-hydroxybutyrate, methylsuccinate, and lysine. Regarding associations, positive relationships were found between fecal methylsuccinate and liver fibrosis scores, as well as between CACs and the NAFLD fibrosis score. Negative relationships were found between *Thiorhodococcus* and troponin I, and between CACs and GFR.

On the other hand, compared with male patients, female patients depicted higher plasma ALP concentrations and hepatic steatosis index, but lower serum creatinine, urate concentrations, and epicardial adipose tissue (EAT) volume. In addition, females showed a lower abundance of bacteria from Clostridia and a higher abundance of *Bacteroides thetaiotaomicron* and *Phascolarctobacterium faecium*. Also, decreased fecal butyrate and hypoxanthine and increased fecal succinate were shown in females. Positive relationships showed between the species *Bacteroides thetaiotaomicron* and *Phascolarctobacterium faecium* with plasma ALP as well as between Clostridia and serum creatinine and urate. Instead, negative relationships were shown between *Tindallia magadiensis* and the hepatic steatosis index.

Concerning the tissue/organ-specific insulin resistance in T2DM patients, significant differences were found in patients caused by myocardial IR and liver IR where two phenotypes of T2DM patients were analyzed, with IR and IS. Patients with myocardial IR presented lower global insulin sensitivity (IS_{clamp}) and higher levels of many cardiovascular and hepatic risk factors, such as higher total cholesterol/HDL ratio and liver stiffness measurement (LSM) value, than T2DM patients with myocardial IS. Alterations in GM, plasma and fecal metabolites were also found in patients with myocardial IR. Therefore, Faith's phylogenetic diversity index, the abundance of Thermicanales, the concentration of fecal arabinose, β-galactose, ribose, aspartate, lactate, and histidine, and the concentration of plasma creatinine, myo-inositol, threonine, β-galactose, glycerol, and choline were decreased, while the abundance of *Eubacterium callanderi* and the concentration of plasma VLDL(CH_3) were increased. Regarding associations between myocardial IR and IS patients, IS_{clamp} was found to be positively correlated with fecal β-galactose and the genera *Caloramator* and *Desulfosporosinus*. These genera and the species *Coprobacillus cateniformi*s were also positively associated with myocardial IS. Finally, bacteria from Thermicanales were negatively correlated with hepatic enzymes such as AST, ALT, and GGT.

Regarding liver IR, patients with this affectation depicted higher plasma total bilirubin, GGT, hyaluronic acid concentrations, enhanced liver fibrosis (ELF) score, and higher LSM value, but lower IS_{clamp} and serum chloride levels. Patients with liver IR had an elevated abundance of *Eubacterium* but decreased concentrations of fecal 2-hydroxybutyrate and plasma glycerol. In addition, plasma glycerol was negatively associated with ELF, plasma GGT, hyaluronic acid, and liver ^{18}F-FDG uptake.

Finally, due to the lack of T2DM phenotypes, the relationships between IS of skeletal muscle and brain with clinical parameters, GM, fecal, and plasma metabolites were explored. Skeletal muscle IS was positively related to IS_{clamp}, plasma adiponectin, tyrosine, histidine, and bacteria from Caldilineales, but negatively with plasma ALT, hepatic steatosis index, liver fat content, and Veillonellaceae. Regarding significant brain regions, the left superior temporal gyrus, and right precuneus were positively

associated with HOMA-IR, while the left olfactory bulb was negatively associated. On the other hand, several relationships were obtained between these regions with plasma metabolites and GM. Thus, the left superior temporal gyrus was negatively associated with plasma formate concentration. The left olfactory bulb was negatively associated with the abundance of *Streptococcus vestibularis*, while positively with the abundance of *Desulfosporosinus* and *Caloramator mitchellensis*. In addition, the right precuneus was positively correlated with the abundance of *Megasphaera elsdenii* and negatively with the abundance of the family Caulobacteraceae and the species *Desulfotomaculum indicum.*

In summary, this is the first study to reveal the relationships in T2DM patients between GM, fecal, and plasma metabolomics, showing several differences and associations after comparing with healthy controls. In addition, this is the first study to assess the effects of GM and plasma and fecal metabolomics profiles with tissue/organ-specific IR in the myocardium, liver, skeletal muscle, and brain. Thus, specific gut bacteria, and plasma and fecal metabolites alterations and associations were found. On the other hand, age and gender effects should be considered in the assessments of alterations in T2DM. Our study enhanced the understanding of the roles of GM and fecal and plasma metabolites in T2DM and the specific IR of its key tissue/organs, providing valuable information for the personalized management of T2DM patients. However, further analysis for validation of these findings is required to avoid the limitation of the present thesis.

Resum

La diabetis de tipus 2 (DM2) es considera una creixent epidèmia mundial, associada a diverses comorbiditats, que inclouen les malalties cardiovasculars, malalties del fetge o demències, generant un nombre important de morts cada any. La resistència a la insulina (RI), una condició patològic associada a la DM2, presenta un elevat grau d'heterogeneïtat als diferents òrgans i teixits. Per altra banda, s'ha descobert una relació directa entre la DM2 i alteracions de la microbiota (GM). Però fins ara no s'ha estudiat les relaciones que hi ha entre GM i RI específica d'òrgans i teixits.

A la present tesi s'ha realitzat un estudi pilot amb 46 pacients amb DM2 i 21 voluntaris sans. S'han fet un anàlisi complert basat en la metabolòmica amb resonancia magnética nuclear de plasma i femta, la seqüenciació de la GM, i l'anàlisi de la IR específica en teixits mitjançant 18F-FDG PET/TC abans i després d'un pinçament hiperinsulinic-eugluc èmic.

A la primera part del nostre estudi es va demostrar que hi havien diferencies consistents entre la GM de pacients i de controls sans, afectant la relació Firmicutes/Bacteroidetes i l'abundància de Proteobacteria. A nivell metabolòmic, es van detectar alteracions en els nivells de malonat, isovalerta i 2-hydroxyvalerat en femta, i acetoacetat, lípids:CH2CO, LDL, VLDL(CH3), fosforilcolina, relació glutamina/glutamat y N- proteïnes acetilades del plasma. A més, es va trobar una correlació directa entre alguns d'aquests metabòlits i els nivells de RI, HbAic, insulina plasmàtica i factors de risc cardiovascular.

Al analitzar pacients de dos grups d'edat, és van detectar canvis associats específicament a pacients d'elevada edat, afectant les Chromatiales, així com la concentració de 2-hidroxivalerat, β-hidroxibutirat, metilsuccinat i lisina fecal. També es van detectar canvis associats específicament a uns dels dos gèneres.

En quan a l'análisi de RI específic, es va demostrar una afectació de Thermicanales, Eubacterium callanderi, Caloramator y Desulfosporosinus, i de la concentración d'arabinosa, β-galactosa, ribosa, aspartat, lactat e histidina fecals, així como de la creatinina, VLDL(CH3), treonina, β-galactosa, glicerol, i la colina plasmàtics en

pacients amb RI miocàrdia. A més, en aquests pacients, la β-galactosa fecal i 2 bactèries van correlacionar positivament amb la sensibilitat sistèmica a la insulina (ISclamp) així com la IS miocàrdia. Per altra banda, las Thermicanales van correlacionar negativament amb factors de risc hepàtic.

Els pacients amb RI hepàtica van presentar alteracions en Eubacterium, 2-hidroxibutirat fecal y glicerol plasmàtic. Aquest últim es va associar negativament amb els biomarcadors hepàtics GGT, ELF, àcid hialurònic plasmàtic i la IS hepàtica. En relació al grup de pacients amb IS cerebral, se va detectar una associació directa del bulb olfactiu esquerra i del precuni amb diversos canvis bacterians.

En conclusión, s'han pogut identificar una sèrie de canvis específics en les bactèries intestinals i els metabòlits plasmàtics i fecals associats a la DM2 i a les RIs específiques de miocardi, fetge, múscul esquelètic i cervell. Les molècules i soques bacterianes identificades poden representar interesants candidats com a biomarcadors per a comorbiditats específiques. Per altra banda, aquestes alteracions es poden veure afectades tant per l'edat com per al gènere, que per tant sempre s'ha de tenir en compte per al diagnòstic i tractament de la malaltia.

Resumen

La diabetes tipo 2 (DM2) es una epidemia mundial con una incidencia creciente, que puede generar una serie de comorbilidades, como las enfermedades cardiovasculares, la enfermedad del hígado graso no alcohólico o la demencia, provocando muchas muertes cada año. La resistencia a la insulina (RI), condición patológica relacionada con la DM2 y comorbilidades, presenta un alto grado de heterogeneidad en los diferentes órganos/tejidos. Recientemente, se descubrió que las alteraciones de la microbiota intestinal (GM) estaban asociadas con la DM2. Sin embargo, a día de hoy no se han estudiado las relaciones entre GM y la RI específica de órgano y tejido en la DM2.

En el presente trabajo se ha realizado un estudio clínico piloto con 46 pacientes con DM2 y 21 voluntarios sanos. Se realizó un estudio completo de los sujetos, aplicando la metabolómica basada en resonancia magnética nuclear (RMN) de muestras plasmáticas y fecales, un análisis IR específico de órgano/tejido mediante 18F-FDG PET/TC antes y después del pinzamiento hiperinsulinémico-euglucémico, y la determinación de la GM por secuenciación de próxima generación.

En una primera parte de nuestro estudio, se realizó una comparación general entre pacientes con DM2 y controles sanos. Como previsto, los pacientes mostraron niveles elevados de RI y diferentes factores de riesgo hepático y cardiovascular. En el estudio de la GM, se confirmaron alteraciones significativas, afectando la relación Firmicutes/Bacteroidetes y la abundancia de las Proteobacteria. En el estudio metabolómico, se detectaron alteraciones en el malonato, isovalerato y 2-hidroxivalerato en heces, y cambios en el acetoacetato, lípidos:CH_2CO, LDL(CH_3), LDL(cadena alifática), VLDL(CH_3), fosforilcolina, relación glutamina/glutamato y N-proteínas acetiladas del plasma Además, varios de estos metabolitos tuvieron una correlación directa con los niveles de RI, la HbA1c, la insulina plasmática y los factores de riesgo cardiovascular.

Cuando comparamos pacientes de mediana edad con pacientes de edad avanzada,

detectamos una menor abundancia de bacterias de Chromatiales, pero una mayor concentración de 2-hidroxivalerato, β-hidroxibutirato, metilsuccinato y lisina fecales. Además, se identificaron cambios específicos asociados al género de los pacientes con DM2.

En cuanto al análisis de los cambios asociados a RI específicos, se puedo demostrar que la abundancia de Thermicanales, *Caloramator* y *Desulfosporosinus*, y la concentración de arabinosa, β-galactosa, ribosa, aspartato, lactato e histidina fecales, así como la creatinina, mioinositol, treonina, β-galactosa, glicerol, y la colina plasmáticas disminuyeron en pacientes con IR miocárdica, mientras que la abundancia de *Eubacterium callanderi* y la concentración plasmática de VLDL(CH_3) aumentaron. Además, se encontró que la β-galactosa fecal y 2 bacterias correlacionaron positivamente tanto con la sensibilidad sistémica a la insulina (IS_{clamp}) así como con la IS miocárdica. Las Thermicanales se correlacionaron negativamente con los factores de riesgo hepático.

Los pacientes con RI hepática presentaron alteraciones en *Eubacterium*, 2-hidroxibutirato fecal y glicerol plasmático. Este último se asoció negativamente con los biomarcadores hepáticos GGT, ELF, el ácido hialurónico plasmático e IS hepático. Además, el IS muscular esquelético se relacionó con IS_{clamp}, adiponectina plasmática, ALT, tirosina e histidina, índice de esteatosis hepática y contenido de grasa hepática, así como Caldilineales y Veillonellaceae. Con respecto a los grupos de IS cerebrales, el bulbo olfativo izquierdo yl precúneo se pueden asociar con cambios bacterianos.

En conclusión, tanto la DM2, como las RIs específicas de miocardio, hígado, músculo esquelético y cerebro se pudieron correlacionar con cambios en las bacterias intestinales y metabolitos plasmáticos y fecales. Además, los efectos de la edad y el género pueden afectar de forma significativa las alteraciones en la DM2. Algunos de los metabolitos y cepas bacterianas identificadas podrán representar interesantes candidatos como biomarcadores para diferentes comorbilidades en DM2.

Index

Abbreviations

^{18}F-FDG	2-deoxy-2-[18F]fluoro-D-glucose
A.U.	arbitrary unit
AC	adenylate cyclase
ACC	acetyl-CoA carboxylase
ACS	acyl-CoA synthase
AD	Alzheimer's disease
AIP	atherogenic index of plasma
ALP	alkaline phosphatase
ALT	alanine aminotransferase
AMPA	α-amino-3-hydroxy-5-methyl-4-isoxazole propionic acid
AMPK	AMP-activated protein kinase
AST	aspartate aminotransferase
AT	adipose tissue
AU	Agatston unit
BBB	blood–brain barrier
BCAA	branched-chain amino acid
BCFA	branched-chain fatty acid
BMI	body mass index
BMRB	Biological Magnetic Resonance Data Bank
bp	base pair
BSA	body surface area
CACs	coronary artery calcium score
CAD	coronary artery disease
CNS	central nervous system
CSF	cerebrospinal fluid
CV	cardiovascular
CV-ANOVA	ANalysis Of VAriance testing of Cross Validation
CVD	cardiovascular disease
Cx	circumflex artery
DAG	diacylglycerol
DPP IV	dipeptidyl peptidase 4
EDTA	ethylenediaminetetraacetic acid
EIA kit	enzyme immunoassay kit
ELF	enhanced liver fibrosis
ELISA	enzyme-linked immunosorbent assay

FDG-6-P	FDG-6-monophosphate
FFA	free fatty acid
FGF21	fibroblast growth factor 21
FIB-4	liver fibrosis index 4
FID	free induction decay
GABA	gamma-aminobutyric acid
GDM	gestational diabetes mellitus
GFR	glomerular filtration rate
GGT	gamma-glutamyl transferase
GIT	gastrointestinal tract
GLP-1	glucagon-like peptide 1
GLUT	glucose transporter protein
GM	gut microbiota
GS	glycogen synthase
GSK-3	glycogen synthase kinase
HA	hyaluronic acid
HbA1c	hemoglobin A1c
HC	hip circumference
HDL	high-density lipoprotein cholesterol
HEC	hyperinsulinemic-euglycemic clamp
HMBD	Human Metabolome Database
HOMA-IR	homeostasis model assessment of insulin resistance
HSL	hormone sensitive lipase
HU	Hounsfield unit
IGT	impaired glucose tolerance
IL-6	interleukin 6
IR	insulin resistance or insulin receptor
IRS	insulin receptor substrate
IS	insulin sensitivity
iv administered	intravenously administered
kg/m^2	kilograms per square meter
kPa	kilopascal
LAD	left anterior descending coronary artery
LCACoA	long chain acyl-CoA
LCFA	long-chain fatty acid
LDL	low-density lipoprotein cholesterol
L-IR	liver insulin resistance
L-IS	liver insulin sensitivity
LM	left main coronary artery

LSM	liver stiffness measurement
LV	left ventricular
MBq/kg	megabecquerels per kilogram of body mass
MBq/kg	megabecquerel per kilogram
MCP-1	monocyte chemoattractant protein-1
mg/dL	milligrams per deciliter
MHz	megahertz
MI	myocardial infarction
min	minute or minutes
mIR	myocardial insulin resistance
mIS	myocardial insulin sensitivity
mM	millimole
MTOR	mammalian/mechanistic target of rapamycin
mU/L	milliunits per liter
NAFLD	non-alcoholic fatty liver disease
NAFLD	nonalcoholic fatty liver disease
NASH	Non-alcoholic steatohepatitis
NCBI	National Center for Biotechnology Information
ng/µl	nanograms per microliter
NMDA	*N*-methyl-D-aspartate
NMR	nuclear magnetic resonance
OGTT	oral glucose tolerance test
OPLS-DA	orthogonal projection to latent structure discriminant analysis
OTUs	Operational Taxonomic Units
PAI	plasminogen activating inhibitor
PCA	principal component analysis
PCoA	principal coordinate analysis
PCR	polymerase chain reaction
PD	Parkinson disease
PET/CT	positron emission tomography - computed tomography
PI3K	phosphatidylinositol 3-kinase
PIIINP	aminoterminal propeptide of type III procollagen
PKA	protein kinase A
PLS	partial least square regression
QUICKI	quantitative insulin sensitivity check index
RCA	right coronary artery
RD^1	relaxation delay
RD^2	radiodensity
SCFA	short-chain fatty acid

SDS	sodium dodecyl sulfate
SEM	standard error of the mean
SGLT2	sodium–glucose cotransporter 2
SHBG	sex hormone-binding globulin
SPECT	single-photon emission computerized tomography
SPM	statistical parametric mapping
SRA	Sequence Read Archive
SUV	standardized uptake value
T1DM	type 1 Diabetes Mellitus
T2DM	type 2 Diabetes Mellitus
TAG	triacylglycerol
TCA	tricarboxylic acid
TG	triglyceride
TIMP-1	tissue inhibitor of metalloproteinase 1
TNF-α	tumor necrosis factor alpha
TSP	3-(Trimethylsilyl)propionic-2,2,3,3-d4 acid
TyG index	triglyceride-glucose index
UV scaling	Unit Variance scaling
VIP	Variable Importance for the Projection
VLDL	very low-density lipoprotein
WC	waist circumference
WHO	World Health Organization
µL	microliter
µM	micromole

1. Introduction

1.1 Diabetes

1.1.1 General overview

Diabetes mellitus is a group of metabolic diseases characterized by persistent hyperglycemia resulting from insufficient insulin production of the pancreas, or the body cells not responding properly to the insulin produced, or both [1]. It may cause long-term micro- and macro-vascular complications leading to many comorbidities such as cardiomyopathies, neuropathies, diabetic retinopathies, nonalcoholic fatty liver disease (NAFLD), nephropathies and stroke, reducing life quality and expectancy of the affected individuals [2]. It was estimated that in 2017, worldwide 424.9 million people were living with diabetes and that the prevalence in adults increased from 4.7% in 1980 to 8.8% in 2017 [3]. Four million deaths were attributable to diabetes and its complications worldwide in 2017 and the annual cost spending on diabetes among adults was up to around 850 billion dollars in 2017 [3]. **Figure 1.1** shows the distribution of adults with diabetes mellitus by regions in the world, where two Asian countries (China and India) and the USA stand out in particular with the highest number of cases [4]. Estimations predict that if we do not take any actions to stop the increase in diabetes, there will be at least 629 million people diagnosed with diabetes by 2045 [3, 5]. Diabetes has become a major health threat in the world and the biggest burden for many families. Many authors considered it a pandemic [6]. Therefore, it is necessary to investigate this pathology to minimize its consequences.

There are two main types of diabetes, type 1 diabetes mellitus (T1DM) and type 2 diabetes mellitus (T2DM), called insulin-dependent diabetes mellitus and non-insulin-dependent diabetes mellitus, respectively [5, 7]. There are some differences between them: 1) T1DM is less prevalent than T2DM and represents around 10% of all cases of diabetes [8]. T2DM is more prevalent and accounts for

about 90% of all diabetic cases [7]. 2) T1DM is an autoimmune disorder caused by a lack of insulin secretion by beta cells of the pancreas and the patients require daily injections of insulin to survive. T2DM is not an autoimmune disorder, resulting from a combination of genetic factors related to impaired insulin secretion, insulin resistance, and environmental factors, and the body can produce insulin but cannot use it effectively [1]. 3) Most cases of T1DM are diagnosed between the ages of 4 and 14, while most people are diagnosed with T2DM after the age of 40 years [1]. Despite that there are several types of diabetes, this thesis is focused on T2DM.

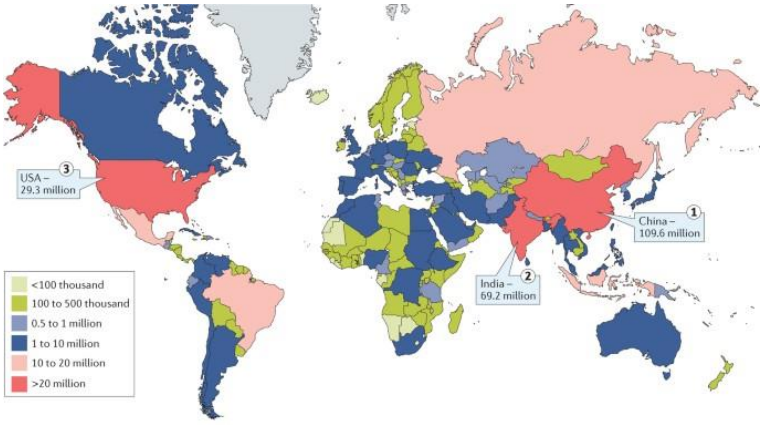

Figure 1.1 Estimated total number of adults (20–79 years) living with diabetes mellitus in 2015. The red color and pink colors indicate more serious areas with the diabetes mellitus pandemic. The figure is from Zheng *et al* [4].

1.1.2 Type 2 Diabetes

1.1.2.1 Overview

T2DM accounts for between 90% and 95% of all diabetic patients, with the highest proportions in low- and middle-income countries or regions [7]. Therefore, T2DM is the most common type of diabetes in the world. The main characteristic symptoms of this type of patient are hyperglycemia, thirst, polyuria, blurred or decreased vision, and weight loss [7]. The most serious clinical manifestations are ketoacidosis or non-ketotic hyperosmolar states such as dehydration, coma, and even death without prompt and effective treatment [7]. However, in the first years of the disease, T2DM

symptoms are often not severe or even absent, causing many individuals with T2DM to remain unknown until biochemical detection or the presence of complications. It is estimated that 30–80% of diabetic cases are undiagnosed [9]. T2DM used to affect mainly adults, but currently can also be found in children, with an alarming annual growth [5].

In the past three decades, epidemiological research on T2DM has improved our understanding of a wide range of risk factors for the development of T2DM, including age, overweight and obesity, unhealthy lifestyles such as unhealthy dietary and sedentary lifestyle, prior gestational diabetes (GDM) and genetic factors [4,7]. Among them, being overweight and obese are the strongest factor leading to T2DM.

1.1.2.2 Diagnostic methods

The current WHO guidelines provide four recommendations for the diagnosis of T2DM [7]. These recommendations (**Table 1.1**) are: 1) fasting plasma glucose ≥ 7.0 mmol/L or ≥ 126 mg/dL, 2) 2-hour post-load plasma glucose after a 75 g oral glucose tolerance test (OGTT) ≥ 11.1 mmol/L or ≥ 200 mg/dL, 3) HbA1c ≥ 6.5% or ≥ 48 mmol/mol and 4) random blood glucose ≥ 11.1 mmol/L or ≥ 200 mg/dL in the presence of signs and symptoms of T2DM. If elevated values are detected in asymptomatic persons, it is recommended to repeat the same tests the next day to confirm the diagnosis.

Table 1.1 Current diagnostic criteria for T2DM.

Number	Diagnostic tests	Diagnostic criteria
1	Fasting plasma glucose	≥ 7.0 mmol/L or ≥ 126 mg/dL
2	2-hour (2-h) post-load plasma glucose after a 75 g OGTT	≥ 11.1 mmol/L or ≥ 200 mg/dL
3	HbA1c	≥ 6.5% or ≥ 48 mmol/mol
4	Random blood glucose in the presence of signs and symptoms of diabetes	≥ 11.1 mmol/L or ≥ 200 mg/dL

Four diagnostic tests for T2DM are currently recommended, shown in **Table 1.1**. Abbreviations: HbA1c, hemoglobin A1c; OGTT, oral glucose tolerance test. This table is summarized by WHO publication [7].

1.1.2.3 Aetiopathology

T2DM is widely regarded as a long-term consequence of multiple risk factors which have been described above. They can be summed up in genetics (family heredity, carrying risk alleles in the *TCF7L2* gene) and environmental factors (lack of exercise, unhealthy diet, stress, hypertension, obesity, and aging) [4]. It is characterized by relative insulin deficiency caused by pancreatic β-cell dysfunction and insulin resistance (IR) in target organs [10]. The pancreas is the only organ in humans to produce and secrete insulin, and it seems incapable of renewing β-cells after the age of 30 years [11]. A decline in function or the destruction of pancreatic β-cells can lead to reduced or no insulin secretion, which severely influences the glucose balance. There are some mechanisms involved in alterations of functions of the pancreas, including genetic factors, insulin resistance, and environmental factors [7].

IR is a common and predominant feature at the early stage of T2DM, caused by impaired insulin sensitivity (IS) in specific organs or improper action of insulin. Due to these reasons, it is compensated by hyperinsulinemia that enables glucose metabolism to remain normal. Individuals with IR or impaired insulin develop postprandial hyperglycemia, which leads to impaired glucose tolerance (IGT) or prediabetes. IGT, or chronic hyperglycemia, further suppresses pancreatic β-cell insulin secretion and worsens IR, resulting in T2DM [12].

1.1.2.4 Complications

Most patients with T2DM have at least one complication and usually several, with cardiovascular complications being the main ones, being also the main cause of death in these patients [13]. The long-term complications traditionally include macrovascular and microvascular complications (**Figure 1.2**) triggered by hyperglycemia [14]. Macrovascular complications include coronary artery disease, peripheral vascular disease, cerebrovascular disease, cardiomyopathy, arrhythmias, and sudden cardiac death [14, 15]. Microvascular complications of T2DM include

diabetic nephropathy, diabetic retinopathy, foot ulcer, and diabetic neuropathy [14, 16].

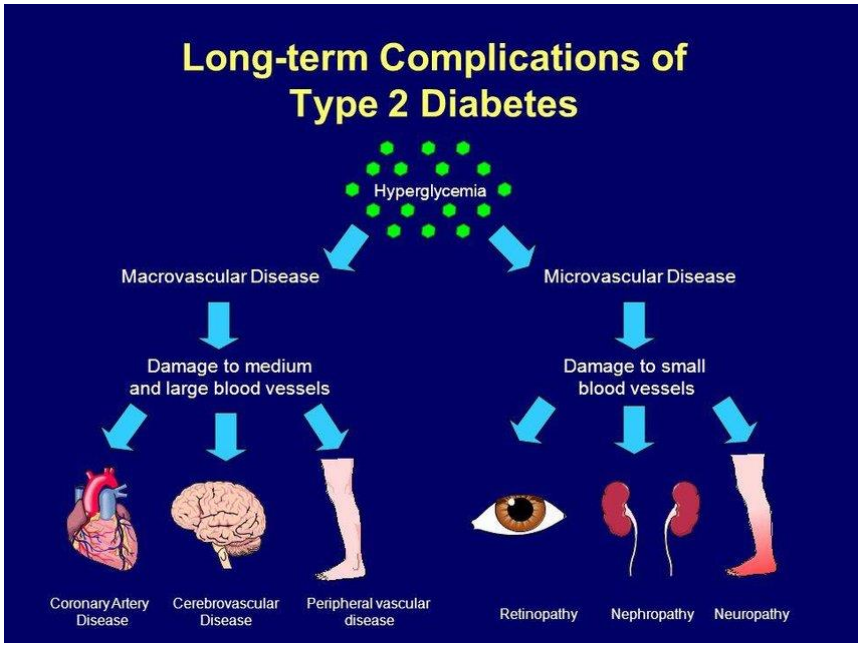

Figure 1.2 Long-term complications of T2DM. Generally, the detrimental effects of hyperglycemia are separated into macrovascular complications and microvascular complications, as shown in the figure. This figure is derived from Seiosuwowei Allen [17].

1.1.2.5 Prevention and management

T2DM is considered a global epidemic by several authors since the population affected by this pathology continues to increase at an alarming rate [3]. In addition to the aforementioned health complications caused by T2DM in patients, there are others related to the economy of the patients and their families as well as to healthcare systems and national economies, through direct medical costs and loss of work and wages [5]. Faced with this global challenge, many efforts through education, media, periodic specialist assessment, and research are being done to prevent this disease [5]. There are effective approaches available to prevent T2DM and its complications such as raising knowledge and awareness of T2DM, receiving regular health evaluations, and maintaining a healthy lifestyle [5]. It has been shown that regular physical activity and the consumption of a healthy diet are valid, favorable, and feasible ways to prevent T2DM [5].

Unfortunately, the food industry continues producing high amounts of ultra-processed food products containing masked sugar and sugary drinks that have been significantly associated with an increased risk of T2DM [18, 19]. Unless governments start to make serious measures to reduce the promotion of these kinds of products, especially for children, a significant reduction of T2DM will be difficult.

Since many patients suffering from T2DM are not diagnosed, an early diagnosis would be the first step for the proper management of patients. After this, a series of cost-effective interventions [5] can be done to improve the patient outcomes such as 1) regular blood glucose control; 2) eating healthy diets avoiding mainly sugar and refined carbohydrates; 3) physical activity; 4) medication, where metformin and insulin are the most habitual drugs used for this type of patients and currently homologs of GLP-1 and inhibitor of SGLT2 and DPP-IV are becoming very important for the treatment of patients; 5) control of blood pressure and lipids to mainly reduce cardiovascular risk; 6) and regular screening of eyes, kidneys, and feet to control diabetic retinopathy, nephropathies, and diabetic foot respectively.

1.1.3 Insulin resistance

1.1.3.1 Overview

Insulin is a hormone produced by the pancreatic β-cells in response to body nutritional stimuli [20]. It controls the excess of blood glucose by a series of actions such as stimulating the uptake of glucose into the cells of the whole body to generate energy; promoting glycogen, fat, and protein synthesis; and inhibiting hepatic glucose production [21, 22]. Therefore, insulin plays a pivotal role in glucose homeostasis in the body.

After the release of insulin from pancreatic β-cells, it enters the bloodstream to target the body cells through the insulin receptors placed on the cell membrane to perform its signaling pathway function, incorporating glucose into the cells [23]. Some key

components taking part in the insulin signaling pathway (**Figure 1.3**) are the insulin receptor, insulin receptor substrate (IRS), phosphatidylinositol 3-kinase (PI3K), glucose transporter protein (GLUT), and Akt/protein kinase B [24]. The glucose transporter GLUT2 in the liver releases glucose, while the insulin-sensitive GLUT4 in the muscle and fat mediates glucose uptake. This Akt protein kinase is required for insulin regulation of the pathways controlling systemic glucose homeostases, such as glucose transport in adipocytes and muscle, inhibition of hepatic gluconeogenesis, and cell autonomous activation of hepatic lipogenesis [25]. When blood glucose levels return to normal (99 mg/dL or lower), it is critical to turn off the insulin signal as soon as possible. Precision modulation of this pathway is crucial for adaptation as the individual transitions from a fed to a fasted state. Uncontrolled activity in the downstream pathways could cause severe metabolic disruptions, most notably insulin resistance [26].

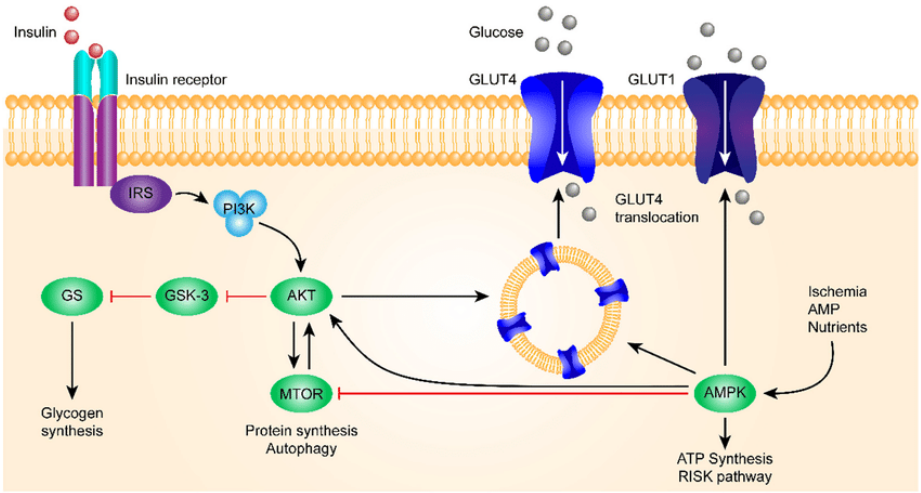

Figure 1.3 Schematic diagram of the general insulin signaling pathway in cells. Insulin binds to the insulin receptor, activating PI3K and, later, AKT, which inhibits GSK-3β. Abbreviations: IRS, insulin receptor substrate; PI3K, phosphatidylinositol 3-kinase; GLUT, glucose transporter protein; GSK-3, glycogen synthase kinase; GS, glycogen synthase; MTOR, mammalian/mechanistic target of rapamycin; AMPK, AMP-activated protein kinase. Black and red arrows indicate phosphorylation activation and inhibition, respectively. The figure is from Arneth *et al* [27].

IR, also known as impaired IS, is present when a normal or high insulin blood level produces a reduced biological response after a nutritional stimulus [28]. In other words, in this situation cells from specific organs and tissues are not sensitive to

insulin and do not incorporate glucose. To compensate for resistance and maintain normal or near-normal blood glucose levels, the pancreas secretes more insulin that results in a state of hyperinsulinaemia, which in turn causes IR [29] and possibly other health problems [30].

Insulin is potent to lower the increasing glucose after food intake and enables the body to maintain blood glucose homeostasis and energy balance. Insulin suppresses hepatic glucose production and stimulates glucose uptake in the muscle and adipose tissue. Besides, insulin is also involved in some signaling pathways in the brain that control both positive and negative aspects of food intake and energy metabolism. Disruption of insulin signaling can then lead to IR and progression toward various metabolic disorders, including cardiovascular disease, obesity, and T2DM [31]. Many mechanisms contribute to the associations between IR and T2DM (**Figure 1.4**). At the molecular level, besides changes in insulin signaling transduction pathways, the mechanisms also include changes in mitochondrial function and glucose metabolism, and free fatty acids (FFAs) in skeletal muscle cells and cardiomyocytes [32].

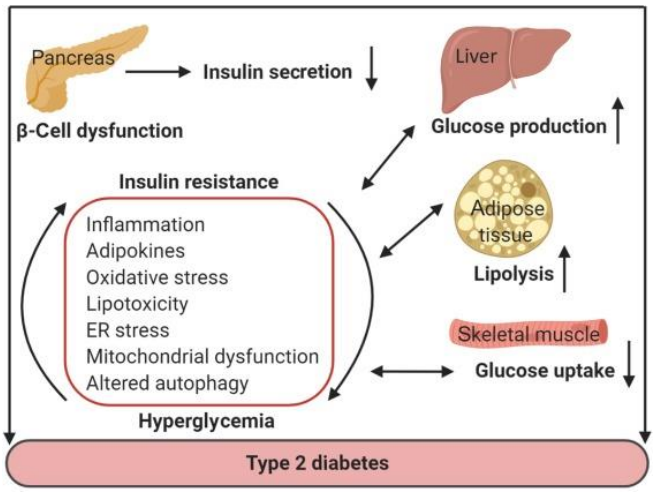

Figure 1.4 Molecular mechanisms of IR and changes in insulin-targeted organs in T2DM. In T2DM, alterations may occur in the pancreas, skeletal muscle, liver, and adipose tissue, among other organs and tissues. Molecular mechanisms of insulin resistance include altered levels of adipokines, oxidative stress, lipotoxicity, mitochondrial dysfunction, and endoplasmic reticulum stress. ER, endoplasmic reticulum. The figure is from Rocha *et al* [36].

Furthermore, oxidative stress has also been implicated in the pathophysiology of IR

both in animals and in cultured cells [33]. In obesity and insulin-resistant states, strong evidence showed that oxidative stress can lead to mitochondrial dysfunction [34]. It is widely acknowledged that inflammatory cytokines, such as interleukin-6 (IL-6) and tumor necrosis factor-α (TNF-α), contribute to IR, which may influence glucose uptake and utilization in the skeletal muscle and affect glucose and fatty acid utilization in the heart [35].

1.1.3.2 Insulin resistance syndrome

Insulin resistance and compensatory hyperinsulinemia in non-diabetic individuals were associated with a cluster of related abnormalities, including some degree of glucose intolerant, essential hypertension, a high plasma triglyceride, and a low high-density lipoprotein (HDL) cholesterol concentration [37]. This cluster of related abnormalities associated with IR/compensatory hyperinsulinemia represented an important clinical syndrome, which was called Syndrome X in 1988, but now is designated as the Insulin Resistance Syndrome [37].

In the present, abnormalities associated with Insulin Resistance Syndrome were summarized to include glucose intolerance, dyslipidaemia, endothelial dysfunction, elevated procoagulant factors, haemodynamic changes, elevated inflammatory markers, abnormal uric acid metabolism, increased ovarian testosterone secretion, and sleep-disordered breathing [37, 38]. Clinical syndromes associated with IR include mainly T2DM, cardiovascular disease (CVD), essential hypertension, polycystic ovary syndrome, non-alcoholic fatty liver disease, certain forms of cancer and sleep apnoea [37, 38].

1.1.3.3 Tissue/Organ-specific insulin resistance

The abnormalities or clinical syndromes related to IR in humans show a high degree of heterogeneity, and severity may vary between different organs [37, 39]. In addition, animal studies prove that the actions of insulin vary according to the physiological

function of the tissues and organs concerned [22, 25]. This has suggested that the studies focused on IR should also focus on individual tissues or organs and not only on the whole body. In fact, this is a good starting point to study T2DM or other metabolic syndrome diseases from an IR-based personalized medicine point of view. The main organs affected by IR are the liver, adipose tissue, skeletal muscle, endothelial cells, brain, and myocardium (**Figure 1.5**). IR in skeletal muscle, myocardium, adipose tissue, liver, and brain were introduced because they are involved in this thesis.

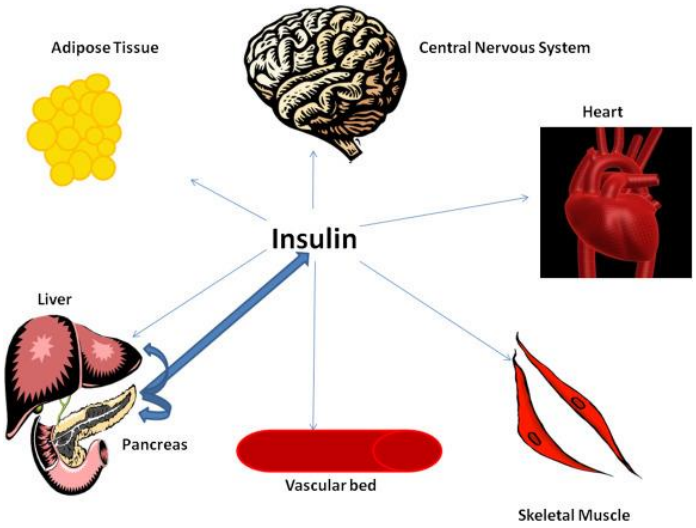

Figure 1.5 Insulin targeted organs or tissues. Major canonical insulin-sensitive tissues are the liver, skeletal muscle, and adipose tissue. However, recent advances demonstrate that both the brain and heart are also insulin-responsive organs. This figure is from Schmidt *et al* [40].

1.1.3.3.1 Skeletal muscle

There are three types of muscle tissue in humans and other vertebrates, namely skeletal muscle, cardiac muscle (myocardium), and smooth muscle, all affected by IR [41].

Skeletal muscle, which is attached to bones, plays a crucial role in providing access to various activities such as walking, running, bowing and maintaining posture, regulating the body temperature, and maintaining systemic glucose metabolism [42]. Skeletal muscle accounts for almost 40% of the body mass [43] and is the main tissue

responsible for insulin-mediated glucose uptake. A hyperinsulinemic-euglycemic clamp (HEC) study on healthy subjects showed that approximately 80% of the whole-body insulin-stimulated glucose is taken up by skeletal muscle and used for glycolysis and glycogen synthesis [44]. In skeletal muscle, the GLUT4 glucose transporter is promoted by insulin to uptake glucose in its cells. In IR conditions such as obesity and T2DM, insulin-stimulated glucose uptake is markedly reduced in skeletal muscle [45, 46]. As a result of this impaired insulin signaling, multiple post-receptor intracellular defects appear, including impaired glucose transport, glucose phosphorylation, and reduced glucose oxidation and glycogen synthesis [47-50]. Interestingly, in a mouse model with a muscle-specific insulin receptor knockout, severe insulin resistance was observed in the muscle but glucose tolerance remained normal [51]. These researchers also found that insulin-stimulated glucose uptake in fat was increased 3-folds and fat mass was increased as well. Besides glucose, FFA can also be utilized by skeletal muscle as a fuel source for energy production, especially under fasting conditions [52]. In myocytes, fatty acids are directed toward the synthesis of lipid metabolites or towards mitochondrial β-oxidation. When fatty acid uptake exceeds the rate of β-oxidation, lipids can accumulate in the muscle, which has subsequent deleterious effects on insulin action. This imbalance between fatty acid uptake and β-oxidation could contribute to muscle IR [53]. In addition, several studies have shown that elevated plasma FFA levels could impair insulin signaling and cause IR in skeletal muscle [54].

Skeletal muscle cells are rich in mitochondria. Mitochondria are organelles that play an important role in the cellular regulation of energy metabolism and that produce the largest amount of ATP through the use of several metabolites as fuel, being glucose the main one [55]. It has been reported that in patients and animals with T2DM, the number and function of mitochondria are reduced in skeletal muscle [56, 57]. Substantial evidence shows that mitochondrial dysfunction and oxidative stress in skeletal muscle are key mechanisms mediating IR [58, 59].

1.1.3.3.2 Myocardium

The myocardium is the muscular layer of the heart wall (**Figure 1.6A**), also called heart muscle or cardiac muscle, the thickest layer between the single-cell endocardium layer and the outer epicardium [60]. It is responsible for the contractile function of the cardiac pump and has distinctive cellular and physiological features that allow it to generate force to maintain adequate tissue and organ perfusion throughout the body [61].

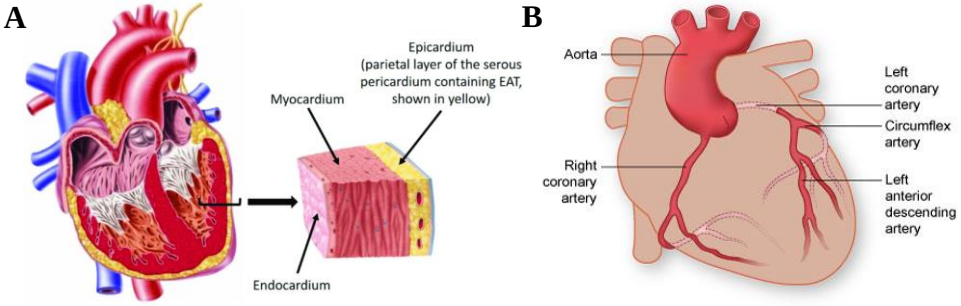

Figure 1.6 Location of the myocardium and its blood supply. A) Layers of tissue surround the heart. B) Myocardium's blood supply comes directly from the system of coronary arteries. There are two main coronary arteries, the left coronary artery (LCA), which branches into the left anterior descending (LAD) coronary artery and the left circumflex (LCx) coronary artery, and the right coronary artery (RCA). The figure A is from Krishnan *et al* [62] and the figure B is from online (www.texasheart.org/heart-health/heart-information-center/topics/the-coronary-arteries/).

The myocardium is made up of cardiac muscle cells called cardiomyocytes (**Figure 1.7**), which are striated, mononuclear muscle cells found exclusively in the heart muscle. For this reason, the myocardium is also known as the striated muscle. A unique cellular and physiological feature of cardiomyocytes is its intercalated discs, which contain cell adhesions such as gap junctions, to facilitate rapid cell-to-cell communication [61]. Functionally, the myocardium relies on electrochemical gradients and potentials to generate contractile force for each heartbeat. The myocardium is found in the walls of all four heart chambers, though it is thicker in the ventricles and thinner in the atria [61].

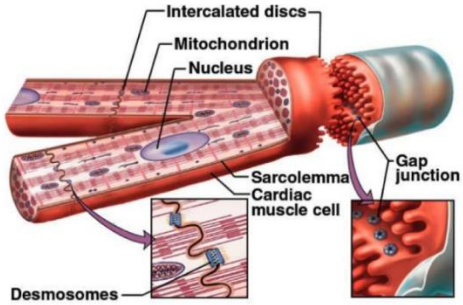

Figure 1.7 Representation of cardiomyocyte structure. The figure depicts the shape of cardiomyocytes (cardiac muscle cells) and intercalated discs, as well as gap junctions. The figure is derived from Fakhrielddine *et al* [63].

The blood supply of the myocardium comes directly from the system of coronary arteries (**Figure 1.6B**) that runs within the epicardial layer. There are two main coronary arteries, the left coronary artery (LCA) and the right coronary artery (RCA), and the former quickly branches into the left anterior descending (LAD) coronary artery and the left circumflex (LCx) coronary artery [61].

While the actions of insulin in the liver, skeletal muscle, and adipose tissue have attracted a lot of attention, its role in the heart has received less attention, basically because its main sources of energy are fatty acids and not glucose, unlike the rest because of its important beta-oxidation equipment [64]. Despite this, the heart uses glucose, commonly when it needs an energy boost, and this process could be compromised by IR, causing deleterious alterations in its operation [65]. The consumption of energy in the myocardium is essential for the cardiac function to maintain a continuous supply of a variety of molecules including oxygen, ADP, creatine, calcium, and other components to the rest of the organs and tissues. Under normal physiological conditions, myocardial metabolic energy is derived from the oxidation of long-chain fatty acids (LCFAs) (60 – 70%), glucose (20%), and lactate (10%) [66]. And when glucose and insulin concentration rise, glucose becomes the favored oxidized substrate of the heart [66]. A large amount of insulin receptors have been found to be located on the surface of cardiomyocytes. Thus, insulin acts directly on the heart muscle, and its action is mediated primarily through PKB/Akt signal

pathway [66]. Similar to the skeletal muscle, activation of insulin signaling pathways in cardiomyocytes leads to an increase in glucose uptake by promoting the translocation of GLUT4, to perform its metabolization via glycolysis [67] (**Figure 1.8**). Thus, insulin promotes glucose in cardiomyocytes as the main cardiac energy substrate, reducing myocardial oxygen consumption and increasing cardiac efficiency [68]. In addition, insulin also participates in the regulation of LCFA uptake, protein synthesis, and vascular activity in the myocardium [66].

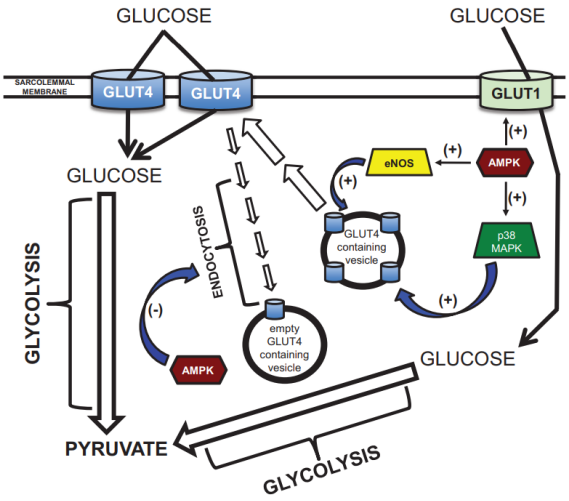

Figure 1.8 The potential mechanisms by which AMPK activation mediates glucose uptake in cardiac myocytes. AMPK activates either p38 MAPK or eNOS, which subsequently increases GLUT4 translocation to the sarcolemmal membrane. The activation of AMPK also facilitates glucose uptake in cardiac myocytes by preventing endocytosis of GLUT4 transporters present at the sarcolemmal membrane. AMPK can also enhance glucose uptake by affecting GLUT1.The figure is from Lee et al [67].

Multiple mechanisms, based mainly on cell and murine model studies, have been proposed to contribute to the increased vulnerability of the heart in insulin-resistant states, such as alterations in myocardial insulin signaling, increased fatty acid utilization, impaired mitochondrial oxidative capacity, mitochondrial dysfunction, decreased cardiac efficiency, excess intramyocardial lipid accumulation, oxidative stress, inflammation, increased apoptosis and myocardial fibrosis, and altered calcium metabolism and signaling [69]. Myocardial IR translates into reduced myocardial insulin sensitivity and compromised intracellular insulin signaling, which adversely affects myocardial mechanical function and tolerance to ischemia and reperfusion.

Myocardial IR, associated with cardiac hypertrophy, can also contribute to the development of heart failure [70].

Structural and functional abnormalities of the myocardium in diabetic patients characterize diabetic cardiomyopathy [71]. Diabetic cardiomyopathy is highly prevalent in asymptomatic T2DM patients, so screening for its presence at the earliest stage of development is very important for T2DM prevention [72]. Since diabetic cardiomyopathy was first recognized and described by Rubler *et al* [73], people found that it was not a rare condition but instead a very common one, and its etiology is primarily due to hyperglycemia, with contributions from the insulin resistance syndrome, which causes left ventricular hypertrophy [74].

1.1.3.3.3 Adipose tissue

In healthy conditions, adipose tissue accounts for about 20% of the body mass in men and about 30% in women [75]. There are two main types of adipose tissue (AT), white and brown. White adipose tissue is the most common type, widely spread throughout the body, and comprises the largest AT volume in most mammals including humans, which is critical for energy storage, endocrine communication, and insulin sensitivity. In contrast, brown adipose tissue, largely present in mammals postnatally and during hibernation, uses energy for non-shivering heat production, which is critical for body temperature maintenance [76].

AT plays a crucial role in the regulation of whole-body fatty acid homeostasis (**Figure 1.9**). Thus, in periods of calorie abundance (after feeding), it stores FFAs in the form of triglycerides through their esterification to glycerol. Insulin stimulates this process—lipogenesis. And at a state of energy shortage (such as during fasting), it releases FFAs back into circulation as a source of energy and fuel for the body [77].

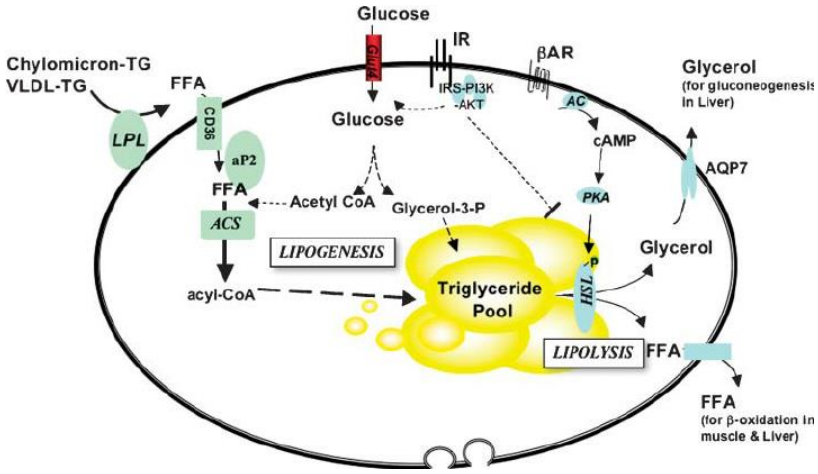

Figure 1.9 Lipid metabolism in adipocytes. Adipocytes function effectively as the body's fuel stores with the biochemical machinery. To this end, it mediates lipogenesis and lipolysis in different conditions. Lipogenesis, conversion of FFA to triglycerides (TG) for storage; lipolysis, breakdown of TG to FFA and glycerol. Adipocytes are insulin-sensitive, and insulin stimulates glucose uptake and lipogenesis and inhibits lipolysis. FFA, free fatty acid; ACS, acyl-CoA synthase; AC, adenylate cyclase; IR, insulin receptor; PKA, protein kinase A; PI3K, phosphatidylinositol 3-kinase; HSL, hormone sensitive lipase. The figure is from Sethi *et al* [78].

AT is the primary site for energy storage. Over the past few decades, it has become clear that adipose tissue is also an endocrine organ, releasing a variety of adipocyte-specific factors known as adipokines [77]. These adipokines are involved in diverse key biological functions such as energy homeostasis, insulin sensitivity, lipid metabolism, inflammation, and immunity [79]. Adipokines include hormones such as leptin, adiponectin, visfatin, apelin, vaspin, hepcidin, chemerin, omentin, and inflammatory cytokines including tumor necrosis factor alpha (TNF-α), interleukin 6 (IL-6), monocyte chemoattractant protein-1 (MCP-1), and plasminogen activating inhibitor (PAI) [80]. Leptin, one of the first discoveries of an adipocyte-derived signaling molecule, has been found to play a profound role in the regulation of body weight and energy homeostasis. Leptin can regulate the appetite to control food intake. A minor increase in leptin concentration reduces the appetite and leads to a decrease in body weight. A decrease in tissue sensitivity to leptin (leptin resistance) was found in obesity, T2DM, and other metabolic disorders, such as IR and dyslipidemia [81]. On the other hand, adiponectin, exclusively secreted by mature adipocytes, acts to increase insulin sensitivity, fatty acid oxidation, as well as energy expenditure and

reduces hepatic glucose production [82]. In contrast to leptin, adiponectin expression and serum concentrations are reduced in insulin-resistant states, including obesity and T2DM [83]. Reduction of adiponectin has been associated with IR, dyslipidemia, and atherosclerosis in humans and animals [84]. In the case of TNF-α, a classical pleiotropic pro-inflammatory cytokine expressed by adipose tissue that appears within minutes of any injury or stress to regulate immune cells [85]. In recent decades, it has also come to be known as an adipokine, promotes insulin resistance, and is associated with obesity and obesity-associated metabolic disease such as T2DM [85]. IL-6, expressed in adipose tissue and other types of cells, is reported to have multiple effects from inflammation to host defense and tissue injury. Plasma IL-6 concentrations were found to be positively correlated with human obesity and IR, and high concentrations of IL-6 were predictive of T2DM [86]. Changes in adipokine levels, induced by obesity, affect the liver and skeletal muscle functions and trigger IR, which are summarized in **Figure 1.10**.

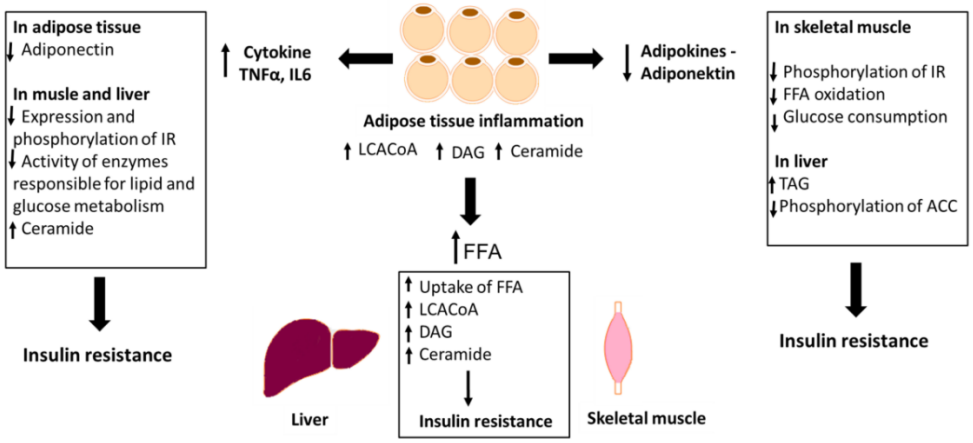

Figure 1.10 Adipocyte dysfunctions linking obesity to insulin resistance and T2DM. IR, insulin receptor; TNF-α, tumor necrosis factor α; IL-6, interleukin 6; FFA, free fatty acids; TAG, triacylglycerol; ACC, acetyl-CoA carboxylase; LCACoA, long-chain acyl-CoA; DAG, diacylglycerol. The figure is from Kojta *et al* [87].

Glucose uptake by adipocytes in the postprandial state is also insulin-dependent via GLUT 4. It is estimated that adipose tissue accounts for about 10% of insulin-stimulated whole-body glucose uptake. In diabetic and IR individuals, adipocytes have reduced GLUT 4 translocation and impaired intracellular signalling

[87]. In addition to stimulating glucose uptake, the actions of insulin on adipose tissue include enhancing triglyceride synthesis and suppressing triglyceride hydrolysis as well as the release of FFAs and glycerol into the circulation [88, 89]. With the development of obesity, the ability of adipocytes to store triglycerides is impaired, and the suppression of lipolysis in adipose tissue by insulin decreases [90]. Consequently, fat is stored in other cell types including liver and skeletal muscle, triggering deleterious effects such as obesity, NAFLD, insulin resistance, and T2DM [91, 92]. Ectopic lipids and their metabolites or increased concentrations of circulating FFAs cause IR in muscle and other tissues. Circulating cytokines released by adipose tissue also contribute to IR in muscle, liver, and other tissues [87], as shown in **Figure 1.10**.

1.1.3.3.4 Liver

The liver is the largest organ in the body and comprises around 2% of an adult's body weight, located between the organs of the gastrointestinal tract and the heart [93]. It is a vital organ that is responsible for a large variety of functions that help to support metabolism, immunity, digestion, detoxification, and vitamin storage among other functions [93]. It is also a unique organ due to its dual blood supply from the portal vein and the hepatic artery (**Figure 1.11**). Oxygenated blood flows in from the hepatic artery, while nutrient-rich blood flows in from the hepatic portal vein [94].

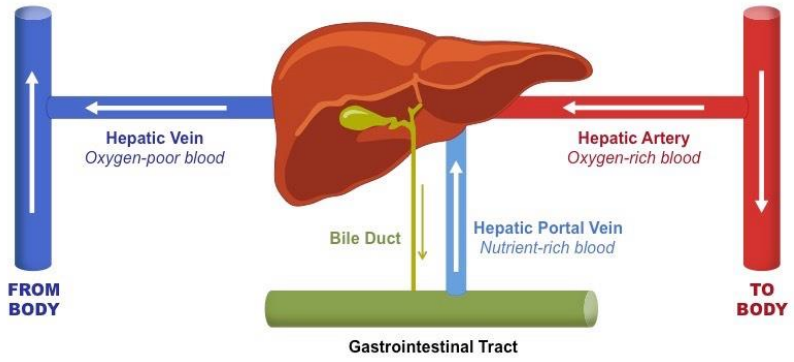

Figure 1.11 Dual blood supply of liver. Oxygen-carrying blood and nutrient-carrying blood pool in the liver. The figure is derived from online (https://ib.bioninja.com.au/options/option-d-human-physiology/d3-functions-of-the-liver/liver-blood-flow.html).

The liver is extremely sensitive to insulin and plays an important role in maintaining blood glucose levels. In the postprandial state, insulin tends to lower blood glucose by stimulating glycogenesis (the process of storing insulin-mediated glucose in the form of glycogen) and suppressing glycogenolysis (the opposite process of glycogenesis, glycogen is converted back to glucose) and gluconeogenesis (glucose synthesis from noncarbohydrate sources) [95], as seen in **Figure 1.12**. The liver accounts for approximately 30% of the whole body's insulin-mediated glucose disposal [24]. On the contrary, during the fasting state, hepatic glycogenolysis and gluconeogenesis are important in maintaining blood glucose concentrations.

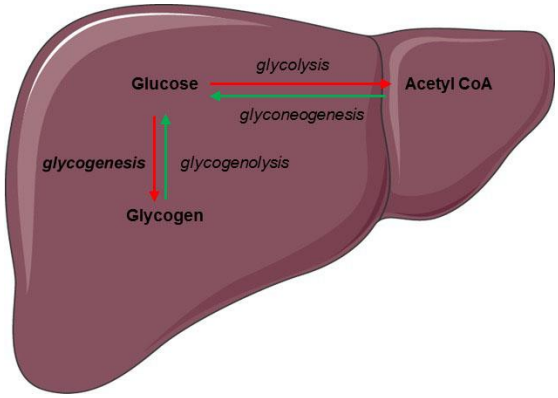

Figure 1.12 Regulation of glucose metabolism by insulin in the liver. In the postprandial state, insulin tends to lower blood glucose by stimulating glycogenesis (left red arrows) and suppressing glycogenolysis and gluconeogenesis (green arrows). The figure is adapted from Rix *et al* [95].

On the other hand, the liver plays a pivotal role in lipid metabolism (**Figure 1.13**) since it can take up FFAs and lipoproteins (complexes of lipid and protein) from the plasma [96]. During fasting or under conditions of low plasma circulating insulin, FFAs derived from the plasma can be metabolized in the mitochondria of hepatocytes via β-oxidation to provide energy or are channeled to ketogenesis [96]. After feeding or under conditions of high plasma circulating insulin, more of FFAs is used for triglyceride synthesis in the liver, which is necessary for very low-density lipoprotein (VLDL) formation. Then, VLDLs carry most of the triglyceride from the liver to the other organs to provide energy [96]. Another important function of the liver is to produce and remove cholesterol in the body. The liver is a key site for endogenous cholesterol synthesis and packages dietary and synthesized cholesterol into

low-density lipoproteins (LDLs), which are secreted into the blood for transport to other tissues. Like triglyceride, cholesterol is also circulated in the plasma as lipoproteins, which are synthesized in the liver. There are two cholesterol-rich lipoproteins, LDLs and high-density lipoproteins (HDLs). HDLs are thought to remove cholesterol from peripheral tissues and transport it to the liver [96]. Because of the above, the liver could be considered the regulator of cholesterol in the body [96]. Cholesterol is essential for all body cells as a major structural component of cell membranes and is also used as a substrate for the synthesis of other steroids such as bile acids, vitamin D, and sex hormones. It is critical to maintaining healthy cholesterol levels. However, elevated total and LDL cholesterol levels in plasma have been demonstrated to be an important risk factor for the development of cardiovascular diseases in humans and laboratory animals [97]. High cholesterol biosynthesis and cholesterol-rich dietary can lead to increase plasma total and LDL cholesterol concentrations [98]. Furthermore, it is well known that the liver serves as an excretory organ, such as the production of bile, which helps break down fats in the small intestine during digestion and eliminate waste [96]. Finally, the liver plays a significant role in the clearance of bilirubin and the metabolism of drugs and xenobiotics [99].

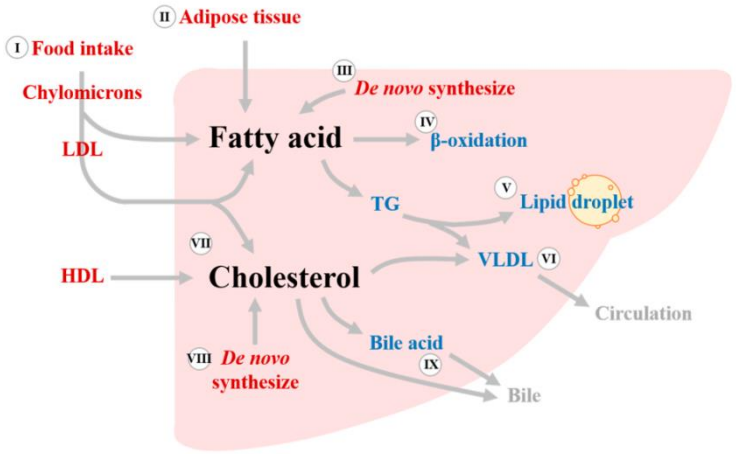

Figure 1.13 Lipid metabolism in the liver. The liver is the main site of fatty acid and cholesterol metabolism. LDL, low-density lipoprotein; VLDL, very low-density lipoprotein; HDL, high-density lipoprotein; TG, triglyceride. The figure is from Liao *et al* [100].

Hepatic IR is characterized by enhanced gluconeogenesis in the fasting state and

impaired suppression of hepatic glucose production in response to insulin in the postprandial state [101]. IR in the liver is the major cause of fasting hyperglycemia in the metabolic syndrome [44]. In a study with mice that had an insulin receptor deletion in hepatocytes, insulin suppression of hepatic glucose production was completely lost [102]. Alterations in lipoprotein metabolism represent a main hepatic manifestation of IR, such as increased circulating levels of FFAs and triglyceride, and decreased clearance of LDL and VLDL [103]. Evidence showed that excess diacylglycerol (DAG) leads to hepatic IR and hyperglycaemia by protein kinase Cε (PKCε) activation and subsequent inhibition of insulin signalling [104]. A study performed on humans revealed that acute elevation of plasma FFA levels produces hepatic IR primarily by inhibiting insulin-mediated suppression of glycogenolysis [105]. Skeletal muscle IR has been demonstrated in rodents to exacerbate NAFLD [106], which is strongly associated with hepatic IR.

Furthermore, hepatocytes can release functional proteins, called hepatokines, which can influence metabolic processes through autocrine, paracrine, and endocrine signaling [107]. These hepatokines include selenoprotein P, sex hormone-binding globulin (SHBG), fibroblast growth factor 21 (FGF21), and adropin. Studies found that SHBG secretion was inversely associated with liver steatosis, cardiometabolic risk, and insulin resistance [108, 109]. FGF21 is reported to induce positive metabolic functions. Administration of recombinant FGF21 to obese mice reversed hepatic steatosis, increased energy expenditure, and improved insulin sensitivity [110].

1.1.3.3.5 Brain

The brain is a complex organ that controls all functions of the body such as thinking, memory, emotion, touch, motor skills, vision, and breathing, and interprets information from the outside world through our five senses: sight, smell, touch, taste, and hearing [111]. The brain is composed of the cerebrum, cerebellum, and brainstem [111]. At the cellular level, it is made up of two types of cells: nerve cells or neurons and glial cells. Neurons convey information through electrical and chemical signals,

and they communicate with each other by exchanging neurotransmitters across a tiny gap called a synapse. Glial cells provide neurons with nourishment, protection, and structural support [111]. There are two sets of blood vessels that supply blood and oxygen to the brain (**Figure 1.14**): the vertebral arteries and the internal carotid arteries [111].

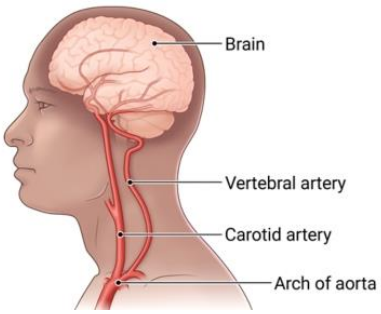

Figure 1.14 Arterial supply to the brain. There are two arteries that are responsible for the blood supply to the brain: the vertebral arteries and the internal carotid arteries. The figure is derived from online (www.cigna.com/es-us/knowledge-center/hw/blood-supply-to-the-brain-tp10153).

Although the roles of insulin in peripheral tissues are well understood, less is known about its multifaceted roles in the brain. Ever since the brain was identified as an insulin-sensitive organ, evidence has rapidly accumulated that insulin actions in the brain produce multiple behavioral and metabolic effects, influencing eating behavior, peripheral metabolism, and cognition [112]. Human and animal studies indicate that insulin influences cerebral bioenergetics, enhances synaptic viability and dendritic spine formation, and increases the turnover of neurotransmitters, such as dopamine. Insulin also has a role in proteostasis, influencing clearance of the amyloid β peptide and phosphorylation of tau, which are hallmarks of Alzheimer's disease (AD) [113]. Moreover, insulin modulates vascular function in the brain through effects on vasoreactivity, lipid metabolism, and inflammation [113]. Disturbances in brain insulin action can be observed in obesity, T2DM, as well as in aging, and dementia [114].

Insulin receptors are expressed on all cell types in the brain and are concentrated in the olfactory bulb, hypothalamus, hippocampus, cerebral cortex, striatum, and

cerebellum [115, 116]. Insulin enters the brain primarily by selective, saturable transport across the capillary endothelial cells of the blood-brain barrier (BBB) [117, 118]. However, it takes a relatively long time for insulin to be transported to neurons from external sources [119, 120]. Insulin has multiple functions in the brain, which are outlined above, and therefore a normal supply of insulin in the brain is very essential for neural function. Recent research suggests that insulin is also synthesized locally in the cerebral cortex, which can ensure a normal concentration of insulin in the brain and provide a rapid way of regulating local microcircuits [120, 121]. Insulin has many roles in neurons. Briefly, insulin enhances neurite outgrowth, modulates catecholamine release and uptake, regulates trafficking of ligand-gated ion channels, regulates expression and localization of gamma-aminobutyric acid (GABA), *N*-methyl-D-aspartate (NMDA), and α-amino-3-hydroxy-5-methyl-4-isoxazole propionic acid (AMPA) receptors, and modulates activity-dependent synaptic plasticity [122]. Concerning glial cells, insulin modulates microglial inflammatory responses [123]. Glucose maintains cerebral energy metabolism in part due to the presence of glucose transporters in endothelial cells of the BBB, neurons, and glial cells, as well as a relatively high plasma glucose concentration [124]. Neuronal glucose uptake depends on the glucose transporter isoforms GLUT1, GLUT3, and GLUT8 on the plasma membrane [124]. Due to the relative abundance in the brain, GLUT3 is considered the major glucose transporter in neurons [125], which is insulin-independent and present in very few other cell types in the body. GLUT-4 is present at a low level in the brain, including the olfactory bulb, the dentate gyrus of the hippocampus, the hypothalamus, and the cortex [126].

Further, insulin signaling in the central nervous system (CNS) regulates metabolic pathways in peripheral tissues such as the liver and adipose tissue, and these effects are thought to be mediated by the actions of insulin in the hypothalamus [122]. The metabolic effects of brain insulin include the suppression of hepatic glucose production [127, 128], hepatic catabolism of branched-chain amino acids [129], hepatic triglyceride secretion and lipolysis in adipose tissue [130]. Brain insulin

actions on other peripheral tissues were summarized previously [114] and depicted in **Figure 1.15**.

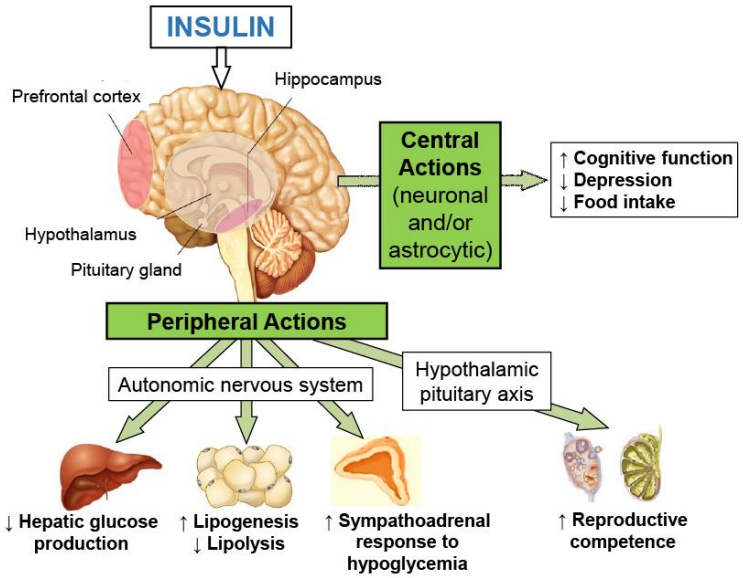

Figure 1.15 Insulin action in the brain regulates both central and peripheral functions. In addition to regulating CNS (via neurons and/or astrocytes) functions, insulin acts in the brain to regulate peripheral functions via the autonomic nervous system and the hypothalamic-pituitary axis. The figure comes from Agrawal *et al* [114].

Similar to the definition of IR, brain IR is defined as the failure of brain cells to respond to insulin [131]. This lack of response could be caused by insulin receptor downregulation, insulin receptor inability to bind insulin, or faulty activation of the insulin signaling cascade [122]. At the cellular level, this dysfunction may manifest as the impairment of neuroplasticity, receptor regulation, or neurotransmitter release in neurons. Or, it may occur as a result of the impairment of processes more directly implicated in insulin metabolism [122]. Functionally, brain IR can manifest as impaired central regulation of nutrient partitioning, cognitive and mood dysfunction, and brain-specific neuropathology and neurodegeneration [122]. T2DM and AD, which some authors classified as “type 3 diabetes”, are both associated with brain IR and brain dysfunction [122, 132].

1.1.3.4 Measurement of insulin resistance

There are a variety of approaches to assess IR in the whole body and specific tissues

or organs [133]. Most IR studies have been performed using the whole-body approach to assess IR due to the simplicity of performing this measurement. Despite this, it is well known that the contribution of each insulin-sensitive organ or tissue can be different for the patient evaluated despite having the same whole-body IR value to other patients [134]. Therefore, several controversial conclusions can be found in the literature due to the use of the whole-body indexes [134, 135].

1.1.3.4.1 Whole-body insulin resistance

The gold standard method to measure whole-body IR is using the hyperinsulinemic-euglycemic clamp (HEC) technique [136]. In this technique, plasma insulin is raised to a constant predetermined level by a continuously primed infusion of exogenous insulin, while plasma glucose is maintained at a constant euglycemic level by adjusting the infusion of exogenous glucose [136]. Under these steady conditions, the rate of infused glucose is equal to the rate of glucose uptake by all the tissues in the body, namely the rate of whole-body glucose disposal. The rate of insulin infusion should be sufficient to suppress endogenous glucose production; 120 $mU/m^2/min$ insulin is a standard insulin infusion rate used in the practice [137]. Despite being the gold standard technique, HEC is invasive with a costly, laborious, and time-consuming procedure [133].

Therefore, several easier and more practical approaches based on indices have been developed, which are derived from measurements of fasting glucose and insulin levels or from the measurement of the dynamic plasma assessment after an oral glucose tolerance test (OGTT). Based on a single fasting blood sample, the homeostatic model assessment of IR (HOMA-IR) [138] and the quantitative insulin sensitivity check index (QUICKI) [139] were developed and have been widely used in the clinical practice and several trials, due to their ease of use and well assessing whole-body IR. Combining the fasting plasma test and the use of OGTT, two more invasive surrogate indices Insulin Sensitivity Index ($ISI_{0,120}$) [140] and the Whole Body Insulin Sensitivity Index (WBISI) [141] are available to choose from.

HOMA-IR is used to quantify IR and beta-cell function from fasting plasma glucose and insulin concentrations. It has proven to be a robust clinical and epidemiological tool for the assessment of whole-body IR. Regarding the QUICKI index, it is also calculated by a formula using fasting plasma glucose and insulin concentrations. It provides a reliable, reproducible, and accurate index of insulin sensitivity with excellent predictive power. Both indices are used in this study.

1.1.3.4.2 Tissue/organ-specific insulin resistance

Tissue or organ-specific IR can be evaluated *ex vivo* or *in vivo*. The *in vivo* approach uses biopsy samples to apply a molecular biology technique to have a surrogate indicator of IR or measure the concentration of radioactive glucose present in the biopsy sample after administering this type of glucose to patients or animals [142, 143]. As for the *in vivo* method, tissue/organ-specific IR can only be assessed using radioactive glucose with dynamic single-photon emission computerized tomography (SPECT) or dynamic or static positron emission tomography (PET) [144, 145] specifically on T2DM patients after an HEC condition, where tissue/organ-specific insulin sensitivity is determined. In the case of dynamic PET evaluation, we always have a surrogate value of IR because the rate of glucose uptake in the organ is determined after comparing it with a control group to establish its rate of reduction. However, in our laboratory, we have used the basis of the dynamic assessment to establish a technique for the first time that allows IR to be quantified by performing two static PET scans on the same fasting patient, at baseline, and after performing an HEC procedure. In each scan, we used half the dose of 2-deoxy-2-[18F]fluoro-D-glucose (^{18}F-FDG) to meet the dosimetric requirements for patients. In addition, this technique can adequately determine the IR because the alterations caused by diets, medications, and exercise, among other causes can be eliminated because the IR is obtained as the difference in the uptake of ^{18}F-FDG in any organ or tissue between the scan performed in HEC and baseline condition (IS in an organ or tissue can be assessed by the formula: $\Delta SUV = SUV_{HEC} - SUV_{baseline}$).

PET is a noninvasive imaging technique providing three-dimensional, whole-body, and quantitative images, which has wide clinical applications in oncology, cardiology, and neurology [146]. In recent years, it was found that the combination of PET and CT (PET/CT) showed more precise anatomical localization of areas of increased metabolic activity than previously one of them alone. It combines the physiological sensitivity of PET with the anatomical accuracy of CT in one imaging session [146].
For instance, currently, a gold standard technique for IR quantification in adipose tissue in humans is the determination of lipolysis fluxes by tracer-dilution techniques during continuous intravenous insulin infusion [147]. In addition, the isotope dilution technique is also a frequent method used to assess hepatic IR [148].
^{18}F-FDG is the most widely used radiotracer for the measurement of tissue glucose uptake in PET due to the following advantages: 1) it has a long half-life (109 minutes); 2) it decays by emitting positrons with the lowest positron energy (511 keV) which contributes to high-resolution imaging and 3) it acts as a glucose analogue and can be transported into the cells by the same carrier as glucose, but its phosphorylated product FDG-6-phosphate can’t enter the standard metabolic pathways and leave the cell slowly, and therefore it is trapped and accumulated in the cells [149]. This 'metabolic trapping' of FDG-6-phosphate forms the basis of the analysis of PET data.

1.1.4 Glucagon-like peptide-1

Glucagon-like peptide 1 (GLP-1) is an incretin hormone secreted by the L-cells of the distal ileum and colon and is generated by tissue-specific posttranslational proteolytic processing of the proglucagon gene [150]. Native GLP-1 is composed of 30 or 31 amino acids, has a very short half-life, and undergoes amination of the C-terminal domain. Bioactive GLP-1 is truncated from GLP-1 (1–37) and exists as two equipotent circulating molecular forms, GLP-1 (7–37) and GLP-1 (7–36 amide). In humans, nearly all circulating GLP-1 is GLP-1 (7–36 amide), accounting for 80% [151]. Nutrients including glucose, fatty acids, and dietary fiber can stimulate the release of this hormone in the digestive tract. Thus, GLP-1 is released in response to

meal intake, affects multiple target tissues throughout the body, and executes key functions such as stimulating pancreatic insulin secretion and inhibiting food intake. After many years of research, it has been recognized to have multifaceted actions in different organs and tissues (**Figure 1.16**) such as the stimulation of insulin secretion from pancreatic β cells, the decrease of gastric emptying, reduction of appetite and food intake, the modulation of rodent β-cell proliferation, and cardio- and neuro-protective effects [152, 153]. Actions of GLP-1 are believed to be mediated by a single G protein-coupled receptor isoform in the cell membrane [150].

One of the most important functions of GLP-1 is its incretin effect or insulinotropic activity, which has attracted numerous and continuous interests, as the stimulation of insulin secretion by GLP-1 is strictly in a glucose-dependent manner [150]. However, GLP-1 is quickly metabolized (in around 2 min in plasma) and inactivated by the enzyme dipeptidyl peptidase IV (DPP-IV) [152], which prevents its broad clinical use. Therefore, different pharmacological approaches aiming to extend the *in vivo* half-life of GLP-1 or to inhibit its inactivation are currently being evaluated, such as GLP-1 analogues exenatide and liraglutide (incretin mimetics), and DPP-IV inhibitors (incretin enhancers) [154]. Incretin mimetics exenatide and liraglutide show reductions in fasting and postprandial glucose concentrations [155]. DPP-IV inhibitors such as sitagliptin and vildagliptin reduce HbA1c by 0.5~1.0% with few adverse events and no weight gain [155]. All these treatments are currently approved in Europe and USA only for specific circumstances in T2DM and obesity. Therefore, despite the incretin mimetics and enhancers being very promising treatments for T2DM and obesity, long-term clinical studies are needed to expand their uses in these pathologies.

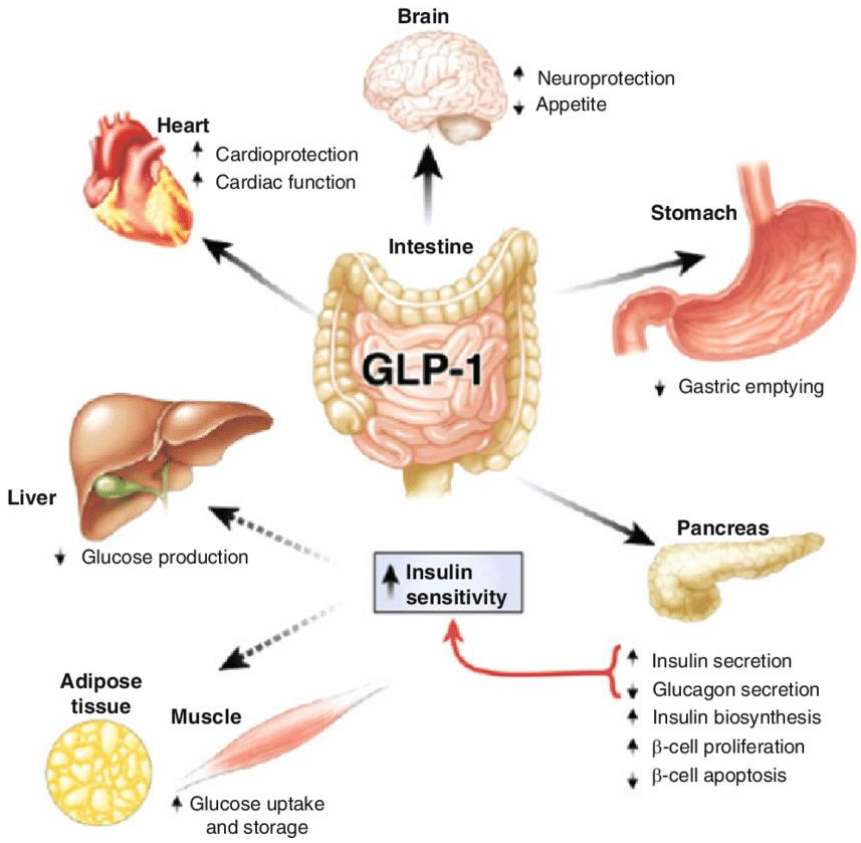

Figure 1.16 Major biological actions of GLP-1 in peripheral tissues. Most GLP-1 effects are mediated by direct interaction with GLP-1 receptors on specific tissues (continuous arrow). However, the actions of GLP-1 in the liver, fat, and muscle most likely occur through indirect mechanisms (discontinuous arrow). The above figure is from Gallwitz *et al* [153].

1.2 Gut microbiota

1.2.1 General overview

Gut microbiota (GM) is an assortment of microorganisms inhabiting the mammalian gastrointestinal tract (GIT). In humans, the number of microorganisms in the GIT has been estimated as many as 10^{14}, which is 10-fold higher than the number of cells in the human body [156]. The number and composition of microbes vary across the length of the GIT, and its richness and diversity are gradually increased from stomach to colon [157] (**Figure 1.17**). Over 70% of all the microbes reside in the colon, but a few of them live in the stomach and duodenum [156]. According to oxygen demand, GM consists of strict anaerobes, facultative anaerobes, and aerobes, with strict anaerobes being the majority [156]. From biological taxonomy, GM consists of

bacteria, archaea, viruses, and eukarya. GM has co-evolved with the host over thousands of years to form an intricate and mutually beneficial relationship, where some bacteria only live in a settled niche, and the microbial composition stays a dynamic homeostasis.

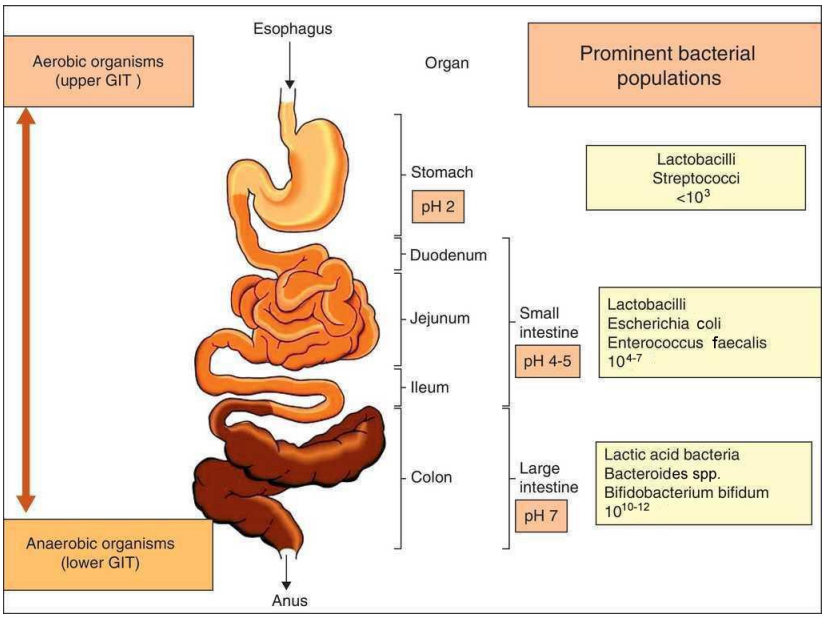

Figure 1.17 Composition and richness of gut microbiota along the gastrointestinal tract. From the stomach to the colon, the pH increases and so does the density of microorganisms. Most aerobic organisms reside in the upper gastrointestinal tract (GIT), while most anaerobic organisms live in the lower GIT. The figure is adapted from Tsabouri *et al* [157].

Currently, the understanding of GM has been greatly improved due to the advent of culture-independent approaches such as high-throughput and low-cost sequencing methods. Thus, more than 50 bacterial phyla and around 500-1000 species have been described [158, 159]. The human gut microbiota is mainly from two phyla: Bacteroidetes and Firmicutes [160]. In bacterial taxonomy, a bacterium is placed within a small but homogenous group in a rank or level, and the most commonly used ranks or levels in their descending order (**Figure 1.18**) are kingdoms, phyla, classes, orders, families, genera, and species. When it comes to talking about an organism, we use the last two taxa, the genus, and the species, because they are more specific. Binomial nomenclature is formally used for naming an organism. It is important to note that the first letter of the genus is always capitalized, and the whole name of the

genus and species is italicized.

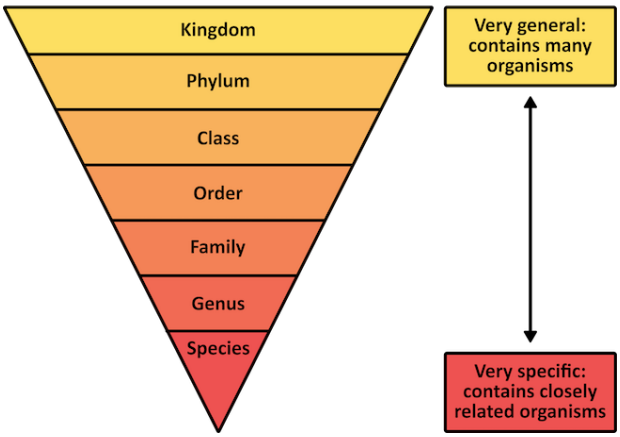

Figure 1.18 Ranks or levels of bacterial taxonomy. The closer the classification is to the genus or species, the more specific it is. Relatively, each kingdom or phylum contains many genera and species. The figure is from online (www.mometrix.com/academy/biological-classification-systems/).

Recent studies show that the function of GM extends far beyond digestion, playing critical roles in host health [161]. The beneficial functions to the host include strengthening gut integrity or shaping the intestinal epithelium, harvesting energy, protecting against pathogens, and regulating host immunity [162]. Therefore, maintaining GM homeostasis is essential to fulfilling the above functions. Many intrinsic and extrinsic factors can affect the distribution and composition of GM, including diet, drugs, probiotics, and antibiotics [163]. On the other hand, when the GM is imbalanced and aberrant, it also may contribute to the pathogenesis of various common metabolic disorders including obesity, T2DM, NAFLD, cardio-metabolic diseases and dementia [161, 164].

1.2.2 Relationships of gut microbiota with Type 2 Diabetes, insulin resistance, and related comorbidities

Over the past few decades, a lot of studies have been performed to explain how GM is involved in the development of the above diseases. There is growing evidence that GM and its alteration interact with other organs, highlighting the concept of the gut-organ axis [165]. **Figure 1.19** depicts the different gut-organ axes and various

diseases associated with GM alterations. Metabolic components serve as communication pathways between the GM and different organs, such as bile acids, short-chain fatty acids (SCFAs), and neurotransmitters [165]. SCFAs are derived from the GM fermentation of indigestible foods and have important metabolic functions [166]. Increasing evidence demonstrates a beneficial role for SCFA in adipose tissue, skeletal muscle, and liver substrate metabolism and function, thereby facilitating improved insulin sensitivity [166].

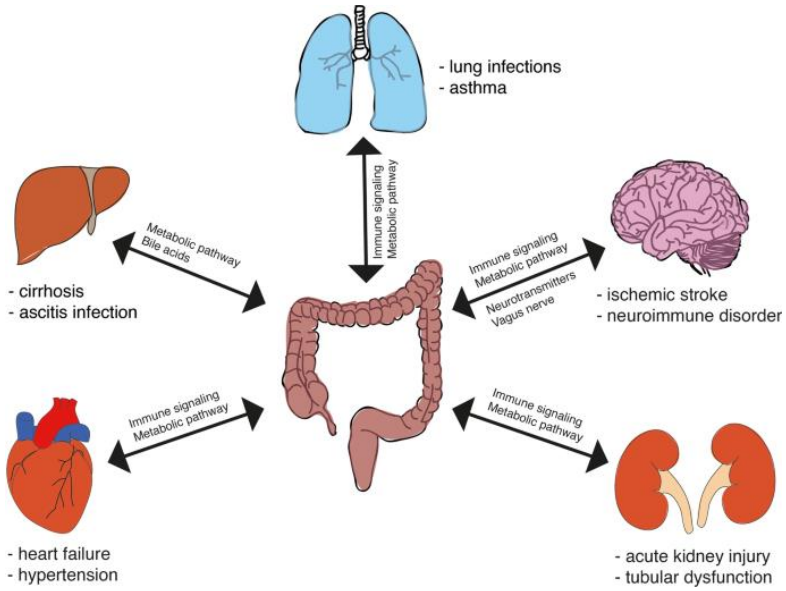

Figure 1.19 Gut-organ axes and disease examples. Through metabolic pathways and immune signalling, GM dysbiosis will affect other organs such as the brain, liver, and heart, and could have an impact on the progression of critical diseases. The figure is from Wozniak *et al* [165].

In addition to IR in some specific tissues/organs described above, the GM may play a role in the IR of these tissues or organs through gut-organ axes [165, 167]. Aberrant alterations in the GM composition have been detected in T2DM patients, including a significant decrease in butyrate-producing bacteria, which are associated with IR and the development of T2DM [168, 169]. Below, a summary of the relationships between GM and T2DM, as well as T2DM-related comorbidities or IR-related diseases is presented.

1.2.2.1 Gut microbiota and Type 2 Diabetes

One of the main features of T2DM is IR in target tissues, which leads to increased

blood concentrations of glucose and insulin. Some studies have shown a relationship between T2DM and changes in the GM composition and the gut itself [168, 170]. For instance, patients with total colectomy show an increased risk of T2DM in comparison to individuals without colectomy [171]. Furthermore, studies in rodents have shown that hyperglycaemia may increase intestinal barrier permeability and subsequently cause a leaky mucosa, allowing permeability of some metabolites to the blood that could alter the metabolism of certain organs [172]. Therefore, there is increasing interest in understanding if an altered GM is involved in triggering either T2DM, a metabolic disease, or problems associated with this disease. A metagenome-wide association study of GM in T2DM showed a moderate degree of gut microbial dysbiosis, including a reduction in the abundance of some universal butyrate-producing bacteria and an elevation in various opportunistic pathogens [168]. Similar results were got in gestational diabetes mellitus [173]. Because most T2DM patients need to take drugs regularly to reduce the glucose blood levels or avoid comorbidities, more conclusive findings are detected in individuals with prediabetes who are drug-naïve, and then the effect of the drug is avoided. Relevant studies indicated that their GM exhibited a loss of butyrate-producing taxa, a reduced abundance of *Akkermansia muciniphila*, and an increased abundance of bacteria with pro-inflammatory potentials such as *Bacteroides vulgatus* and *Prevotella copri* [174, 175]. Altogether, these studies suggest that an aberrant GM might be an important contributor to the development of T2DM.

1.2.2.2 Gut microbiota and cardiovascular disease

Cardiovascular disease (CVD) remains the leading cause of death worldwide, and is estimated to cause 17.9 million deaths globally in 2019, which accounts for 32% of all deaths [176]. CVDs are a group of disorders of the heart and blood vessels and are usually associated with atherosclerosis and increased blood clots, which cause damage to arteries in organs such as the brain, heart, kidneys, and eyes. It includes coronary artery disease (CAD), cerebrovascular disease, peripheral arterial disease,

rheumatic heart disease, and other related conditions [176]. The heart is an important organ for the body and heart disease (cardiopathy) is chosen as a unique type of CVDs to address the relationships with the GM.

1.2.2.2.1 Gut microbiota and cardiopathy

Cardiopathies also called heart diseases include cardiomyopathy, myocardial infarction, heart attack, CAD, and heart failure. Most of these heart diseases are related to the presence of atherosclerotic plaques [177]. Atherosclerosis is a buildup of plaque inside the artery walls, which causes the inside of the arteries to become narrower and slows down the flow of blood to the heart, brain, or other parts of the body. Atherosclerosis can be related to IR, as the affected individuals frequently have clinically silent metabolic dysfunctions for many years, including elevated circulating concentrations of glucose, insulin, and lipids in addition to IR [161]. Furthermore, it has been proven that arteriosclerosis affects the gut microbiota [178]. Patients with ischaemic heart failure were recently found an abnormal GM, which was an increased abundance of genera *Ruminococcus*, *Acinetobacter,* and *Veillonella* and a decreased abundance of genera *Alistipes*, *Faecalibacterium* and *Oscillibacter* [178]. In addition, subjects with atherosclerotic cardiovascular disease were reported an enriched abundance of Enterobacteriaceae, including *Escherichia coli*, *Klebsiella spp.*, and *Enterobacter aerogenes* [179].

Diabetes mellitus and obesity, as the two most important factors, can definitely increase cardiovascular risk [180]. Some altered gut bacteria include the above-mentioned in the studies of T2DM and heart diseases, which are associated with CVD. Therefore, these studies demonstrated that GM is related to the development of cardiovascular risk factors that can further result in CVDs.

1.2.2.3 Gut microbiota and fatty liver disease

Fatty liver disease is a condition caused by an excess of fat storage in the liver. There are two types of fatty liver disease: NAFLD and alcoholic liver disease.

NAFLD comprises a wide spectrum of hepatic pathology ranging from simple steatosis causing the non-alcoholic fatty liver to non-alcoholic steatohepatitis (NASH) and even cirrhosis [181, 182]. NAFLD is a common disease in many countries, frequently diagnosed in overweight or obese individuals, with a prevalence of up to 20–40% in the adult population [183]. NAFLD is considered the hepatic manifestation of metabolic syndrome. Therefore, IR is frequently found in patients with NAFLD and is thought to contribute to the pathogenesis partly by enhancing lipolysis in the adipose tissue, and subsequently increasing the flux of free fatty acids into the liver [184]. Recent studies suggested that in addition to IR, GM may also have a potential role in the pathogenesis of NAFLD [185]. For example, a study was shown that the abundance of the bacterial genera *Clostridium*, *Anaerobacter*, *Streptococcus*, *Escherichia*, and *Lactobacillus* was increased in individuals with NAFLD, whereas *Oscillibacter*, *Flavonifaractor*, *Odoribacter*, and *Alistipes* were decreased [186]. Furthermore, in comparison to healthy controls, the percentage of Proteobacteria, Enterobacteriaceae, and *Escherichia spp.* is elevated in patients with NASH [187].

1.2.2.4 Gut microbiota and dementia

Dementia is a general term used to describe a group of symptoms that affect memory, thinking, comprehension, calculation, learning capacity, orientation, language, and judgement [188]. Dementia is a pathological condition that is the main cause of disability and dependence in elderly people worldwide [188]. In 2019, it was estimated that 55.2 million people were living with dementia. It was the seventh leading cause of death worldwide, accounting for 1.6 million deaths [188]. Among all types of dementia, Alzheimer's disease (AD) is the most common form of dementia

and approximately accounts for 60-80% of cases [189]. Growing evidence supports the notion that AD is fundamentally a metabolic disease in which brain glucose utilization and energy production are impaired [190, 191]. In fact, some authors considered AD as Type 3 Diabetes [132] and it has been associated with progressive brain IR and insulin deficiency [113, 192]. On the other hand, the role of GM in the brain-gut axis has been identified and studied [193]. Therefore, the contribution of intestinal bacteria to cognitive dysfunction, specifically to the development of AD was delineated. For example, a cross-sectional clinical trial comparing control individuals with AD patients showed a decreased microbial diversity as well as significant differences in bacterial abundance including decreased Firmicutes and *Bifidobacterium* and increased Bacteroidetes in AD patients [194].

1.3 Metabolomics

1.3.1 General overview

Metabolomics is the large-scale and comprehensive study of metabolites, within biofluids, cells, tissues, or organisms [195]. Metabolites are small to medium-sized molecules derived from cellular metabolism, and their concentrations can directly reflect the underlying biochemical activity and physiological state of cells or tissues [196]. Collectively, these small molecules and their interactions within a biological system are regarded as the metabolome [197]. Metabolomics provides a “snapshot” in time of all metabolites present in a biological sample, which directly represents the molecular phenotype in contrast with other “omics” which provide former steps, such as genetic or proteomic information. Therefore, metabolomics is a powerful approach for the detection of temporal physiological changes in real time and can complement transcriptomics, genomics, and proteomics [198].

Comprehensive metabolomic profiling has been made possible thanks to two important advancements in recent decades. First, computational tools and resources for automating the analysis of spectra and extracting meaningful biochemical

information have been developed, which allow the interpretation of metabolite data in the context of its relationship to metabolic pathways [199, 200]. Second, advances in the sensitivity and specificity of small molecule detection methods enable the characterization and quantification of complex metabolic profiles in biological samples, allowing the simultaneous measurement of dozens or even hundreds of metabolites in a single sample [201, 202]. Currently, metabolomics is widely utilized for identifying disease biomarkers, aiding in drug discovery, and studying plants, bacteria, nutrition, and the environment [203].

In metabolomics, three analytical chemistry strategies are used – untargeted, semi-targeted, and targeted methods. Both untargeted and semi-targeted methods are typically applied in hypothesis-generating studies, aimed to identify and quantify metabolites as many as possible [204]. Semi-targeted metabolomics is a technique for quantifying hundreds of known metabolites and simultaneously detecting thousands of unknown features [205]. In contrast, targeted approaches analyze a relatively smaller subset of biochemically annotated and relevant metabolites for validating and translating hypothesis-generating studies. Untargeted and semi-targeted metabolomics provide the opportunity to observe unexpected changes, while targeted metabolomics offers higher sensitivity and selectivity [195]. Often, the choice of technique is determined by the experimental objective and the type of sample/matrix.

The most frequently used analytical platforms for metabolomics are nuclear magnetic resonance (NMR) spectroscopy and gas- or liquid-chromatography coupled to mass spectrometry (GC-MS or LC-MS). In the MS platform, both LC and GC are used for metabolite separation. MS and NMR are very effective and comprehensive to analyze the molecular composition of a sample, but both have their pros and cons [205]. On the one hand, MS has high sensitivity and selectivity, but quantification is more time-consuming and it is destructive to the samples. NMR, on the other hand, has very high reproducibility, and provides an easy quantification as well as deeper structural information, but has low sensitivity and selectivity [206]. As such, NMR and MS are complementary analytical techniques that can assist us in identifying

metabolites. In this study, NMR spectroscopy was the selected analytical technique.

1.3.2 Nuclear Magnetic Resonance metabolomics

NMR is a spectroscopic technique that uses the energetic transition of nuclear spins in the presence of a strong magnetic field to detect molecules. Nuclear spins encode information about the chemical environment and thus the molecular structure [205]. The first NMR spectrum was published in the 1940s [207]. As a tool in analytical chemistry, NMR can be applied in numerous areas and has proven to be a powerful tool in life sciences, particularly in the identification and structural elucidation of organic compounds, particularly metabolites [208]. Since NMR was first used in metabolic studies by Wilson and Burlingame [209], it has contributed significantly to our knowledge of metabolism and metabolic processes for about 50 years.

An NMR spectrometer consists of three main components: a superconducting magnet, a probe, and a complex electronic system (console) controlled by a workstation, as shown in **Figure 1.20**. The NMR spectrum provides the following information for each metabolite: the number of signals produced by protons, the position of the signals, the integration and intensity of the signals, and the splitting of the signals produced [210]. All these information is used for the elucidation of compounds from NMR spectra.

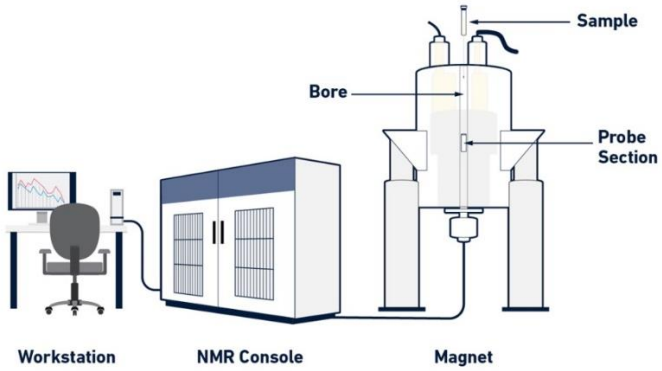

Figure 1.20 General design of an NMR spectrometer with its principal components. An NMR instrument generally contains three components: a superconducting magnet, a probe, and an NMR console controlled by a workstation. The figure is from online (www.technologynetworks.com/analysis/articles/nmr-spectroscopy-principles-interpreting-an-nmr-spectrum-and-common-problems-355891).

The workflow pattern of NMR-based metabolomics (**Figure 1.21**) can be divided into four steps: sample preparation, NMR acquisition, data analysis, and biological interpretation [211].

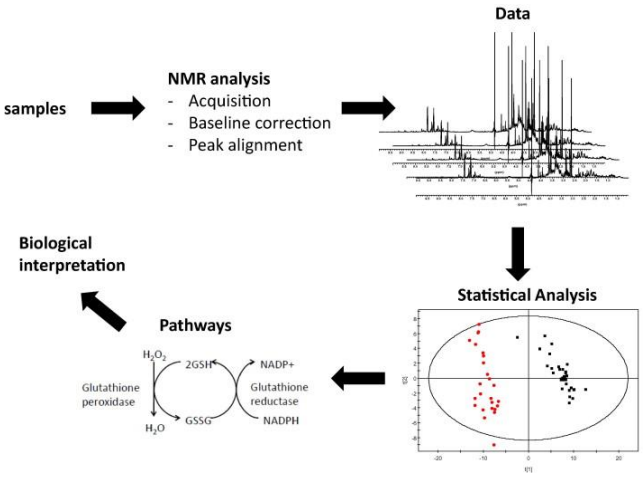

Figure 1.21 General workflow of NMR-based metabolomics. Typically, an NMR-based metabolomics study includes the following steps: sample preparation, NMR acquisition, data analysis, and biological interpretation. The above figure is from Brennan *et al* [211].

1.3.2.1 Sample preparation

A wide variety of body samples can be used for NMR-based metabolomics, including saliva, nasal lavage, exhaled breath condensate, sweat, blood, plasma, serum, urine, and feces [212]. In addition, biopsy samples such as tissues and tumors and *in vitro* cell systems such as yeast, tumor cells, and bacteria also can be used for NMR spectroscopy [213]. Liquid samples, like plasma, can be directly measured, while for semi-solid samples, like feces, an extraction procedure has to be carried out to remove macromolecules or particles [213]. It is generally acknowledged that a standard operating procedure for sample acquisition, processing, and storage is very critical. For instance, if blood samples are used for the metabolomics study, lithium heparin tubes are recommended for blood collection [214], rather than EDTA-containing tubes, because EDTA produces additional resonances. Following collection, samples should be kept cold or frozen immediately and transferred to the lowest temperature (e.g., -80 ℃) as soon as possible to minimize metabolite degradation. In addition, unnecessary freeze/thaw cycles should be avoided [215]. Also, the pH of the samples

has a significant impact on the chemical shifts in the NMR spectra. It is important to adjust the pH, which is frequently done by adding a phosphate buffer at pH 7.4 [211].

1.3.2.2 NMR acquisition

The vast majority of NMR-based metabolomics studies, such as our studies, are performed by using one-dimensional proton (^{1}H) NMR spectroscopy (^{1}H-NMR). This is because ^{1}H atoms are existed in almost all organic compounds and thus in nearly every known metabolite [216]. In ^{1}H-NMR, a large and powerful magnet is used to align protons present in a sample that is loaded into an NMR glass tube. Several types of magnets can be used, ranging from a field strength of 250 to 900 MHz. The higher the field strength, the more sensitive the NMR spectrometer is, and lower concentrations of metabolites can be detected. With modern NMR equipment, samples can be continually loaded and removed with a robot sample exchanger that runs for days or weeks at a time. Over the past decades, the use of cryogenically cooled probes or cryoprobes dramatically increases signal sensitivity by a factor of three to four [217].

The principles of ^{1}H NMR are not fully described here, as they have been well described previously [218]. A crucial aspect of spectral acquisition in aqueous samples is the suppression of the water signal. In extracted samples, this issue can be solved by the use of >99.9% deuterated solvents (e.g., D_2O) [216]. In light of the complex profiles obtained for biofluids such as plasma/serum and urine, it is important to use one-dimensional spectra in combination with two-dimensional NMR experiments such as TOCSY, ^{1}H J-RES and ^{1}H-^{13}C HSQC for metabolites identification [211]. Furthermore, for plasma samples, the broad protein signals have to be removed with special pulse sequences [211]. For metabolites identification, the chemical shifts and multiplicity patterns have to be compared with reference databases, such as Human Metabolome Database (HMDB) [219] and Biological Magnetic Resonance Databank (BMRB) [220] as well as spiking samples with reference standards [206].

1.3.2.3 Data analysis

After NMR data acquisition, two tasks need to be done: NMR data preprocessing and multivariate data analysis [221]. The preprocessing procedures in an NMR-based metabolomics study include baseline correction, alignment, binning, and normalization. Typically, each laboratory has a preferred approach for baseline correction. Peak alignment is an important preprocessing step, which generally includes initial alignment and local alignment. Each spectrum is initially aligned to an internal standard: commonly, 3-(Trimethylsilyl)propionic-2,2,3,3-d4 acid (TSP) at 0.0 ppm is used for this [211]. Various alignment algorithms have been proposed for local alignment [211], which are not introduced here. Following peak alignment, the spectra are segmented into bins or buckets, and the spectral intensity within each bin is calculated. These bins can be of equal size (for example 0.04 ppm) or variable sized, as in our studies [222]. Recently, many software packages have emerged for the automated or semi-automated quantification of metabolites in NMR spectra, such as MetaboHunter, MetaboMiner, BQuant, and BATMAN [211]. Normalization is a mathematical operation that attempts to account for the sample's overall concentration. There are numerous approaches to normalization, the most common of which is to normalize each spectrum to its total intensity [211].

Once preprocessing is complete, the pipeline moves on to multivariate statistical analysis, which involves supervised and unsupervised data analysis. Unsupervised data analysis seeks to gain a general understanding of the data and identify any underlying trends. Principal Component Analysis (PCA) is one of the most popular techniques in unsupervised data analysis to identify potential outliers, assess the overall quality of the data, and explore metabolite differences between groups [198, 211]. Supervised techniques are used to identify spectral signals that differ between groups or classes and require prior knowledge of class membership. The two most popular methods employed in supervised data analysis, are Partial Least Squares Discriminant Analysis (PLS-DA) and Orthogonal Projection to Latent Structure

Discriminant Analysis (OPLS-DA) [211]. These two methods aid in the identification of the important variables, but they both have the risk of overfitting the data. Therefore, it is essential to validate every model. Permutation testing and cross-validation are methods for validating the model [211].

Finally, the metabolic profile can also be correlated with other variables, for instance, relevant clinical parameters, through a multivariate regression analysis, for instance, Partial Least Squares (PLS) [223] or univariable regression analysis such as Spearman or Pearson correlation analysis [224].

1.3.2.4 Biological interpretation

Statistical analysis usually yields a list of metabolites that are significantly associated with a phenotype, but it is challenging to gain biological insights from this analysis. Hence, biological data interpretation is needed. The first step in this process is usually the mapping of known metabolites onto biological pathways. Several well-documented public databases contain meticulously curated data on metabolites, metabolic reactions, enzymes, genes, proteins, and pathways, such as KEGG, Reactome, and MetaCyc databases [198]. Also, some open-source tools (Metscape, MetaboAnalyst, and VANTED) and commercial tools (MetaCore, Ingenuity Pathway Analysis) make use of pathway information and provide various methods for mapping experimentally observed changes onto metabolic pathways [198]. Placing compounds in metabolic pathways facilitates the connection of observed changes to previously reported biological observations.

In addition to mapping metabolites to pathways, it is frequently useful to be able to assess the relative importance of different pathways. Enrichment analysis can be used to complete this task, and typically produces a ranked list of pathways as well as a list of experimental compounds mapped to them [198]. Due to a relatively small number of identified metabolites measured in a given study, the statistical power of enrichment testing is not very high. One significant limitation of all the above

pathway mapping techniques is the relatively low coverage of experimentally measured metabolites in pathway databases [198].

1.3.3 Metabolomics studies in Type 2 Diabetes, insulin resistance, and related comorbidities

GM is responsible for the production and transformation of metabolites and takes part in several essential metabolic functions, including SCFAs production, amino acid synthesis, bile acid transformation as well as hydrolysis and fermentation of non-digestible substrates [225]. Changes in GM have been described above in metabolic diseases such as T2DM and related comorbidities, and the related metabolite alterations can be identified by metabolomics techniques.

1.3.3.1 Metabolomics and Type 2 Diabetes

Several alterations of metabolites in plasma, serum, or feces in T2DM patients have been reported. T2DM patients had a lower level of fecal propionic acid, valeric acid, and butyric acid, and a higher level of succinate after comparing with the controls [226]. However, the results of the total concentration of SCFAs in feces are inconsistent [226, 227]. However, a large number of human studies have consistently demonstrated that high levels of branched-chain amino acids (BCAAs) and aromatic amino acids (AAAs) in biological samples (plasma, feces, and urine) are associated with IR and have the potential to predict the development of diabetes and obesity [228, 229]. In fact, high serum concentrations of alanine, phenylalanine, glutamate, valine, leucine, isoleucine, tyrosine, ornithine, and lysine were linked to an increased risk of T2DM incidence, whereas high concentrations of glutamine were linked to a lower risk [230]. For example, a high plasma concentration of total BCAAs was found highly associated with an increased risk of T2DM [231, 232]. In terms of bile acid metabolism, an increase of deoxycholic acid in plasma was reported in T2DM patients [233].

1.3.3.2 Metabolomics and cardiovascular disease

Metabolomics has also been used to discover a link between host metabolism and incident CVD biomarkers. In an independent large clinical cohort (n = 1,876 subjects), many plasma metabolites were reproducibly correlated with CVD risks, and after structural validation, three of them were linked to phosphatidylcholine metabolism — choline, betaine, and trimethylamine-N-oxide (TMAO) [234]. Subsequent studies have confirmed a link between elevated plasma TMAO and increased cardiovascular and mortality risk in a wide range of populations [235, 236]. As mentioned above, BCAAs are found to be associated with IR, T2DM, and heart diseases. Plasma BCAA levels were also demonstrated to be of an independent predictive value for CVD risk prediction [237]. Furthermore, the levels of different lipoproteins detected in plasma have been associated with cardiovascular diseases, and NMR-based plasma profiling is currently applied as a screening method for cardiovascular risk [238, 239].

1.3.3.2.1 Metabolomics and cardiopathy

As mentioned above, cardiopathy is a group of heart diseases, belonging to CVD. There has been a lot of interest in seeing if metabolomic profiling can identify people with a higher risk for ischemic heart disease due to underlying atherosclerosis. Specifically, several studies have shown that plasma TMAO is a significant predictor of atherosclerosis as well as incident risk for myocardial infarction (MI) and stroke [240, 241]. Another MS-based metabolomic profiling discovered that in blood samples, higher levels of 18:2 monoglyceride or lower levels of 18:2 lysophosphatidylcholine and 28:1 sphingomyelin are associated with an increased risk of incident events of CAD [242]. Similar results were also found in patients with angina or MI [243]. Compared with healthy controls, increased plasma levels of pyruvate and lactate, and BCAAs leucine and isoleucine were observed in patients with heart failure [244].

1.3.3.3 Metabolomics and fatty liver disease

Untargeted metabolomics has also been applied to acquire knowledge about metabolic liver diseases. The metabolism of amino acids, fatty acids, and vitamins differed significantly between patients who suffered from NAFLD and NASH and healthy controls [245]. Patients with NASH had higher plasma levels of BCAAs, as well as phenylalanine, glutamate, and aspartate versus the healthy controls [246]. Another study also confirmed these patterns of change in levels of circulating BCAAs [247]. On the contrary, in subjects with NASH, the blood concentration of lysophosphocholine (16:0) was lower than in subjects without NASH [248]. Interestingly, in individuals with NASH, more ethanol produced by the aberrant GM was discovered compared with healthy individuals [249].

1.3.3.4 Metabolomics and dementia

Metabolomics advances have revealed the complexities of the dynamic changes associated with the progression of several pathologies related to dementia in T2DM such as Parkinson disease (PD) and AD, the more common one [189]. A clinical trial using unbiased lipidomics and metabolomics approaches discovered 34 significantly altered metabolites in the brain samples from AD patients after comparing them with the control subjects [250]. These metabolites were mapped onto six metabolic pathways and one of them, the alanine, aspartate, and glutamate metabolism, indicated the strongest correlations with AD status. In another untargeted metabolomics study, six unsaturated fatty acids (linoleic acid, linolenic acid, docosahexaenoic acid, eicosapentaenoic acid, oleic acid, and arachidonic acid) were identified to correlate with AD pathology as well as its clinical symptoms [251]. Cerebrospinal fluid (CSF) is the extracellular fluid that surrounds the brain and is an ideal source for determining neurobiochemical changes in the central nervous system of AD patients. Compared with lean volunteers, eight metabolites were significantly increased in the CSF samples of AD patients, including one acylcarnitine, two

sphingomyelins, and five glycerophospholipids [252]. Regarding Parkinson disease, a significant reduction in tryptophan, creatinine, and 3-hydroxyisovalerate levels in CSF was reported in PD patients compared to healthy subjects [253]. Further, in a double-cohort study, eighteen PD-specific plasma metabolites were identified, and among them, seven long-chain acylcarnitines decreased in both groups of PD patients when compared with the corresponding controls [254].

Chapter 1:
Gut microbiota and metabolomics alterations caused by T2DM

2.1 Introduction

An introduction to the alteration in gut microbiota and plasma and feces metabolomics caused by T2DM has been addressed in the general introduction of this thesis. However, there are some topics not previously addressed such as age- and sex-related differences in T2DM in terms of the gut microbiota, metabolomics, and IR that we will introduce in this chapter. Aging is an inevitable process in living beings and then in humans. With the increase in life expectancy, humans are living to a very old age along with the health problems associated with aging. Aging causes a series of transformations from organs to cellular organelles and leads to a wide variety of altered functions, which increase the risks of the development of some age-related diseases including diabetes [255, 256]. Therefore, it is very important to take into account the age factor in the study of T2DM. Also, gender has a much wider influence on disease than is usually acknowledged, and funding agencies from Europe and North America have implemented policies to support and mandate researchers to consider gender at all levels of medical research [257]. Therefore, it should be taken into account in the study of metabolic disorders, especially T2DM. The impact of age and gender on T2DM will be introduced taking into account the following aspects: gut microbiota, metabolomics, IR, and cardiovascular and hepatic risk factors.

2.1.1 Age-related changes in gut microbiota, metabolome, insulin resistance, and cardiovascular and hepatic risk factors caused by T2DM

As described above, the aging process induces many transformations, ranging from organs to cellular organelles, and as a consequence, leads to physiological, sensory, cognitive, and physical function changes [255]. Therefore, aging is widely regarded as a risk factor for T2DM [4].

2.1.1.1 Gut microbiota

As was described in the general introduction, the composition of the gut microbiota plays an essential role in human health, and it stays a dynamic homeostasis [162]. The use of molecular and genetic methods in recent years has expanded our understanding of intestinal flora, including its establishment, composition, and evolution. The gut microbiota composition is shaped in early life (0~3 years) and established as an adult-like configuration after the age of 3 years, then remaining relatively stable in adulthood [258, 259]. However, the structural changes and compositional evolution of gut flora from the adult stage to the elderly stage remain unclear. A study involving more than 1000 healthy Chinese individuals aged from 3 to over 100 years found that the gut microbiota differed little between individuals aged from 30 to >100, but varied dramatically in persons around 20 years [260]. Another study of 367 healthy Japanese subjects also found that the gut microbiota changed with age before 20 years, but had different results over 70 years in comparison to adulthood [261]. In this Japanese population study, a decrease in Lachnospiraceae and *Bifidobacterium*, and an increase in Proteobacteria and *Bacteroides* were observed in the elderly subjects (>70 years). Further, one more study performed on healthy subjects showed a pronounced difference in core microbiota between the elderly and younger adults because the elderly adults had a higher percentage of *Bacteroides spp.* and different abundance patterns of *Clostridium* groups [262].

Regarding T2DM, a moderate degree of gut microbial dysbiosis was found in T2DM patients after comparing with healthy individuals, manifested as an increase of opportunistic pathogens and sulphate-reducing bacteria and a reduction of butyrate-producing species [168]. Karlsson *et al* also observed similar alterations of microbiota in a study performed with European diabetic women [173]. These studies suggested that the intestinal microbiome might be an important contributor to the development of T2DM. However, to the best of our knowledge, no studies have been performed to determine the changes or evolution of the intestinal microbiota in patients with T2DM from adulthood to the elderly.

2.1.1.2 Metabolomics

2.1.1.2.1 Plasma

Metabolomic approaches, widely used in clinical trials, have also been applied to study the variation of the metabolomic profile of biofluids and tissues upon age. A "normal" plasma metabolome was defined by Trabado *et al* by analyzing plasma samples from 800 French healthy volunteers aged between 18 and 86. They found that older subjects (>60 years) had higher levels of sphingomyelins and phosphatidylcholines than younger subjects [263]. Another study about plasma metabolic profiles was conducted on 146 healthy subjects, aged from 30 to 100 [264]. This study showed alterations in ten species of plasmatic metabolites that were correlated with age, six were finally identified. Among them, one proteolytic product increased with age, while one hydroxyl fatty acid, one polyunsaturated fatty acid, two phospholipids, and one prostaglandin decreased with aging.

However, few plasma metabolomics studies have revealed age-related changes in T2DM. This may be because it is difficult to recruit a group of basically similar T2DM patients (similar medication treatment, weight, and other influencing factors). Several studies have described the metabolic differences in plasma or serum samples between older persons with or without diabetes. For instance, diabetic older adults aged around the age of 73 years old were shown higher levels of the amino acids alanine, glutamate, and proline and lower levels of arginine and citrulline [265]. When incorporated in archived blood samples obtained approximately 15 years ago, the study showed a greater accumulation of alanine and proline in diabetic older subjects. In addition, an interesting study examined the associations of 10-year plasma metabolite changes with subsequent T2DM risk [266]. In that study, the top three high T2DM risk-associated 10-year changes were found: isoleucine, leucine, and valine, which all belong to branch-chain fatty acids (BCAAs), and at the same time, the top three low T2DM risk-associated 10-year metabolite changes were also determined: N-acetylaspartic acid, C20:0 lysophosphatidylethanolamine, and C16:1

sphingomyelin.

2.1.1.2.2 Feces

Not like plasma, to date, only a few metabolomics studies have used feces to describe metabolic differences related to age. A study performed in healthy Danes found the largest systemic variation in fecal metabolome between young adults (18 years old) and elderly (65-80 years old): fecal concentrations of short-chain fatty acids (SCFAs) butyric acid and acetic acid were higher in young adults, while amino acids isoleucine, leucine, valine, and alanine were higher in the elderly [267]. In male BALB/c mice, an aging signature of fecal metabolomics was unveiled previously [268]. Compared to young mice (3-month-old), feces from old mice (16-month-old) had higher levels of 4-hydroxyphenylacetate and histidine, with lower levels of α-ketoisocaproate, α-ketoisovalerate, β-hydroxybutyrate, methionine, isoleucine and bile salts. However, no studies have reported the age-related difference in fecal metabolites between T2DM patients of different ages.

2.1.1.3 Insulin resistance and T2DM

The relationship between aging and IR is well documented [269, 270]. Older subjects with a mean age of 69 years had a higher probability to manifest IR (significant elevation of serum glucose and insulin levels) measured during the OGTT test than younger subjects [270]. They demonstrated that older subjects had a post-receptor defect in insulin action because insulin binding to isolated adipocytes and monocytes was similar in the older and younger groups. The post-receptor defect caused peripheral IR. In coherence with this, older age is a major risk factor for T2DM [4] and epidemiological studies reported that the incidence of T2DM was much higher in the elderly than in young people [271]. For example, one review provides a comprehensive perspective on the increased incidence of T2DM in older people due in part to the aging of the skeletal muscle [272]. During skeletal muscle aging, some

changes may occur, such as mitochondrial dysfunction, oxidative stress, increased inflammation, and intramyocellular lipid accumulation, which may affect skeletal muscle insulin sensitivity and therefore increase the risk of IR and T2DM. Accordingly, the aging process can trigger metabolic abnormalities related to IR and T2DM.

2.1.1.4 Cardiovascular and hepatic risk factors

By far, age is the most important risk factor for cardiovascular disease (CVD) [273]. In general, the effects of aging are considered unavoidable and irreversible. Besides age, cardiovascular risk factors also include high blood pressure, high cholesterol, smoking, T2DM, etc [274]. Both serum total cholesterol and blood pressure increase as age increases and the absolute difference in the risk of coronary heart disease was largest in the oldest age group [275]. A large-scale study in the Finnish population showed that serum cholesterol levels continuously increased from 25-29 years of age to 45-49 years of age in men, and continued to rise in women until 60-64 years of age [276]. Adults with diabetes are thought to have a high CVD risk. Diabetes patients are up to four times more likely to develop CVD than non-diabetics [277]. Diabetic men and women entered the high-risk CVD category after 40 years old, and younger diabetic people (age 40 or younger) did not seem to be at high risk of CVD [277]. Atherosclerosis is also a cumulative process, starting at an early age [278]. So far, differences in CVD risk factors such as plasma levels of total cholesterol, HDL cholesterol, LDL cholesterol, triglyceride, and atherosclerotic plaque in T2DM caused by age were not addressed.

Aging is also a key risk factor in the development of liver-related diseases [279]. With the aging process, liver structure and function are gradually altered, as well as liver cell changes [280]. Research has proven that the volume and blood flow of the liver decreases gradually with age [279]. In a human study, as humans got older, serum levels of gamma-glutamyltransferase (GGT) and alkaline phosphatase (ALP) were elevated while the level of serum bilirubin was gradually reduced [281]. Experiments

on male C57BL/6J mice demonstrated that plasma activity of aspartate aminotransferase (AST) was significantly higher in old mice, with marked histological signs of hepatic inflammation and fibrosis after comparing with young mice [282].

NAFLD refers to a group of conditions caused by an accumulation of fat in the liver and develops in 4 main stages: steatosis, NASH (accompanied by inflammation resulting from damaged hepatic cells), liver fibrosis, and liver cirrhosis (the most severe stage) [181, 182]. According to epidemiological surveys, the prevalence rate of NAFLD showed an increasing tendency as one got older [283, 284]. In addition, a cross-sectional study reported that elderly NAFLD patients (age ≥65 years) were more likely to have NASH and advanced fibrosis than nonelderly patients (18-64 years) [285]. NAFLD and T2DM are known to frequently coexist and act synergistically to increase the risk of adverse clinical outcomes [286]. One study reported that the prevalence of ultrasonographic NAFLD was 69.4% in 180 patients with T2DM and another study evidenced that 87% of 204 T2DM patients had NAFLD on histology [287, 288]. However, no one has addressed age differences in hepatic physiological function and markers of NAFLD and liver fibrosis in T2DM individuals.

2.1.2 Gender-related changes in gut microbiota, metabolome, insulin resistance, and cardiovascular and hepatic risk factors caused by T2DM

There is mounting evidence that sex differences are very important in the epidemiology, pathophysiology, treatment, and outcomes of many diseases, such as diabetes [289, 290]. The International Diabetes Federation reports that in 2019, there are more deaths associated with diabetes among women (2.3 million) than men (1.9 million) in adults aged from 20 to 79 [291]. Obesity, the most critical risk factor of T2DM, is more common in women than in men [292]. Previous studies have

suggested that endogenous sex hormones play an important role in the development of T2DM [109]. Therefore, sex and gender differences in T2DM studies should be taken into account.

2.1.2.1 Gut microbiota

Several studies have concluded that gender is one of the main variables affecting gut microbiota [293, 294]. Nowadays, gender differences in gut microbiota have not been reported in childhood, maybe owing to gonadal hormone quiescence [294]. A large-scale study identified a different gut microbiota in a 19- to 24-year-old cohort of healthy Chinese individuals (55 females and 80 males), finding the largest differences in the abundance of operational taxonomic units (OTUs) [260]. They speculated that these findings could be explained by the changes in sex steroid hormone levels at this age period. Roles of gender and sex hormones in gut microbiota were further summarized by Kichul Yoon *et al* [294], and the concept of "microgenderome" was proposed [295]. Tomohisa Takagi *et al* also studied gender-related differences in the gut microbiota in 277 healthy subjects aged 20 to 89 years [296]. Concerning the diversity analysis of gut microbiota in these subjects, significant microbial structural differences using β-diversity indexes were disclosed between male and female subjects, whereas no statistical differences were shown for all α-diversity indexes. In addition, significant differences in gut microbes at the genus level were found between genders. Thus, an increase in representative genera *Prevotella*, *Megamonas*, *Fusobacterium*, and *Megasphaera* was shown in male subjects and an increase in representative genera *Bifidobacterium*, *Ruminococcus*, and *Akkermansia* in female subjects. Moreover, in a study of 1135 individuals, females showed a greater microbial diversity and a higher abundance of *Akkermansia muciniphila* than males [297].

The roles of gut microbiota in T2DM have been delineated and understood previously [168, 169], however, up to now, to our knowledge, no research can be found comparing the gut microbiota between adult T2DM women and men. In 2021, there is

little gender difference in the overall prevalence of diabetes (10.2% in women, 10.8% in men), but the number of deaths due to diabetes in adults is higher in women than in men [298]. And some women are exposed to gestational diabetes, which is a transient condition that occurs in pregnancy and induces long-term risks of T2DM [299].

2.1.2.2 Metabolomics

2.1.2.2.1 Plasma

There are many differences in the physiology, functions, and quality of metabolism based on gender, which can affect the human metabolome [300, 301]. Therefore, there is a growing interest to identify sex-related metabolic features, which are fundamental to the delivery of personalized healthcare services including personalized nutrition. The aforementioned study performed on 800 French healthy individuals not only determined the age effects in plasma metabolome but also explored the impact of gender in plasma metabolome [263]. Thus, they found that males had higher concentrations of branched-chain amino acids, creatinine, and lysophosphatidylcholines, and lower concentrations of phosphatidylcholines and sphingomyelins in comparison with females. On the other hand, a comprehensive metabolomic study performed in serum samples of 903 women and 853 men indicated that more than 1/3 of all metabolites displayed significant differences between both genders [302].

Although changes in metabolic profiles in T2DM have been studied in several types of samples [230, 303, 304], the sex-specific metabolic signatures in the pathology have rarely been examined. To our knowledge, only one article showed sex differences in fasting urine and plasma metabolomics in the run-in period in healthy and T2DM subjects [305]. Their results presented a clear discrimination by plasma metabolomic analysis between healthy females and males and between diabetic females and males. They also obtained similar results in the urine metabolomic analysis. However, the authors did not provide metabolite differences in plasma and

urine samples between females and males with T2DM.

2.1.2.2.2 Feces

Compared to blood samples, feces are less often used to study gender differences in metabolomics, possibly because stool samples need to be processed before being used in metabolomics instruments. The above study in healthy Danes not only investigated the influence of age on the fecal metabolome but also explored the sex influence [267]. In the old age group (65−80 years old), levels of fecal metabolites valeric acid, isovaleric acid, butyric acid, and ethanol were consistently higher in males than in females. In the young age group (18 years old), fecal valeric acid and propionic acid were significantly higher in males. Even though fecal metabolic alterations caused by T2DM have been reported [304], the sex differences in fecal metabolites in the disease have not yet been investigated.

2.1.2.3 Insulin resistance

In recent decades, researchers have recognized gender differences in insulin sensitivity in humans [306]. Females differ substantially from males in the susceptibility to develop IR and in the degrees of IR due to several features.

First, in body composition, for a given body mass index, men had higher lean mass while women had higher adiposity [307]. In addition, men were reported to have more visceral and hepatic adipose tissue, associated with increased IR, whereas women had more peripheral or subcutaneous adipose tissue [307].

Second, sex hormones are different in women and men [109]. For example, estrogens have many beneficial effects on insulin sensitivity and adipose tissue distribution, and also have anti-inflammatory properties, which may help to build a more insulin-sensitive environment in women at fertile age [307]. In this line, an excess of androgens in women was associated with an increased IR [308, 309]. In addition, in diabetic animal models, estrogen was found to protect against hyperglycemia by

reducing hepatic glucose production and enhancing glucose transport in the muscle [307]. Further, estrogen seems to be implicated in the protection of pancreatic β-cell function and survival in the condition of oxidative stress [310].

Third, adiponectin levels were reported to be markedly higher in women than in men [311, 312]. Adiponectin is a hormone produced exclusively by adipose tissue, which arouses enough interest of researchers because it can lower hepatic glucose production and improve insulin sensitivity in muscle and liver by decreasing triglyceride content [313] and its supplement might provide a novel treatment for IR and T2DM.

2.1.2.4 Cardiovascular and hepatic risk factors

The role of sex is a fundamental issue in medicine and is getting more and more attention nowadays. Like age, gender differences in cardiovascular risk factors have also been discovered. In a large-scale Finnish population, all different age groups consistently showed cardiovascular risk factors: smoking was more common in men than in women, total cholesterol, blood pressure, and BMI were higher in men, but HDL cholesterol was lower ($p<0.001$) [275]. They also indicated that diabetes, as one cardiovascular risk factor, had similar prevalence in both genders. In concordance with the above results, another population-based study performed on a large number of adults living in Ontario, Canada proved that men had higher rates of CVD than women in those without the established coronary disease [277]. And diabetic men entered the high-risk category earlier than diabetic women (age 47.9 vs 54.3). In addition, they discovered that diabetic men were 1.22 times more likely to have acute myocardial infarction than diabetic women.

Sexual dimorphism in the liver has early been discovered and addressed, and it is regarded that the hepatic tissue exhibits significant sexual dimorphism due to the different metabolic needs for male and female reproduction [314]. The liver is a target organ for sex hormones as its cells express estrogen receptors and the androgen receptor in both men and women [315]. Ample evidence indicates that the prevalence

of NAFLD is higher in men than in women, regardless of age [316, 317]. Gender differences also exist for the major risk factors of NAFLD. In rodent NASH models, fed with a methionine choline-deficient diet, compared to female rats, male rats developed more severe steatosis ($p < 0.001$), had higher liver lipid content ($p < 0.05$) and higher serum alanine transaminase (ALT) levels ($p < 0.005$) [318]. As depicted in the general introduction, the liver is the main location of lipid metabolism. A cross-sectional analysis conducted in a cohort of 10761 Chinese adults indicated that in both NAFLD and non-NAFLD states, men had significantly higher levels of ALT, triglyceride, and triglyceride/HDL-cholesterol than women, with lower levels of total cholesterol, HDL-cholesterol and LDL-cholesterol [319]. They identified some independent predictors of NAFLD and demonstrated that among these factors, triglyceride was associated much stronger with NAFLD in men than in women. As described above, T2DM is usually concurrent with NAFLD [286]. In T2DM patients, the prevalence of NAFLD was also reported to be significantly higher in males than in females [320, 321]. However, studies about sex differences in NAFLD risk factors and liver fibrosis markers are still lacking in T2DM.

2.2 Hypothesis and Objectives

The number of patients affected by T2DM has increased considerably, and new treatments of this disease have emerged. However, the exact changes that take place in the gut microbiota, the fecal and the plasma metabolome have not been studied in detail. Based on previous findings, we hypothesize that specific gut bacteria as well as some fecal and plasma metabolites are involved in T2DM, and are related to GLP-1 release. Moreover, we hypothesize that the effect of T2DM on metabolism and bacteria differs between females and males, and between different age ranges. In this context, the objective of the work presented in this chapter is to identify changes in the metabolome and the gut microbiota related to T2DM, and how they are correlated with each other. To this end, we proposed the following specific objectives:

- To investigate the alterations of gut microbiota and fecal and plasma metabolite profiles in T2DM patients compared to healthy individuals through next-generation sequencing and NMR spectrum techniques
- To study the correlations between the most important clinical variables related to T2DM or its comorbidities.
- To identify some specific gut bacteria related to plasma GLP-1, as well as fecal and plasma metabolites
- To identify age-driven changes in the gut microbiota and fecal and plasma metabolite profiles by comparison of middle-aged and old-aged T2DM subjects.
- To identify sex-related differences by comparison of females and males with T2DM.

As a result, our studies will provide insight into changes in the gut microbiome at each taxonomic level in T2DM patients, as well as the alterations of the metabolome and biochemical and anthropometrical features related to T2DM associated with this microbial metabolism. These changes will be compared for middle and older aged patients, and females and males. We expect to provide detailed information on gut microbiota and metabolomic profiles and emphasize the importance of age and gender in the management of T2DM, especially for the application of personalized dietary interventions.

2.3 Materials and methods

2.3.1 Subjects

This proof-of-concept clinical trial comprised of forty-six T2DM patients and twenty-one healthy volunteers was conducted according to the tenets of the Helsinki Declaration. The Ethics Committee of the Vall d'Hebron University Hospital approved all procedures (protocol number PR(AG)01/2017). Written informed consent was obtained from all the participants before any planned action. T2DM subjects were

recruited at the Outpatient Department of the Endocrinology Service of Vall d'Hebron University Hospital. 250 clinical records of T2DM patients were reviewed where 72 met the inclusion criteria but only 46 agreed to participate in the clinical trial. Healthy volunteers were recruited at the Outpatient Department of the Endocrinology Service of two hospitals (Vall d'Hebron University Hospital and Dr. Josep Trueta University Hospital).

For all subjects participating in the study, the following exclusion criteria were applied: 1) age < 20 years, 2) taking medications related to insulin, 3) previous CVD events or other comorbidities related to T2DM, 4) alcohol consumers, 5) smokers who no stopped smoking at least ≤ 1 year before recruitment 6) missing blood or feces samples. Moreover, T2DM patients had to meet the following extra inclusion criteria: 1) fasting glucose ≥ 126 mg/dL, 2) HbA1c ≥ 6.5%, 3) no contraindication or claustrophobia for the PET/CT, 4) no concomitant pathologies related to a short life expectancy, such as cancers, hemafecia and irritable bowel syndrome, 5) diagnosis of T2DM at least 5 years before the screening, 6) patients with T2DM controlled at least one year before the inclusion in the study and 7) no other previous type of diabetes diagnosed.

In the current study, sixteen T2DM patients and twelve healthy individuals matched by age (average age: 58 and 56, respectively) and gender (female/male: 8/8 and 6/6, respectively) were included to determine the alterations caused by T2DM in patients and associations after comparing with healthy subjects in terms of gut microbiota and metabolites. Subsequently, in addition to the above T2DM patients, other twenty-eight T2DM patients (female/male: 13/15) who were more than 64 years old were pooled into an older T2DM group to assess the effect of age on T2DM. Further, twenty-two age-matched T2DM females and males (average age was both 66) were included to determine the effect of gender respectively on gut microbiota and metabolites alteration caused by T2DM.

2.3.2 Sample collection

Blood samples were collected from the patients and controls after a minimum of ten hours of fasting state, stored at 4℃ immediately, and processed (described below) within the first hour. Participants collected fecal samples after defecation, which were delivered to the hospital quickly in ice. Later fecal samples were aliquoted and stored at -80 ℃ immediately.

2.3.3 Anthropometric and biochemical measurement

Biochemical analyses were performed at the Biochemistry Core Facilities of the Vall d'Hebron University Hospital. For all participants, the plasma concentrations of glucose, insulin, glycated haemoglobin (HbA1c), high-density lipoprotein (HDL), low-density lipoprotein (LDL), triglycerides (TG), total cholesterol, hepatic enzymes AST, ALT, GGT and ALP, electrolytes sodium, potassium, phosphate, calcium and chloride, total protein, albumin, creatinine, and among other biochemical parameters were determined according to standard assays of the Biochemistry Core Facilities.

For further insights into T2DM, some specific indicators were just measured in patients, such as leptin, interleukin-6, total GLP-1, troponin I, total free fatty acids, adiponectin, and the enhanced liver fibrosis (ELF) test. The plasma concentrations of GLP-1, adiponectin, and troponin I were determined by GLP-1 EIA Kit (YK160, Yanaihara Institute Inc., Japan), Adiponectin ELISA Kit (KAPME09, DIAsource ImmunoAssays, Belgium) and Atellica IM High-Sensitivity Troponin I Assay (Siemens Healthineers, USA), respectively. All procedures were followed by the manufacturer's instructions of the kits. The ELF test was adopted to evaluate the liver function, including 3 assays: hyaluronic acid (HA), tissue inhibitor of metalloproteinase 1 (TIMP-1), and aminoterminal propeptide of type III procollagen (PIIINP). Their concentrations were measured in the ADVIA Centaur® automated immunoassay analyzer (Siemens Healthcare Inc., USA) by commercial kits bought from Siemens Healthineers company. ELF value was calculated by the algorithm

[322]: 2.278 + 0.851 ln(HA) + 0.751 ln(PIIINP) + 0.394 ln(TIMP1).

Anthropometric measurement for all participants was done in the Endocrinology Department at Vall d'Hebron University Hospital, including body mass, height, waist circumference, and hip circumference. All indexes used in the studies were listed in **Table 2.1**.

Table 2.1 Indexes used in the study.

Indexes	Cut-off values	Cut-off values referred to	Formula referred to
BMI	Obesity (≥30) Normal weight (18.5~24.9)	[323]	weight (kg)/[height $(m)^2$]
HOMA-IR	Insulin resistant (>3.8) Normal (≦1.4)	[324, 325]	[138]
QUICKI	Normal (>0.333)	[326]	[139]
TyG index	Insulin resistant (>8.8)	[327]	[327]
AIP	High CVD risk (>0.24)	[328]	[329]
NAFLD liver fat score	NAFLD (>-0.64)	[330]	[330]
Liver fat content	—	—	[330]
Hepatic steatosis index	NAFLD (>36) Normal (<30)	[331]	[331]
Fatty liver index	Fatty liver (≥60) Normal (<30)	[332]	[332]
FIB-4	Liver fibrosis (>3.25) Normal (<1.45)	[333]	[333]
NAFLD fibrosis score	Advanced fibrosis (>0.676) Normal (<-1.455)	[334]	[334]

BMI, body mass index; HOMA-IR, homeostasis model assessment of insulin resistance; QUICKI, quantitative insulin sensitivity check index; TyG index, triglyceride-glucose index; FIB-4, liver fibrosis index 4; AIP, atherogenic index of plasma.

2.3.4 Transient elastography

Liver stiffness measurement (LSM) was performed for all T2DM patients using transient elastography (FibroScan 502 Touch, Echosens, Paris, France), which is a noninvasive technique to estimate the severity of fibrosis. As described previously by

our group, measurements were performed by standard procedures when patients were under fasting conditions [335]. At least ten successful acquisitions, expressed in kilopascal (kPa), were performed on each patient, and an interquartile to median ratio should be lower than 30% [335]. LSM values ≥ 6 kPa were considered abnormal and suggestive of mild liver fibrosis/disease [335].

2.3.5 Fecal DNA extraction

The procedures for fecal DNA extraction were adapted from Yu *et al* [336]. Briefly, frozen fecal samples were scraped and weighed 300~500 mg. Immediately, 1 mL lysis buffer (500 mM NaCl, 50 mM Tris-HCl, pH 8.0, 50 mM EDTA, and 4% sodium dodecyl sulfate (SDS)) was added to a 2 mL Eppendorf tube containing the feces. Samples were homogenized by resuspension using a micropipette and vortexed, then heated at 88 ℃ for 15 min, with gentle shaking every 5 min. The supernatant was harvested by centrifugation at 16,000 g and 4 ℃ for 5 min. Then, the precipitate was resuspended in 300 μL of fresh lysis buffer and then the above incubation and centrifugation steps were repeated. Both supernatants were pooled together and steps 6 to 10 of the extraction protocol of Yu *et al* were applied [336]. At that moment, fecal DNA was dissolved in Tris-EDTA buffer and was purified by QIAamp® Fast DNA Stool Mini Kit (Qiagen, Germany). Briefly, the above fecal DNA solution (about 200 μL) was added to 700 μL InhibitEX Buffer and vortexed for 1 min. Then, the mixed solution was incubated on a heating block at 70 ℃ for 5 min, vortexed for 15 s, and centrifuged at 10,000 g for 2 min. In order to harvest more fecal DNA, the resulting supernatant was divided into four 1.5 mL Eppendorf tubes in a volume of 200 μL. Each tube was added 1.5 μL DNase-free RNase (10 mg/mL) and incubated at 37 ℃ for 15 min. Subsequently, 7.5 μL of proteinase K and 200 μL Buffer AL were added and then the protocol “Isolation of DNA from Stool for Pathogen Detection” of the Qiagen kit was followed from step 7 to the end. Before adding the Buffer AW1 from the kit, the solutions from the same feces should go through the QIAamp spin column

successively.

The extracted genomic fecal DNA was assessed to determine its quality and concentration before applying metagenomic sequencing. First, the purity of fecal DNA was determined by Nanodrop 2000 spectrophotometer (Thermo Fisher Scientific, USA): a 260/280 ratio of around 1.80 was considered pure. Second, DNA concentration was measured by Nanodrop and fluorometer with the Quant-iT PicoGreen dsDNA assay (Invitrogen, USA). Third, the integrity of DNA samples was assessed by agarose gel electrophoresis, by detecting a clear band around the size of 17 kb [337]. Last, the presence of PCR inhibitors was evaluated by amplifying DNA samples with or without dilution by 16S universal primers 27F/1492R [338]. Only if fecal DNA samples fulfilled all these tests, they were used for further analysis.

2.3.6 Illumina MiSeq sequencing

After assessing the quality and concentration, fecal DNA samples were sequenced in ATLAS Biolabs GmbH (Berlin, Germany) using the Illumina MiSeq platform. The protocol of sequencing preparation is described in dx.doi.org/10.17504/protocols.io.nuudeww. Barcoded primers 515F–806R [339] targeting the V4 region of the 16S rRNA gene were used for PCR amplification. Each sample was amplified in triplicate and the amplified products were pooled together. The expected size of amplicons is around 300–350 bp. The amplicons of all samples were verified by agarose gel and quantified by Quant-iT PicoGreen dsDNA assay (Invitrogen, USA). The 16S library was set up by combining an equal amount of amplicon from each sample (240 ng) and cleaned by using UltraClean PCR Clean-Up Kit (Mo Bio, USA). Then, one aliquot of the library was sequenced on the MiSeq platform with 5-10% PhiX.

Raw sequence reads were processed according to the BaseSpace 16S Metagenomics App (Illumina) and QIIME 2 pipelines [340]. Sequences were clustered into OTUs at a similarity threshold ratio of 97% and were performed for taxonomy classification by q2-feature-classifier in QIIME 2 [341]. The raw sequence data for the 16S rRNA gene

can be accessed from NCBI Sequence Read Archive (SRA) database with accession ID PRJNA810955 after the released date.

2.3.7 Plasma and fecal metabolomics

2.3.7.1 Sample preparation

Blood samples obtained from the Vall d'Hebron University Hospital were processed by the following protocol: 2 mL of Histopaque® 1119 and 1077 (Sigma-Aldrich, UK) were successively added to a 15-mL clean centrifuge tube. Then, blood samples were added after gentle shaking and centrifuged at 300 g and 4 ℃ for 30 min. The upper light-yellow layer (plasma) was transferred into a 2 mL clean Eppendorf tube and stored at -80 ℃ until metabolomics analysis, while other layers were separated for other uses. A few blood samples from healthy controls were processed as described previously [206]. Briefly, blood samples were centrifuged at 300g for 20 min in a vacutainer tube without any component. The obtained plasma was transferred to an Eppendorf tube and stored at -80 ℃ until their metabolomics analysis.

For NMR sample preparation, plasma samples were thawed on ice. 300 μL plasma was added to 300 μL of 10% D_2O buffer (5 mM TSP, 140 mM phosphate buffer, 0.04% NaN_3, pH 7.4). Then, 550 μL of the mixed solution was transferred into a 5-mm NMR tube for analysis.

The procedures of fecal metabolite extraction were performed following previous studies in our group [206]. Briefly, frozen fecal samples were thawed on ice, and 100 mg feces were balanced and transferred into a 1.5 mL Eppendorf tube and homogenized with 1 mL 0.1M phosphate D_2O buffer (with 5 mM TSP, pH 7.4). Samples went through 3 freeze and thaw cycles by alternate immersion into liquid nitrogen and tap water and were subsequently centrifuged at 15,000g for 15 min after a 15-second vortex. The supernatant was collected and stored at -80 ℃ until analysis.

For NMR sample preparation, the fecal supernatant was thawed on the ice, and 600 μL was transferred to the NMR tube directly.

2.3.7.2 NMR spectra acquisition

All NMR spectra were acquired at 27 ℃ on a Bruker 600 MHz spectrometer (Rheinstetten, Germany) with a TCI cryoprobe and processed under the Topspin 3.2 software (Bruker). D_2O was set as the solvent of the field frequency, a 4 seconds relaxation delay (RD) was incorporated between free induction decays (FIDs) and water suppression by presaturation was applied. 64 K data points were digitalized over a spectral width of 30 ppm for an optimal baseline correction. For the quantification of lipoproteins, additional diffusion-edited experiments were carried out to reduce the interference of the small metabolite signals. FID values were multiplied by an exponential function with a 0.5 Hz line broadening factor. The reference of plasma and feces was α-glucose anomeric doublet (δ 5.23) and TSP signal (0), respectively. ^{1}H-NMR signals were assigned to their corresponding metabolites with the assistance of 2-dimensional NMR Experiments and spectral databases such as the Human Metabolome Database (HMBD) [219] and Biological Magnetic Resonance Data Bank (BMRB) [220].

For ambiguous cases, the assignment was confirmed by adding a reference compound to the sample and repeating the spectra, to verify that signals match. In order to reduce the difference in concentration and experimental error, all spectra were normalized to total intensity. Optimal integration regions were defined for each compound and integration was conducted with Global Spectral Deconvolution in MestreNova 8.1 (Mestrelab Research, Spain). Impurity signals from Ficoll substances (Histopaque$^{@}$ 1119 and 1077) were excluded from the integration.

2.3.7.3 Metabolomics data analysis

For metabolomics data analysis, principal component analysis (PCA), partial least

square regression (PLS), and orthogonal-orthogonal projection to latent structure discriminant analysis (OPLS-DA) or partial least squares discriminant analysis (PLS-DA) were performed using SIMCA-P 14.1 (Umetrics, Sweden). When the initial OPLS-DA models were not optimal, they were improved, if possible, by VIP-based variable selection. PLS, OPLS-DA, and PLS-DA models were validated by the permutation plot (100 fold) and the reliability of these models was assessed by ANalysis Of VAriance testing of Cross-Validated predictive residuals (CV-ANOVA) in SIMCA-P. During the OPLS-DA or PLS-DA analysis, variables with VIP values > 1.0 were considered to do further relevant analysis.

The identified significant metabolites were submitted for statistical analysis (see below).

2.3.8 Hyperinsulinemic-euglycemic clamp

Hyperinsulinemic-euglycemic clamp (HEC) technique is a gold standard method to measure whole-body insulin sensitivity (IS). The applied procedure followed previous protocols [136, 342] with a minor modification. Briefly, after overnight fasting, patients lay on a stretcher, and two catheters were inserted in the antecubital vein of each arm. The left catheter was used to obtain arterialized venous blood samples and the right one was used to administer constant infusions of insulin and glucose. The right arm was also the place where Fluorine-18-deoxyglucose (FDG) was administered. The body surface area (BSA) of each patient was calculated by the formula [343]: BSA (m^2) = (weight (kg) × height (cm)/3600)$^{1/2}$. Initially, 1 UI/mL insulin solution was infused at a speed of 80 mU/m^2/min, and after 5 min the insulin infusion rate was reduced to 60 mU/m^2/min, and at the same time the injection of 10 % glucose solution was started at an initial rate of 2 mg/kg/min. The blood glucose concentration was determined every 5 min by a glucometer (Accu-check Aviva, Roche, Sant Cugat del Valles, Barcelona, Spain) and the glucose infusion rate was adjusted to maintain plasma glucose concentration at 88.3–99.1 mg/dL. After the second 5 min, the insulin infusion rate was reduced to 40 mU/m^2/min and then

maintained constant during the rest of the HEC procedure. The whole HEC procedure lasted 120 min and insulin sensitivity was assessed as the mean glucose infusion rate during the final 40 min. In this stationary phase, the glucose infusion rate equals the glucose uptake rate of the body, which is a measure of whole-body insulin sensitivity.

2.3.9 Statistical analysis

Statistical analysis was mainly performed in GraphPad Prism 8.0.1 (San Diego, USA). Normal distribution was analyzed for all quantitative data by D'Agostino & Pearson test or Shapiro-Wilk test. An unpaired t-test was used for comparing variables from two groups which both passed the normality test and data were expressed as mean ± standard error of the mean (SEM). Mann-Whitney unpaired test was used to compare the variables from two groups that didn't show the normal distribution and descriptive data were shown as median (interquartile range). Differences with $p<0.05$ were considered significant differences between groups. Spearman's correlation analysis was conducted between different variables and a $p<0.05$ was associated with a significant correlation between variables.

2.4 Results

2.4.1 Effect of T2DM related to gut microbiota on the middle-aged population

2.4.1.1 Anthropometric and biochemical characteristics

Anthropometric and biochemical characteristics of healthy individuals and age-matched T2DM patients are summarized in **Table 2.2**. As expected, patients with T2DM had higher plasma concentrations of glucose and insulin ($p<0.01$) as well as higher HbA1c levels and HOMA-IR value ($p<0.001$), and TyG index ($p<0.01$). Additionally, the QUICKI value was calculated to quantify the systemic insulin sensitivity of both cohorts, being drastically lower ($p<0.001$) in diabetic patients as expected.

Regarding fingerprints related to CVD risk, the plasma concentration of triglyceride, the triglyceride/HDL ratio, and the atherogenic index of plasma (AIP) were increased significantly ($p<0.05$) in T2DM adults while the plasma concentration of HDL was reduced ($p<0.05$). It is worth mentioning that waist circumference, waist/hip ratio, and BMI were prominently higher ($p<0.001$) in the T2DM group because most patients were obese (BMI>30 kg/m^2). Interestingly, hip circumference has no difference between the two groups.

Concerning liver function and pathology, the AST/ALT ratio was reduced significantly ($p<0.05$) in T2DM. In addition, this group of patients had higher NAFLD liver fat score, liver fat content, fatty liver index, and hepatic steatosis index ($p<0.001$), suggesting liver steatosis and therefore NAFLD. In addition, the NAFLD fibrosis score was increased in the T2DM group ($p<0.01$). The concentration of serum albumin and sodium was decreased significantly ($p<0.01$) in the T2DM group, but they were still in the normal range.

Table 2.2 Anthropometric and biochemical parameters of T2DM patients and healthy individuals.

	Control	T2DM
Number	12	16
Male/Female	6/6	8/8
Age	55.67 ± 1.10	58.44 ± 1.10
Waist circumference (cm)	87.56 ± 3.71	105.40 ± 2.05 ***
Hip circumference (cm)	102.0 (96.5-105.5)	106.0 (99.3-115.4)
Waist/hip ratio	0.86 (0.79-0.94)	0.97 (0.95-1.03) ***
BMI (kg/m^2)	24.62 ± 0.90	30.63 ± 0.96 ***
Glucose (mg/dL)	89.33 ± 2.37	121.10 ± 8.13 **
HbA1c (%)	5.5 (5.4-5.8)	7.3 (6.4-7.6) ***
Insulin (mU/L)	5.31 (1.75-7.27)	14.31 (9.39-18.89) ***
HOMA-IR	1.14 (0.39-1.45)	3.96 (2.44-5.57) ***
QUICKI	0.418 ± 0.027	0.318 ± 0.007 ***
Albumin (g/dL)	4.51 ±0.06	4.26 ±0.06 **
Sodium (mmol/L)	141.2 (140.3-142.8)	139.4 (138.2-140.5) **
Potassium (mmol/L)	4.000 (3.900-4.273)	4.035 (3.735-4.323)
HDL (mg/dL)	60.83 ± 5.07	46.50 ± 2.57 *
Triglyceride (mg/dL)	69.0 (52.5-105.8)	101.5 (82.3-144.3) *
Triglyceride/HDL ratio	1.20 (0.81-2.15)	2.22 (1.62-2.85) *
AIP	0.11 ± 0.09	0.38 ± 0.06 *
TyG index	8.12 ± 0.15	8.75 ± 0.13 **
AST (IU/L)	27.00 (25.50-34.50)	22.00 (18.25-30.75)
ALT (IU/L)	19.00 (17.25-25.25)	18.00 (16.25-38.50)
GGT (IU/L)	23.5 (12.5-33.0)	20.5 (16.0-28.5)
AST/ALT ratio	1.23 (1.05-1.58)	1.01 (0.80-1.20) *
NAFLD liver fat score	–1.98 (–2.26 ~ –1.67)	1.07 (0.83-1.98) ***
Liver fat content (%)	2.17 (1.91-2.42)	8.69 (7.09-11.37) ***
Fatty liver index	25.01 (6.45-34.87)	70.17 (51.28-75.24) ***
Hepatic steatosis index	32.11 ± 1.59	41.98 ± 1.05 ***
FIB-4	1.09 (1.02-1.80)	1.03 (0.83-1.29)
NAFLD fibrosis score	–2.44 ± 0.44	–0.87 ± 0.26 **

Abbreviations: BMI, body mass index; HbA1c, hemoglobin A1c; HOMA-IR, homeostasis model assessment of insulin resistance; QUICKI, quantitative insulin sensitivity check index; HDL, high-density lipoprotein cholesterol; TyG index, triglyceride-glucose index; FIB-4, liver fibrosis index 4; AIP, atherogenic index of plasma; GGT, gamma-glutamyl transferase; AST, aspartate aminotransferase; ALT, alanine aminotransferase; NAFLD; non-alcoholic fatty liver disease. * $p<0.05$, ** $p<0.01$, *** $p<0.001$

2.4.1.2 Gut microbiota analyses between T2DM patients and controls

2.4.1.2.1 Composition and diversity analysis of gut microbiota

After the 16S rRNA gene amplicon sequencing of samples, no significant difference in the total sequence and quality-filtered reads between groups was found (**Supplementary Figure 2.1** in Annex). The rarefaction curve showed that the sequencing depth was enough for the analysis. Also, the number of observed features, Shannon's diversity index, and Faith's phylogenetic diversity index, which reflect the species richness of a community, didn't show differences between the control and T2DM group, nor Pielou's evenness index, an indicator for species evenness of a community.

Although we did not find changes in microbial diversity in T2DM, we could identify alterations in gut microbiota composition, as can be seen in **Figure 2.1**. Thus, the relative abundance of Firmicutes decreased statistically while Bacteroidetes and Proteobacteria increased significantly in the T2DM group ($p<0.05$). For dominant families (**Figure 2.1B**), the proportion of Ruminococcaceae was dramatically lower while Bacteroidaceae, Enterobacteriaceae, and Veillonellaceae were significantly higher in T2DM ($p<0.05$).

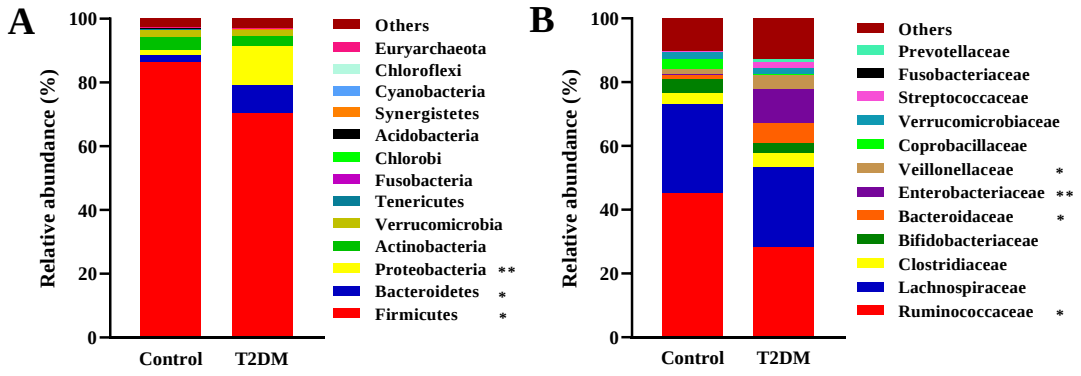

Figure 2.1 Alterations of gut microbiota in T2DM. A) and B) showed the relative abundance of gut bacteria at the phylum and family levels respectively. * and ** indicated that between the control group and T2DM group $p<0.05$ and $p<0.01$ respectively.

In humans, Firmicutes and Bacteroidetes are the two most dominant phyla in the gastrointestinal (GI) tract, and their relative abundance account for more than 90% [344]. Changes in the Firmicutes/Bacteroidetes ratio are regarded as gut dysbiosis and can lead to various pathologies such as obesity and inflammatory bowel disease [345]. As displayed in **Figure 2.2**, the Firmicutes/Bacteroidetes ratio decreased remarkably ($p<0.05$) in the T2DM group, indicating that gut dysbiosis occurred in T2DM patients.

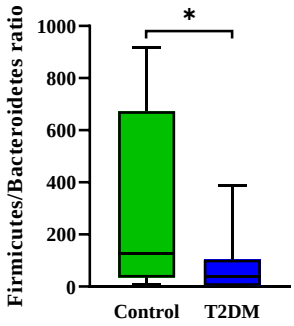

Figure 2.2 The ratio of relative abundance of Firmicutes and Bacteroidetes. It was significantly lower in the T2DM group than in the control group. * indicated $p<0.05$.

2.4.1.2.2 Alteration of significant gut bacteria between T2DM and controls

Faced with a large number of data, multivariate orthogonal projection to latent structure discriminant analysis (OPLS-DA) or partial least squares discriminant analysis (PLS-DA) models were built to grab the most relevant changes in gut bacteria between groups. As depicted in **Figure 2.3A and B**, score plots of principal component analysis (PCA) and OPLS-DA showed a separation for the control and T2DM group. Based on OPLS-DA models, VIP (variable importance for the projection) values were used to obtain the main variables altered between groups. VIP values >1 were considered as relevant alterations associated with T2DM and therefore submitted to univariate analyses.

From phylum to genus levels (**Figure 2.3C**), Firmicutes, Clostridia, Clostridiales, Ruminococcaceae, and *Faecalibacterium* decreased significantly ($p<0.05$) in T2DM while Proteobacteria, Gammaproteobacteria, Enterobacteriales, Enterobacteriaceae

and *Escherichia* increased (p<0.01). At the species level, only *Faecalibacterium prausnitzii* was found to decrease in T2DM (p<0.01).

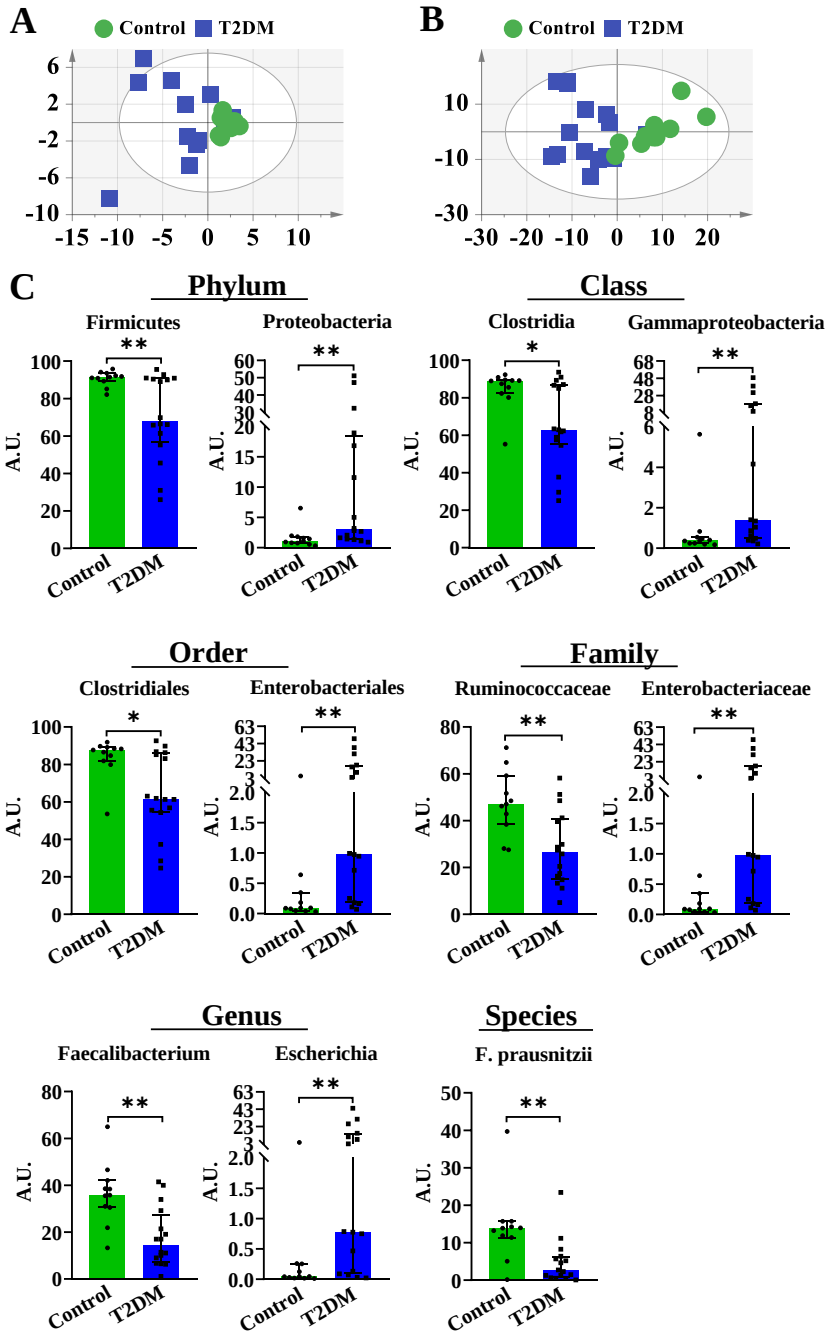

Figure 2.3 Significant gut bacteria that change between T2DM and controls. A) showed the score plot of PCA and the parameters of the model were: Pareto scaling, R2X(cum)= 0.935, Q2(cum)= 0.513. B) displayed the score plot of the variable selected OPLS-DA and the parameters of the model were: Pareto scaling, R2Y(cum)= 0.559, Q2(cum)= 0.338. Permutation test: R2= (0.0, 0.217), Q2= (0.0, -0.314), p from CV-Anova = 0.050. C) showed the relative abundance of the most relevant gut bacteria with VIP value >1 and p-value from the Mann-Whitney test <0.05. F. prausnitzii, *Faecalibacterium prausnitzii*. Data were shown as the median and interquartile range in all bar plots. * and ** indicated p<0.05 and p<0.01 respectively. A.U., arbitrary units.

2.4.1.2.3 Association of gut microbiota with biochemical and anthropometrical variables

To evaluate the association of T2DM-altered biochemical and anthropometric parameters with the gut microbiota, partial least square (PLS) regression analyses were carried out and depicted in **Figure 2.4**. Only biochemical variables HbA1c, insulin, and AIP had a good relationship with altered gut bacteria.

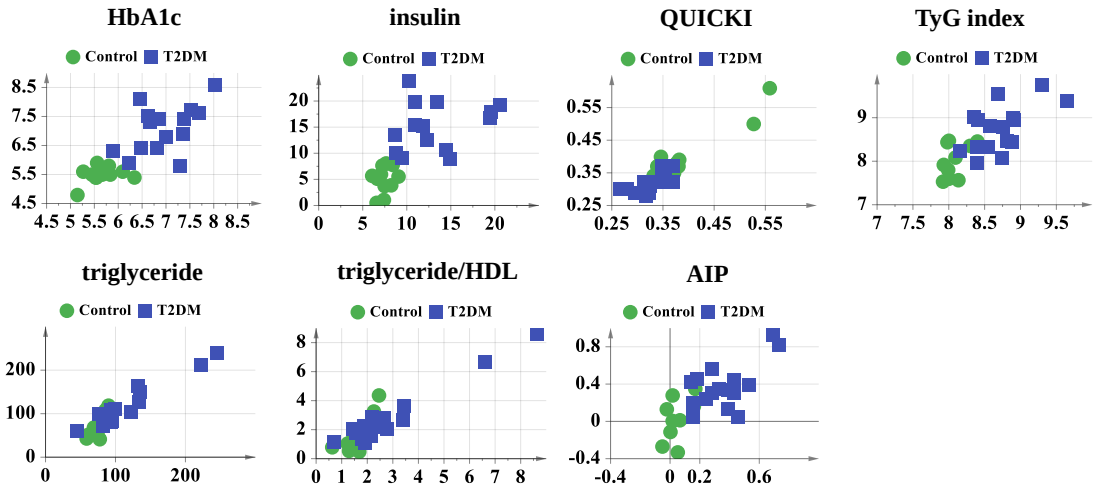

Figure 2.4 PLS analyses of altered gut bacteria versus significant biochemical and anthropometric parameters between the control and T2DM group. PLS plots were only shown if the p-value of the CV-Anova was <0.05. All models were obtained after univariate (UV) scaling. The parameters of the models were: HbA1c, R2Y(cum)= 0.648, Q2(cum)= 0.438. Permutation test: R2=(0.0, 0.533), Q2=(0.0, -0.072), p from CV-Anova = 0.017. Insulin, R2Y(cum)= 0.441, Q2(cum)= 0.330. Permutation test: R2=(0.0, 0.326), Q2=(0.0, -0.108), p from CV-Anova = 0.012. QUICKI, R2Y(cum)= 0.849, Q2(cum)= 0.427. Permutation test: R2=(0.0, 0.594), Q2=(0.0, -0.171), p from CV-Anova = 0.046. TyG index, R2Y(cum)= 0.555, Q2(cum)= 0.241. Permutation test: R2=(0.0, 0.270), Q2=(0.0, -0.102), p from CV-Anova = 0.042. Triglyceride, R2Y(cum)= 0.885, Q2(cum)= 0.530. Permutation test: R2=(0.0, 0.610), Q2=(0.0, -0.190), p from CV-Anova = 0.044. Triglyceride/HDL, R2Y(cum)= 0.873, Q2(cum)= 0.533. Permutation test: R2=(0.0, 0.616), Q2=(0.0, -0.159), p from CV-Anova = 0.0497. AIP, R2Y(cum)= 0.550, Q2(cum)= 0.247. Permutation test: R2=(0.0, 0.273), Q2=(0.0, -0.106), p from CV-Anova = 0.044.

2.4.1.3 Fecal metabolomics analyses between T2DM patients and controls

2.4.1.3.1 Identification of significant fecal metabolites associated with T2DM

As depicted in **Figure 2.5A** and **B**, PCA and OPLS-DA analysis evidenced a clear separation between the control and the T2DM group. Fecal metabolites with VIP values >1 based on the OPLS-DA model were submitted to univariate analysis to confirm their significance. As shown in **Figure 2.5C**, isovalerate and 2-hydroxyvalerate were reduced ($p<0.05$) in the T2DM group, while malonate was increased ($p<0.001$).

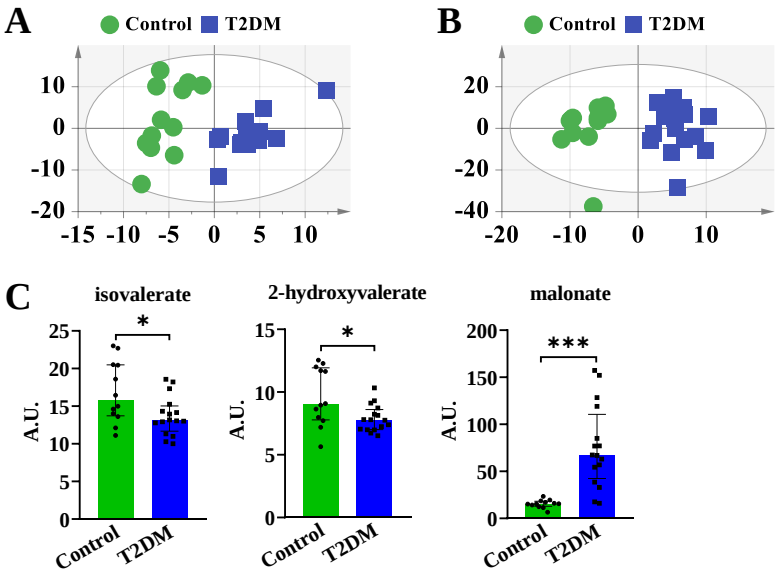

Figure 2.5 Relevant fecal metabolites associated with T2DM. A) showed the score plot of the PCA model of fecal metabolic profiles, and the parameters of the model were: UV scaling, R2X(cum)= 0.671, Q2(cum)= 0.396. B) displayed the score plot of the OPLS-DA model of fecal metabolic profiles, and the parameters of the model were: Pareto scaling, R2Y(cum)= 0.892, Q2(cum)= 0.649. Permutation test: R2= (0.0, 0.502), Q2= (0.0, -0.823), p from CV-Anova = 5.6×10^{-4}. C) showed the normalized concentration of the most relevant fecal metabolites with VIP value >1 and p-value from the Mann-Whitney test <0.05. Data were shown as the median and interquartile range in all bar plots. * and *** indicated $p<0.05$ and $p<0.001$ respectively. A.U., arbitrary units.

2.4.1.3.2 Association of fecal metabolic profile with biochemical and anthropometrical variables

PLS regression analyses of fecal metabolic profiles versus significant biochemical and anthropometric parameters including risk factor indexes were carried out, as depicted in **Figure 2.6**. A high number of PLS correlations were obtained. In detail, all significant anthropometric parameters (waist circumference, waist/hip ratio, and BMI) were strongly correlated with fecal metabolic profiles. Furthermore, also important biochemical parameters such as plasma glucose, insulin, HOMA-IR, QUICKI, and HbA1c, showed robust correlations with fecal metabolomic profiles. For CVD-related markers (HDL, triglyceride, triglyceride/HDL ratio, AIP, and TyG index), only moderate models could be obtained. Regarding liver pathological risk factor indexes, PLS regression models were only obtained for the hepatic steatosis index, fatty liver index and NAFLD liver fat score, but not for the NAFLD fibrosis score.

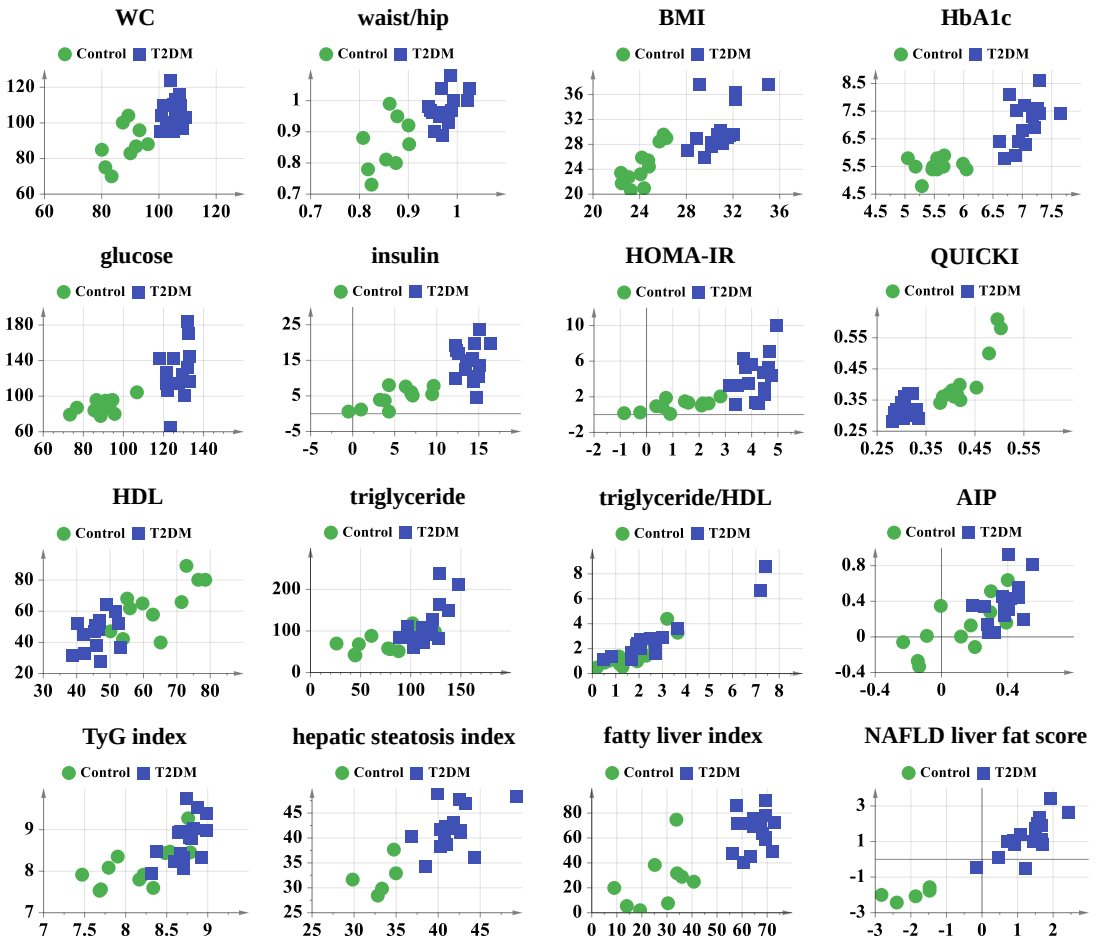

Figure 2.6 PLS analyses of fecal metabolic profiles versus significant biochemical and anthropometric parameters related to T2DM. PLS plots were only shown if the p-value of the CV-Anova was <0.05. Univariate scaling was applied to all data. The parameters of the models were: Waist circumference (WC), R2Y(cum)= 0.525, Q2(cum)= 0.324. Permutation test: R2= (0.0, 0.369), Q2= (0.0, -0.121), p from CV-Anova = 0.013. Waist/hip ratio, R2Y(cum)= 0.556, Q2(cum)= 0.314. Permutation test: R2= (0.0, 0.354), Q2= (0.0, -0.129), p from CV-Anova = 0.019. BMI, R2Y(cum)= 0.625, Q2(cum)= 0.399. Permutation test: R2= (0.0, 0.312), Q2= (0.0, -0.152), p from CV-Anova = 0.0017. HbA1c, R2Y(cum)= 0.658, Q2(cum)= 0.512. Permutation test: R2= (0.0, 0.285), Q2= (0.0, -0.164), p from CV-Anova = 1.8×10^{-4}. Glucose, R2Y(cum)= 0.487, Q2(cum)= 0.277. Permutation test: R2= (0.0, 0.361), Q2= (0.0, -0.125), p from CV-Anova = 0.024. Insulin, R2Y(cum)= 0.581, Q2(cum)= 0.326. Permutation test: R2= (0.0, 0.337), Q2= (0.0, -0.118), p from CV-Anova = 0.0088. HOMA-IR, R2Y(cum)= 0.497, Q2(cum)= 0.250. Permutation test: R2= (0.0, 0.321), Q2= (0.0, -0.128), p from CV-Anova = 0.027. QUICKI, R2Y(cum)= 0.705, Q2(cum)= 0.333. Permutation test: R2= (0.0, 0.592), Q2= (0.0, -0.183), p from CV-Anova = 0.026. HDL, R2Y(cum)= 0.541, Q2(cum)= 0.284. Permutation test: R2= (0.0, 0.345), Q2= (0.0, -0.118), p from CV-Anova = 0.018. Triglyceride, R2Y(cum)= 0.441, Q2(cum)= 0.243. Permutation test: R2= (0.0, 0.360), Q2= (0.0, -0.097), p from CV-Anova = 0.035. Triglyceride/HDL, R2Y(cum)= 0.888, Q2(cum)= 0.557. Permutation test: R2= (0.0, 0.752), Q2= (0.0, -0.196), p from CV-Anova = 0.031. AIP, R2Y(cum)= 0.507, Q2(cum)= 0.323. Permutation test: R2= (0.0, 0.312), Q2= (0.0, -0.131), p from CV-Anova = 0.0076. TyG index, R2Y(cum)= 0.507, Q2(cum)= 0.345. Permutation test: R2= (0.0, 0.328), Q2= (0.0, -0.121), p from CV-Anova = 0.005. Hepatic

steatosis index, R2Y(cum)= 0.591, Q2(cum)= 0.404. Permutation test: R2= (0.0, 0.388), Q2= (0.0, -0.138), p from CV-Anova = 0.0094. Fatty liver index, R2Y(cum)= 0.599, Q2(cum)= 0.425. Permutation test: R2= (0.0, 0.351), Q2= (0.0, -0.136), p from CV-Anova = 0.0023. NAFLD liver fat score, R2Y(cum)= 0.847, Q2(cum)= 0.476. Permutation test: R2= (0.0, 0.700), Q2= (0.0, -0.120), p from CV-Anova = 0.038. AIP, atherogenic index of plasma. BMI, body mass index; HOMA-IR, homeostasis model assessment of insulin resistance; QUICKI, quantitative insulin sensitivity check index; TyG index, triglyceride-glucose index.

2.4.1.4 Plasma metabolomics analyses of T2DM patients and controls

2.4.1.4.1 Identification of significant plasma metabolites

Similarly, multivariate PCA and OPLS-DA were applied to reduce the dimensionalities of the metabolomics data. As evidenced in **Figure 2.7A** and **B**, both PCA and OPLS-DA analysis clearly showed a significant difference between T2DM and healthy controls. Altered plasma metabolites are shown in **Figure 2.7C**, including those with VIP value >1 in the OPLS-DA model, and $p<0.05$ in the univariate analyses. The concentrations of LDL(CH_3), LDL(aliphatic chain), VLDL(CH_3), phosphorylcholine, and N-acetylated proteins were reduced in T2DM patients while acetoacetate and lipids:CH_2CO were increased ($p<0.001$).

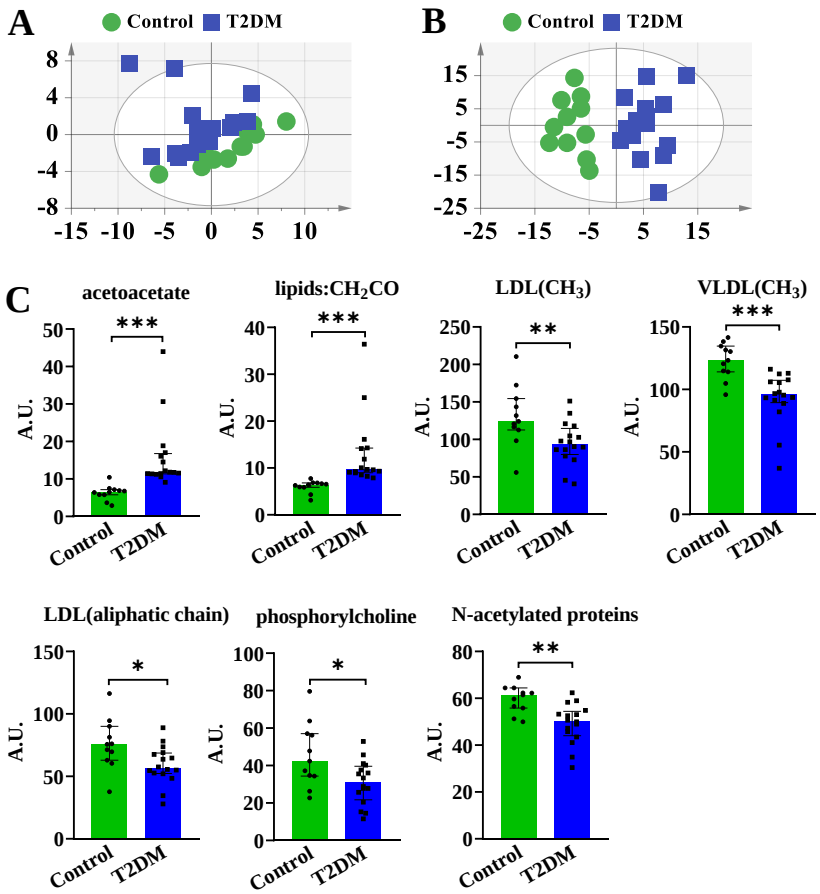

Figure 2.7 Relevant plasma metabolites associated with T2DM. A) depicted the score plot of the PCA model of plasma metabolic profiles, with the following model parameters: UV scaling, R2X(cum)= 0.853, Q2(cum)= 0.596. B) depicted the score plot of the OPLS-DA model of plasma metabolic profiles, with the model parameters: Pareto scaling, R2Y(cum)= 0.848, Q2(cum)= 0.603. Permutation test: R2= (0.0, 0.439), Q2= (0.0, -0.991), p from CV-Anova = 0.055. C) depicted bar plots of the normalized concentration values of the most relevant plasma metabolites with VIP value >1 and p-value from the Mann-Whitney test <0.05. Data were shown as the median and interquartile range in all bar plots. *, ** and *** indicated p<0.05, p<0.01 and p<0.001 respectively. A.U., arbitrary units.

It has been reported that in plasma, high levels of glutamate and low levels of glutamine are associated with an increased risk of T2DM. The imbalance of plasma glutamine and glutamate can predict the occurrence of T2DM [346]. This was confirmed in our study because the concentration of glutamine and glutamate were reduced and increased respectively in the T2DM group. Thus, the plasma glutamine/glutamate ratio was reduced dramatically (p<0.001) in the T2DM group, as shown in **Figure 2.8**.

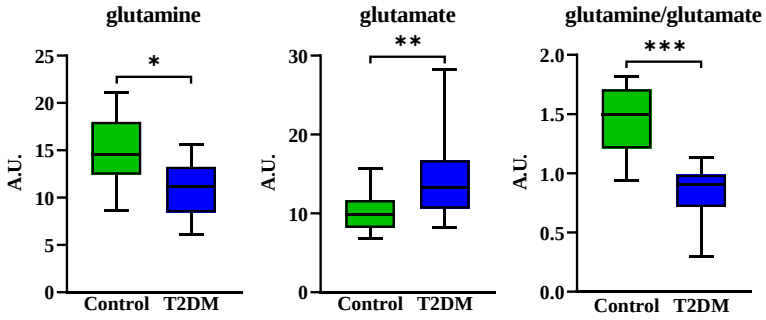

Figure 2.8 Changes of plasma metabolites glutamine and glutamate in T2DM. Compared with the control group, the concentration of glutamine reduced while the concentration of glutamate increased significantly. Thus, the ratio of glutamine/glutamate decreased drastically in the T2DM group. *, ** and *** indicated $p<0.05$, $p<0.01$ and $p<0.001$ respectively.

2.4.1.4.2 Association of plasma metabolic profile with biochemical and anthropometrical variables

Similar to the fecal metabolic profiles, PLS regression analyses of plasma metabolic profiles versus significant biochemical and anthropometric parameters were performed, as displayed in **Figure 2.9**. Regarding the anthropometric variables, robust PLS models could only be obtained for waist circumference and BMI (with p-value from CV-Anova <0.05). Moreover, PLS models could be obtained for the biochemical parameters HbA1c, glucose, insulin, HOMA-IR, and QUICKI. In addition, regression models were also obtained for CVD risk factor markers, including HDL, triglyceride, triglyceride/HDL ratio, AIP, and TyG index. For significant hepatic risk factor markers, only two robust models were obtained using the fatty liver index and NAFLD fibrosis score with plasma metabolic profiles.

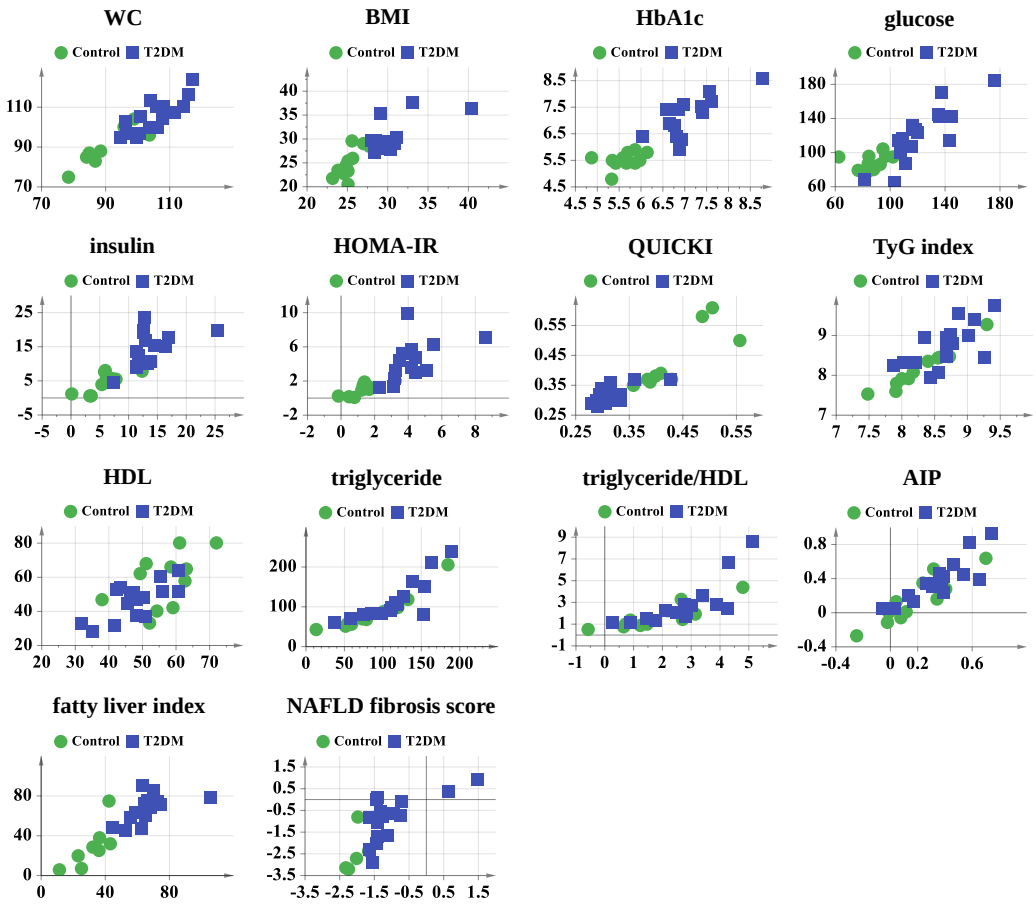

Figure 2.9 PLS analyses of plasma metabolic profiles versus significant biochemical and anthropometric parameters related to T2DM. PLS plots were only shown if the p-value from the CV-Anova was <0.05. UV scaling was applied in all models. The parameters of the models were: Waist circumference (WC), R2Y(cum)= 0.835, Q2(cum)= 0.592. Permutation test: R2=(0.0, 0.335), Q2=(0.0, -0.321), p from CV-Anova = 0.047. BMI, R2Y(cum)= 0.671, Q2(cum)= 0.452. Permutation test: R2=(0.0, 0.266), Q2=(0.0, -0.229), p from CV-Anova = 0.0077. HbA1c, R2Y(cum)= 0.805, Q2(cum)= 0.566. Permutation test: R2=(0.0, 0.379), Q2=(0.0, -0.292), p from CV-Anova = 0.014. Glucose, R2Y(cum)= 0.724, Q2(cum)= 0.479. Permutation test: R2=(0.0, 0.365), Q2=(0.0, -0.244), p from CV-Anova = 0.017. Insulin, R2Y(cum)= 0.651, Q2(cum)= 0.500. Permutation test: R2=(0.0, 0.252), Q2=(0.0, -0.247), p from CV-Anova = 0.0024. HOMA-IR, R2Y(cum)= 0.601, Q2(cum)= 0.446. Permutation test: R2=(0.0, 0.285), Q2=(0.0, -0.196), p from CV-Anova = 0.0059. QUICKI, R2Y(cum)= 0.768, Q2(cum)= 0.458. Permutation test: R2=(0.0, 0.250), Q2=(0.0, -0.231), p from CV-Anova = 0.009. TyG index, R2Y(cum)= 0.682, Q2(cum)= 0.623. Permutation test: R2=(0.0, 0.057), Q2=(0.0, -0.175), p from CV-Anova = 8.12×10^{-6}. HDL, R2Y(cum)= 0.457, Q2(cum)= 0.362. Permutation test: R2=(0.0, 0.097), Q2=(0.0, -0.131), p from CV-Anova = 0.0045. Triglyceride, R2Y(cum)= 0.772, Q2(cum)= 0.721. Permutation test: R2=(0.0, 0.053), Q2=(0.0, -0.178), p from CV-Anova = 2.26×10^{-7}. Triglyceride/HDL, R2Y(cum)= 0.629, Q2(cum)= 0.557. Permutation test: R2=(0.0, 0.069), Q2=(0.0, -0.164), p from CV-Anova = 5.74×10^{-5}. AIP, R2Y(cum)= 0.800, Q2(cum)= 0.754. Permutation test: R2=(0.0, 0.054), Q2=(0.0, -0.179), p from CV-Anova = 4.99×10^{-8}. Fatty liver index, R2Y(cum)= 0.713, Q2(cum)= 0.510. Permutation test: R2=(0.0, 0.280), Q2=(0.0, -0.226), p from CV-Anova = 0.0062. NAFLD fibrosis score, R2Y(cum)= 0.531, Q2(cum)= 0.342. Permutation test: R2=(0.0, 0.112), Q2=(0.0, -0.125), p from CV-Anova = 0.023.

2.4.1.5 Correlations between gut microbiota, metabolomics, biochemical and anthropometrical variables as well as liver and cardiovascular risk factor indexes of T2DM patients and controls

2.4.1.5.1 Relationships of relevant gut bacteria, fecal metabolites, and plasma metabolites with biochemical and anthropometrical parameters and risk factor indexes

In order to confirm the association of individual bacteria and metabolites with biochemical and anthropometrical variables, Spearman's correlation analyses were performed (**Figure 2.10A)**. Only the most important bacteria, fecal, and plasma metabolites obtained from the OPLS-DA analysis in the above sections and important bacterial and plasma metabolite ratios defined as Firmicutes/Bacteroidetes and glutamine/glutamate were selected for this analysis.

Regarding the most important fecal metabolites, 2-hydroxyvalerate was negatively associated with plasma insulin and HOMA-IR and positively with QUICKI ($p<0.05$). Additionally, 2-hydroxyvalerate was also correlated negatively with plasma glucose, while isovalerate was positively associated with QUICKI and HDL ($p<0.05$). On the other hand, fecal metabolites isovalerate and 2-hydroxyvalerate were negatively associated with CVD-related risk factor biomarkers such as triglyceride, triglyceride/HDL, AIP, and TyG index ($p<0.05$). Moreover, malonate was positively correlated with plasma glucose, insulin, HOMA-IR, HbA1c, BMI, waist circumference, and NAFLD fibrosis score ($p<0.05$) while negatively with QUICKI ($p<0.01$). Additionally, only malonate was positively correlated with triglyceride/HDL ratio and AIP ($p<0.05$).

Concerning the most relevant plasma metabolites, four plasma metabolites such as LDL(CH_3), LDL(aliphatic chain), phosphorylcholine, and N-acetylated proteins were

negatively associated with plasma glucose, insulin, HOMA-IR, TyG index, and the most significant CVD biomarkers (triglyceride, triglyceride/HDL, AIP, and TyG index) and positively to QUICKI ($p<0.01$). Curiously, acetoacetate and lipids:CH_2CO had exactly opposite associations with the above-mentioned biochemical parameters and indexes. On the other hand, VLDL(CH_3) and N-acetylated proteins were negatively associated with HbA1c and the NAFLD fibrosis score ($p<0.05$). Furthermore, VLDL(CH_3) and phosphorylcholine were also negative with BMI ($p<0.05$). Additionally, LDL(CH_3), LDL(aliphatic chain), and phosphorylcholine were negatively linked with the fatty liver index and the liver fat content ($p<0.05$) and positively with HDL ($p<0.001$). It should be noted that all plasma metabolites had marked associations with triglyceride and triglyceride-related parameters ($p<0.05$), except for VLDL(CH_3). Furthermore, the plasma glutamine/glutamate ratio had a prominent relationship with all biochemical, anthropometrical parameters and CVD and hepatic risk factor markers analyzed except for AST/ALT. Briefly, it had negative correlations with all significant anthropometric variables, HOMA-IR, triglyceride-related markers, and all liver indexes, and positive connections were found for QUICKI, HDL, albumin, and sodium.

Regarding the association of the most relevant gut bacteria obtained from the OPLS-DA analysis (11 bacteria at different taxonomic levels) with the biochemical and anthropometrical parameters, most of them had significant associations with HbA1c such as Firmicutes, Proteobacteria, *Faecalibacterium prausnitzii*, and *Escherichia*. However, these bacteria did not have significant relationships with insulin, HOMA-IR, and QUICKI. Only the genus *Faecalibacterium* and the species *Faecalibacterium prausnitzii* seemed to be correlated with them (for example, spearman correlation results of *Faecalibacterium prausnitzii* and HOMA-IR were: rho= -0.38, p= 0.05) while a negative relationship of *Faecalibacterium* and *Faecalibacterium prausnitzii* was detected with the NAFLD fibrosis score ($p<0.05$). Moreover, *Faecalibacterium prausnitzii* was negatively associated with the waist/hip ratio, plasma glucose, and HbA1c ($p<0.05$). Additionally, the Gammaproteobacteria,

Enterobacteriales, Enterobacteriaceae, and *Escherichia* had positive associations with the waist/hip ratio ($p<0.05$). The Firmicutes/Bacteroidetes ratio was negatively associated with the waist circumference, waist/hip ratio, and fatty liver index ($p<0.05$).

2.4.1.5.2 Relationships between gut microbiota and metabolomics

The relationships between the most important gut bacteria and feces and plasma metabolites were investigated, as shown in **Figure 2.10B** and **C**.

Regarding fecal metabolites, malonate had a significant relationship with most of the relevant gut bacteria. In addition, 2-hydroxyvalerate was positively associated with *Ruminococcaceae* and *Faecalibacterium* ($p<0.05$). Moreover, the Firmicutes/Bacteroidetes ratio was positively linked to isovalerate ($p<0.05$).

For plasma metabolites, VLDL(CH_3) was surprisingly and significantly associated with all relevant gut bacteria (positively associated with bacteria on the left side and negatively associated with bacteria on the right side) ($p<0.05$). Compared with VLDL(CH_3), acetoacetate and lipids:CH_2CO showed an inverse association with some gut bacteria such as Firmicutes, Proteobacteria, *Ruminococcaceae*, *Faecalibacterium* and *Faecalibacterium prausnitzii* ($p<0.05$). Regarding the glutamine/glutamate ratio, it had a positive relationship with all reduced gut bacteria such as the phylum Firmicutes and the species *Faecalibacterium prausnitzii* and negative with Proteobacteria and Gammaproteobacteria ($p<0.05$). It was worth noting that the glutamine/glutamate ratio was positively correlated with the Firmicutes/Bacteroidetes ratio ($p<0.01$), while two plasma metabolites acetoacetate and lipids:CH_2CO were negatively correlated with the bacterial ratio ($p<0.05$).

Regarding the associations of plasma and fecal metabolites, **Figure 2.10C** depicted that several fecal and plasma metabolites were closely related and influenced by each other. Thus, plasma metabolites LDL(CH_3), LDL(aliphatic chain), and N-acetylated

proteins were positively associated with fecal metabolites 2-hydroxyvalerate, and isovalerate ($p<0.05$) while plasma metabolites acetoacetate and lipids:CH_2CO were inversely related to them. Instead, the plasma VLDL(CH_3) and N-acetylated proteins had negative relationships with fecal malonate, which were also positively associated with plasma metabolites acetoacetate and lipids:CH2CO ($p<0.001$). Interestingly, the plasma glutamine/glutamate ratio was significantly linked to all significant fecal metabolites (positively correlated with 2-hydroxyvalerate, and isovalerate ($p<0.05$) while negatively with malonate ($p<0.01$)).

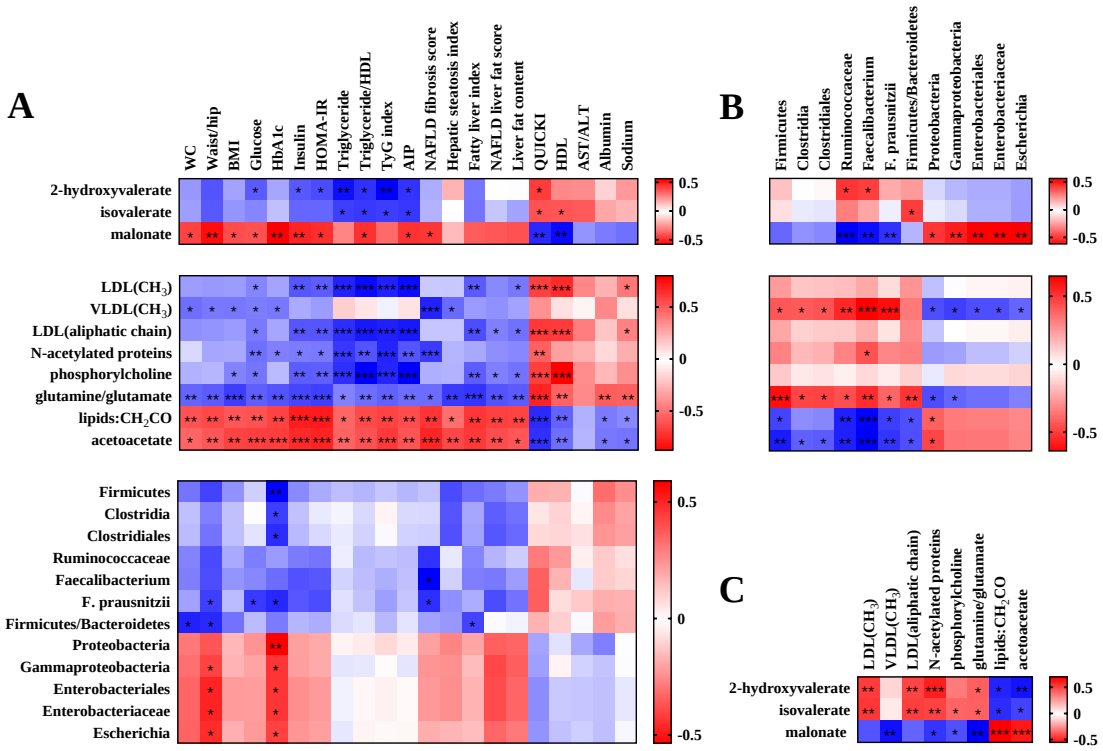

Figure 2.10 Spearman's correlation analyses in the control and T2DM groups. A) Correlations of significant anthropometric and biochemical variables with the most relevant fecal metabolites (up), plasma metabolites (middle), and gut bacteria(down). B) Correlations of the most relevant gut bacteria with the most relevant fecal metabolites (up) and plasma metabolites (down). C) Correlations of the most relevant plasma metabolites with the most relevant fecal metabolites. *, ** and *** indicated $p<0.05$, $p<0.01$ and $p<0.001$, respectively. F. prausnitzii, *Faecalibacterium prausnitzii*. WC, waist circumference; AIP, atherogenic index of plasma. BMI, body mass index; HOMA-IR, homeostasis model assessment of insulin resistance; QUICKI, quantitative insulin sensitivity check index; TyG index, triglyceride-glucose index; AST, aspartate aminotransferase; ALT, alanine aminotransferase; NAFLD, non-alcoholic fatty liver disease; HDL, high-density lipoprotein cholesterol.

2.4.2 Effect of age on T2DM patients

2.4.2.1 Anthropometric and biochemical parameters

In order to see how the different variables associated with T2DM change with age, a middle-aged (58.44 ± 1.10 years) and an older-aged (70.68 ± 0.74 years) T2DM group was compared.

Concerning anthropometric traits (**Table 2.3**), no significant differences were found between both cohorts of patients. However, some differences were found for biochemical parameters. Thus, sodium and potassium, key electrolytes to maintain physiological functions, were reduced and increased, respectively, in older patients ($p<0.05$). Although the concentration of AST and ALT did not show an apparent difference between both groups, their ratio as well as the plasma GGT levels increased dramatically in the older-aged T2DM patients ($p<0.05$).

On the other hand, important biochemical parameters for evaluating insulin's actions were assessed in T2DM patients, such as C-peptide, GLP-1, and the whole-body insulin sensitivity IS_{clamp}. However, we did not find a significant difference in these parameters between middle- and older-aged T2DM patients. Nevertheless, parameters related to comorbidities associated with T2DM such as troponin I and the glomerular filtration rate (GFR) were elevated and decreased dramatically ($p<0.01$) in the older-aged T2DM group, respectively. Further, the blood creatinine ($p=0.096$) and urea ($p=0.060$) showed a tendency to increase with the age. Interestingly, hepatic indexes of fibrosis such as FIB-4 ($p<0.001$), NAFLD fibrosis score ($p<0.01$), and ELF ($p=0.050$) raised drastically in older-aged patients, while four hepatic indexes related to steatosis, NAFLD liver fat score, liver fat content, hepatic steatosis index, and fatty liver index were scarcely altered.

Table 2.3 Biochemical and anthropometrical parameters of middle-aged and older-aged T2DM patients.

	Middle-aged T2DM	**Old-aged T2DM**
Number	16	28
Male/Female	8/8	15/13
Age	58.44 ± 1.10	70.68 ± 0.74 ***
Waist/hip ratio	0.97 (0.95-1.03)	0.98 (0.94-1.04)
BMI (kg/m^2)	30.63 ± 0.96	31.72 ± 0.80
Glucose (mg/dL)	121.10 ± 8.13	127.29 ± 5.23
HbA1c (%)	7.3 (6.4-7.6)	7.2 (6.6-7.5)
Insulin (mU/L)	14.31 (9.39-18.89)	17.36 (10.53-31.59)
HOMA-IR	3.96 (2.44-5.57)	5.30 (3.54-9.07)
QUICKI	0.318 ± 0.007	0.300 ± 0.006
C-peptide (ng/mL)	1.88 ± 0.26	1.97 ± 0.21
IS_{clamp} [mg/(kg ·min)]	1.710 (1.468-1.968)	1.375 (1.005-1.850)
Total GLP-1 (ng/ml)	1.13 ± 0.24	1.42 ± 0.18
TyG index	8.79 (8.32-9.02)	9.02 (8.39-9.48)
Sodium (mmol/L)	139.4 (138.2-140.5)	137.8 (135.4-139.2) *
Potassium (mmol/L)	4.035 (3.735-4.323)	4.310 (4.188-4.510) *
Total free fatty acids (mmol/L)	0.79 (0.60-0.84)	0.66 (0.56-0.77)
Fructosamine (µmol/L)	256.5 (238.0-275.5)	255.5 (233.3-287.3)
Adiponectin (µg/ml)	4.04 (3.14-6.41)	3.11 (1.90-7.41)
Troponin I (pg/mL)	3.5 (3.0-9.8)	8.0 (5.0-12.0) **
Interleukin-6 (pg/mL)	2.34 (1.56-3.45)	2.19 (1.50-4.47)
Urea (mg/dL)	37.81 ± 4.05	44.93 ± 2.75 $
Creatinine (mg/dL)	0.70 (0.62-0.83)	0.88 (0.64-1.03) $
GFR (ml/min/1,73 m2)	90.0 (90.0-90.0)	80.5 (61.0-90.0) **
AST (IU/L)	22.00 (18.25-30.75)	25.00 (22.00-40.75)
ALT (IU/L)	18.00 (16.25-38.50)	20.50 (16.00-29.50)
GGT (IU/L)	20.5 (16.0-28.5)	29.0 (19.0-52.8) *
AST/ALT ratio	1.01 (0.80-1.20)	1.31 (0.96-1.52) **
NAFLD liver fat score	1.07 (0.83-1.98)	1.67 (0.87-3.56)
Liver fat content (%)	8.69 (7.09-11.37)	9.13 (7.36-14.29)
Fatty liver index	70.17 (51.28-75.24)	84.01 (46.50-94.77)
Hepatic steatosis index	41.98 ± 1.05	41.26 ± 1.10
FIB-4	1.03 (0.83-1.29)	1.73 (1.25-2.73) ***
NAFLD fibrosis score	–0.87 ± 0.26	0.48 ± 0.25 **
ELF	9.018 ± 0.137	9.510 ± 0.176 $

Abbreviations: BMI, body mass index; HbA1c, hemoglobin A1c; HOMA-IR, homeostasis model

assessment of insulin resistance; QUICKI, quantitative insulin sensitivity check index; IS_{clamp}, insulin sensitivity measured during the HEC clamp; GLP-1, glucagon-like peptide 1; TyG index, triglyceride-glucose index; GGT, gamma-glutamyl transferase; AST, aspartate aminotransferase; ALT, alanine aminotransferase; GFR, glomerular filtration rate; NAFLD; non-alcoholic fatty liver disease; FIB-4, liver fibrosis index 4; ELF, enhanced liver fibrosis. *, ** and *** indicated $p<0.05$, $p<0.01$ and $p<0.001$, respectively. $, $0.05<p<0.1$.

2.4.2.2 Effect of age on the alterations of gut microbiota

2.4.2.2.1 Biodiversity and microbial composition analyses

As shown in **Supplementary Figure 2.2** in Annex, a marginal difference can be seen between middle-aged and old-aged diabetic groups from sequencing reads, observed features, and three alpha-diversity indexes. Similarly, as depicted in **Supplementary Figure 2.3** in Annex, no significant differences in the gut microbiota composition between the groups at the phylum and family level were detected. Despite that, compared with the middle-aged T2DM group, the average percentage of phylum Proteobacteria and family Enterobacteriaceae was reduced in the older T2DM group, while phylum Verrucomicrobia and families Verrucomicrobiaceae and Streptococcaceae were increased.

2.4.2.2.2 Identification of altered gut bacteria between middle-aged and old-aged T2DM patients

Multivariate analyses were performed for gut bacteria profiles between the two cohorts of diabetic patients of different ages. A moderate PCA discriminant model was only obtained by using all significant gut bacteria ($p<0.05$), as depicted in **Figure 2.11A** and **B**. There was considerable overlap between the middle-aged and old-aged groups in PCA and PLS-DA plots. Based on the PLS-DA model, significant variables with VIP values >1 were shown in **Figure 2.11C**. Compared with the middle-aged

T2DM subjects, the relative abundance of Chromatiales, Chromatiaceae, Moraxellaceae, and *Thiorhodococcus* was reduced and *Blautia schinkii* increased ($p<0.05$) in old-aged T2DM patients.

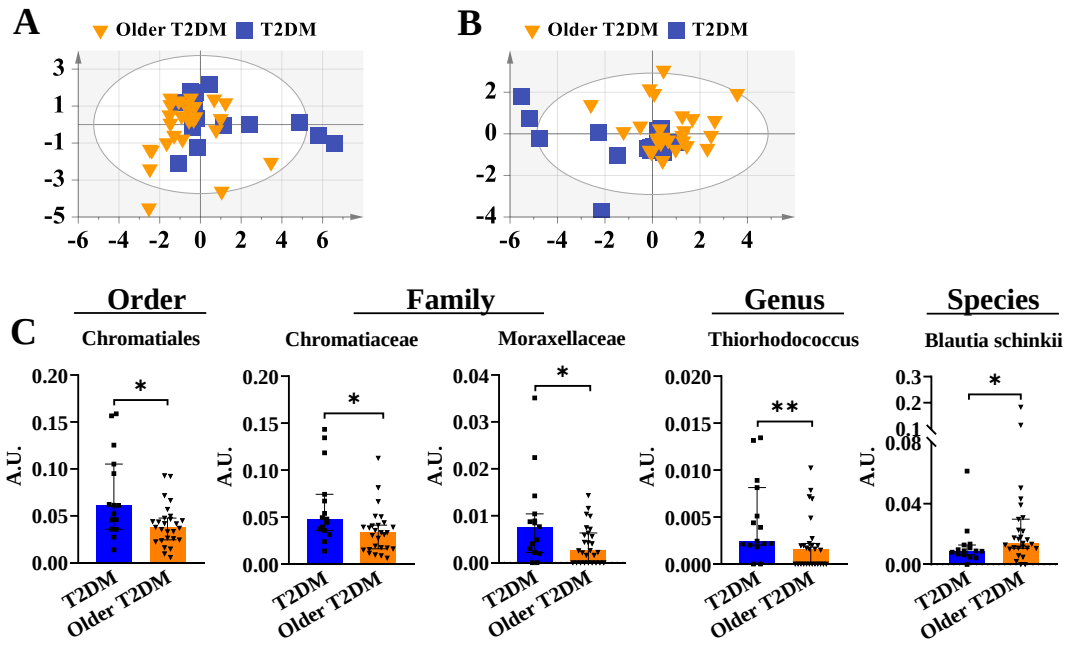

Figure 2.11 Distinct gut bacteria between middle-aged and old-aged T2DM patients. A) showed the PCA score plot of significant gut bacteria, and the parameters of the PCA model were: UV scaling, R2X(cum)= 0.568, Q2(cum)= 0.309. B) displayed the PLS-DA score plot of significant gut bacteria, and the parameters of the model: UV scaling, R2Y(cum)= 0.336, Q2(cum)= 0.136. Permutation test: R2=(0.0, 0.163), Q2=(0.0, -0.171), p from CV-Anova = 0.193. C) showed the relative abundance of the most relevant gut bacteria with VIP value >1 and p-value from the Mann-Whitney test <0.05. Data were shown as the median and interquartile range in all bar plots. * and ** indicated $p<0.05$ and $p<0.01$ respectively. A.U., arbitrary units.

2.4.2.2.3 Association of gut microbiota with biochemical variables

Multivariate linear regression analysis was conducted between gut microbiota and all significant biochemical variables, but no models could be obtained.

2.4.2.3 Fecal metabolomics analyses between middle-aged and old-aged T2DM patients

2.4.2.3.1 Identification of the most important altered fecal metabolites

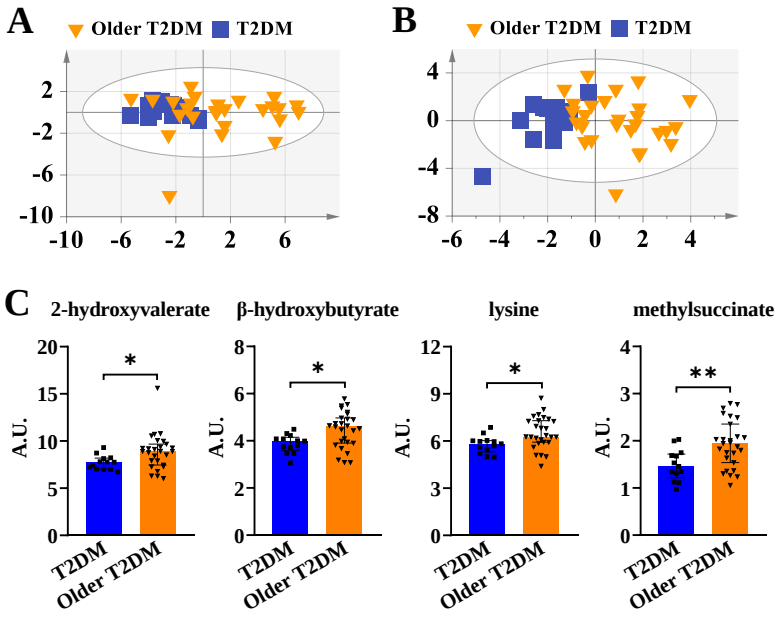

Figure 2.12 The most important fecal metabolites altered between middle-aged and old-aged T2DM patients. A) showed the PCA score plot of significant fecal metabolites, and the parameters of the PCA model were: UV scaling, R2X(cum)= 0.783, Q2(cum)= 0.414. B) displayed the OPLS-DA score plot of significant fecal metabolites, and the parameters of the model: Pareto scaling, R2Y(cum)= 0.527, Q2(cum)= 0.362. Permutation test: R2=(0.0, 0.194), Q2=(0.0, -0.276), p from CV-Anova = 0.0028. C) showed the normalized concentration of the most relevant fecal metabolites with VIP value >1 and p-value from the Mann-Whitney test <0.05. Data were shown as the median and interquartile range in all bar plots. * and ** indicated p<0.05 and p<0.01 respectively. A.U., arbitrary units.

Unlike gut microbiota, robust models were obtained for fecal metabolites between middle-aged and old-aged T2DM patients, as depicted in **Figure 2.12A** and **B**. The PCA and OPLS-DA plots showed a proper separation between the two groups, especially the OPLS-DA plot. From this model, several relevant fecal metabolites could be identified (**Figure 2.12C**). Thus, fecal 2-hydroxyvalerate, β-hydroxybutyrate, methylsuccinate, and lysine increased (p<0.05).

2.4.2.3.2 Association of fecal metabolic profiles with biochemical variables

PLS regression analyses were carried out for fecal metabolites versus all significant biochemical variables between both cohorts of patients (**Supplementary Figure 2.4** in Annex). Only one robust model could be obtained, showing that fecal metabolites of middle-aged and old-aged T2DM patients tended to associate with NAFLD fibrosis score.

2.4.2.4 Alteration of plasma metabolomics between middle-aged and old-aged T2DM patients

Discriminant analyses of plasma metabolic profiles were performed between middle-aged and old-aged T2DM groups, but no model could be obtained. PCA indicated that there was no difference in plasma metabolites between both groups (**Supplementary Figure 2.5** in Annex), which was also confirmed by univariate comparison analysis.

2.4.2.5 Relationships between gut microbiota, fecal metabolomics, and biochemical variables in middle-aged and old-aged T2DM patients

Spearman's correlation analyses of different parameters were performed between middle-aged and old-aged T2DM patients (**Figure 2.13**).

Regarding significant biochemical variables, only three showed significant associations with fecal metabolites (**Figure 2.13A**). In detail, the NAFLD fibrosis score and FIB-4 were positively associated with the fecal metabolites methylsuccinate. In addition, the NAFLD fibrosis score also correlated positively with β-hydroxybutyrate ($p<0.05$).

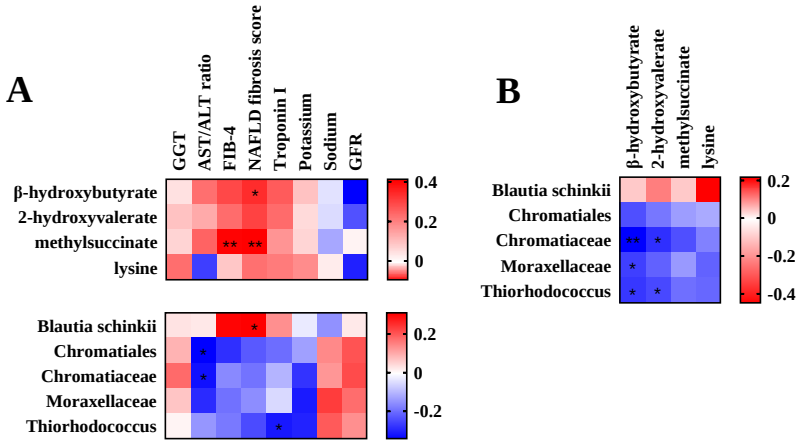

Figure 2.13 Spearman's correlation analyses in middle-aged and old-aged T2DM groups. A) Correlations of significant biochemical parameters with the most relevant fecal metabolites and gut bacteria. B) Correlations of the most relevant fecal metabolites with gut bacteria. GGT, gamma-glutamyl transferase; AST, aspartate aminotransferase; ALT, alanine aminotransferase; GFR, glomerular filtration rate; FIB-4, liver fibrosis index 4. * and ** indicated $p<0.05$ and $p<0.01$ respectively.

Regarding the associations of significant biochemical variables with selected gut bacteria, the AST/ALT ratio was negatively associated ($p<0.05$) with the bacteria Chromatiales and Chromatiaceae. On the other hand, the NAFLD fibrosis score had a positive relationship with the species *Blautia schinkii* ($p<0.05$). Finally, troponin I had a negative association with the genus *Thiorhodococcus* ($p<0.05$).

Concerning the relationship between gut bacteria and fecal metabolites, only significant negative correlations were found. Thus, Chromatiaceae and *Thiorhodococcus* were associated ($p<0.05$) with β-hydroxybutyrate, and 2-hydroxyvalerate. In addition, Moraxellaceae were related to β-hydroxybutyrate ($p<0.05$).

2.4.3 Effect of gender on T2DM patients

A total of forty-six T2DM patients (female/male: 24/22) were selected to study gender-based differences in the disease. After matching sex, both twenty-two females and males were included in the following study.

2.4.3.1 Biochemical and anthropometrical variables

A comparative analysis of the biochemical and anthropometrical variables between female and male T2DM patients was done to evaluate the effect of gender on T2DM patients, which was summarized in **Table 2.4**. There, the parameters regarding waist and hip circumferences, as well as glucose, insulin, HOMA-IR, HbA1c, GLP-1 and IS_{clamp} and CVD risk factors such as HDL, LDL, and triglyceride, were not different between female and male patients. However, the ratio between waist and hip circumferences was drastically higher in male subjects ($p<0.001$). Regarding BMI, there was no significant difference between cohorts, even though the BMI of female T2DM patients tended to be a bit higher than male patients. On the other hand, plasma levels of leptin were dramatically higher in female patients ($p<0.001$). Even though normalized by BMI, the leptin/BMI ratio was still higher in female patients ($p<0.001$). In contrast, the serum levels of urate and creatinine were higher in male patients ($p<0.05$). In terms of liver enzymes, only ALP was increased prominently in female patients ($p<0.01$). Moreover, the hepatic steatosis index was higher in female T2DM patients ($p<0.05$).

Table 2.4 Biochemical and anthropometrical parameters of female and male T2DM patients.

	Female T2DM	**Male T2DM**
Number	22	22
Age	66.45 ± 1.76	65.50 ± 1.31
Waist circumference (cm)	105.5 ± 2.5	109.4 ± 1.8
Hip circumference (cm)	107.0 (99.0-123.0)	109.5 (100.8-113.5)
Waist/hip ratio	0.94 (0.90-0.98)	1.02 (0.97-1.08) ***
BMI (kg/m^2)	32.30 (28.63-36.60)	29.83 (27.99-32.65)
Leptin (ng/mL)	47.7 (29.8-63.0)	8.3 (5.2-25.3) ***
Leptin/BMI ratio	1.43 (1.03-1.93)	0.30 (0.18-0.85) ***
Glucose (mg/dL)	128.5 ± 7.4	127.8 ± 6.7
HbA1c (%)	7.4 (6.9-7.7)	6.8 (6.4-7.4)
Insulin (mU/L)	18.11 (11.92-31.55)	15.48 (10.03-19.39)
C-peptide (ng/mL)	2.12 ± 0.25	1.82 ± 0.20
HOMA-IR	5.28 (3.25-9.98)	4.74 (2.96-6.30)

QUICKI	0.300 ± 0.008	0.306 ± 0.007
IS_{clamp} [mg/(kg ·min)]	1.56 ± 0.10	1.56 ± 0.14
Total GLP-1 (ng/mL)	1.52 ± 0.23	1.16 ± 0.18
Total cholesterol (mg/dL)	176.6 ± 5.8	171.9 ± 10.7
HDL (mg/dL)	49.09 ± 2.32	43.64 ± 2.25
LDL (mg/dL)	100.82 ± 5.31	98.50 ± 7.73
Triglyceride (mg/dL)	122.00 (87.25-180.50)	105.50 (82.75-180.25)
Troponin I (pg/mL)	5.0 (3.0-11.0)	9.0 (4.8-11.0)
Urea (mg/dL)	36.0 (29.5-57.5)	38.5 (31.0-44.0)
Urate (mg/dL)	5.27 ± 0.31	6.19 ± 0.33 *
Interleukin-6 (pg/mL)	3.33 (1.62-5.50)	2.02 (1.50-2.98)
Creatinine (mg/dL)	0.63 (0.54-0.90)	0.85 (0.75-1.00) **
ALP (IU/L)	88.82 ± 6.46	64.77 ± 3.29 **
GGT (IU/L)	25.50 (15.50-36.00)	26.00 (16.75-36.25)
AST/ALT ratio	1.17 (0.99-1.47)	1.12 (0.86-1.36)
Hepatic steatosis index	43.43 ± 1.16	40.20 ± 0.98 *
NAFLD liver fat score	1.90 (0.86-3.46)	1.28 (0.96-2.36)
Liver fat content (%)	9.42 (7.22-15.81)	8.67 (7.76-13.07)
Fatty liver index	70.54 ± 5.28	71.17 ± 4.36
FIB-4	1.26 (0.83-1.80)	1.57 (1.14-2.28)
ELF	9.40 ± 0.20	9.18 ± 0.15
NAFLD fibrosis score	–0.33 (–1.08 ~ 0.52)	0.29 (–0.68 ~ 1.25)

Abbreviations: BMI, body mass index; HbA1c, hemoglobin A1c; HOMA-IR, homeostasis model assessment of insulin resistance; QUICKI, quantitative insulin sensitivity check index; IS_{clamp}, insulin sensitivity measured during the HEC clamp; GLP-1, glucagon-like peptide 1; HDL, high-density lipoprotein cholesterol; LDL, low-density lipoprotein cholesterol; GGT, gamma-glutamyl transferase; ALP, alkaline phosphatase; AST, aspartate aminotransferase; ALT, alanine aminotransferase; NAFLD; non-alcoholic fatty liver disease; FIB-4, liver fibrosis index 4; ELF, enhanced liver fibrosis. *, ** and *** indicated $p<0.05$, $p<0.01$ and $p<0.001$, respectively.

2.4.3.2 Effect of gender on gut microbiota alteration

2.4.3.2.1 Gut microbiota composition and diversity analyses

In order to show alterations in gut microbiota between female and male T2DM patients, fecal DNA was sequenced and compared. All diversity indexes were nearly the same in both groups, including the Shannon-Wiener index, Faith's phylogenetic

diversity index, and Pielou's evenness index, as can be seen in **Supplementary Figure 2.6** in Annex. In addition, the relative abundance of dominant gut bacteria at phylum and family level were not significantly different as can be shown in **Supplementary Figure 2.7** in Annex. However, several changes are noteworthy. The abundance of phyla Proteobacteria, Actinobacteria, and Verrucomicrobia and families Bifidobacteriaceae, Enterobacteriaceae, Verrucomicrobiaceae, and Streptococcaceae were higher in female T2DM, while phylum Firmicutes and families Lachnospiraceae and Veillonellaceae were lower.

2.4.3.2.2 Identification of significant gut bacteria differences between female and male T2DM

PCA analysis of sequence data was carried out but the little separation was found between female and male patients in the PCA score plot (**Figure 2.14A**). Concerning discriminant analysis between both genders, neither OPLS-DA nor PLS-DA models could be obtained. Despite this, statistics using univariate analysis of the variables were performed. Compared with female T2DM patients, the relative abundance of class Clostridia, order Clostridiales, and four species *Roseburia faecis, Tindallia magadiensis*, *Mycoplasma edwardii*, and *Peptoniphilus coxii* seemed to be significantly elevated ($p<0.05$) in male patients while three species *Bifidobacterium gallicum, Bacteroides thetaiotaomicron* and *Phascolarctobacterium faecium* decreased ($p<0.05$).

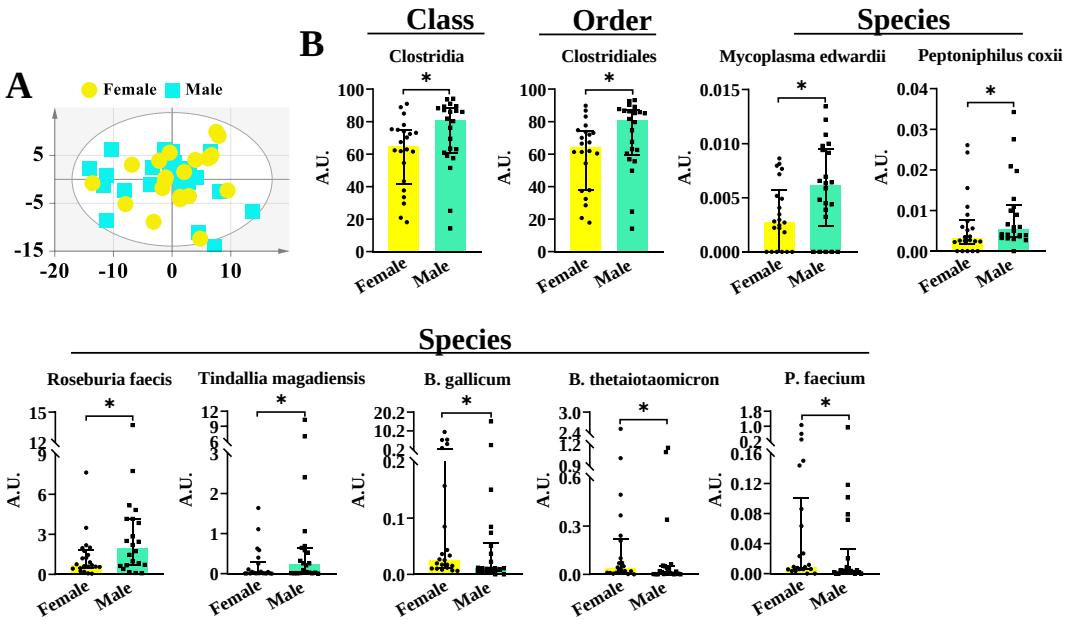

Figure 2.14 Significant gut bacteria that differ between female and male T2DM adults. A) showed the PCA score plot of metagenomic data, and the parameters of the PCA model were: UV scaling, R2X(cum)= 0.177, Q2(cum)= 0.038. B) displayed the relative abundance of significant gut bacteria with a p-value from the Mann-Whitney test <0.05. Data were shown as the median and interquartile range in all bar plots. B. gallicum, *Bifidobacterium gallicum*; B. thetaiotaomicron, *Bacteroides thetaiotaomicron*; P. faecium, *Phascolarctobacterium faecium*. * indicated p<0.05. A.U., arbitrary units.

2.4.3.2.3 Association of gut microbiota with biochemical and anthropometrical parameters

Multivariate regression analyses of gut microbiota with significant biochemical and anthropometrical parameters were carried out for female and male T2DM groups. Only one model could be established between gut bacteria and these parameters (**Supplementary Figure 2.8** in Annex), but it was not very powerful.

2.4.3.3 Alteration of fecal metabolomics between female and male T2DM patients

2.4.3.3.1 Identification of altered fecal metabolites

Similar to the gut microbiota, no separation between men and women was detected in the PCA score plot (**Figure 2.15A**). Furthermore, no discriminant models (OPLS-DA or PLS-DA) could be obtained for fecal metabolomics between female and male T2DM patients. Therefore, only univariate analysis was performed between both genders. As evidenced in **Figure 2.15B**, the concentration of fecal metabolites butyrate and hypoxanthine was increased ($p<0.05$) in males while succinate was reduced.

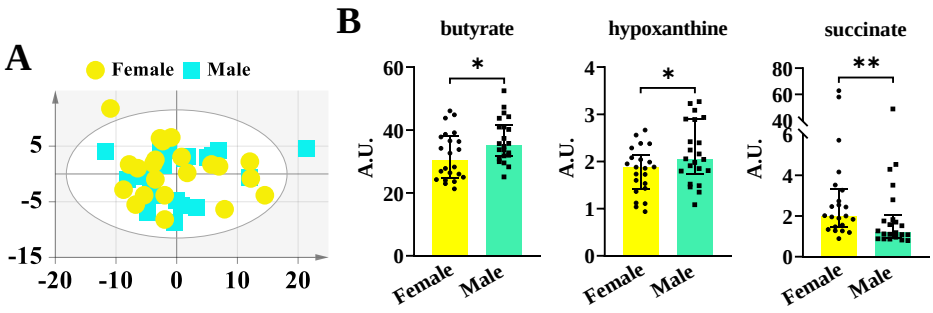

Figure 2.15 Significant fecal metabolites between female and male T2DM subjects. A) showed the PCA score plot of fecal metabolomics data and the parameters of the PCA model were: UV scaling, R2X(cum)= 0.660, Q2(cum)= 0.317. B) showed the normalized concentration of significant fecal metabolites with a p-value from univariate comparison analysis <0.05. Data were shown as the median and interquartile range in all bar plots. * and ** indicated $p<0.05$ and $p<0.01$ respectively. A.U., arbitrary units.

2.4.3.3.2 Association of fecal metabolic profiles with anthropometric and biochemical variables

Multiparametric regression analyses were done for fecal metabolites versus all significant anthropometric and biochemical variables (**Supplementary Figure 2.9** in

Annex). Even so, the waist/hip ratio and blood urate did not show a good correlation with fecal metabolites between both T2DM genders.

2.4.3.4 Alteration of plasma metabolomics between female and male T2DM

In terms of plasma metabolic profiles, the PCA plot did not show any difference between female and male subjects (**Supplementary Figure 2.10** in Annex). Furthermore, no discriminant models were obtained for both group of T2DM patients, either. Univariate statistical analysis further confirmed this result.

The association between plasma metabolomics and significant anthropometric and biochemical variables was also studied by multivariate regression analysis. As depicted in **Supplementary Figure 2.11** in Annex, only one PLS model could be obtained.

2.4.3.5 Correlations between gut microbiota, fecal metabolomics, anthropometric and biochemical variables in female and male T2DM patients

2.4.3.5.1 Relationships of gut microbiota, fecal metabolomics with anthropometric and biochemical parameters

Spearman's correlation analysis represented by heatmaps was performed for significant gut microbiota, metabolomics, biochemical and anthropometrical variables obtained from the above gender analyses (**Figure 2.16**). Regarding the association between biochemical and anthropometrical data with fecal metabolites, plasma ALP, leptin, and the leptin/BMI ratio were positively associated with succinate ($p<0.05$). In addition, blood creatinine was positively linked to butyrate ($p<0.01$).

Concerning the relationship between biochemical and anthropometrical variables and gut bacteria, the hepatic enzyme ALP was positively associated with *Bacteroides thetaiotaomicron* and *Phascolarctobacterium faecium* ($p<0.05$). In addition, positive correlations were also found between plasma creatinine with *Roseburia faecis*, the class Clostridia and the order Clostridiales ($p<0.05$), and for plasma urate with the class Clostridia and order Clostridiales. Only one negative correlation was obtained between the hepatic steatosis index and *Tindallia magadiensis* ($p<0.05$).

2.4.3.5.2 Relationships between gut microbiota and fecal metabolites

After performing the analysis, only the fecal metabolites succinate and hypoxanthine were negatively associated with the species *Mycoplasma edwardii* and *Bifidobacterium gallicum* respectively ($p<0.01$). On the contrary, hypoxanthine was positively linked to the bacteria Clostridia, Clostridiales, *Roseburia faecis*, and *Peptoniphilus coxii* ($p<0.05$). And fecal SCFA butyrate had a significant and positive correlation with *Peptoniphilus coxii* ($p<0.01$).

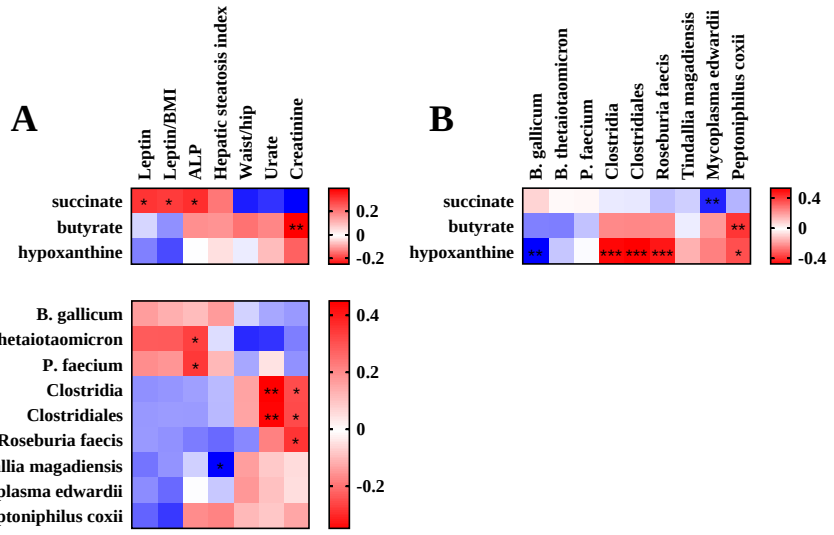

Figure 2.16 Spearman's correlation analyses in female and male T2DM patients. A) Correlations of significant anthropometric and biochemical parameters with significant fecal metabolites and gut bacteria. B) Correlations of significant fecal metabolites with significant gut bacteria. BMI, body mass index; ALP, alkaline phosphatase. B. gallicum, *Bifidobacterium gallicum*; B. thetaiotaomicron, *Bacteroides thetaiotaomicron*; P. faecium, *Phascolarctobacterium faecium*. *, ** and *** indicated $p<0.05$, $p<0.01$ and $p<0.001$, respectively.

2.5 Discussion

The current study integrates for the first time data from gut microbiota, fecal metabolites, and plasma metabolites of T2DM patients, to figure out the gut microbiota and metabolic alterations of T2DM and their relationships. Moreover, we have studied the gut microbiota at the genus and species level to go deeper and better detail the alterations caused by T2DM. We further studied the association of these alterations between them and with relevant anthropometric and biochemical parameters related to T2DM and its consequences. In addition, the effects of age and sex on the alteration and associations were evaluated in patients with T2DM by identifying and selecting specific variables or parameters of patients. We selected the most relevant gut bacteria, fecal metabolites, and plasma metabolites by discriminant models (OPLS-DA or PLS-DA) and univariate analysis, and picked out the significant anthropometric and biochemical parameters by univariate analysis.

2.5.1 Alterations in T2DM patients

For the interpretation of these results, it is important to take into account that by doing a representative selection of T2DM patients, they could also be partially affected by other disorders diagnosed or not, which in turn can also alter the composition of blood and feces. For instance, the average BMI of T2DM patients is significantly higher than that of controls (30.63 ± 0.96 vs 24.62 ± 0.90), indicating that most T2DM patients were obese, as usually happens in this type of patients because obesity is an important risk factor for the development of T2DM [347] and therefore expected. Furthermore, NAFLD liver fat score, fatty liver index, and NAFLD fibrosis score were high in T2DM individuals, suggesting excess fat infiltration and fibrosis that could affect the liver [331, 333]. NAFLD and NASH are usually observed in T2DM patients [286], which was also demonstrated by hepatic risk factor markers in our study. In addition, even though the T2DM patients included in this trial did not have a history of any cardiovascular events, they presented signs of cardiovascular risk

defined by increased plasma triglycerides, AIP, and TyG index [329].

The metagenomic study of gut bacteria further revealed a certain degree of dysbiosis in the gut microbiota of people with T2DM (**Figure 2.1**), as already detected in previous studies [168]. We found that the abundance of the most dominant phylum Firmicutes decreased dramatically while Bacteroidetes and Proteobacteria increased in T2DM patients. These results are in coherence with a previous study, which also found a significant reduction in bacteria Firmicutes and a trend to increase in bacteria of the phylum Bacteroidetes in T2DM patients [348]. In addition, recently Zhao *et al* reported opposite results about the phyla Firmicutes and Bacteroidetes, which are in disagreement with the current study, but they showed an increase of Proteobacteria in T2DM, in coherence with our results [304]. Therefore, in our study the Firmicutes/Bacteroidetes ratio was expected to reduce significantly in the patients, further confirming a gut dysbiosis that may be accompanied by some pathologies [345].

At smaller levels, corresponding bacteria from the phyla Firmicutes and Proteobacteria were determined in the patients. Concerning changes in gut bacteria at genus and species level, we revealed in T2DM patients a significant decrease in *Faecalibacterium prausnitzii* and an increase in *Escherichia spp* (**Figure 2.3**). This is consistent with the study performed by Qin *et al* where they found that *Faecalibacterium prausnitzii*, one butyrate-producing bacterium, was enriched in the control group while *Escherichia coli*, as one opportunistic pathogen, was enriched in the T2DM group [168]. An increase in *Escherichia coli* was reported to be related to NASH [187], and subcutaneously infusion of this bacteria into mice could induce obesity and IR [349].

The metabolomics study confirmed that these changes in the gut microbiota composition also affected the metabolomics profile of feces. For instance, we found two kinds of fecal valerates (isovalerate and 2-hydroxyvalerate) decreased in the T2DM samples (**Figure 2.5**). Our results were in accordance with previous studies, which demonstrated that compared with the healthy subjects, the concentrations of

short-chain fatty acids (SCFAs) including valeric acid were predominantly reduced in the T2DM patients [226, 304]. Valeric acid, as one SCFA, has been found to affect the pathogenesis of AD by reducing aggregations of Aβ, and the reduction of valeric acid and other SCFAs may promote Aβ accumulation in the brain [350]. In addition, we found that the concentration of fecal metabolite malonate increased in T2DM dramatically ($p<0.001$). This is following the study of Fikri *et al* where they reported that T2DM patients also had a slightly significant increase of plasmatic malonate [351]. Malonate was found to be robustly protective against cardiac ischemia/reperfusion injury [352]. In our study, the increase of malonate in T2DM patients may be due to cardiac ischemia.

Concerning plasma metabolites (**Figure 2.7**), we found that low-density lipoproteins including LDL(CH_3) and LDL(aliphatic chain) were reduced in T2DM patients as well as very-low-density lipoprotein VLDL(CH_3). These results seem to be different from previously reported studies where they found that the total concentrations of LDL and VLDL were significantly higher in patients with T2DM compared with the controls [353, 354]. However, it is important to take into account the size of the lipoproteins in every case. For instance, the amount of large LDL particles have shown to decrease in a prior study [355], which could be the change detected by our diffusion-edited NMR experiment, which filters the signals from large molecules.

Besides the lipoproteins, we observed that acetoacetate and lipids:CH_2CO were increased markedly in T2DM. The change in acetoacetate is in concordance with the results obtained by Andersson-Hall *et al* [356]. Acetoacetate can act as an energy source for the body, especially preferred by cardiac muscle and renal cortex [357]. This increase could compensate for the energy deficit caused by IR as well as lipids:CH_2CO. Additionally, Wu *et al* reported that acetoacetate could ameliorate AD symptoms in mice [358]. On the other hand, the importance of glutamine for cell survival and proliferation is widely accepted [359]. Many previous studies found that T2DM patients presented an imbalance of plasma glutamine and glutamate (decreased glutamine and increased glutamate) [230, 346]. Therefore, the glutamine/glutamate ratio has been widely used for predicting T2DM incidence [346]. In our study, T2DM

subjects had lower plasma glutamine and higher glutamate than controls, and in consequence, had a lower glutamine/glutamate ratio (**Figure 2.9**). These findings are in harmony with previous research [230, 303].

Once the alteration of the gut microbiota and metabolites has been determined, we would like to know in more detail the association of these alterations with parameters related to the pathophysiology of T2DM and its associated consequences, mainly cardiovascular and hepatic. Therefore, PLS regression analysis was used to find the associations between multiple clinical variables and altered gut microbiota and metabolites as well as the relations between them. Our results revealed that the best correlation could be obtained with the fecal metabolome. All significant altered anthropometric parameters in T2DM patients (waist circumference, the waist/hip ratio, and BMI) and biochemical markers related to T2DM (plasma glucose, insulin, HOMA-IR, QUICKI, and HbA1c) showed a robust association with fecal metabolic profiles (**Figure 2.6**). Thus, a feces analysis could be an interesting alternative for the diagnosis and management of T2DM, especially at early stages, when the biochemical blood variables may still not be altered. Interestingly, only a few clinical parameters presented a robust correlation with gut bacteria (**Figure 2.4**), revealing that bacterial metabolism seemed to be more sensitive to T2DM disorder than the gut bacteria profile. Concerning plasma metabolic profiles, some associations could be found with clinical parameters (**Figure 2.9**), but much less than in feces. This may be partially due to the lower variability and higher homeostasis of metabolites in plasma. In summary, only HbA1c and insulin correlated properly with gut microbiome and fecal and plasma metabolomics, and therefore with the control of T2DM and the insulin release and function.

To go into more detail about the associations, correlation analysis (**Figure 2.10**) were done between altered gut microbiota and metabolites with the biochemical and anthropometrical variables or with the association between them. Thus, the fecal metabolites 2-hydroxyvalerate and malonate were significantly correlated with

fingerprints of T2DM including plasma glucose, insulin, and the IR indexes HOMA-IR and QUICKI. To our knowledge, this is the first time that this kind of correlation is detected. This result is also in line with our previous analysis, where both metabolites were identified as being significantly different in T2DM patients and healthy controls. As a result, these two fecal metabolites must be considered in future studies relating to the management of T2DM in patients because they appear to be more implicated in IR.

Concerning correlation with plasma metabolites, it is interesting that all relevant plasma metabolites changed in T2DM had significant associations with plasma glucose, and except for plasma metabolite VLDL(CH_3), all of them were significantly linked to plasma insulin, HOMA-IR, and QUICKI. On the other hand, the glutamine/glutamate ratio was found negatively associated with plasma glucose, insulin, and HOMA-IR and positively with QUICKI. This was also in concordance with previous studies [360].

Regarding gut bacteria, only a few significant correlations were obtained. Thus, HbA1c showed a significant association with most of the relevant gut bacteria. On the other hand, *Faecalibacterium prausnitzii* was negatively connected to fasting plasma glucose, which was consistent with a previous study [349]. *Faecalibacterium prausnitzii*, as the most abundant commensal bacteria, is reported to play important roles in gut homeostasis, such as fermenting glucose to acetate, butyrate, D-lactate, and formate [361], processes that seem to be altered in T2DM. Further, the Firmicutes/Bacteroidetes ratio showed a negative association with the anthropometric parameters waist circumference and waist/hip ratio. This ratio has already been previously related to obesity in a recent study where it was reported that the Firmicutes/Bacteroidetes ratio was significantly decreased after BMI reduction [362]. Though our result is not related to BMI, the fact that it is related to waist circumference, which is usually indirectly related to weight, indicates that this bacterium very probably plays an important role in obesity, which triggers diabetes. However, further studies are needed to confirm this assumption.

To discover more information about the relationship between gut bacteria and metabolites, we also identified connections between gut bacteria and fecal and plasma metabolites. In this analysis, only the fecal metabolite malonate and the plasma metabolite VLDL(CH_3) evidenced significant associations with most significant bacteria such as bacteria *Faecalibacterium* and *Escherichia*. Therefore, both metabolites could be interesting candidates as indicators for an alteration of the gut microbiota related to T2DM that can be more easily measured than gut bacteria. Further, the most dominant genus *Faecalibacterium* was positively correlated with fecal metabolite 2-hydroxyvalerate, which decreased in T2DM and was related to IR, and was negatively correlated with plasma metabolite acetoacetate, which increased in T2DM and was related to IR, CVD, and AD. Then, this genus seems to play important roles in the development of IR in T2DM as has been described previously either in obesity or T2DM [363, 364]. These relationships further confirmed the important roles of *Faecalibacterium* in T2DM. Finally, we found that the Firmicutes/Bacteroidetes ratio was positively linked to the plasma glutamine/glutamate ratio which is more related to the development of T2DM. This result is described here for the first time and is coherent with the finding that oral L-glutamine supplementation changed the composition of the gut microbiota in overweight and obese people, reducing the Firmicutes/Bacteroidetes ratio [365]. Therefore, both ratios are very important in the development of T2DM and need to be taken into account in the management of patients.

2.5.2 Aging effects on T2DM

After studying the effects of gut microbiota and fecal and plasma metabolites on T2DM, we were interested in studying the effect of age on T2DM. To our knowledge, this type of study has never been addressed in the literature and could be important for a better understanding of T2DM and the management of patients. We are interested in this study because we detected an increased risk for pathological problems derived from T2DM with increased age in the cohort of patients studied. For instance, the

plasma troponin I level (a marker of myocardial infarction) was markedly increased in old-aged patients, indicating a possible higher risk of myocardial infarction despite it being still within a normal range because this parameter is only altered after infarction [366]. Further, the glomerular filtration rate (GFR) (the best available indicator of overall kidney function [367]) was lower in elderly patients, accompanied by higher plasma levels of urea and creatinine. These changes suggested that older T2DM patients were more susceptible to kidney inflammation and disease. Significant differences were also found between middle-aged and old-aged T2DM patients in liver fibrosis indexes such as FIB-4 and NAFLD fibrosis score. These results indicated that elderly T2DM patients were more likely to suffer from liver fibrosis and then liver pathology. This could be explained because T2DM patients have a high prevalence of suffering NAFLD and over time could develop symptoms of NASH [286].

Because of the small age difference and the small number of patients, only a few gut bacteria and fecal metabolites were found altered between middle-aged and old-aged T2DM patients, while plasma metabolites showed no difference. Regarding alterations in gut microbiota, bacteria Chromatiales, Chromatiaceae, Moraxellaceae, and *Thiorhodococcus* were found to decrease in old-aged patients (**Figure 2.11**). The genus *Thiorhodococcus* belongs to Chromatiaceae, a family of purple sulfur bacteria within the order Chromatiales of the class Gammaproteobacteria. Most members from Chromatiaceae typically grow under anoxic conditions [368]. In terms of Moraxellaceae, they are also a family of Gammaproteobacteria, including a few pathogenic species. Not much information is available about the above-altered bacteria. However, from the class level, Gammaproteobacteria is found to be implicated in the development of NAFLD [369, 370], a most common comorbidity of T2DM. On the other hand, the species *Blautia schinkii* was elevated in old-aged T2DM subjects. Nonetheless, further research is needed to determine the roles of these bacteria in T2DM patients from middle age to old age.

Regarding the fecal metabolome (**Figure 2.12**), three fatty acid derivates (2-hydroxyvalerate, β-hydroxybutyrate, methylsuccinate) were increased in old-aged

T2DM individuals. Both β-hydroxybutyrate and methylsuccinate were shown in some literature to play a role in the brain, and β-hydroxybutyrate was found to attenuate AD pathology [371, 372]. In addition, the amino acid lysine was also found to increase in old-aged T2DM. High plasma levels of lysine were associated with an increased risk of T2DM incidence [230].

Further, relationships were explored between gut bacteria, fecal metabolites, and biochemical parameters. Fecal metabolites β-hydroxybutyrate and methylsuccinate were both positively correlated with NAFLD fibrosis score. However, Haam *et al* revealed a different result that β-hydroxybutyrate was inversely associated with hepatic fibrosis [373]. It is possible because they acquire metabolites from urine, which are different from feces. This is the first study to elucidate that *Blautia schinkii* is positively associated with NAFLD fibrosis score and *Thiorhodococcus* is negatively associated with plasma troponin I. Associations between gut bacteria and fecal metabolites were also examined in our study, but only several significant negative associations were found. Further study on a large-scale cohort is necessary to confirm these findings.

2.5.3 Gender effects on T2DM

Currently, some attention has been paid to the gender effect in the development of several pathologies, including T2DM, with clear differences attributed to gender [289, 290]. Therefore, the different effects of gender on T2DM were also considered in this study, which to our knowledge has not been previously addressed. Even though there was no difference in waist and hip circumferences between the two groups, male subjects with T2DM had a much higher waist/hip ratio. This can be explained by a prior study that levels of T2DM are greater in middle-aged men than in women [374]. Plasma levels of leptin were higher in female patients, even when normalized by BMI. This is in accordance with a study performed in the Spanish population where researchers also observed higher plasma leptin levels in women than in men [375]. Both T2DM women and men included in our study had higher plasma leptin levels

than the reference value (23.75 ng/mL in women and 6.45 ng/mL in men), suggesting that they may have leptin resistance [375]. In T2DM, men had higher levels of waste product urate and creatinine than women, indicating men are more susceptible to kidney dysfunction. This is in agreement with previous findings in a variety of renal diseases, where men develop renal failure more quickly than women [376] Regarding liver physiopathology, T2DM females had higher plasma concentrations of ALP and higher scores of hepatic steatosis index. This indicated that they had a greater infiltration of fat in the liver and had a more advanced NAFLD stage than men. This is also found by Balakrishnan *et al* that women have a higher risk of advanced fibrosis than men once NAFLD is established in both sexes, especially after the age of 50 [377].

On the other hand, several differences were evidenced for gut bacteria and fecal metabolites between T2DM women and men. Thus, the percentage of the class Clostridia, which we already found decreased in T2DM patients compared to controls, was markedly lower in T2DM females than in males. Accumulating evidence suggests that Clostridia are profoundly involved in the maintenance of overall gut function, particularly in the production of SCFAs [378] that exert beneficial effects on inflammatory status and insulin sensitivity and regulate related diseases, such as CVD [379], AD [380] and NAFLD [381]. A significant reduction of Clostridia may impair gut homeostasis, and this process seems to be increased in women and then the deleterious process coming from its depletion is enhanced in this gender. Moreover, at a smaller level, we also found that one order and three species from the class Clostridia such as Clostridiales, *Roseburia faecis*, *Tindallia magadiensis*, and *Peptoniphilus coxii* were lower in T2DM females. These results further strengthened our above observations and provide us with more details about the alterations produced in the Clostridia class in females. On the contrary, females had a higher abundance of *Bacteroides thetaiotaomicron* and *Phascolarctobacterium faecium* than males in T2DM. *Bacteroides thetaiotaomicron*, an opportunistic pathogen, can produce succinate to facilitate the growth of *Phascolarctobacterium faecium* [382]. This was proved by our fecal metabolomic result that succinate was found to be

increased in T2DM females. In addition, *Bacteroides thetaiotaomicron* treatment in mice contributes to increased fat deposition and impaired glucose tolerance [383]. These indicated that conditions of T2DM were more severe in females than in males, probably driven by this bacterium.

The differences in fecal metabolites in T2DM between both genders were in coherence with the differences detected in gut microbiota. Thus, the fecal metabolite butyrate was found to reduce prominently in T2DM females, which could be a consequence of the significant reduction of gut bacteria from Clostridia. Butyrate, an important SCFA, is believed to play protective roles against obesity and related metabolic diseases including T2DM and NAFLD [384]. The concentration of fecal hypoxanthine was also decreased in T2DM females in our study. One previous study found that the concentration of hypoxanthine in whole blood was higher in T2DM patients than in controls, suggesting that it may play a role in the development of the disease [385]. Above metabolomics results confirmed that females with T2DM suffer from more severe metabolic disorders than males.

Correlation analysis to show the associations between anthropometric and biochemical parameters, gut bacteria, and fecal metabolites were further examined for the above explanations. There were only a few significant associations. Therefore, the fecal metabolite succinate showed a positive relationship with biochemical parameters leptin and ALP that were shown gender differences. This is in accordance with the above observations where this metabolite as well as both biochemical parameters was increased in T2DM females. Both abnormal leptin levels and elevated fecal metabolite succinate are associated with more pathophysiology in T2DM patients [386]. On the other hand, the fecal metabolite butyrate was found to be positively related to serum creatinine concentration. In addition, a negative association was found between the hepatic steatosis index and *Tindallia magadiensis*. It is the first time that this relationship has been described for T2DM; the altering of both variables corresponds to what was seen in the current study performed in T2DM patients since *Tindallia magadiensis* belongs to the bacteria class Clostridia. This indicates again

that this class is strongly related to the pathogenesis of T2DM. Regarding correlations between gut bacteria and fecal metabolites, Clostridia and its members (Clostridiales, *Roseburia faecis*, and *Peptoniphilus coxii*) were found to be positively related to the fecal metabolite hypoxanthine. Similar to what was shown in mice [387], this result again shows that Clostridia are important in T2DM and that gender influences the alterations of this type of bacteria. Finally, the species *Peptoniphilus coxii* was positively related to fecal butyrate, suggesting that it may help to produce butyrate [388] and then execute some beneficial effects [384] for male patients.

2.5.4 Limitations

Despite the fact that we have obtained many novel data in the three studies carried out with these subjects, it is important to take into account that the current studies show some limitations. In the first place, the number of subjects in this first pilot clinical trial was very small. On the other hand, it would be interesting to also have a control group in the age and gender studies but unfortunately, we have no access to old-aged controls and additionally, we need to take into account the difficulty of these for not having pathologies. Further, the difference in age between the two T2DM groups is very small. Therefore, future studies are required to overcome these problems and obtain more robust results.

2.6 Conclusions

Our study revealed a close relationship between the alterations in anthropometric factors, biochemical factors, the fecal metabolome, the plasma metabolome, and gut bacteria in T2DM patients. In summary, the following conclusions can be reached:

- Our study confirmed that T2DM patients had severe IR, as well as NAFLD, and increased CVD and kidney risks factors.
- Alterations in gut microbiota composition, rather than in gut microbial diversity were found in T2DM patients. For example, patients had a lower abundance of Firmicutes and a lower ratio of Firmicutes/Bacteroidetes than controls, with a higher abundance of Proteobacteria. At a smaller level, a lower abundance of *Faecalibacterium prausnitzii* and a higher abundance of *Escherichia* were found in patients.
- Alterations were also found in fecal and plasma metabolites in T2DM patients, such as fecal 2-hydroxyvalerate, malonate, and plasma lipoprotein LDL, phosphorylcholine, and acetoacetate, as well as the ratio of plasma glutamine/glutamate.
- All above significantly altered fecal and plasma metabolites showed significant correlations with IR and CV risk factors. However, no bacteria were found to be significantly correlated with systemic IR indices.
- Multivariate regression analysis showed HbA1c and plasma insulin levels had a significant association with gut microbial profiles as well as fecal and plasma metabolic profiles.
- Age and gender need to be taken into account in the management of T2DM. In our study, age and gender generated significant differences in the gut microbiota composition and fecal metabolites, instead of plasma metabolites. In age effects, gut bacteria from Chromatiales, and fecal metabolites β-hydroxybutyrate, methylsuccinate and lysine should be considered in future studies. On the other hand, in gender effects, bacteria from Clostridia and

species *Bacteroides thetaiotaomicron*, as well as fecal butyrate, succinate and hypoxanthine, were found to play important roles.

Chapter 2:

Gut microbiota and metabolomics related to tissue/organ-specific insulin resistance in T2DM: a study of liver, heart, skeletal muscle and brain

3.1 Introduction

In this chapter, we studied the effect of the gut microbiota as well as plasma and fecal metabolomics on the liver, heart, skeletal, and brain IR. However, the basic functions of some insulin-targeted tissues or organs and their roles in maintaining glucose homeostasis have been introduced in chapter 1 as well as the causes of this specific IR. Despite this, no more studies have been addressed to study the role of tissue/organ-specific IR due to the difficulties of its measurement. This can only be performed *in vitro* thought the use of tissue/organ biopsies for molecular biology studies or *in vivo* using dynamics (SPECT or PET) or static radioactive techniques (PET) where our group has established a new method as been mentioned in the chapter 1 [144, 145]. The use of biopsies, apart from being a highly invasive and unethical technique to measure the IR of a tissue or organ, only provides us with information on a part of the mentioned tissue and/or organ that may not be representative and therefore we may fall into errors. Instead, the *in vivo* radioactive techniques solve all these problems using two static ^{18}F-FDG PET/CT assessments, one in baseline and another after an HEC procedure that is a complex procedure for their clinical daily use, even in clinical trials. This allowed us to determine the insulin sensitivity of organs and tissues in patients with T2DM accurately, as well as to learn more about the relationship between the gut microbiota and fecal metabolomics in this pathophysiology, as well as the relationship of all these variables with the plasma metabolomics.

T2DM is a global health threat and has received much attention. However, many different complications, particularly in different organs and tissues, have been reported in people with T2DM related to systemic IR due to the above-mentioned difficulties. Then IR is an independent risk factor for comorbidities in T2DM such as heart failure, sarcopenia, dementia, or hepatic pathologies [37, 70, 132, 286]. However, it is well known that sometimes tissue/organ-specific IR is different from

systemic indexes of IR [389]. This is tricky and difficult for the researcher to deal with. Then, studies are being carried out to study tissue/organ-specific IR mainly in animals and in animals through knock-out animal models (knocking out insulin receptors in adipose tissue) [390] and some, like the case of our research group, even in patients. However, to the best of our knowledge, there are few studies linking the effects of gut microbiota and its associated metabolomic profile with tissue/organ-specific IR. Therefore, the roles of gut microbiota and metabolites in tissue/organ-specific insulin resistance will be introduced below.

3.1.1 Roles of gut microbiota in tissue/organ-specific insulin resistance

As we have introduced previously in **Section 1.2.2.1**, changes in gut microbiota have been described in T2DM and some related complications, indicating that the gut microbiota plays key roles in these pathologies that usually have been characterized by the presence of IR [168, 178, 185, 240, 351]. Therefore, a link between gut microbiota and IR has been suggested in several studies [167, 170, 240, 391]. Imbalanced gut microbiota appears to interfere with intestinal permeability and increase lipopolysaccharide (LPS) absorption [167], which induces a chronic subclinical inflammatory process and leads to IR via activation of Toll-like receptor 4 (TLR4) [167, 391]. Furthermore, a decrease in some specific gut bacteria such as *Faecalibacterium prausnitzii* and *Roseburia intestinalis* altered in T2DM causes a decrease in circulating SCFAs [168], which may also contribute to decreased insulin sensitivity. In addition, some specific gut bacteria have also been reported to have associations with HOMA-IR [392], a systemic IR index. However, up to now, rare studies have investigated whether tissue-specific IR is related to specific gut bacteria. In this study, for the first time, we are going to study the effect of the altered gut microbiota in specific IR on the liver, brain, heart, and skeletal muscle in T2DM patients.

3.1.2 Roles of metabolites in tissue/organ-specific insulin resistance

Several studies have described the metabolic changes in tissue/organ-specific IR in animal models, and have elucidated the relationships between some metabolites and specific IR in humans. For example, a study performed in muscle- and liver-specific IR mouse models indicated that concentrations of intracellular long-chain fatty acyl CoA, ceramide, and diacylglycerol were significantly increased in the skeletal muscle of the mice and they associated it with muscle-IR. In addition, the authors found that concentrations of intracellular long-chain fatty acyl CoA were significantly increased in the liver of the liver-IR of these mice [393]. On the other hand, a plasma lipidomics study in overweight/obese non-diabetic patients revealed that skeletal muscle insulin sensitivity was associated with higher plasma lysophosphatidylcholine concentrations, and hepatic IR with higher plasma triacylglycerol (TAG) and diacylglycerol concentrations and a lower abundance of odd-chain and very-long-chain TAG in women [394]. An NMR-based metabolomics study in obese patients showed that both liver and muscle IR was associated with elevated branched-chain amino acids, lactate and triglycerides, and lower glycine levels [395]. In addition, they found that only liver IR was associated with lower ketone body levels and elevated ketogenic amino acids, which suggested decreased ketogenesis.

However, in most studies performed on patients, tissue-specific IR was measured by surrogate indices based on fasting biochemical analysis and OGTT test [395, 396].

3.2 Hypothesis and Objectives

We hypothesize that some different gut bacteria, as well as fecal and plasma metabolites, are related to specific IR of different organs and tissues in T2DM patients and risk factors of comorbidities associated with T2DM. These differences can provide important key information to explain and deepen pathological events in patients. Furthermore, the alterations shown in this pilot clinical trial could be used as prognostic biomarkers, after confirmation by further studies.

Specifically, this chapter has the following aims:

1) To identify specifically altered gut bacteria as well as specific fecal and plasma metabolites in the tissue/organ of stratified patients for liver-or-myocardial IR and IS phenotypes, based on PET/CT imaging data of glucose uptake after HEC
2) To assess the association of significant imaging variables (used to determine tissue/organ-specific IR (PET) or structural alterations (CT)) from the liver, heart, skeletal muscle, and brain) with gut microbiota, metabolomics, biochemical and anthropometrical parameters.
3) To identify some specific gut bacteria related to plasma GLP-1, as well as fecal and plasma metabolites
4) To determine the differences caused by gender and age in the objectives of points 1) and 2).

3.3 Materials and methods

3.3.1 Subjects

As described in chapter 1, forty-six T2DM patients were recruited from the Outpatient Department of the Endocrinology Service Vall d'Hebron University Hospital (Barcelona, Spain), who had been diagnosed at least 5 years. The criteria of patients have also been described in chapter 1. All participants were informed before the studies and the consent documents were obtained.

All patients received an ^{18}F-FDG PET/CT scan at baseline and after HEC respectively, the procedures of which are introduced below. Specific tissue IS was determined by measuring the increment in ^{18}F-FDG uptake after HEC. After HEC, seventeen patients indicated a striking enhancement of myocardial ^{18}F-FDG uptake and twenty-five a marginal increase, thus revealing myocardial IS (mIS) and IR (mIR) respectively [390]

On the other hand, after HEC, thirteen patients exhibited an increase in liver ^{18}F-FDG uptake and twenty-eight a reverse decrease, indicating liver IR (L-IR) and IS (L-IS), respectively. It is age-and-gender matched between patients with mIS and mIR, and between patients with L-IS and L-IR.

Despite the fact that the myocardium and the liver showed these two phenotypes in T2DM patients, brain and skeletal muscle did not show any using the brain PET data or difference of ^{18}F-FDG uptake in skeletal muscle. Thus, all patients (n=46) were included for just correlation analysis between IS in these tissues and sequencing and metabolomics data. On the other hand, the statistical analysis was only performed to obtain the alteration between two groups for both liver and myocardial phenotypes due to the absence of a healthy control group.

3.3.2 Methods referred to in Chapter 1

Biochemical and anthropometric measurement, fecal sample collection and extraction, sequencing and metabolomics, HEC clamp as well as statistical analysis are referred to in sections 2.3.2 to 2.3.9.

3.3.3 Positron emission tomography/computed tomography

3.3.3.1 PET/CT scanning

Two ^{18}F-FDG PET/CT scans were performed for each T2DM patient in a random order within 2 days. Before each PET/CT scan, patients stopped the uptake of any medications for 24 hours and fasted at least for 8 hours. A dose of 1.9 MBq/kg of ^{18}F-FDG was intravenously (iv) administered to the patients before each scan session. A 12-min whole-body PET/CT scan (initial scan) followed by a 6-min cardiac PET scan (initial scan) was performed for 60 minutes after iv administration of 18F-FDG in the patients. The second injection of ^{18}F-FDG was performed at least 1.5 hours after starting the HEC procedure and only when the concentration of three consecutive plasma glucose levels (5 min intervals) was in the range of 100 ± 15 mg/dL. HEC was maintained for 60 min after the ^{18}F-FDG injection and then was stopped. Patients were then again scanned (HEC scan) in the same conditions as the baseline scan. Insulin sensitivity (IS) of each tissue or organ was determined as the difference in standardized uptake value (ΔSUV) of ^{18}F-FDG between the HEC and baseline scans.

3.3.3.2 PET/CT acquisition

PET/CT imaging was acquired in a Biograph mCT 64S scanner (Siemens Healthcare, Erlangen, Germany). Coronary synchronized CT Calcium Scoring acquisition was performed before the PET scan with the following acquisition parameters: tube

voltage = 80 kV, pitch = 0.9 pixel, spacing = 0.7168 mm isotropic, tube current = 126 mA, exposure time = 0.5 second, image matrix size = 512 × 512 and slice thickness = 0.6 mm.

Imaging data were reconstructed with 3 iterations and 21 subsets and Gaussian filtering (order 3), with attenuation, scatter and point spread function corrections, and also with the application of time of flight methods. For the whole body, pixel spacing was 2.03642 × 2.03642 mm, and matrix size was 200 × 200 with a slice thickness of 3 mm. For the cardiac bed, Gaussian filtering (order 3) with 3 iterations and 21 subsets, all corrections, ZOOM value 2 were used, and pixel spacing was 1.59095 × 1.59095 mm and matrix size was 256 × 256 with a slice thickness of 2.027 mm.

3.3.3.3 PET/CT imaging data processing and analysis

PET images in DICOM format were first normalized for body weight and injected dose, by using the PET DICOM Extension available in 3D Slicer software [397, 398]. After normalization, the PET images and corresponding CT images were cropped to contain only the heart and neighboring ascending and descending aorta and saved in NIfTI format. Then, image processing and analysis were performed with the Carimas software (version 2.9, Turku, Finland Proper, Finland). Initially, the myocardium of the normalized HEC scan images was automatically segmented by using Carimas's automatic segmentation tool, followed by a manual adjustment when necessary, while taking into consideration the anatomical information from the co-registered CT images. The protocol of the cardiac segmentation was evaluated and approved by radiologists from Nuclear Medicine Department, which specialized in cardiac imaging. Once the myocardium was segmented, total SUVbw (standardized uptake value normalized by body weight) values were obtained. For liver and skeletal muscle, the analysis of DICOM formats was performed similarly to the heart but using the 3D Slicer software [397, 398] without cropping the images. CT images were used for segmentation and the PET images were used to obtain the ^{18}F-FDG uptake. Similar to the myocardium, segmentations were confirmed by radiologists from Nuclear

Medicine Department, who specialized in the liver and skeletal muscle imaging respectively to obtain the SUVbw values for further analysis.

CT Calcium Scoring was determined using a semi-automatic methodology by syngo.via cardiac CT software (version 5.01, Siemens Healthineers, Erlangen, Germany). Patients were classified as low or moderate cardiovascular risk (<400 AU) or high risk (>400 AU) based on their Agatston units (AU). Differences in frequency between groups were analyzed by Fisher's exact test. The radiodensity of the myocardium, skeletal muscle, and liver was obtained after the tissue/organ segmentation of the CT image using the CT Calcium Scoring images in DICOM format with the 3D Slicer.

Epicardial adipose tissue (EAT) was characterized by using a 3D Slicer from non-contrast CT images. Radiodensity values between -250 and -30 Hounsfield units (HU) were considered as EAT, as previously described [399]. EAT volume, radiodensity and thickness values were quantified and included in comparisons.

Brain analysis was done by voxel-based mapping analysis of PET images using the SPM8 software (https://www.fil.ion.ucl.ac.uk/spm/software/spm8/) running on Matlab for Windows (version 7.7, MathWorks, USA). Spatially normalized glucose metabolism images were smoothed with a 12-mm full-width Gaussian kernel at half-maximum. SPM was used to compare data between the baseline scan and the HEC scan. Significant responses were identified where voxel level p-value<0.001 and cluster size≥100 voxels. Voxel values of significant clusters in each patient were quantified and included in comparisons.

3.4 Results

3.4.1 Myocardial insulin resistance

In our group, we have determined two T2DM patient phenotypes in terms of myocardial IR according to their myocardial ^{18}F-FDG uptake after HEC [389]. Thus, patients were stratified into two groups, myocardial IR (mIR) and myocardial IS (mIS), depending on whether they had a significant increase in FDG uptake or not after the HEC procedure. As shown in **Figure 3.1**, after the HEC scan, mIS patients had a striking enhancement of ^{18}F-FDG uptake ($p<0.001$), while mIR patients had small or no ^{18}F-FDG uptake. In addition, myocardial radiodensity (mRD) was significantly increased in the mIR group ($p<0.05$). Therefore, our myocardial analyses were performed using both cohorts separately to show the alteration of GM and plasma and fecal metabolomics between both cohorts to establish possible metabolites or GM altered with the myocardial IR. Subsequently, we studied the associations of any metabolites or gut bacteria with myocardial insulin resistance using all patients from both cohorts in the same analysis to have a broad spectrum of patients with myocardial IR.

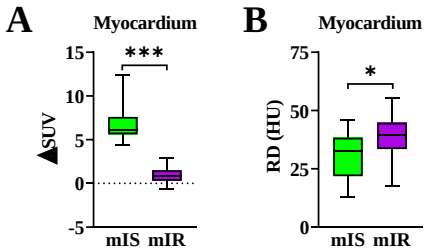

Figure 3.1 PET and CT imaging data analyses for the myocardium. A) Differences in standardized uptake value (ΔSUV) in the myocardium. B) Radiodensity (RD) of the myocardium. * and *** indicated $p<0.05$, and $p<0.001$, respectively. HU, Hounsfield units.

3.4.1.1 Anthropometric and biochemical parameters

As described above, according to myocardial ^{18}F-FDG uptake, seventeen T2DM patients (8 males / 9 females) were classified into the mIS group, and twenty-five patients (13 males / 12 females) were classified into the mIR group.

A comparative anthropometric and biochemical analysis was conducted between mIS and mIR patients, as summarized in **Table 3.1**. Patients were matched by gender and age and all anthropometric parameters, including the waist/hip ratio and BMI, did not show a significant difference between both cohorts. Compared with mIR patients, mIS patients had significantly higher whole-body insulin sensitivity (IS_{clamp}) ($p<0.01$), measured during HEC. Without being statistically significant, the systemic insulin sensitivity index QUICKI ($p=0.090$) showed a tendency to increase in patients with mIS while the insulin resistance index HOMA-IR ($p=0.089$) tended to decrease. Furthermore, the ratio of total cholesterol/HDL and the plasma concentration of total protein and albumin were prominently higher ($p<0.05$) in mIR patients. The concentration of calcium and chloride (two of the major blood electrolytes) was markedly elevated and decreased ($p<0.05$) respectively, in mIR subjects. Moreover, mIR patients tended to have higher levels of interleukin 6 (IL-6) ($p=0.052$), an inflammatory cytokine. Additionally, higher levels of liver enzymes AST, ALT, and GGT were observed in mIR patients ($p<0.01$). On the other hand, the NAFLD liver fat score and liver fat content were raised significantly ($p<0.05$) in patients with mIR. Finally, liver fibrosis index FIB-4 and the concentration of hyaluronic acid were increased ($p<0.05$) in mIR patients.

In summary, most biochemical indicators for T2DM complications, mainly related to liver pathology, were increased in the mIR group.

Table 3.1 Anthropometric and biochemical parameters of mIS and mIR patients.

	mIS	**mIR**
Number	17	25
Male/Female	8/9	13/12
Age	67.12 ± 2.03	65.08 ± 1.28

Waist/hip ratio	0.98 (0.95-1.06)	0.97 (0.92-1.04)
BMI (kg/m^2)	31.62 ± 1.12	31.59 ± 0.70
Glucose (mg/dL)	122.41 ± 7.96	130.40 ± 6.73
HbA1c (%)	6.96 ± 0.15	7.30 ± 0.18
Insulin (mU/L)	15.12 (9.31-19.24)	17.84 (11.51-33.85)
HOMA-IR	3.88 (3.19-5.28)	5.67 (3.68-10.36) $
QUICKI	0.31 (0.30-0.32)	0.30 (0.28-0.32) $
IS_{clamp} [mg/(kg·min)]	1.84 ± 0.15	1.34 ± 0.09 **
TyG index	8.72 ± 0.14	9.03 ± 0.10 $
Total GLP-1 (ng/mL)	1.42 ± 0.27	1.42 ± 0.16
Total cholesterol/HDL ratio	3.50 ± 0.20	4.14 ± 0.22 *
Total protein (g/dL)	6.80 (6.55-7.05)	7.20 (6.85-7.55) *
Albumin (g/dL)	4.1 (3.9-4.3)	4.4 (4.1-4.5) *
Interleukin-6 (pg/mL)	1.87 (1.50-3.70)	3.01 (1.81-5.89) $
Calcium (mg/dL)	9.3 (9.1-9.6)	9.7 (9.4-9.8) *
Chloride (mmol/L)	105 (103-109)	103 (102-105) *
AST (IU/L)	21.0 (17.0-23.5)	30.0 (22.0-44.0) **
ALT (IU/L)	17.0 (14.5-21.0)	29.0 (17.5-39.5) **
ALP (IU/L)	81.47 ± 7.87	74.76 ± 4.67
GGT (IU/L)	19.0 (13.5-28.0)	29.0 (23.0-51.5) **
AST/ALT ratio	1.14 (0.91-1.34)	1.07 (0.85-1.38)
NAFLD liver fat score	1.05 (0.47-1.75)	2.36 (1.04-4.44) *
Liver fat content (%)	8.32 (6.83-9.00)	13.07 (8.33-15.83) *
Fatty liver index	70.84 (46.29-89.27)	78.13 (61.01-92.89)
Hepatic steatosis index	40.90 (36.58-48.42)	41.71 (38.91-46.27)
FIB-4	1.18 (0.82-1.53)	1.73 (1.03-2.88) *
NAFLD fibrosis score	–0.44 ± 0.29	0.27 ± 0.31
ELF	9.07 ± 0.14	9.48 ± 0.17
TIMP-1 (ng/mL)	253.9 (230.9-290.0)	299.3 (219.8-335.2)
PIIINP (ng/mL)	7.82 (5.88-9.23)	6.57 (5.72-9.65)
Hyaluronic acid (ng/mL)	37.07 (27.49-46.97)	66.60 (32.25-98.20) *

BMI, body mass index; HbA1c, hemoglobin A1c; IS_{clamp}, insulin sensitivity measured during the HEC clamp; HOMA-IR, homeostasis model assessment of insulin resistance; QUICKI, quantitative insulin sensitivity check index; TyG index, triglyceride-glucose index; GLP-1, glucagon-like peptide 1; HDL, high-density lipoprotein cholesterol; GGT, gamma-glutamyl transferase; AST, aspartate aminotransferase; ALT, alanine aminotransferase; ALP, alkaline phosphatase; NAFLD; non-alcoholic fatty liver disease; FIB-4, liver fibrosis index 4; ELF, enhanced liver fibrosis; TIMP-1, tissue inhibitor of metalloproteinase 1; PIIINP, aminoterminal propeptide of type III procollagen. *, $p<0.05$; **, $p<0.01$; $, $0.05<p<0.1$.

3.4.1.2 Liver fibrosis measured by transient elastography

Continued with the biochemical analysis, the degree of hepatic fibrosis of patients was measured by FibroScan. As depicted in **Figure 3.2**, the results showed the LSM value was higher in mIR than in mIS ($p<0.05$).

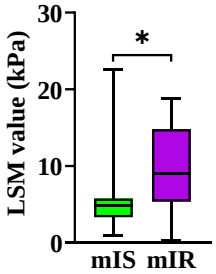

Figure 3.2 Liver fibrosis measurement in mIS and mIR groups. * indicated $p<0.05$. LSM, liver stiffness measurement; kPa, kilopascal.

3.4.1.3 Gut microbiota analyses between mIS and mIR

3.4.1.3.1 Gut microbiota composition and diversity analysis

Gut microbiota sequence data were analyzed for the mIS and mIR groups, as displayed in **Supplementary Figure 3.1** in Annex. The number of total sequence reads and filtered reads showed no difference between both cohorts of T2DM patients. In alpha diversity analysis, Faith's phylogenetic diversity index decreased apparently in the mIR group ($p<0.05$), as well as the number of observed features ($p=0.075$).

The relative abundance of major gut bacteria at the phylum and family level of both patient groups are shown in **Supplementary Figure 3.2** in Annex. The same kinds of bacteria were found in mIS and mIR, nevertheless, some differences in their average abundance could be detected. Compared with the mIS group, the percentage of Bacteroidetes, Proteobacteria, and Verrucomicrobia at the phylum level was elevated in the mIR group, while Firmicutes, Actinobacteria, and Fusobacteria were reduced.

At the family level, the proportion of Bacteroidaceae, Enterobacteriaceae, Veillonellaceae, Verrucomicrobiaceae, and Streptococcaceae increased in the mIR group, while Ruminococcaceae, Lachnospiraceae, Bifidobacteriaceae, and Fusobacteriaceae decreased.

3.4.1.3.2 Identification of the most relevant alterations in gut microbiota between mIS and mIR

In order to analyze the differences in gut microbiota, multivariate analyses were conducted between mIS and mIR groups. Although no clear separation was observed in the PCA plot (**Figure 3.3A**), a robust PLS-DA model was established by all significant gut bacteria, as depicted in **Figure 3.3B**.

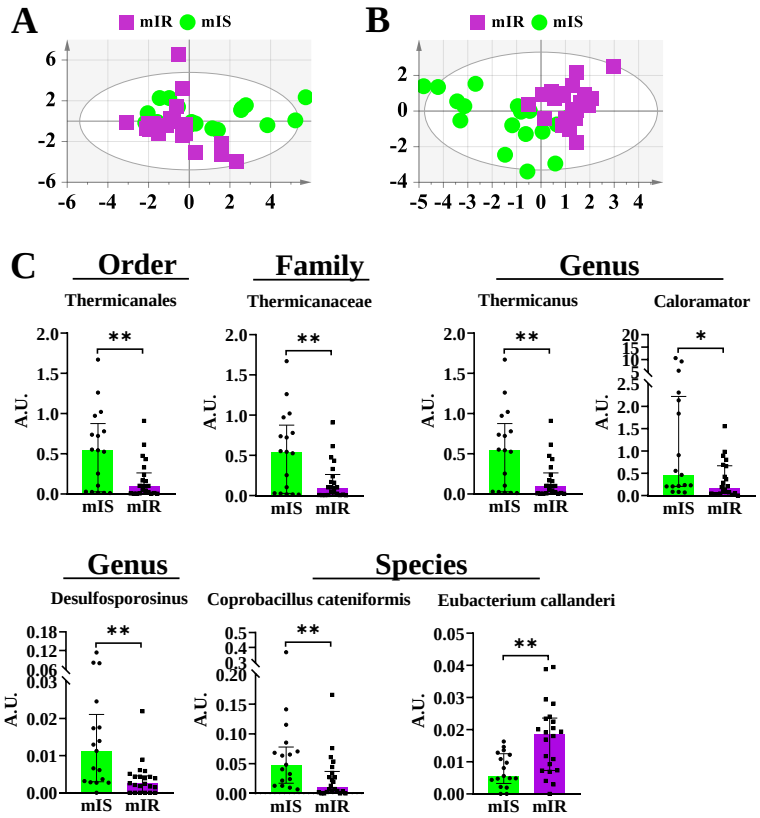

Figure 3.3 Most relevant gut bacteria differing between patients with mIS and mIR. A) showed the PCA score plot of significant gut bacteria, and the parameters of the PCA model were: UV scaling, R2X(cum)= 0.501, Q2(cum)= 0.008. B) depicted the PLS-DA score plot of significant gut bacteria, and

the parameters of the model were: UV scaling, R2Y(cum)= 0.632, Q2(cum)= 0.272. Permutation test: R2=(0.0, 0.295), Q2=(0.0, -0.234), p from CV-Anova = 0.074. C) displayed relative abundance of the most relevant gut bacteria with VIP value >1 and significant p-value from Mann-Whitney test <0.05. Data were shown as the median and interquartile range in all bar plots. * and ** indicated p<0.05 and p<0.01 respectively. A.U., arbitrary units.

Based on the PLS-DA model, the most important gut bacteria were obtained by VIP value >1 and submitted to univariate analysis, as shown in **Figure 3.3C**. Thus, the abundance of order Thermicanales, family Thermicanaceae, genera *Thermicanus*, *Caloramator*, and *Desulfosporosinus*, and species *Coprobacillus cateniformis* was prominently reduced in the mIR group (p<0.05), while species *Eubacterium callanderi* was raised (p<0.01).

3.4.1.3.3 Multivariate regression analysis of gut microbiota with biochemical variables

To complete the analysis, multivariate linear regression (PLS) was conducted between the gut bacterial profile and all significant biochemical variables between mIR and mIS cohorts (**Table 3.1**). No valid models were obtained in any case.

3.4.1.4 Fecal metabolomics analysis between mIS and mIR patients with T2DM

3.4.1.4.1 Identification of the most relevant fecal metabolites

The fecal metabolome of the mIS and the mIR groups was determined by ^{1}H-NMR spectroscopy, as described in the Materials and Methods section. Then, PCA analysis was performed to establish possible differences between both groups, This analysis showed a slight separation between both groups (**Figure 3.4A**), nevertheless, no discriminant models could be obtained for the separation of mIS and mIR. Therefore, data were only analyzed by univariate analysis using Mann-Whitney non-parametric test. Interestingly, several fecal metabolites were reduced (p<0.05) in mIR patients,

including the sugars arabinose, β-galactose, and ribose, and the amino acids aspartate and histidine, and lactate (**Figure 3.4B**).

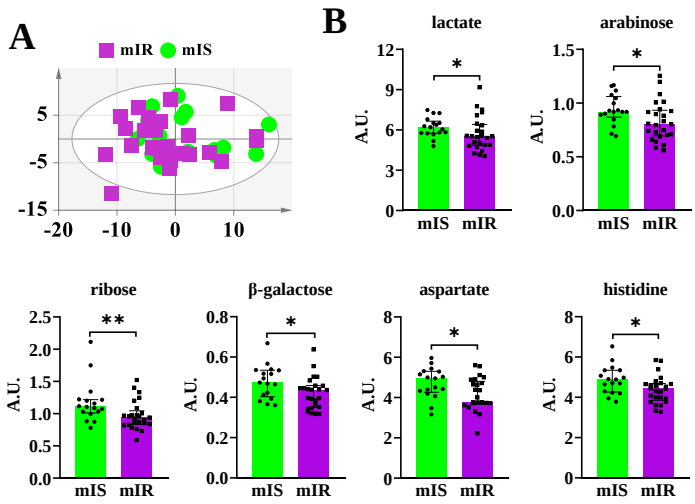

Figure 3.4 Fecal metabolites that are significantly altered between mIS and mIR cohorts. A) showed the PCA score plot of fecal metabolomics data, and the parameters of the PCA model were: UV scaling, R2X(cum)= 0.674, Q2(cum)= 0.306. B) displayed normalized concentrations of significant fecal metabolites indicating significance from univariate analysis $p<0.05$. Data were shown as the median and interquartile range in all bar plots. * and ** indicated $p<0.05$ and $p<0.01$ respectively. A.U., arbitrary units.

3.4.1.4.2 Multivariate regression analysis of fecal metabolomics with biochemical variables

Multivariate linear regression analysis was conducted for fecal metabolomics and all significant biochemical variables between the mIS and mIR groups of T2DM patients (**Table 3.1**). Only one weak PLS model was obtained, for the correlation with the hepatic enzyme GGT, as displayed in **Supplementary Figure 3.3** in Annex.

3.4.1.5 Plasma metabolomics analyses between mIS and mIR

3.4.1.5.1 Identification of the most relevant plasma metabolites

The plasma metabolome of mIS and mIR patients was obtained by ^{1}H-NMR spectroscopy, as described in the Materials and Methods section. In order to reduce

the dimensionality of the database and capture the most important variables, PCA and PLS-DA analyses were carried out with the plasma metabolites.

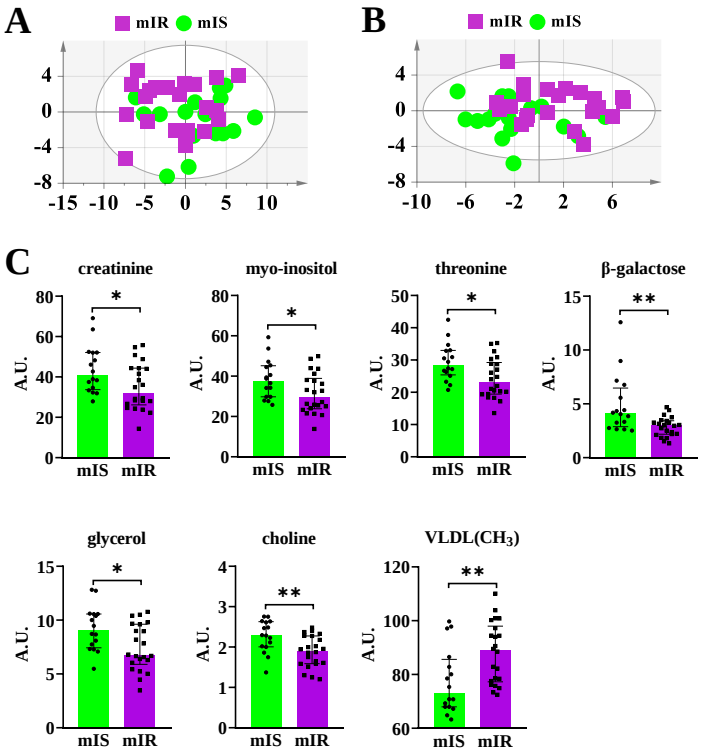

Figure 3.5 Relevant plasma metabolites that were different between mIS and mIR groups. A) showed the score plot of the PCA model of plasma metabolic profiles, and the parameters of the model were: UV scaling, R2X(cum)= 0.874, Q2(cum)= 0.567. B) displayed the score plot of the PLS-DA model of plasma metabolic profiles, and the parameters of the model: UV scaling, R2Y(cum)= 0.57, Q2(cum)= 0.218. Permutation test: R2=(0.0, 0.318), Q2=(0.0, -0.245), p from CV-Anova = 0.153. C) depicted normalized concentrations of the most relevant plasma metabolites with VIP value >1 and p-value from the Mann-Whitney test <0.05. * and ** indicated $p<0.05$ and $p<0.01$, respectively. A.U., arbitrary units.

As exhibited in **Figure 3.5**, a partial separation between groups was observed in the PCA model, and a moderate PLS-DA model separating the mIS and mIR groups was obtained. The most important metabolites in the separation were selected by VIP value >1 of the PLS-DA model and a significant p-value in the following univariate analysis shown in **Figure 3.5C**. As a result, lower levels ($p<0.05$) of six plasma metabolites including creatinine, myo-inositol, threonine, β-galactose, glycerol, and choline, and a pretty higher level ($p<0.01$) of VLDL(CH_3) were found in mIR patients.

3.4.1.5.2 Multivariate regression analysis of plasma metabolomics with biochemical variables

Regression analysis was also performed to determine the relationship between the plasma metabolomic profiles and all significant biochemical parameters between mIR and mIS cohorts (**Table 3.1**). Nevertheless, as a result, only one weak PLS model could be obtained with the correlation of plasma albumin, as depicted in **Supplementary Figure 3.4** in Annex.

3.4.1.6 Associations between gut microbiota, metabolomics, myocardial IR (obtained by PET), myocardial structural changes (obtained by CT image), liver stiffness measurements, and biochemical parameters that differ between mIS and mIR groups

The association of all the altered variables between the mIS and mIR groups was obtained in the section. Thus, it is intended to find the relationship between biochemical alterations, myocardial IR, and structural affectation with the intestinal microbiota and plasmatic and fecal metabolites, as well as the association between biota and metabolomics. This study was conducted using all T2DM patients together to have a broad spectrum of variables for association studies.

3.4.1.6.1 Relationships of gut microbiota and metabolomics with biochemical variables

Although no general correlation between bacterial and metabolomic profiles with significant biochemical parameters could be established, we found some relevant individual relationships as shown in **Figure 3.6A**.

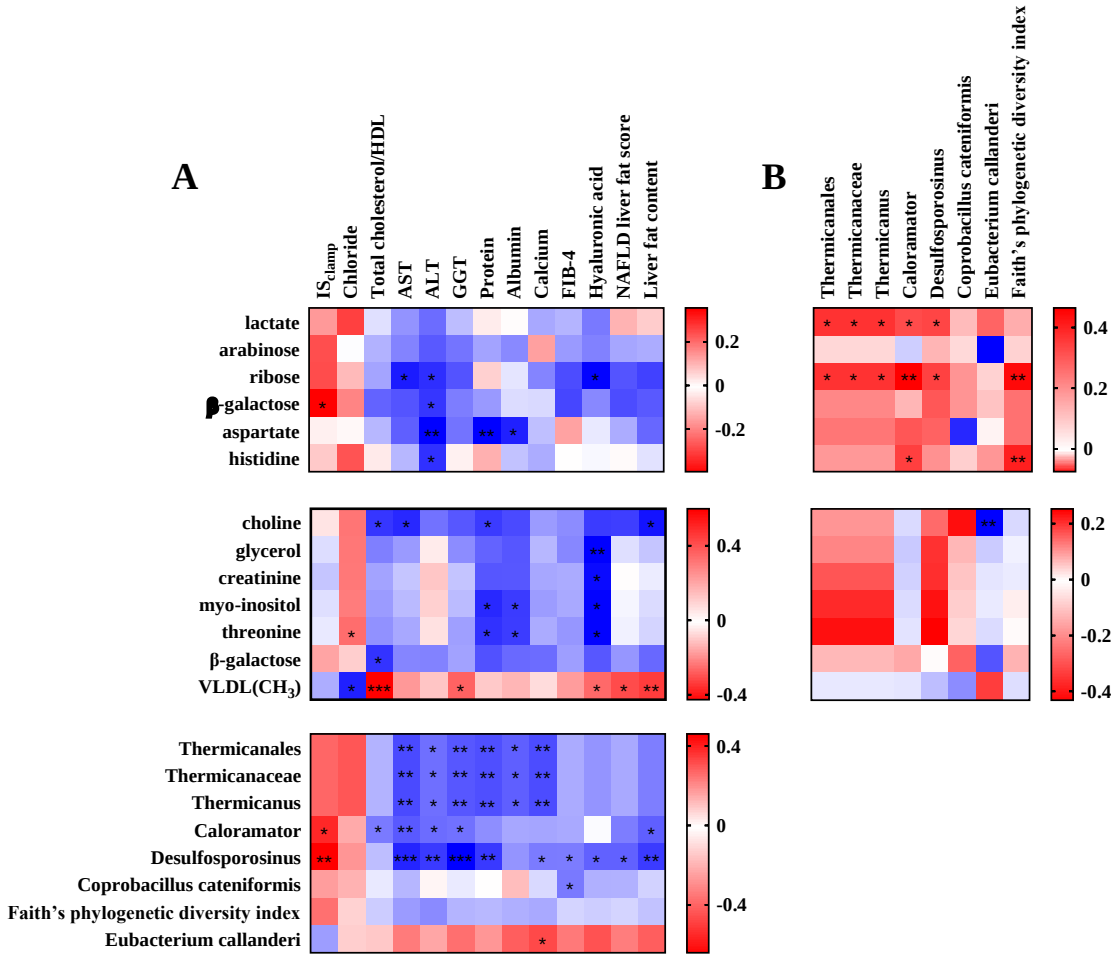

Figure 3.6 Spearman correlation analyses between gut microbiota, metabolomics, and biochemical parameters in the mIS and mIR groups. A) Correlations of significant biochemical parameters with significant fecal metabolites (upper), the most relevant plasma metabolites (middle), and gut bacteria and alpha diversity index (lower). B) Correlations of the most relevant gut bacteria and alpha diversity index with significant fecal (upper) and plasma metabolites (lower). No significant correlations were found between significant fecal and plasma metabolites. IS_{clamp}, insulin sensitivity measured during the HEC clamp; HDL, high-density lipoprotein cholesterol; GGT, gamma-glutamyl transferase; AST, aspartate aminotransferase; ALT, alanine aminotransferase; NAFLD; non-alcoholic fatty liver disease; FIB-4, liver fibrosis index 4. *, ** and *** indicated $p<0.05$, $p<0.01$ and $p<0.001$, respectively.

For fecal metabolites, IS_{clamp} was positively related to β-galactose ($p<0.05$), while the hepatic enzymes AST and ALT were negatively related to ribose ($p<0.05$). Furthermore, ALT also showed negative associations with β-galactose, aspartate, and histidine ($p<0.05$). Biochemical variables total protein and albumin correlated negatively with fecal aspartate ($p<0.05$).

Regarding the plasma metabolites, no significant correlation was obtained for IS_{clamp}. However, plasma VLDL(CH_3) was positively linked with total cholesterol/HDL, GGT, hyaluronic acid, NAFLD liver fat score, and liver fat content, and inversely related with chloride ($p<0.05$). On the contrary, choline was negatively related to some of the previously mentioned variables. In addition, negative relationships between total protein and albumin with plasma myo-inositol and threonine were proved ($p<0.05$).

For the most relevant gut bacteria, two genera *Caloramator* and *Desulfosporosinus* were positively associated with IS_{clamp} while inversely to liver enzymes AST, ALT, and GGT ($p<0.05$). In particular, *Desulfosporosinus* was also negatively correlated with all significant markers of liver physiology ($p<0.05$). Regarding, Thermicanales taxa, including Thermicanaceae and *Thermicanus*, were negatively associated with all hepatic enzymes, total proteins, albumin, and calcium ($p<0.05$). However, *Eubacterium callanderi* was positively linked with plasma calcium ($p<0.05$).

3.4.1.6.2 Relationships of gut microbiota with metabolomics in mIS and mIR

We further wanted to know if we could identify any specific correlations between gut bacteria and feces/plasma metabolites. As depicted in **Figure 3.6B**, only significant positive correlations were found between gut bacteria and fecal metabolites, while only one negative correlation was found between gut bacteria and plasma metabolites. Thus, fecal lactate and ribose were related to Thermicanales taxa, *Caloramator*, and *Desulfosporosinus* ($p<0.05$). Further, the genus *Caloramator* was associated with fecal histidine ($p<0.05$). On the other hand, *Eubacterium callanderi* showed a pronounced association with plasmatic choline ($p<0.01$).

Faith's phylogenetic diversity index, as mentioned above, revealed a significant difference between mIS and mIR cohorts of T2DM patients. It was found to be significantly associated only with fecal metabolites, as indicated in **Figure 3.6B**, where Faith's phylogenetic diversity index showed positive associations with ribose, and histidine ($p<0.01$).

3.4.1.6.3 Relationships of myocardial IR (obtained by PET), myocardial structural changes (obtained by CT image), liver stiffness measurements, biochemical parameters, gut microbiota and metabolomics in mIS and mIR

After a comparison of the imaging data between the mIS and the mIR groups, we further wanted to establish their relationships with other significant variables. We found some marked correlations between imaging variables and biochemical parameters, depicted in **Figure 3.7A**. Myocardial ΔSUV had a positive correlation with IS_{clamp} and serum chloride but had a negative correlation with hepatic markers total cholesterol/HDL ratio, AST, ALT, GGT, NAFLD liver fat score, and liver fat content and total protein ($p<0.05$). CT imaging variable mRD was negatively associated with IS_{clamp}, while positively with total cholesterol/HDL ratio, and liver fat content ($p<0.05$). Moreover, LSM values were positively related to GGT and liver fat content ($p<0.05$).

There were also some significant associations between imaging variables and fecal metabolites, as delineated in **Figure 3.7B**. Myocardial ΔSUV showed a positive association with the most significant fecal metabolites, including arabinose, β-galactose, ribose, aspartate, and histidine ($p<0.05$). Myocardial radiodensity (mRD) was negatively related to fecal ribose, as well as LSM values with β-galactose ($p<0.05$).

Furthermore, some significant correlations were also found between plasma metabolites and imaging variables (**Figure 3.7C**). ΔSUV in the myocardium was positively associated with plasma choline and β-galactose while inversely with VLDL(CH_3) ($p<0.05$). And mRD and LSM values had a negative association with plasma β-galactose ($p<0.05$). On the contrary, LSM values were shown a positive association with VLDL(CH_3) ($p<0.05$)

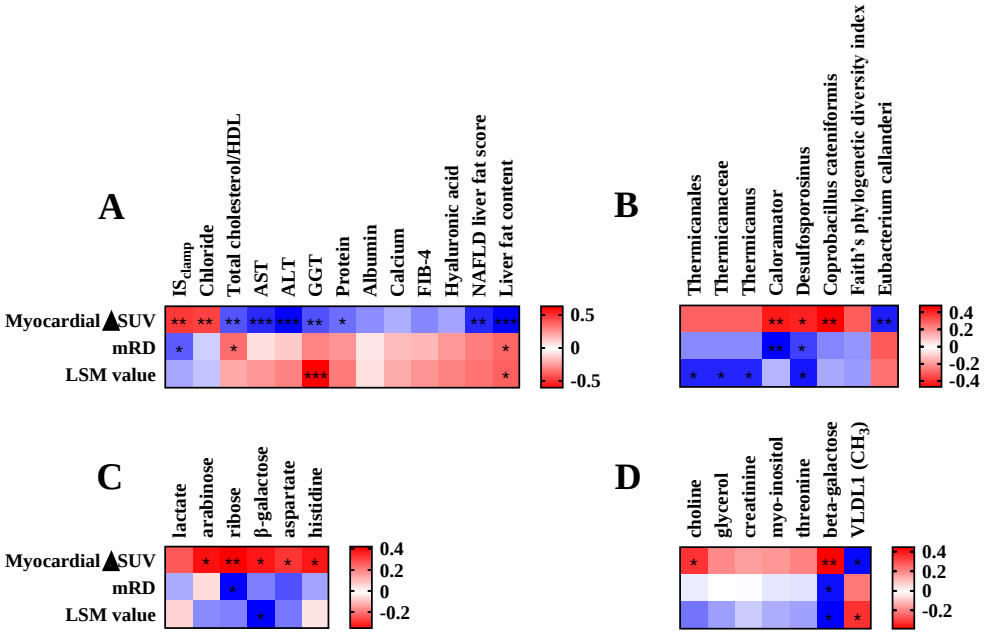

Figure 3.7 Spearman correlation analyses of significant imaging variables and LSM value with metabolomic, bacterial, and biochemical parameters in mIS and mIR groups. Correlations of myocardial ΔSUV, mRD, and LSM value with A) altered biochemical parameters, B) gut bacteria and alpha diversity index, C) fecal metabolites, and D) plasma metabolites in mIR and mIS cohorts. IS_{clamp}, insulin sensitivity measured during the HEC clamp; HDL, high-density lipoprotein cholesterol; GGT, gamma-glutamyl transferase; AST, aspartate aminotransferase; ALT, alanine aminotransferase; NAFLD; non-alcoholic fatty liver disease; FIB-4, liver fibrosis index 4; ΔSUV, differences in standardized uptake value; mRD, myocardial radiodensity; and LSM, liver stiffness measurement. *, ** and *** indicated p<0.05, p<0.01 and p<0.001, respectively.

Furthermore, the correlations between gut bacteria and imaging variables were studied as well, as depicted in **Figure 3.7D**. Myocardial ΔSUV indicated a positive connection to the genera *Caloramator*, *Desulfosporosinus*, and species *Coprobacillus cateniformis*, but presented an inverse connection to the species *Eubacterium callanderi* (p<0.01). And mRD presented negative associations with *Caloramator* and *Desulfosporosinus* (p<0.05). LSM values were negatively associated with Thermicanales taxa, and *Desulfosporosinus* (p<0.05)

3.4.2 Liver insulin resistance

Aside from the two phenotypes related to the myocardium discovered in our research group, two phenotypes related to the liver were also discovered, such as liver insulin resistance (L-IR) and liver insulin sensitivity (L-IS), which were discovered when considering ^{18}F-FDG uptake in the liver by PET. L-IS was characterized by a decrease in FDG uptake after HEC, while L-IR by an increase in FDG uptake, as shown in **Figure 3.8**. Therefore, they had a dramatic difference in ΔSUV. However, the liver radiodensity did not have any difference between the two groups.

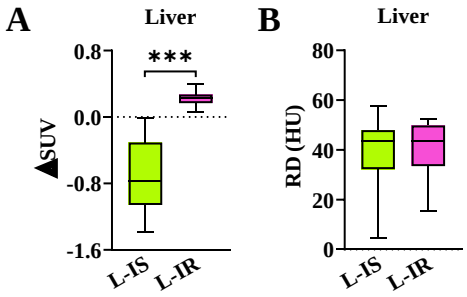

Figure 3.8 PET and CT imaging data analyses for the liver. A) Differences in standardized uptake value (ΔSUV) in the liver. B) Radiodensity (RD) of the liver. *** indicated p<0.001. HU, Hounsfield units.

3.4.2.1 Anthropometric and biochemical parameters of T2DM patients

A comparison of the major anthropometric and biochemical parameters of L-IS and L-IR patients is summarized in **Table 3.2**. Patients were gender and age matches, and the anthropometric parameters including the BMI and waist/hip ratio showed no statistical difference between L-IS and L-IR phenotypes. IS_{clamp} was higher in the L-IS group than in the L-IR group ($p<0.05$), although no evident difference in glucose, insulin, and HbA1c and HOMA-IR and QUICKI indices were found between both groups. However, the plasma concentration of GLP-1 tended to be increased in L-IR

patients, without reaching statistical significance (p=0.091). Furthermore, total bilirubin concentration increased markedly in L-IR patients (p<0.05), as well as the conjugated bilirubin showed a trend to increase (p=0.056). In terms of liver enzymes, only GGT was elevated prominently in L-IR (p<0.05). Regarding the ELF score and the concentration of hyaluronic acid, they also were increased in patients with L-IR (p<0.05). On the contrary, chloride was decreased in L-IR patients (p<0.05).

Table 3.2 Anthropometric and biochemical information between L-IS and L-IR.

	L-IS	**L-IR**
Number	28	13
Male/Female	14/14	6/7
Age	66.50 ± 1.38	65.62 ± 1.82
Waist/hip ratio	0.97 (0.95-1.06)	0.98 (0.90-1.02)
BMI (kg/m^2)	30.57 (28.59-35.73)	30.69 (28.49-34.35)
Glucose (mg/dL)	126.9 ± 6.2	126.5 ± 10.1
HbA1c (%)	7.01 ± 0.14	7.39 ± 0.26
Insulin (mU/L)	16.75 (9.92-23.69)	17.56 (11.60-42.77)
HOMA-IR	4.76 (3.08-7.20)	5.37 (3.83-12.98)
QUICKI	0.304 ± 0.007	0.299 ± 0.011
IS_{clamp} [mg/(kg ·min)]	1.66 ± 0.11	1.26 ± 0.11 *
Total GLP-1 (ng/mL)	0.96 (0.29-1.73)	1.85 (0.79-2.09) $
Interleukin-6 (pg/mL)	2.10 (1.50-4.33)	3.41 (2.23-5.86)
Urea (mg/dL)	40.46 ± 2.62	42.85 ± 5.10
Total protein (g/dL)	7.02 ± 0.12	7.21 ± 0.12
Total bilirubin (mg/dL)	0.45 (0.35-0.62)	0.67 (0.57-0.93) *
Conjugated bilirubin (mg/dL)	0.20 (0.19-0.25)	0.24 (0.23-0.29) $
Chloride (mmol/L)	104.8 ± 0.6	101.9 ± 1.3 *
Troponin I (pg/mL)	6.5 (3.3-10.8)	6.0 (3.0-10.5)
Adiponectin (μg/mL)	3.22 (2.33-5.70)	5.29 (2.09-6.34)
GGT (IU/L)	22.5 (16.3-29.0)	34.0 (26.0-123.50) *
NAFLD liver fat score	1.67 (0.58-2.94)	1.72 (1.02-5.72)
Liver fat (%)	8.67 (6.89-13.28)	9.98 (7.79-16.22)
Hepatic steatosis index	42.38 ± 1.06	41.40 ± 1.30
Fatty liver index	69.32 ± 4.55	77.42 ± 5.50
FIB-4	1.28 (0.93-2.00)	1.42 (0.97-3.08)
ELF	9.14 ± 0.13	9.76 ± 0.26 *
TIMP-1 (ng/mL)	266.3 (230.4-309.1)	266.1 (217.6-428.5)
PIIINP (ng/mL)	7.42 ± 0.36	8.12 ± 1.28
Hyaluronic acid (ng/mL)	39.81 (28.62-75.62)	86.18 (37.72-153.30) *
NAFLD fibrosis score	–0.07 ± 0.25	0.23 ± 0.45

BMI, body mass index; HbA1c, hemoglobin A1c; IS_{clamp}, insulin sensitivity measured during the HEC clamp; HOMA-IR, homeostasis model assessment of insulin resistance; QUICKI, quantitative insulin sensitivity check index; TyG index, triglyceride-glucose index; GLP-1, glucagon-like peptide 1; GGT, gamma-glutamyl transferase; NAFLD; non-alcoholic fatty liver disease; FIB-4, liver fibrosis index 4; ELF, enhanced liver fibrosis; TIMP-1, tissue inhibitor of metalloproteinase 1; PIIINP, aminoterminal propeptide of type III procollagen. *, p<0.05; $, 0.05<p<0.1

3.4.2.2 Liver fibrosis measured by transient elastography

Further, the degree of liver fibrosis in patients was measured by transient elastography. As depicted in **Figure 3.9**, the results showed the LSM value was higher in L-IR than in L-IS (p<0.05).

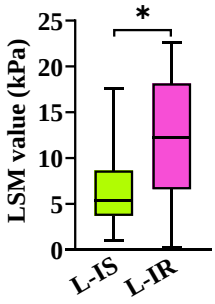

Figure 3.9 Liver fibrosis measurements in L-IS and L-IR groups. * indicated p<0.05. LSM, liver stiffness measurement; kPa, kilopascal.

3.4.2.3 Alterations of the gut microbiota between L-IS and L-IR phenotypes of T2DM patients

3.4.2.3.1 Composition and diversity of the gut microbiota

Fecal DNA sequencing data were analyzed for the L-IS and L-IR groups, as displayed in **Supplementary Figure 3.5** in Annex. The number of total reads and filtered reads was found significantly lower in the L-IR group (p<0.05). All samples reached a plateau in the rarefaction curve, which meant our sequencing depth was enough for

further analysis. Compared with the L-IS group, Shannon's diversity index (p=0.071) and Pielou's evenness index (p=0.080) showed a trend to increase in L-IR, without reaching statistical significance.

Gut bacteria at the phylum and family level showed some altered tendencies between both liver phenotypes of T2DM patients (**Supplementary Figure 3.6** in Annex**)**. At the phylum level, Firmicutes tended to increase in L-IR while Proteobacteria, Actinobacteria, Verrucomicrobia, and Fusobacteria tended to decrease. At the family level, the abundance of Ruminococcaceae, Clostridiaceae, and Streptococcaceae was elevated in L-IR patients while the abundance of Bifidobacteriaceae, Enterobacteriaceae, Verrucomicrobiaceae, and Fusobacteriaceae was reduced.

3.4.2.3.2 Altered gut bacteria between L-IS and L-IR phenotypes of T2DM patients

In order to identify the gut bacteria related to liver IR, a multivariate analysis was conducted with the gut sequencing data of both groups. As depicted in **Figures 3.10A** and **B**, even though the PCA model did not show a very clear separation, the OPLS-DA discriminant model demonstrated the potential to separate samples from the two groups. The variables with VIP values >1 and p values <0.05 from the Mann-Whitney test were considered the most significant. Applying these criteria, only one genus *Eubacterium* was found to be altered in patients with L-IR ($p<0.05$) (**Figure 3.10C**). We further tried to perform a multivariate regression analysis of significant biochemical variables versus the GM, but we did not obtain any valid model.

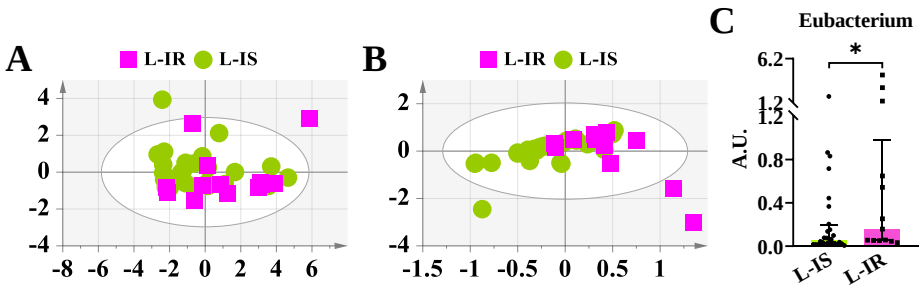

Figure 3.10 The most relevant gut bacteria between patients with L-IS and L-IR. A) showed the PCA score plot of significant gut bacteria, and the parameters of the PCA model were: UV scaling, R2X(cum)= 0.716, Q2(cum)= 0.454. B) presented the OPLS-DA score plot of significant gut bacteria, and the parameters of the model were: Pareto scaling, R2Y(cum)= 0.373, Q2(cum)= 0.247. Permutation test: R2=(0.0, 0.071), Q2=(0.0, -0.221), p from CV-Anova = 0.033. C) displayed the relative abundance of the most relevant gut bacteria with VIP value >1 and p-value from the Mann-Whitney test <0.05. * indicated p<0.05. A.U., arbitrary units.

3.4.2.4 Fecal metabolomics analyses of L-IS and L-IR patients

3.4.2.4.1 Identification of the most relevant fecal metabolites altered in liver insulin resistance phenotypes

PCA analysis and discriminant analysis were performed to reduce the dimensionalities of fecal metabolomics data and to capture the most important variables. As shown in **Figure 3.11**, both PCA and PLS-DA plots showed a separation between the samples from the two groups. Interestingly, the L-IS samples were divided into two clusters, one that overlapped with the L-IR samples, and one that was very clearly separated from the L-IR samples. After a selection guided by VIP values and univariate statistics, fecal metabolite 2-hydroxybutyrate was found to be reduced in L-IR (p<0.05).

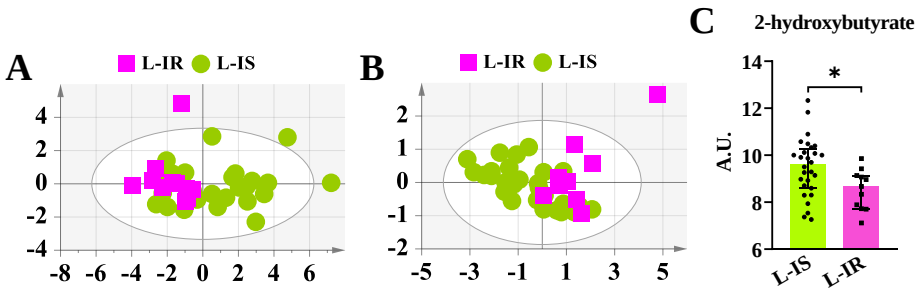

Figure 3.11 The most relevant fecal metabolites between patients with L-IS and L-IR. A) showed

the score plot of the PCA model of fecal metabolic profiles, and the parameters of the model were: UV scaling, R2X(cum)= 0.626, Q2(cum)= 0.296. B) displayed the score plot of the PLS-DA model of fecal metabolic profiles, and the parameters of the model were: Pareto scaling, R2Y(cum)= 0.350, Q2(cum)= 0.177. Permutation test: R2=(0.0, 0.131), Q2=(0.0, -0.190), p from CV-Anova = 0.104. C) showed the normalized concentration of the most relevant fecal metabolites with VIP value >1 and p-value <0.05 from the Mann-Whitney test. * indicated p<0.05. A.U., arbitrary units.

3.4.2.4.2 Multivariate regression analysis of fecal metabolomics with biochemical variables

Correlation between fecal metabolic profiles and significant biochemical parameters was conducted by PLS regression analysis. As a result, a good model was obtained against the total bilirubin, as displayed in **Supplementary Figure 3.7** in Annex.

3.4.2.5 Comparison of plasma metabolites between L-IS and L-IR patients

3.4.2.5.1 Identification of significantly altered plasma metabolites between L-IS and L-IR patients

In PCA analysis of plasma metabolomics data, no clustering could be detected between L-IS and L-IR patients (**Figure 3.12A**). Further, no discriminant model could be established between both groups. However, applying univariate analysis, one significant plasma metabolite, glycerol, could be identified as decreased in the L-IR group (**Figure 3.12B**).

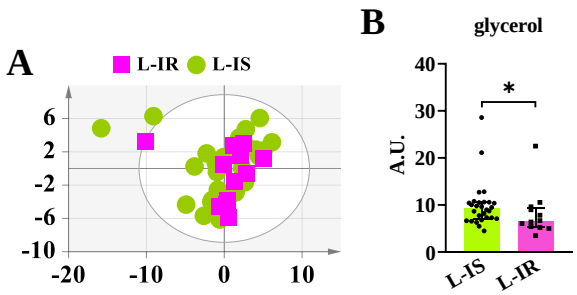

Figure 3.12 Significant plasma metabolites between L-IS and L-IR. A) showed the PCA score plot of plasma metabolomics data and the parameters of the PCA model were: UV scaling, R2X(cum)= 0.844, Q2(cum)= 0.657. B) displayed the normalized concentration of significant plasma metabolites with a p-value from univariate analysis <0.05. * indicated p<0.05. A.U., arbitrary units.

3.4.2.5.2 Multivariate regression analysis of plasma metabolomics with biochemical variables

In order to find the associations between plasma metabolites and significant biochemical parameters, multivariate regression analysis was performed. Two PLS models were obtained that correlate the plasma metabolome, as reflected in **Supplementary Figure 3.8** in Annex. However, these two plots did not indicate an association between plasma metabolic profiles and IS_{clamp} or hyaluronic acid.

3.4.2.6 Correlations between gut microbiota, metabolomics, liver IR (obtained by PET), liver stiffness measurements, and biochemical parameters in L-IS and L-IR groups

3.4.2.6.1 Relationships of biochemical characteristics with gut microbiota and metabolomics

Spearman's correlation analyses were done between all metabolomic, gut bacteria, and biochemical variables that differed significantly between L-IS and L-IR. Significant relationships were only found between the biochemical parameters GGT,

ELF, hyaluronic acid, and plasma metabolite glycerol that were negatively associated (**Figure 3.13**).

Initially, in our research plans, we want to identify some specific gut bacteria related to GLP-1, as well as fecal and plasma metabolites. However, the plasma GLP-1 concentration was only measured for T2DM patients and was not observed significant differences in any above studies. Only patients with L-IS and L-IR showed a tendency to be significantly different (p=0.091). We also performed a correlation analysis between GLP-1, gut bacteria, and fecal and plasma metabolites to see if any significant correlations could be obtained. Also, no significant correlations were found, and it just tended to correlate positively with the genus *Eubacterium* (rho= 0.291, p= 0.085).

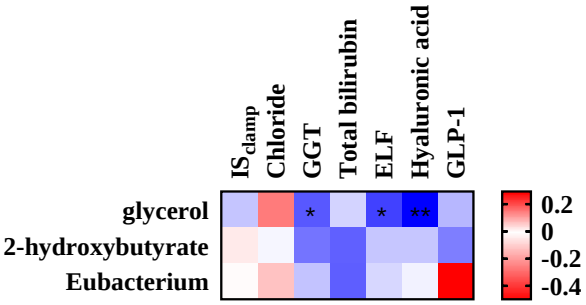

Figure 3.13 Spearman correlation analyses between biochemical parameters and plasma glycerol in patients with L-IS and L-IR. No significant correlations were found between biochemical parameters, *Eubacterium*, and fecal 2-hydroxybutyrate, between plasma glycerol, fecal 2-hydroxybutyrate, and *Eubacterium*. GGT, gamma-glutamyl transferase; ELF, enhanced liver fibrosis; GLP-1, glucagon-like peptide 1; IS_{clamp}, insulin sensitivity measured during the HEC clamp. * and ** indicated $p<0.05$ and $p<0.01$, respectively.

3.4.2.6.2 Relationships of liver IR (obtained by PET), liver stiffness measurements with significant biochemical, gut microbiota, and metabolomics variables in L-IS and L-IR

Significant PET variable liver ΔSUV and FibroScan data also correlated with relevant metabolomic, gut bacteria, and biochemical variables, and the results are summarized in **Figure 3.14**. IS_{clamp} was negatively related to liver ΔSUV, while plasma GGT level

was positively to liver ΔSUV and LSM value ($p<0.01$). Regarding gut bacteria, fecal and plasma metabolites, only plasma metabolite glycerol had significant correlations as negatively correlated with liver ΔSUV ($p<0.05$).

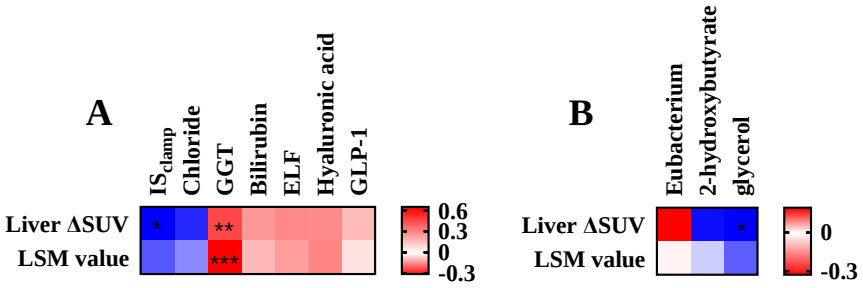

Figure 3.14 Spearman correlation analyses of liver ΔSUV and LSM value with metabolomic, bacterial, and biochemical variables in patients with L-IS and L-IR. Correlations of myocardial ΔSUV, and LSM value with A) altered biochemical parameters, B) gut bacteria *Eubacterium*, fecal 2-hydroxybutyrate, and plasma glycerol in L-IR and L-IS patients. GGT, gamma-glutamyl transferase; ELF, enhanced liver fibrosis; GLP-1, glucagon-like peptide 1; IS_{clamp}, insulin sensitivity measured during the HEC clamp; LSM, liver stiffness measurement; ΔSUV, differences in standardized uptake value. *, ** and *** indicated $p<0.05$, $p<0.01$, and $p<0.001$, respectively.

3.4.3 Skeletal muscle insulin resistance

We could not divide T2DM patients by skeletal muscle IR phenotypes because the data did not show different behavior from T2DM patients. Therefore, only correlation studies were performed.

3.4.3.1 Associations of the skeletal muscle insulin sensitivity with gut microbiota, plasma/fecal metabolomics, and biochemical and anthropometric data

Spearman's correlation analysis was performed for all patients (n= 46) between skeletal muscle ΔSUV and data from the anthropometric and biochemical analysis, metabolomics, and fecal sequencing. Significant correlations were shown in **Figure 3.15**. Several biochemical parameters, but not anthropometric parameters, presented

significant relationships with skeletal muscle ΔSUV. Thus, IS_{clamp} and adiponectin showed positive correlations, while ALT, hepatic steatosis index, and liver fat content had inverse correlations ($p<0.05$). However, skeletal muscle ΔSUV did not correlate significantly with HOMA-IR and QUICKI. Plasma metabolites, not fecal metabolites, were found to be significantly associated with skeletal muscle ΔSUV. Namely, plasma metabolites tyrosine and histidine had positive associations with skeletal muscle ΔSUV ($p<0.05$).

Moreover, in the gut microbiota, Caldilineales taxa (Caldilineaceae, *Caldilinea*, *Caldilinea tarbellica*) were positively associated with skeletal muscle ΔSUV ($p<0.05$). In addition, genera *Desulfosporosinus* and *Mogibacterium* and species *Carboxydocella ferrireducens* were also positively associated with skeletal muscle ΔSUV, while the family Veillonellaceae was negatively associated ($p<0.01$).

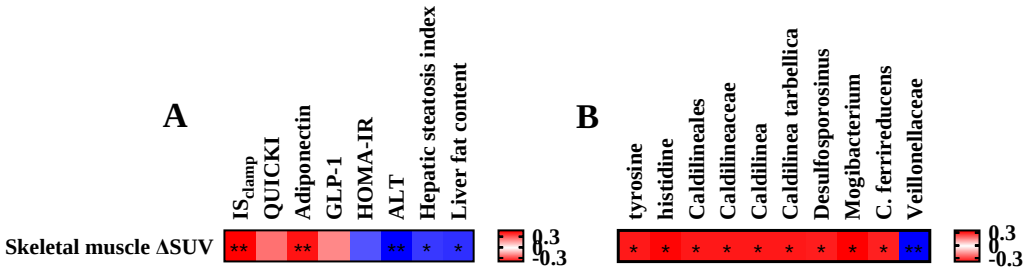

Figure 3.15 Spearman correlation analyses of skeletal muscle ΔSUV with anthropometric and biochemical parameters, gut microbiota, fecal and plasma metabolomics in all T2DM patients. Significant correlations were not observed between skeletal muscle ΔSUV and defined fecal metabolites, but were found between skeletal muscle ΔSUV and plasma metabolites tyrosine and histidine. IS_{clamp}, insulin sensitivity measured during the HEC clamp; GLP-1, glucagon-like peptide 1; HOMA-IR, homeostasis model assessment of insulin resistance; QUICKI, quantitative insulin sensitivity check index; ALT, alanine aminotransferase; ΔSUV, differences in standardized uptake value. * and ** indicated $p<0.05$ and $p<0.01$, respectively.

3.4.4 Brain insulin resistance and sensitivity

SPM analysis of brain images was done between HEC - baseline PET scans to show the insulin-sensitive regions of T2DM patients and between baseline – HEC PET scans to determine the insulin-resistant regions of T2DM patients. As shown in

Figure 3.16, when HEC minus baseline (IS regions), a significant increase was observed in cerebellar vermis VI, left parahippocampal gyrus, right hippocampus, left amygdala, left olfactory bulb, and left middle cingulate gyrus. Reversely, when baseline minus HEC (IR regions), a significant decrease was obtained in the right superior temporal gyrus, left superior temporal gyrus, and right precuneus.

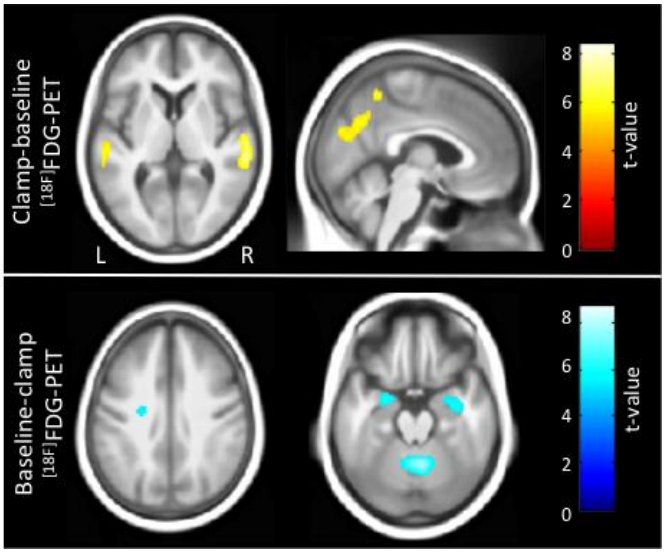

Figure 3.16 Voxel-based statistical parametric mapping analyses of brain PET images. Representative sections showed the HEC clamp effects. Six significant clusters (superior row) were found in the condition of HEC minus baseline, including the cerebellar vermis VI, left parahippocampal gyrus, right hippocampus, left amygdala, left olfactory bulb, and left middle cingulate gyrus. Three significant clusters (lower row) were found in the condition of baseline minus HEC, including the right superior temporal gyrus, left superior temporal gyrus, and right precuneus. Results have been overlaid over a mean structural image and the color scale represents the corresponding t-value at the voxel level. Images were shown by neurological convention (R: right, L: left).

Then, no phenotypes were shown in this type of analysis and then only correlation studies using the affected regions of each patient were performed to know the gut microbiota, plasma/feces metabolomics, and biochemical and anthropometrical parameters associated with these insulin-responsive brain regions.

3.4.4.1. Associations of the brain insulin resistance and sensitivity regions with gut microbiota, plasma/fecal metabolomics, and biochemical and anthropometric data

^{18}F-FDG SUV values of altered brain clusters, which represented insulin resistance and sensitivity (**Figure 3.16**), were used to perform Spearman's correlation analyses with anthropometric and biochemical parameters, metabolomics data, and fecal sequencing data in all T2DM patients, as delineated in **Figure 3.17**.

Biochemical parameters, but not anthropometric parameters, showed a significant association with nine brain clusters, as shown in **Figure 3.17A**. Thus, insulin, NAFLD liver fat score, and liver fat content were negatively correlated with voxel values of cerebellar vermis VI, left parahippocampal gyrus, and left olfactory bulb, while they were positively associated with voxel values of left superior temporal gyrus and right precuneus ($p<0.01$). Similarly, HOMA-IR was negatively related to voxel values of the left olfactory bulb, but positively with voxel values of the left superior temporal gyrus and right precuneus ($p<0.01$), while QUICKI had opposite relationships to HOMA-IR. NAFLD liver fat score and liver fat content exhibited positive associations with voxel values of the right superior temporal gyrus. Moreover, total and conjugated bilirubin showed positive associations with the voxel values of the left middle cingulate gyrus ($p<0.01$). Finally, adiponectin was positively associated with voxel values of the left olfactory bulb, while negatively with the right precuneus ($p<0.01$).

Regarding plasma metabolites, few significant correlations were obtained (**Figure 3.17B**). Plasma LDL(aliphatic chain) was positively associated with voxel values of the left amygdala ($p<0.01$). Finally, plasma formate showed a positive association with the cerebellar vermis VI, and an inverse association with the left superior temporal gyrus ($p<0.01$).

Compared to plasma metabolites, a bit more significant correlations were obtained for fecal metabolites (**Figure 3.17C**). Thus, voxel values of cerebellar vermis VI, left

parahippocampal gyrus and right hippocampus were positively related with fecal methylamine, and aspartate ($p<0.01$). Furthermore, ribose was positively correlated with voxel values of cerebellar vermis VI and left parahippocampal gyrus, while was negatively with the right superior temporal gyrus ($p<0.01$). Moreover, fecal arabinose, sarcosine, and histidine were positively linked to the left parahippocampal gyrus and right hippocampus, while were inversely to the right superior temporal gyrus ($p<0.01$). Voxel values of the right hippocampus showed positive relationships with fecal β-hydroxybutyrate, β-galactose, trimethylamine, and fumarate ($p<0.01$). In addition, the left amygdala was positively associated with fecal uridine, uracil, benzoate, and nicotinate ($p<0.01$).

Regarding gut bacteria (see **Figure 3.17D**), voxel values of cerebellar vermis VI and left parahippocampal gyrus exhibited positive relationships with the abundance of the genus *Alkaliphilus* and species *Propionispora hippie* ($p<0.01$). On the other hand, the class Clostridia was positively linked to voxel values of cerebellar vermis VI ($p<0.01$). Moreover, the left parahippocampal gyrus was found to be positively associated with Thermi taxa (class Deinococci) and Firmicutes taxa (family Peptococcaceae, genus *Sedimentibacter*, and species *Sporosarcina pasteurii*) ($p<0.01$). On the contrary, the left parahippocampal gyrus and right hippocampus were negatively associated with the family Lactobacillaceae and genus *Lactobacillus* ($p<0.01$). Moreover, voxel values of the left amygdala were positively associated with order Natranaerobiales, genus *Chlorobaculum* and species *Anaerobranca zavarzinii*, *Ruminococcus bromii* and *Coprococcus catus* ($p<0.01$). Furthermore, voxel values of the left olfactory bulb showed positive connections to *Desulfosporosinus* and *Caloramator mitchellensis*, and negative to *Streptococcus vestibularis* ($p<0.01$). Finally, the left middle cingulate gyrus was positively linked to genera *Oribacterium* and *Holdemania*, while was oppositely with Erysipelotrichaceae taxa (genus *Erysipelothrix*, species *Erysipelothrix muris*), genera *Eubacterium* and *Weissella* and species *Clostridium cadaveris* ($p<0.01$). Despite all these connections, few significant relationships were found between gut bacteria and the remaining three IR brain regions (baseline-HEC). Thus, voxel values of the right superior temporal gyrus had positive correlations with *Streptococcus*

vestibularis, and negative with genus *Holdemania* and species *Sporosarcina pasteurii* ($p<0.01$). On the other hand, the right precuneus was positively associated with *Megasphaera elsdenii*, while was oppositely with the family Caulobacteraceae and species *Desulfotomaculum indicum* ($p<0.001$).

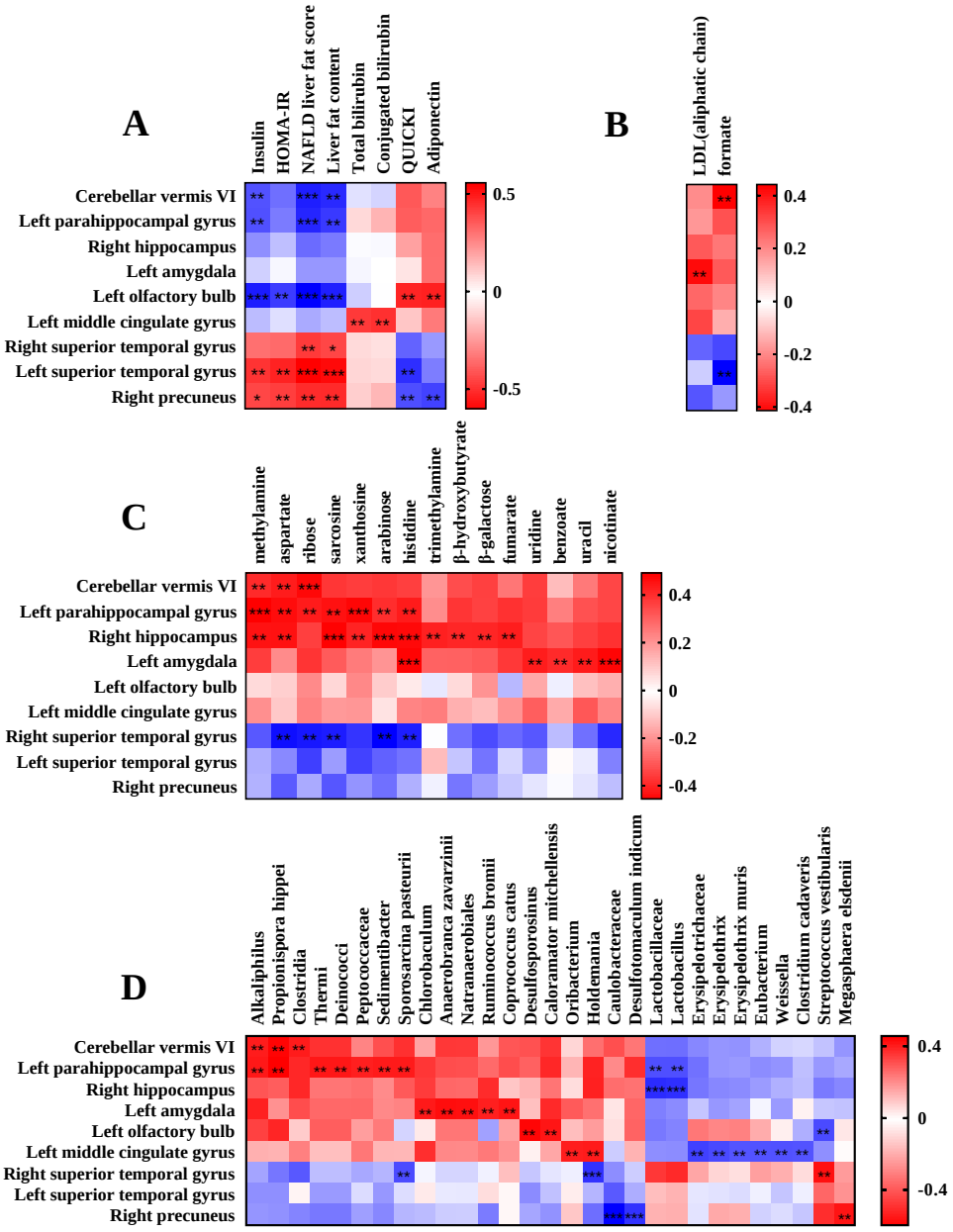

Figure 3.17 Spearman correlation analyses of cerebral insulin sensitivity. A) Biochemical variables. B) Plasma metabolic profiles. C) Fecal metabolic profiles. D) Gut microbiota. If bacteria at different taxonomic levels had an equal abundance in each patient, only bacteria at the lowest level were chosen to be shown in the heatmap. Only variables with rho>0.4 or rho<-0.4 ($p<0.0063$) are shown. HOMA-IR, homeostasis model assessment of insulin resistance; QUICKI, quantitative insulin sensitivity check index; NAFLD, non-alcoholic fatty liver disease; LDL, low-density lipoprotein. ** and *** indicated $p<0.01$ and $p<0.001$, respectively.

3.4.5 Comparison of PET/CT images of middle-aged and old-aged T2DM patients

In the previous sections, the effect of tissue/organ-specific insulin resistance and structure on the gut microbiota and blood and fecal composition in T2DM patients has been analyzed based on PET/CT imaging. Following the rationale of Chapter 1, in this section, we tried to see the effect of age on these differences.

3.4.5.1 Alterations in PET/CT imaging between middle-aged and old-aged T2DM patients

Translated PET/CT imaging data were analyzed and a comparison between middle-aged and old-aged T2DM subjects was carried out. Several significant differences were found in CT images, shown in **Figure 3.18**, but not in PET data. Older diabetic patients tended higher calcifications in all plaques, but these differences were only statistically significant for LM plaque and the sum of calcifications in all coronary arteries (total plaques).

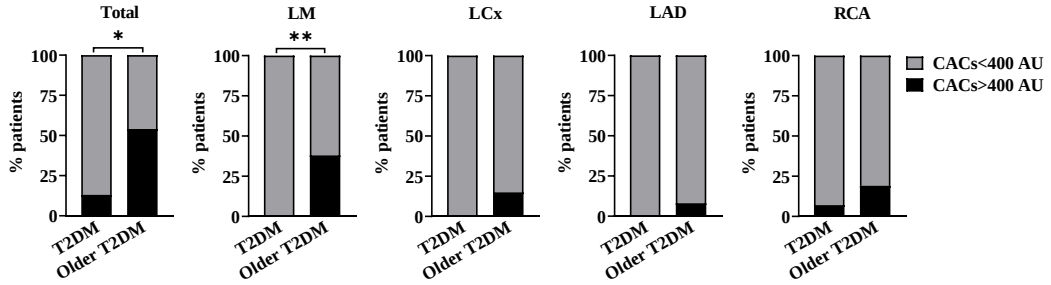

Figure 3.18 Frequency of coronary artery calcium scores (CACs) higher than 400 AU in different plaques between middle-aged and old-aged T2DM patients. The left anterior descending artery (LAD), left circumflex artery (LCx), left main coronary artery (LM), and right coronary artery (RCA) are coronary territories in the myocardium and total plaques are the sum of plaques in the whole myocardium. Results are shown per % of patients with CACs > or ≤400 Agatston Units (AU). Differences in frequency between groups were analyzed by Fisher's exact test. *, $p<0.05$; **, $p<0.01$.

3.4.5.2 Correlations of significant CT imaging results with significant biochemical parameters, fecal metabolites, and gut bacteria between middle-aged and old-aged T2DM patients

Spearman's correlation analysis was performed for calcifications of significantly altered coronary arteries (LM and total plaques in myocardium) with significant results in Chapter 1 between both age groups. It should be remembered that plasma metabolites were not found to have any differences between both groups of T2DM patients, so they were not included in the correlation analysis. As depicted in **Figure 3.19**, both LM plaque and total plaques were positively correlated with GGT, NAFLD fibrosis score, and troponin I, while negatively with GFR ($p<0.05$). Further, total plaques were also positively associated with FIB-4 ($p<0.01$).

Regarding fecal metabolites, as seen in **Figure 3.19B**, total plaques were positively associated with β-hydroxybutyrate, 2-hydroxyvalerate, and lysine ($p<0.05$). No significant connections were found for gut bacteria.

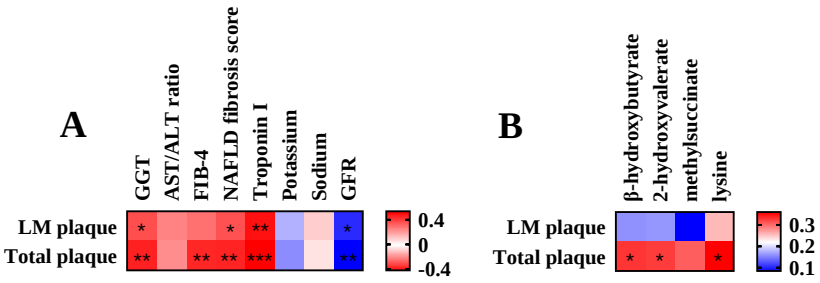

Figure 3.19 Spearman correlation analyses of significant imaging variables in middle-aged and old-aged T2DM patients. Correlations of the significant calcification territories in myocardium with A) biochemical parameters, B) the most relevant fecal metabolites, and plasma glycerol. No significant associations were found between the significant calcification territories in the myocardium and the most relevant gut bacteria. GGT, gamma-glutamyl transferase; AST, aspartate aminotransferase; ALT, alanine aminotransferase; GFR, glomerular filtration rate; FIB-4, liver fibrosis index 4; NAFLD; non-alcoholic fatty liver disease. *, ** and *** indicated $p<0.05$, $p<0.01$ and $p<0.001$, respectively.

3.4.6 Comparison of PET/CT images of female and male T2DM patients

In the previous sections, the effect of tissue/organ-specific insulin resistance and structure on the gut microbiota and blood and fecal composition in T2DM patients has been analyzed based on PET/CT imaging. Following the rationale of Chapter 1, in this section, we tried to see the effect of gender on these differences.

3.4.6.1 Alterations in PET/CT imaging between female and male T2DM patients

All PET and CT imaging data used to determine tissue/organ-specific IR and structural alterations respectively were done univariable analysis between both genders. As delineated in **Figure 3.20**, several significant differences in CT data, not in PET data, were obtained. Radiodensity (RD) of the skeletal muscle was increased in female T2DM patients ($p<0.05$). However, epicardial adipose tissue (EAT) volume was higher in males ($p<0.05$).

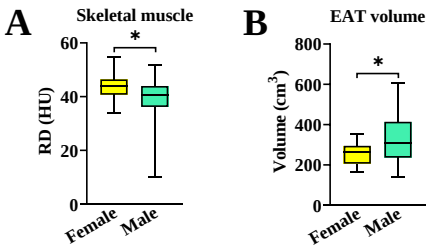

Figure 3.20 CT imaging data analyses between female and male T2DM patients. A) Radiodensity (RD) in the skeletal muscle. B) Epicardial adipose tissue (EAT) volume. HU, Hounsfield unit. * indicated $p<0.05$.

3.4.6.2 Correlations of significant CT imaging alterations with significant biochemical and anthropometric parameters, fecal metabolites, and gut bacteria between female and male T2DM patients

Correlation analysis of significant PET/CT imaging variables between genders was performed with significant differences in biochemical and anthropometric parameters, fecal metabolites, and gut bacteria. As depicted in **Figure 3.21A**, skeletal muscle RD was negatively associated with the waist/hip ratio ($p<0.05$). On the contrary, the waist/hip ratio and plasma creatinine concentration were positively related to EAT volume ($p<0.05$).

On the other hand, plasma metabolites were not used in the correlation analysis since no significant difference between both gender groups. Only one significant correlation was shown between altered fecal metabolites and CT imaging variables (**Figure 3.21B**). Thus, EAT volume was positively associated with the SCFA butyrate ($p<0.05$). Finally, no associations were found between the CT imaging variables and the gut microbiota in terms of gender.

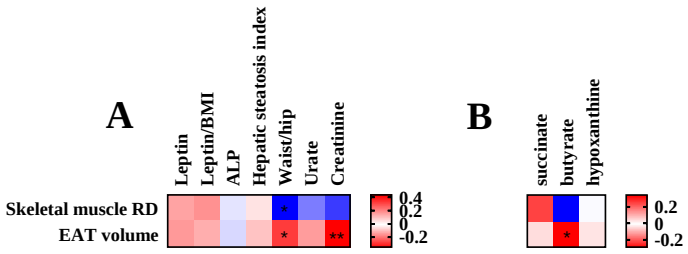

Figure 3.21 Spearman correlation analyses of significant imaging variables in T2DM females and males. Correlations of significant CT imaging variables with A) significant biochemical and anthropometric parameters, and B) fecal metabolites. No significant associations were found between significant CT imaging variables and significant gut bacteria. BMI, body mass index; ALP, alkaline phosphatase; RD, radiodensity; EAT, epicardial adipose tissue. * and ** indicated $p<0.05$ and $p<0.01$, respectively.

3.5 Discussion

The present chapter aimed to extend the understanding of tissue/organ-specific insulin resistance in T2DM by studying, for the first time, its relationship with the gut microbiota and fecal and plasmas metabolome. Two different T2DM phenotypes were addressed previously by our group in terms of insulin-mediated ^{18}F-FDG uptake in the myocardium after HEC, insulin sensitive (mIS), and insulin resistant (mIR) [389]. We defined mIS as a striking increment in myocardial ^{18}F-FDG uptake. On the contrary, we defined mIR as a pathological response to the HEC, namely, a marginal increase in myocardial ^{18}F-FDG uptake. This difference in glucose uptake is similarly expressed before in skeletal muscle between T2DM patients and controls following an HEC [400]. They found that T2DM patients had a blunted increment in intramyocellular glucose-6-phosphate concentrations, compared with controls.

At the same time, we also found two other phenotypes in patients: a marginal increase in hepatic ^{18}F-FDG uptake after HEC and a decrease in hepatic ^{18}F-FDG uptake. According to the availability of ^{18}F-FDG, if the myocardial tissue of the patient has a striking increased uptake of ^{18}F-FDG, the liver should have decreased uptake of ^{18}F-FDG. Therefore, reduced ^{18}F-FDG uptake in the liver after HEC was classified as L-IS, while increased ^{18}F-FDG uptake in the liver was classified as L-IR.

Although the skeletal muscle and brain regions did not show any phenotypes in the patients, correlation analysis was also performed. In addition, these will provide the differences between using systemic IR indexes such as HOMA-IR (evaluated in chapter 1) or tissue/organ-specific insulin resistance in T2DM. On the other hand, the effects of gender and age in terms of tissue/organ-specific insulin resistance were assessed. As result we found, both in mIR and in L-IR patients, insulin sensitivity ISclamp and electrolyte chloride were decreased. On the contrary, the concentrations of plasma GGT and hyaluronic acid were increased in these patients.

3.5.1 Alterations caused by myocardial and hepatic IR

3.5.1.1 Biochemical parameters and LSM value

Although long-chain fatty acid is the preferent energy source for the heart, as described in the introduction [66], glucose becomes the favored oxidized substrate when glucose and insulin concentrations are increased, as the HEC clamp condition of our study [66].

In the first section of the chapter, T2DM patients with myocardial insulin sensitivity (mIS) were studied and compared with patients affected by myocardial insulin resistance (mIR). As expected, mIS patients showed higher systemic insulin sensitivity (IS_{clamp}), compared with mIR patients. Interestingly, on the contrary, mIR patients have also an increase of liver enzymes, hepatic steatosis and fibrosis indexes, such as the AST, ALT, GGT, NAFLD liver fat score, liver fat content, FIB-4 score, and LSM value, suggesting that they had more severe NAFLD and higher risks of liver fibrosis. These are in coherence with previously described results for both phenotypes of T2DM patients [335, 389].

In the liver phenotype study, as in the mIR patients, IS_{clamp} and serum chloride concentrations were reduced in L-IR patients. This may be a cause or consequence of IR in the myocardium and liver. Previous studies demonstrated that chloride is a key electrolyte for regulating plasma volume during worsening heart failure [401] and its recovery [402]. Thus, the reduction of serum chloride in mIR and L-IR patients may be associated with myocardial ischemia and increased CV risks.

Fibroscan is a useful test to stage liver fibrosis [403]. Compared with their counterparts, the LSM value in mIR patients and L-IR patients was both elevated significantly and its median value was all higher than 6, indicating that these patients had significant liver fibrosis [335]. In this abnormal condition, we found that these

two types of patients both had increased plasma GGT and hyaluronic acid levels. In addition, L-IR patients presented higher total bilirubin levels and ELF scores, which further reflected aberrant liver condition [404].

3.5.1.2 Gut microbiota

Regarding alterations of gut microbiota, one alpha diversity index—Faith's phylogenetic diversity index was shown a significant reduction in the mIR group, but another alpha diversity index—Shannon's diversity index did not show this significant result. Then, we observed the changes in gut microbiota composition caused by mIR. We found that many specific gut bacteria decreased prominently in mIR patients, including the order Thermicanales, family Thermicanaceae, genera *Thermicanus*, *Caloramator*, and *Desulfosporosinus* and species *Coprobacillus cateniformis*. On the other hand, the species *Eubacterium callanderi* was found to be increased in these patients. It is the first time to describe these results in T2DM patients with myocardial IR.

Different from the myocardial study, very few significant results in the gut microbiota were obtained in the hepatic study. All alpha diversity indexes did not indicate significant differences between L-IS and L-IR groups. And only one genus, *Eubacterium*, showed a significant increase in L-IR patients. *Eubacterium callanderi*, an anaerobic, rod-shaped, and non-spore-forming bacterium, belongs to the genus *Eubacterium* within the phylum Firmicutes [405], and has thus far only been isolated from ruminal content and pig feces [406]. It has been reported as the causative agent in a single case of bacteremia [407]. Our study suggested that the increase of *Eubacterium callanderi* may play an important role in mIR patients, as well as the genus *Eubacterium* in L-IR patients, but further studies are required to reveal the function and mechanism of this species in the patients.

3.5.1.3 Fecal metabolomics

Concerning fecal metabolomics, no fecal metabolites were found to be elevated significantly in mIR patients or L-IR patients. In other words, we only found that several fecal metabolites were reduced in these two types of patients when compared with their counterparts, such as β-galactose, ribose, arabinose, aspartate, histidine, lactate, and 2-hydroxybutyrate. These results are first described in T2DM phenotypes. Beta-galactose, ribose, and arabinose are the three main monosaccharides. Compared with mIS patients, mIR patients had lower concentrations of these monosaccharides, probably because of lower carbohydrate metabolism caused by systemic IR and myocardial IR. For instance, galactose is a key source of energy in humans and an important structural element in complex molecules [408]. Recently, it has been reported to be beneficial in many diseases, particularly those affecting the brain [409, 410]. A decreased level of fecal aspartic acid was also reported previously in T2DM rats [411]. Aspartic acid has been linked to several important biological functions, including NADH transport to mitochondria, alanine generation, and gluconeogenesis. It was also linked to depression and dementia as a neurotransmitter [411].

Many previous studies revealed that plasma 2-hydroxybutyrate levels were higher in T2DM patients than in healthy controls [412, 413]. Vangipurapu *et al* revealed that 2-hydroxybutyrate significantly increased the risk of T2DM by 32% and was significantly associated with the risk of incident T2DM and IR, and also associated with reduced insulin secretion [414]. We found that fecal 2-hydroxybutyrate concentration was markedly lower in L-IR patients than in L-IS patients. Our disparity in 2-hydroxybutyrate results could be attributed to differences in feces and plasma, as well as different comparison subjects.

3.5.1.4 Plasma metabolomics

In addition, plasma metabolomics was also conducted for patients in our study. A previous NMR analysis of plasma lipoproteins indicated that the concentrations of

VLDL of different sizes were all significantly increased in T2DM patients [415]. We obtained higher plasma VLDL(CH_3) concentrations in mIR patients, which suggested higher CV risk [416]. However, it was not observed in L-IR patients. In the plasma, we also observed reduced β-galactose in mIR patients. A previous study found some abnormalities in inositol metabolism in association with IR in a mouse model, and insulin-sensitising effects of dietary myo-inositol supplementation [417]. In our study, plasma concentrations of myo-inositol were lower in mIR patients than in mIS patients, most likely due to myocardial IR. Choline is an essential nutrient for humans and plays important roles in human metabolism as a methyl donor, a precursor for the neurotransmitter acetylcholine, and a component of cell membranes [418]. Besides, choline is also a major precursor for TMAO. Although some studies have shown that choline and its metabolites are related to CVD risk and T2DM [234, 419, 420], another study reported that plasma TMAO and related metabolites were not significantly associated with T2DM, and plasma choline was associated with greater IS [421]. In the current study, we found that plasma choline was lower in mIR patients, possibly due to lower IS. Commonly, mIR and L-IR patients both exhibited decreased concentrations of plasma glycerol. In IR states, increased lipolysis leads to the overproduction of glycerol from triglycerides [422]. A prospective study on a large-scale Finnish population has demonstrated that higher serum glycerol levels are associated with an increased risk for T2DM [423]. Our results for the plasma metabolite glycerol were obtained in T2DM subgroups, which have not been described before.

3.5.2 Associations with systemic IR and tissue/organ-specific IR

Although the widely-used systemic IR indexes HOMA-IR and QUICKI did not show significant differences between groups of myocardial and hepatic studies, the IS_{clamp} did. Additionally, myocardial ΔSUV obtained from PET imaging analysis represents

myocardial IS, because a previous study from our group showed that myocardial ΔSUV was negatively correlated with HOMA-IR in all included T2DM patients (n= 35) and in mIR patients, but not in those with mIS [389]. In the hepatic study, as shown in **Figure 3.22**, liver ΔSUV was positively correlated with HOMA-IR in the included T2DM patients (n= 35) and in L-IS patients, but not in those with L-IR. Therefore, liver ΔSUV can be considered liver IR. Although skeletal muscle ΔSUV did not show significant correlations with HOMA-IR (data not shown), it had positive correlations with IS_{clamp} (**Figure 3.15**). Thus, skeletal muscle ΔSUV can be defined as skeletal muscle IS. Concerning the brain regions, the left olfactory bulb, left superior temporal gyrus and right precuneus were significantly related to IR indicators HOMA-IR and QUICKI (**Figure 3. 17**). The imaging data of the left olfactory bulb represents IS of the region, the data of the left superior temporal gyrus and right precuneus represents IR of these regions. Then, specific gut bacteria related to systemic IS and tissue/organ-specific IR or IS were identified, as well as fecal and plasma metabolites.

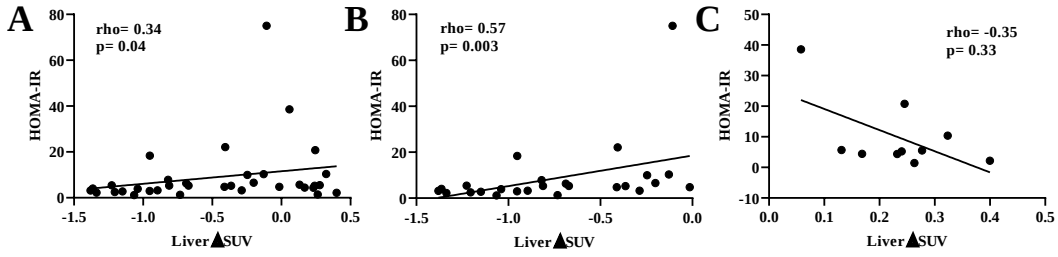

Figure 3.22 Correlation analyses between liver ΔSUV and HOMA-IR in A) all T2DM patients with liver phenotypes, B) L-IS patients, and C) L-IR patients.

3.5.2.1 Specific gut bacteria

In the myocardial study, two genera *Caloramator* and *Desulfosporosinus* were positively correlated with systemic IS (IS_{clamp}), and also with myocardial IS. But the species *Coprobacillus cateniformis* was only positively associated with myocardial IS, and the species *Eubacterium callanderi* was only negatively associated with

myocardial IS. These results were obtained for the first time, and are interesting to be verified in future research. However, in the hepatic study, the genus *Eubacterium* did not have significant associations with IS_{clamp} or liver IR.

Regarding skeletal muscle IS, it was positively related to Caldilineales taxa, genera *Desulfosporosinus* and *Mogibacterium*, and the species *Carboxydocella ferrireducens*, but negatively to the family Veillonellaceae. The family Veillonellaceae has been reported to be positively associated with liver fibrosis severity, HbA1c, and adipose tissue IR in non-obese subjects [424]. In addition, Veillonellaceae was found to be associated with higher serum insulin concentrations and caecal TNF-α mRNA levels in mice [425]. Our research is the first to show a link between Veillonellaceae and skeletal muscle IS, as well as other above bacteria.

Among the above three brain regions, only the left olfactory bulb and right precuneus depicted significant correlations with gut microbiota. Of note, the genus *Desulfosporosinus*, which has shown positive associations with myocardial and skeletal muscle IS above, also showed positive associations with left olfactory bulb IS. *Desulfosporosinus* is a genus of strictly anaerobic, sulfate-reducing bacteria, and is commonly found in soil [426]. However, reports about the associations between *Desulfosporosinus* and IS are very scarce. One study described that all species from *Desulfosporosinus* can produce trimethylamine [427], which can be taken up by hepatocytes and oxidized to TMAO [428]. TMAO was generally regarded as a deleterious dietary gut microbiome metabolite in studies on patients and animal models of NAFLD, cognitive diseases, and T2DM [427]. However, TMAO has also been summarized to have positive effects involving anti-oxidative or anti-inflammatory effects observed in the liver, adipose tissue, skeletal muscle, and pancreatic β-cells under stress from over-nutrition models [427]. The genus *Desulfosporosinus* in our study may be linked with IS in the myocardial tissue, skeletal muscle, and the left olfactory bulb by beneficial TMAO effects.

The olfactory bulb is an essential structure in the olfactory system devoted to the sense of smell [429]. The precuneus is a brain region involved in a variety of complex functions including mental imagery strategies and memory [430]. Besides

Desulfosporosinus, the left olfactory bulb IS was also shown positive associations with *Caloramator mitchellensis*, but inverse associations with *Streptococcus vestibularis*. On the other hand, the right precuneus IR was positively associated with *Megasphaera elsdenii*, while was oppositely with the family *Caulobacteraceae* and the species *Desulfotomaculum indicum*. *Megasphaera elsdenii* is an important ruminal bacterium from the family Veillonellaceae. Wang *et al* found that the richness of *Megasphaera* was positively correlated with HOMA-IR in patients with diabetic peripheral neuropathy [431]. This is the first time that the relationships between these bacteria and brain IR or IS regions have been established, and further research is needed to gain a thorough understanding.

3.5.2.2 Specific fecal metabolites

Concerning fecal metabolites, β-galactose showed positive associations with systemic IS (IS_{clamp}) and myocardial IS. Another two monosaccharides ribose and arabinose also depicted positive associations with myocardial IS. Ribose is an important substrate of ATP synthesis. The results suggested that these monosaccharides may be involved in insulin-mediated myocardial energy metabolism. Further, two amino acids aspartate and histidine also showed positive correlations with myocardial IS. Our previous study on obese patients found that fecal histidine had a negative association with HOMA-IR [206]. Our finding indicates that the fecal metabolite histidine is not only associated with systemic insulin sensitivity, but also with myocardial IS. However, no fecal metabolites were found to be inversely associated with myocardial IS. Meanwhile, fecal metabolites were not found to be significantly correlated with liver IR, skeletal muscle IS, and brain insulin-related regions.

3.5.2.3 Specific plasma metabolites

Regarding plasma metabolites, β-galactose also exhibited positive associations with myocardial IS, further demonstrating the crucial roles of β-galactose in patients and

myocardial IS. Moreover, like β-galactose, plasma choline was also shown positive associations with myocardial IS. Our previous study indicated that plasma choline had a negative correlation with HOMA-IR [206]. However, another report showed an opposite correlation [432]. Plasma lipoprotein VLDL(CH_3) levels were negatively associated with myocardial IS. Associations between plasma lipoprotein and HOMA-IR depend on the particle size [433, 434], Jason *et al* revealed that the production rate of plasma $VLDL_1$ (Sf 60–400), not $VLDL_2$ (Sf 20–60), was significantly and positively correlated with HOMA-IR [433]. Although correlations between these plasma metabolites and myocardial IS have never been described before, they are almost consistent with the findings in systemic IR.

In terms of hepatic IR, plasma glycerol showed a negative association in this study, which differed from previous reports. Glycerol is a substrate for gluconeogenesis, and increased hepatic delivery of glycerol caused by adipose tissue IR drives gluconeogenesis and results in hepatic IR [435, 436]. For skeletal muscle IS, two plasma amino acids tyrosine and histidine had positive associations. However, plasma tyrosine concentrations have been reported to have a positive correlation with IR [206, 437]. L-histidine is a component of carnosine, present in skeletal muscle [438]. The supplementation of histidine was reported to improve IR, reduce BMI, and fat mass, and suppress inflammation and oxidative stress in obese women with metabolic syndrome [439]. These findings support our results about the relationship between plasma histidine and skeletal muscle IS. Finally, for brain IR or IS regions, left superior temporal gyrus IR correlated negatively with plasma formate. This metabolite was found to be negatively associated with HOMA-IR and BMI in our previous study [206]. This is the first time a relationship between brain IR regions and the metabolite has been depicted, and more research is needed to obtain a more robust result.

3.5.2.4 Biochemical parameters (CV and hepatic risk factors)

In addition, the relationships between CV and hepatic risk factors and systemic IS and

tissue/organ-specific IR or IS were also determined in the study. The latest publication from our group demonstrated that liver tests can be used to identify myocardial IR in T2DM patients [335]. Consistently, we found that hepatic risk factors including liver enzymes (AST, ALT, and GGT), NAFLD liver fat score and liver fat content, as well as liver fibrosis measures (LSM value), were negatively associated with myocardial IS. In addition, we also found that the CV risk factor total cholesterol/HDL ratio had a negative correlation with myocardial IS. Individuals with high total cholesterol/HDL ratios have been demonstrated to be insulin resistant for many years [440]. Of note, the serum concentration of an electrolyte, chloride, which was reduced in both mIR and L-IR patients, showed a positive association with myocardial IS, but no significant association with liver IR. As described above, studies from Kataoka *et al* implicated an important role of chloride in the worsening and recovery of heart failure [401, 402].

In the past decade, the role of insulin resistance in the pathogenesis of NAFLD and NASH has been better elucidated [184, 441]. Our study found that plasma GGT levels and LSM values correlated positively with liver IR. Previous studies showed that elevated GGT levels are a marker for hepatic steatosis and hepatic insulin resistance [442] and that LSM values had a positive correlation with HOMA-IR [443].

As introduced above, skeletal muscle is an insulin-dependent tissue and accounts for the majority (about 60-70%) of whole-body insulin-mediated glucose uptake [24]. Thus, our results showed that skeletal muscle IS was positively related to whole-body IS (IS_{clamp}). Adiponectin, which is only secreted by mature adipocytes, has many beneficial effects, the most important of which is increasing IS [82]. We also found that skeletal muscle IS was positively associated with plasma adiponectin levels. This is in coherence with a previous finding that plasma adiponectin concentration was positively associated with the fold increase in skeletal muscle insulin receptor tyrosine phosphorylation [444], an important step in the insulin-signaling cascade. On the contrary, three hepatic risk factors were shown negative associations with skeletal muscle IS, including plasma ALT levels, hepatic steatosis index, and liver fat content. Higher plasma ALT levels were suggested to be associated with IR, and

hypoadiponectinemia in adolescents [445]. Previous studies consistently showed that liver steatosis is associated with IR in skeletal muscle [446].

Interestingly, plasma adiponectin levels and hepatic risk factors were also correlated with brain IS or IR regions in our study. In detail, adiponectin was positively correlated with left olfactory bulb IS, while inversely with right precuneus IR. A study in aged mice reveals that adiponectin can enhance neuronal IS through AMPK activation and chronic adiponectin deficiency leads to cerebral IR [447]. This study suggests that adiponectin also mediates effects in the brain. Additionally, NAFLD liver fat score and liver fat content were positively related to IR in the left superior temporal gyrus and right precuneus but were negative to left olfactory bulb IS. These results were obtained for the first time. Recently, NAFLD has emerged as an important disease linked to the development of cognitive impairment and dementia [448, 449]. More studies are warranted to disclose the relationships of hepatic risk factors with brain IR.

3.5.3 Age and gender effects

Continuing from Chapter 1, age and gender differences in T2DM patients in PET/CT imaging were investigated. In Chapter 1, older patients presented higher risks of myocardial infarction, kidney dysfunction, and liver fibrosis than middle-aged patients. Through PET/CT imaging techniques, older patients found a higher frequency of CACs > 400 AU in LM plaque and total plaque. Since CACs are the most sensitive and noninvasive tool in assessing cardiovascular risk [450], our results suggested that older T2DM patients were at a very high risk of developing cardiovascular events. Rodgers *et al* also outlined that the aging and elderly population was especially vulnerable to cardiovascular disease [451]. The frequency of LM plaque and the total plaque was not found to be significantly associated with the relevant gut microbes but was found to be positively related with hepatic risk factors (GGT and NAFLD fibrosis score) and increased risk of myocardial infarction. Most fecal metabolites showed significant correlations with total plaques, instead of

LM plaque.

In Chapter 1, T2DM women presented more serious NAFLD, while T2DM men showed the potential to suffer from kidney problems. An analysis of PET/CT images showed a significantly reduced ^{18}F-FDG uptake in the spleen after HEC and a lower radiodensity in the skeletal muscle in males. In contrast, a bigger EAT volume and no difference in EAT radiodensity was observed in males, compared to females. Recent studies showed that both EAT radiodensity and EAT volume were independently associated with human coronary atherosclerosis [452, 453]. It suggested that T2DM men had a higher risk of coronary atherosclerosis than T2DM women. Few significant correlations were obtained between PET/CT imaging variables, gut bacteria, and fecal metabolites.

3.5.4 Limitations

Finally, we have to comment on some limitations of the data presented in this chapter. For instance, we study the myocardial IR and hepatic IR in the same cohorts, therefore, a part of the patients would manifest both myocardial and hepatic IR through observations of ^{18}F-FDG uptake, and some other patients only had one of them. But we did not consider the influence of hepatic IR when we studied myocardial IR. Similarly, we did not consider the effect of myocardial IR when we investigated hepatic IR. As described in chapter 1, the number of patients in both groups of one study was small. Further, a long-term study for the patients with mIR or L-IR is required to confirm our described relationships between gut microbiota, metabolomics, and specific insulin resistance. Despite these limitations, our studies are the first to establish a relationship between specific insulin resistance measured by real glucose uptake, and gut microbiota, as well as metabolomics.

3.6 Conclusion

The study presented in this chapter allows us to draw the following conclusions:

- T2DM patients with the mIR phenotype were characterized by a reduced systemic IS index, more severe NAFLD, and increased risk of liver fibrosis and coronary atherosclerosis, compared with mIS patients.
- Alterations in gut microbiota, fecal and plasma metabolites such as decreased proportions of Thermicanales taxa, *Caloramator*, *Desulfosporosinus*, reduced fecal β-galactose and lactate and increased plasma VLDL(CH_3) in mIR patients after comparing with mIS patients. Regarding associations, the genera *Caloramator*, *Desulfosporosinus*, and fecal β-galactose were positively associated with IS_{clamp} and the myocardial IS, while *Eubacterium callanderi* and plasma VLDL(CH_3) were negatively associated with myocardial IS.
- Several alterations were also found in L-IR patients, including a higher abundance of *Eubacterium*, and lower concentrations of fecal 2-hydroxybutyrate and plasma glycerol after comparing with L-IS patients. Additionally, plasma GGT concentration correlated positively with liver IR, while plasma metabolite glycerol correlated negatively with liver IR.
- Skeletal muscle IS was positively related to IS_{clamp}, plasma adiponectin, tyrosine, and histidine and negatively with ALT, hepatic steatosis index, and liver fat content. Regarding gut bacteria, skeletal muscle IS was positively associated with Caldilineales taxa, while inversely with Veillonellaceae.
- Several significant associations were obtained for brain IS/IR regions with GM. Thus, the left olfactory bulb showed positive associations with *Desulfosporosinus* and *Caloramator mitchellensis*, but negative associations with *Streptococcus vestibularis*. The right precuneus was positively related with *Megasphaera elsdenii*, while inversely with Caulobacteraceae and *Desulfotomaculum indicum*.
- Old-aged T2DM patients further showed higher atherosclerotic risk than middle-aged patients. CACs in the left main coronary artery and total coronary

territories were positively related with GGT, NAFLD fibrosis score, and troponin I, but negatively with glomerular filtration rate.

- Several imaging differences were shown between T2DM females and males. In detail, females had higher radiodensity of skeletal muscle but lower EAT volume.

4. General conclusions

As a result of the work presented in chapters 1 and 2, we draw the following conclusions from this thesis:

- The results presented in the first part of the thesis, comparing T2DM patients with healthy controls, provided results that were in coherence with previous studies, such as an increased abundance of Proteobacteria in patients and a decreased glutamine/glutamate ratio.
- Regarding the age and gender in T2DM, we detected changes that were associated with these features, confirming that gender and age effects should be taken into account during patients' management.
- Several differences were detected between both myocardial and liver phenotypes, including CV and hepatic risk factors, GM, as well as fecal and plasma metabolites.
- Despite skeletal muscle and brain did not show any IR phenotypes, they were found to be related to some specific gut bacteria, and plasma or fecal metabolites.
- While no direct correlation with systemic IR parameters like HOMA was detected in T2DM, we were able to identify a series of bacteria and metabolites that correlated with specific IR in different tissues/organs, representing interesting biomarker candidates for specific comorbidities.

5. Funding

The research involved in the thesis was funded by the Carlos III Health Institute and the European Regional Development Fund (PI16/02064 and PI20/01588) and AGAUR (2017SGR1303 and 2017SGR1144). The Ph.D. student was supported by a scholarship from China Scholarship Council with No.201706180010.

6. Publications

During this thesis, several works have been done and are going to be published soon. And I have participated in the following publication:

Palomino-Schätzlein M, Mayneris-Perxachs J, Caballano-Infantes E, Rodríguez MA, Palomo-Buitrago M-E, **Xiao X**, Mares R, Ricart W, Simó R, Herance JR, Fernández-Real J-M: Combining metabolic profiling of plasma and faeces as a fingerprint of insulin resistance in obesity. Clinical Nutrition 2020, 39(7):2292-2300.

7. References

1. Ozougwu J, Obimba K, Belonwu C, Unakalamba C: The pathogenesis and pathophysiology of type 1 and type 2 diabetes mellitus. *Journal Physiology and Pathophysiology* 2013, 4(4):46-57.
2. Harding JL, Pavkov ME, Magliano DJ, Shaw JE, Gregg EW: Global trends in diabetes complications: a review of current evidence. *Diabetologia* 2019, 62(1):3-16.
3. IDF Diabetes Atlas Eighth edition, 8th edn. Brussels: International Diabetes Federation; 2017.
4. Zheng Y, Ley SH, Hu FB: Global aetiology and epidemiology of type 2 diabetes mellitus and its complications. *Nature Reviews Endocrinology* 2018, 14(2):88-98.
5. Global report on diabetes. Geneva: World Health Organization; 2016.
6. Susan van D, Beulens JWJ, Yvonne T. van der S, Grobbee DE, Nealb B: The global burden of diabetes and its complications: an emerging pandemic. *European journal of cardiovascular prevention and rehabilitation* 2010, 17(1_suppl):s3-s8.
7. Classification of diabetes mellitus. Geneva: World Health Organization; 2019.
8. Paschou SA, Papadopoulou-Marketou N, Chrousos GP, Kanaka-Gantenbein C: On type 1 diabetes mellitus pathogenesis. *Endocrine Connections* 2018, 7(1):R38-R46.
9. Zimmet P, Alberti KGMM, Shaw J: Global and societal implications of the diabetes epidemic. *Nature* 2001, 414(6865):782-787.
10. Chatterjee S, Khunti K, Davies MJ: Type 2 diabetes. *The Lancet* 2017, 389(10085):2239-2251.
11. Perl S, Kushner JA, Buchholz BA, Meeker AK, Stein GM, Hsieh M, Kirby M,

Pechhold S, Liu EH, Harlan DM *et al*: Significant Human β-Cell Turnover Is Limited to the First Three Decades of Life as Determined by in Vivo Thymidine Analog Incorporation and Radiocarbon Dating. *The Journal of Clinical Endocrinology & Metabolism* 2010, 95(10):E234-E239.

12. Leahy JL: Pathogenesis of Type 2 Diabetes Mellitus. *Archives of Medical Research* 2005, 36(3):197-209.
13. Arnold SV, Khunti K, Tang F, Chen H, Cid-Ruzafa J, Cooper A, Fenici P, Gomes MB, Hammar N, Ji L *et al*: Incidence rates and predictors of microvascular and macrovascular complications in patients with type 2 diabetes: Results from the longitudinal global discover study. *American Heart Journal* 2022, 243:232-239.
14. Fowler MJ: Microvascular and Macrovascular Complications of Diabetes. *Clinical Diabetes* 2008, 26(2):77-82.
15. Viigimaa M, Sachinidis A, Toumpourleka M, Koutsampasopoulos K, Alliksoo S, Titma T: Macrovascular Complications of Type 2 Diabetes Mellitus. *Current Vascular Pharmacology* 2020, 18(2):110-116.
16. Litwak L, Goh S-Y, Hussein Z, Malek R, Prusty V, Khamseh ME: Prevalence of diabetes complications in people with type 2 diabetes mellitus and its association with baseline characteristics in the multinational A1chieve study. *Diabetology & Metabolic Syndrome* 2013, 5(1):57.
17. Seiosuwowei A: Compare and contrast the efficacy of angiotensin converting enzymes (ACE) inhibitors and angiotensin II receptor blockers (ARBs) on type 2 diabetic patients with hypertension. Cambridge: Anglia Ruskin University; 2016.
18. Moradi S, Hojjati Kermani MA, Bagheri R, Mohammadi H, Jayedi A, Lane MM, Asbaghi O, Mehrabani S, Suzuki K: Ultra-Processed Food Consumption and Adult Diabetes Risk: A Systematic Review and Dose-Response Meta-Analysis. In: *Nutrients.* vol. 13; 2021.
19. Wang M, Yu M, Fang L, Hu R-Y: Association between sugar-sweetened beverages and type 2 diabetes: A meta-analysis. *Journal of Diabetes*

Investigation 2015, 6(3):360-366.

20. Newsholme P, Gaudel C, McClenaghan NH: Nutrient Regulation of Insulin Secretion and β-Cell Functional Integrity. In: *The Islets of Langerhans.* Edited by Islam MS. Dordrecht: Springer Netherlands; 2010: 91-114.
21. Cruz-Pineda WD, Parra-Rojas I, Rodríguez-Ruíz HA, Illades-Aguiar B, Matia-García I, Garibay-Cerdenares OL: The regulatory role of insulin in energy metabolism and leukocyte functions. *Journal of Leukocyte Biology* 2022, 111(1):197-208.
22. Janus A, Szahidewicz-Krupska E, Mazur G, Doroszko A: Insulin Resistance and Endothelial Dysfunction Constitute a Common Therapeutic Target in Cardiometabolic Disorders. *Mediators of Inflammation* 2016, 2016:3634948.
23. Cheatham B, Kahn CR: Insulin Action and the Insulin Signaling Network*. *Endocrine Reviews* 1995, 16(2):117-142.
24. Wilcox G: Insulin and insulin resistance. *Clinical Biochemist Reviews* 2005, 26(2):19-39.
25. Czech MP: Insulin action and resistance in obesity and type 2 diabetes. *Nature Medicine* 2017, 23(7):804-814.
26. Boucher J, Kleinridders A, Kahn CR: Insulin receptor signaling in normal and insulin-resistant states. *Cold Spring Harb Perspect Biol* 2014, 6(1):1-23.
27. Arneth B, Arneth R, Shams M: Metabolomics of Type 1 and Type 2 Diabetes. In: *International Journal of Molecular Sciences.* vol. 20; 2019.
28. Cefalu WT: Insulin Resistance: Cellular and Clinical Concepts. *Experimental Biology and Medicine* 2001, 226(1):13-26.
29. Shanik MH, Xu Y, Škrha J, Dankner R, Zick Y, Roth J: Insulin Resistance and Hyperinsulinemia: Is hyperinsulinemia the cart or the horse? *Diabetes Care* 2008, 31(Supplement_2):S262-S268.
30. Nolan CJ, Ruderman NB, Kahn SE, Pedersen O, Prentki M: Insulin Resistance as a Physiological Defense Against Metabolic Stress: Implications for the Management of Subsets of Type 2 Diabetes. *Diabetes* 2015, 64(3):673-686.
31. Sharma MD, Garber AJ, Farmer JA: Role of Insulin Signaling in Maintaining

Energy Homeostasis. *Endocrine Practice* 2008, 14(3):373-380.

32. Abel ED, Litwin SE, Sweeney G: Cardiac Remodeling in Obesity. *Physiological Reviews* 2008, 88(2):389-419.
33. Samuel Varman T, Shulman Gerald I: Mechanisms for Insulin Resistance: Common Threads and Missing Links. *Cell* 2012, 148(5):852-871.
34. Bugger H, Abel ED: Mitochondria in the diabetic heart. *Cardiovascular Research* 2010, 88(2):229-240.
35. Abel ED, O'Shea KM, Ramasamy R: Insulin Resistance: Metabolic Mechanisms and Consequences in the Heart. *Arteriosclerosis, Thrombosis, and Vascular Biology* 2012, 32(9):2068-2076.
36. Rocha M, Apostolova N, Diaz-Rua R, Muntane J, Victor VM: Mitochondria and T2D: Role of Autophagy, ER Stress, and Inflammasome. *Trends in Endocrinology & Metabolism* 2020, 31(10):725-741.
37. Reaven GM: The insulin resistance syndrome. *Current Atherosclerosis Reports* 2003, 5(5):364-371.
38. Reaven G: The metabolic syndrome or the insulin resistance syndrome? Different names, different concepts, and different goals. *Endocrinology and Metabolism Clinics* 2004, 33(2):283-303.
39. Unnikrishnan AG: Tissue-specific insulin resistance. *Postgraduate Medical Journal* 2004, 80(946):435.
40. Schmidt SL, Hickey MS: Regulation of Insulin Action by Diet and Exercise. *Journal of Equine Veterinary Science* 2009, 29(5):274-284.
41. Bach AD, Stern-Straeter J, Beier JP, Bannasch H, Stark GB: Engineering of muscle tissue. *Clinics in Plastic Surgery* 2003, 30(4):589-599.
42. Goodman CA, Hornberger TA, Robling AG: Bone and skeletal muscle: Key players in mechanotransduction and potential overlapping mechanisms. *Bone* 2015, 80:24-36.
43. Wang J, Khodabukus A, Rao L, Vandusen K, Abutaleb N, Bursac N: Engineered skeletal muscles for disease modeling and drug discovery. *Biomaterials* 2019, 221:119416.

44. DeFronzo RA, Tripathy D: Skeletal Muscle Insulin Resistance Is the Primary Defect in Type 2 Diabetes. *Diabetes Care* 2009, 32(suppl_2):S157-S163.

45. DeFronzo RA, Gunnarsson R, Björkman O, Olsson M, Wahren J: Effects of insulin on peripheral and splanchnic glucose metabolism in noninsulin-dependent (type II) diabetes mellitus. *The Journal of Clinical Investigation* 1985, 76(1):149-155.

46. Mitrakou A, Kelley D, Veneman T, Jenssen T, Pangburn T, Reilly J, Gerich J: Contribution of Abnormal Muscle and Liver Glucose Metabolism to Postprandial Hyperglycemia in NIDDM. *Diabetes* 1990, 39(11):1381-1390.

47. Cusi K, Maezono K, Osman A, Pendergrass M, Patti ME, Pratipanawatr T, DeFronzo RA, Kahn CR, Mandarino LJ: Insulin resistance differentially affects the PI 3-kinase– and MAP kinase–mediated signaling in human muscle. *The Journal of Clinical Investigation* 2000, 105(3):311-320.

48. Bouzakri K, Koistinen AH, Zierath RJ: Molecular Mechanisms of Skeletal Muscle Insulin Resistance in Type 2 Diabetes. *Current Diabetes Reviews* 2005, 1(2):167-174.

49. Karlsson HKR, Zierath JR: Insulin signaling and glucose transport in insulin resistant human skeletal muscle. *Cell Biochemistry and Biophysics* 2007, 48(2):103-113.

50. Bajaj M, DeFronzo RA: Metabolic and molecular basis of insulin resistance. *Journal of Nuclear Cardiology* 2003, 10(3):311-323.

51. Kim JK, Michael MD, Previs SF, Peroni OD, Mauvais-Jarvis F, Neschen S, Kahn BB, Kahn CR, Shulman GI: Redistribution of substrates to adipose tissue promotes obesity in mice with selective insulin resistance in muscle. *The Journal of Clinical Investigation* 2000, 105(12):1791-1797.

52. Park SS, Seo Y-K: Excess Accumulation of Lipid Impairs Insulin Sensitivity in Skeletal Muscle. In: *International Journal of Molecular Sciences.* vol. 21; 2020.

53. Zhang L, Keung W, Samokhvalov V, Wang W, Lopaschuk GD: Role of fatty acid uptake and fatty acid β-oxidation in mediating insulin resistance in heart

and skeletal muscle. *Biochimica et Biophysica Acta (BBA) - Molecular and Cell Biology of Lipids* 2010, 1801(1):1-22.

54. Boden G: Fatty acid—induced inflammation and insulin resistance in skeletal muscle and liver. *Current Diabetes Reports* 2006, 6(3):177-181.
55. Brand MD, Orr AL, Perevoshchikova IV, Quinlan CL: The role of mitochondrial function and cellular bioenergetics in ageing and disease. *British Journal of Dermatology* 2013, 169(s2):1-8.
56. Kelley DE, He J, Menshikova EV, Ritov VB: Dysfunction of Mitochondria in Human Skeletal Muscle in Type 2 Diabetes. *Diabetes* 2002, 51(10):2944-2950.
57. Ritov VB, Menshikova EV, Azuma K, Wood R, Toledo FGS, Goodpaster BH, Ruderman NB, Kelley DE: Deficiency of electron transport chain in human skeletal muscle mitochondria in type 2 diabetes mellitus and obesity. *American Journal of Physiology-Endocrinology and Metabolism* 2009, 298(1):E49-E58.
58. Lowell BB, Shulman GI: Mitochondrial Dysfunction and Type 2 Diabetes. *Science* 2005, 307(5708):384-387.
59. Petersen KF, Dufour S, Befroy D, Garcia R, Shulman GI: Impaired Mitochondrial Activity in the Insulin-Resistant Offspring of Patients with Type 2 Diabetes. *New England Journal of Medicine* 2004, 350(7):664-671.
60. Laflamme MA, Sebastian MM, Buetow BS: 10 - Cardiovascular. In: *Comparative Anatomy and Histology.* Edited by Treuting PM, Dintzis SM. San Diego: Academic Press; 2012: 135-153.
61. Tran DB, Weber C, Lopez RA: Anatomy, Thorax, Heart Muscles. Internet: StatPearls; 2022.
62. Krishnan A, Sharma H, Yuan D, Trollope AF, Chilton L: The Role of Epicardial Adipose Tissue in the Development of Atrial Fibrillation, Coronary Artery Disease and Chronic Heart Failure in the Context of Obesity and Type 2 Diabetes Mellitus: A Narrative Review. In: *Journal of Cardiovascular Development and Disease.* vol. 9; 2022.

63. Bader F, Bendahmane M, Saad M, Talhouk R: Derivation of a new macroscopic bidomain model including three scales for the electrical activity of cardiac tissue; 2020.

64. Grynberg A, Demaison L: Fatty Acid Oxidation in the Heart. *Journal of Cardiovascular Pharmacology* 1996, 28.

65. Lopaschuk GD, Karwi QG, Tian R, Wende AR, Abel ED: Cardiac Energy Metabolism in Heart Failure. *Circulation Research* 2021, 128(10):1487-1513.

66. Bertrand L, Horman S, Beauloye C, Vanoverschelde J-L: Insulin signalling in the heart. *Cardiovascular Research* 2008, 79(2):238-248.

67. Lee CT, Ussher JR, Mohammad A, Lam A, Lopaschuk GD: 5′-AMP-activated protein kinase increases glucose uptake independent of GLUT4 translocation in cardiac myocytes. *Canadian Journal of Physiology and Pharmacology* 2014, 92(4):307-314.

68. Iliadis F, Kadoglou N, Didangelos T: Insulin and the heart. *Diabetes Research and Clinical Practice* 2011, 93:S86-S91.

69. Riehle C, Abel ED: Insulin Signaling and Heart Failure. *Circulation Research* 2016, 118(7):1151-1169.

70. Zheng L, Li B, Lin S, Chen L, Li H: Role and mechanism of cardiac insulin resistance in occurrence of heart failure caused by myocardial hypertrophy. *Aging*, 11(16):6584-6590.

71. Miki T, Yuda S, Kouzu H, Miura T: Diabetic cardiomyopathy: pathophysiology and clinical features. *Heart Failure Reviews* 2013, 18(2):149-166.

72. Tarquini R, Lazzeri C, Pala L, Rotella CM, Gensini GF: The diabetic cardiomyopathy. *Acta Diabetologica* 2011, 48(3):173-181.

73. Rubler S, Dlugash J, Yuceoglu YZ, Kumral T, Branwood AW, Grishman A: New type of cardiomyopathy associated with diabetic glomerulosclerosis. *The American Journal of Cardiology* 1972, 30(6):595-602.

74. Bell DSH: Diabetic Cardiomyopathy. *Diabetes Care* 2003, 26(10):2949-2951.

75. Lohman TG: Skinfolds and Body Density and Their Relation to Body Fatness:

A Review. *Human Biology* 1981, 53(2):181-225.

76. Tsubota A, Okamatsu-Ogura Y, Bariuan JV, Mae J, Matsuoka S, Nio-Kobayashi J, Kimura K: Role of brown adipose tissue in body temperature control during the early postnatal period in Syrian hamsters and mice. *Journal of Veterinary Medical Science* 2019, 81(10):1461-1467.
77. Galic S, Oakhill JS, Steinberg GR: Adipose tissue as an endocrine organ. *Molecular and Cellular Endocrinology* 2010, 316(2):129-139.
78. Sethi JK, Vidal-Puig AJ: Thematic review series: Adipocyte Biology. Adipose tissue function and plasticity orchestrate nutritional adaptation. *Journal of Lipid Research* 2007, 48(6):1253-1262.
79. Waki H, Tontonoz P: Endocrine Functions of Adipose Tissue. *Annual Review of Pathology: Mechanisms of Disease* 2007, 2(1):31-56.
80. Ahima RS: Adipose Tissue as an Endocrine Organ. *Obesity* 2006, 14(S8):242S-249S.
81. Gruzdeva O, Borodkina D, Uchasova E, Dyleva Y, Barbarash O: Leptin resistance: underlying mechanisms and diagnosis. *Diabetes, Metabolic Syndrome and Obesity: Targets and Therapy* 2019, 12:191-198.
82. Yanai H, Yoshida H: Beneficial Effects of Adiponectin on Glucose and Lipid Metabolism and Atherosclerotic Progression: Mechanisms and Perspectives. In: *International Journal of Molecular Sciences.* vol. 20; 2019.
83. Achari AE, Jain SK: Adiponectin, a Therapeutic Target for Obesity, Diabetes, and Endothelial Dysfunction. In: *International Journal of Molecular Sciences.* vol. 18; 2017.
84. Kadowaki T, Yamauchi T: Adiponectin and Adiponectin Receptors. *Endocrine Reviews* 2005, 26(3):439-451.
85. Sethi JK, Hotamisligil GS: Metabolic Messengers: tumour necrosis factor. *Nature Metabolism* 2021, 3(10):1302-1312.
86. Bastard J-P, Jardel C, Bruckert E, Blondy P, Capeau J, Laville M, Vidal H, Hainque B: Elevated Levels of Interleukin 6 Are Reduced in Serum and Subcutaneous Adipose Tissue of Obese Women after Weight Loss*. *The*

Journal of Clinical Endocrinology & Metabolism 2000, 85(9):3338-3342.

87. Kojta I, Chacińska M, Błachnio-Zabielska A: Obesity, Bioactive Lipids, and Adipose Tissue Inflammation in Insulin Resistance. In: *Nutrients.* vol. 12; 2020.

88. Saponaro C, Gaggini M, Carli F, Gastaldelli A: The Subtle Balance between Lipolysis and Lipogenesis: A Critical Point in Metabolic Homeostasis. In: *Nutrients.* vol. 7; 2015: 9453-9474.

89. Boden G: Obesity and Free Fatty Acids. *Endocrinology and Metabolism Clinics of North America* 2008, 37(3):635-646.

90. Guilherme A, Virbasius JV, Puri V, Czech MP: Adipocyte dysfunctions linking obesity to insulin resistance and type 2 diabetes. *Nature Reviews Molecular Cell Biology* 2008, 9(5):367-377.

91. Goodpaster BH, Wolf D: Skeletal muscle lipid accumulation in obesity, insulin resistance, and type 2 diabetes. *Pediatric Diabetes* 2004, 5(4):219-226.

92. Liu Q, Bengmark S, Qu S: The role of hepatic fat accumulation in pathogenesis of non-alcoholic fatty liver disease (NAFLD). *Lipids in Health and Disease* 2010, 9(1):42.

93. Kalra A, Yetiskul E, Wehrle CJ, Tuma F: Physiology, liver. Internet: StatPearls; 2022.

94. Deheragoda M: Normal Liver Anatomy and Introduction to Liver Histology. In: *Textbook of Pediatric Gastroenterology, Hepatology and Nutrition: A Comprehensive Guide to Practice.* Edited by Guandalini S, Dhawan A. Cham: Springer; 2022: 739-742.

95. Rix I, Steen Pedersen J, Storgaard H, Gluud LL: Cardiometabolic effects of antidiabetic drugs in non-alcoholic fatty liver disease. *Clinical Physiology and Functional Imaging* 2019, 39(2):122-127.

96. Tso P, McGill J: The Physiology of the Liver. In.: Academia; 2003: 514-525.

97. Wang DQH: Regulation of Intestinal Cholesterol Absorption. *Annual Review of Physiology* 2007, 69(1):221-248.

98. Wang HH, Liu M, Li X, Portincasa P, Wang DQH: Impaired intestinal

cholecystokinin secretion, a fascinating but overlooked link between coeliac disease and cholesterol gallstone disease. *European Journal of Clinical Investigation* 2017, 47(4):328-333.

99. Virović-Jukić L, Živković M: Liver Function. In: *Gastrointestinal Complications of Diabetes : A Comprehensive Guide.* Edited by Duvnjak M, Smirčić-Duvnjak L. Cham: Springer; 2018: 267-274.
100. Liao C-J, Huang P-S, Chien H-T, Lin T-K, Yeh C-T, Lin K-H: Effects of Thyroid Hormones on Lipid Metabolism Pathologies in Non-Alcoholic Fatty Liver Disease. In: *Biomedicines.* vol. 10; 2022.
101. Cherrington AD: Banting Lecture 1997. Control of glucose uptake and release by the liver in vivo. *Diabetes* 1999, 48(5):1198-1214.
102. Michael MD, Kulkarni RN, Postic C, Previs SF, Shulman GI, Magnuson MA, Kahn CR: Loss of Insulin Signaling in Hepatocytes Leads to Severe Insulin Resistance and Progressive Hepatic Dysfunction. *Molecular Cell* 2000, 6(1):87-97.
103. Biddinger SB, Hernandez-Ono A, Rask-Madsen C, Haas JT, Alemán JO, Suzuki R, Scapa EF, Agarwal C, Carey MC, Stephanopoulos G *et al*: Hepatic Insulin Resistance Is Sufficient to Produce Dyslipidemia and Susceptibility to Atherosclerosis. *Cell Metabolism* 2008, 7(2):125-134.
104. Perry RJ, Samuel VT, Petersen KF, Shulman GI: The role of hepatic lipids in hepatic insulin resistance and type 2 diabetes. *Nature* 2014, 510(7503):84-91.
105. Boden G, Cheung P, Stein TP, Kresge K, Mozzoli M: FFA cause hepatic insulin resistance by inhibiting insulin suppression of glycogenolysis. *American Journal of Physiology-Endocrinology and Metabolism* 2002, 283(1):E12-E19.
106. Kim JK, Zisman A, Fillmore JJ, Peroni OD, Kotani K, Perret P, Zong H, Dong J, Kahn CR, Kahn BB *et al*: Glucose toxicity and the development of diabetes in mice with muscle-specific inactivation of GLUT4. *The Journal of Clinical Investigation* 2001, 108(1):153-160.
107. Meex RCR, Watt MJ: Hepatokines: linking nonalcoholic fatty liver disease

and insulin resistance. *Nature Reviews Endocrinology* 2017, 13(9):509-520.

108. Peter A, Kantartzis K, Machann J, Schick F, Staiger H, Machicao F, Schleicher E, Fritsche A, Häring H-U, Stefan N: Relationships of Circulating Sex Hormone–Binding Globulin With Metabolic Traits in Humans. *Diabetes* 2010, 59(12):3167-3173.
109. Ding EL, Song Y, Malik VS, Liu S: Sex Differences of Endogenous Sex Hormones and Risk of Type 2 DiabetesA Systematic Review and Meta-analysis. *JAMA* 2006, 295(11):1288-1299.
110. Xu J, Lloyd DJ, Hale C, Stanislaus S, Chen M, Sivits G, Vonderfecht S, Hecht R, Li Y-S, Lindberg RA *et al*: Fibroblast Growth Factor 21 Reverses Hepatic Steatosis, Increases Energy Expenditure, and Improves Insulin Sensitivity in Diet-Induced Obese Mice. *Diabetes* 2009, 58(1):250-259.
111. Anatomy of the Brain [https://mayfieldclinic.com/pe-anatbrain.htm]
112. Kullmann S, Heni M, Hallschmid M, Fritsche A, Preissl H, Häring H-U: Brain Insulin Resistance at the Crossroads of Metabolic and Cognitive Disorders in Humans. *Physiological Reviews* 2016, 96(4):1169-1209.
113. Kellar D, Craft S: Brain insulin resistance in Alzheimer's disease and related disorders: mechanisms and therapeutic approaches. *The Lancet Neurology* 2020, 19(9):758-766.
114. Agrawal R, Reno CM, Sharma S, Christensen C, Huang Y, Fisher SJ: Insulin action in the brain regulates both central and peripheral functions. *American Journal of Physiology-Endocrinology and Metabolism* 2021, 321(1):E156-E163.
115. Marks JL, Porte DJ, Stahl WL, Baskin DG: Localization of insulin receptor mRNA in rat brain by in situ hybridization. *Endocrinology* 1990, 127(6):3234-3236.
116. Unger JW, Betz M: Insulin receptors and signal transduction proteins in the hypothalamo-hypophyseal system: a review on morphological findings and functional implications. *Histology and Histopathology* 1998, 13(4):1215-1224.
117. Baura GD, Foster DM, Porte D, Jr., Kahn SE, Bergman RN, Cobelli C,

Schwartz MW: Saturable transport of insulin from plasma into the central nervous system of dogs in vivo. A mechanism for regulated insulin delivery to the brain. *The Journal of Clinical Investigation* 1993, 92(4):1824-1830.

118. Banks WA, Jaspan JB, Kastin AJ: Selective, Physiological Transport of Insulin Across the Blood-Brain Barrier: Novel Demonstration by Species-Specific Radioimmunoassays. *Peptides* 1997, 18(8):1257-1262.

119. Schwartz MW, Sipols A, Kahn SE, Lattemann DF, Taborsky GJ, Bergman RN, Woods SC, Porte D: Kinetics and specificity of insulin uptake from plasma into cerebrospinal fluid. *American Journal of Physiology-Endocrinology and Metabolism* 1990, 259(3):E378.

120. Csajbók ÉA, Tamás G: Cerebral cortex: a target and source of insulin? *Diabetologia* 2016, 59(8):1609-1615.

121. Clarke DW, Mudd L, Boyd Jr FT, Fields M, Raizada MK: Insulin Is Released from Rat Brain Neuronal Cells in Culture. *Journal of Neurochemistry* 1986, 47(3):831-836.

122. Arnold SE, Arvanitakis Z, Macauley-Rambach SL, Koenig AM, Wang H-Y, Ahima RS, Craft S, Gandy S, Buettner C, Stoeckel LE *et al*: Brain insulin resistance in type 2 diabetes and Alzheimer disease: concepts and conundrums. *Nature Reviews Neurology* 2018, 14(3):168-181.

123. J. Spielman L, Bahniwal M, P. Little J, G. Walker D, Klegeris A: Insulin Modulates In Vitro Secretion of Cytokines and Cytotoxins by Human Glial Cells. *Current Alzheimer Research* 2015, 12(7):684-693.

124. Uemura E, Greenlee HW: Insulin regulates neuronal glucose uptake by promoting translocation of glucose transporter GLUT3. *Experimental Neurology* 2006, 198(1):48-53.

125. Maher F, Vannucci SJ, Simpson IA: Glucose transporter proteins in brain. *The FASEB Journal* 1994, 8(13):1003-1011.

126. Blázquez E, Velázquez E, Hurtado-Carneiro V, Ruiz-Albusac JM: Insulin in the Brain: Its Pathophysiological Implications for States Related with Central Insulin Resistance, Type 2 Diabetes and Alzheimer's Disease. *Frontiers in*

Endocrinology 2014, 5.

127. Pocai A, Lam TKT, Gutierrez-Juarez R, Obici S, Schwartz GJ, Bryan J, Aguilar-Bryan L, Rossetti L: Hypothalamic KATP channels control hepatic glucose production. *Nature* 2005, 434(7036):1026-1031.
128. Obici S, Zhang BB, Karkanias G, Rossetti L: Hypothalamic insulin signaling is required for inhibition of glucose production. *Nature Medicine* 2002, 8(12):1376-1382.
129. Shin Andrew C, Fasshauer M, Filatova N, Grundell Linus A, Zielinski E, Zhou J-Y, Scherer T, Lindtner C, White Phillip J, Lapworth Amanda L *et al*: Brain Insulin Lowers Circulating BCAA Levels by Inducing Hepatic BCAA Catabolism. *Cell Metabolism* 2014, 20(5):898-909.
130. Scherer T, O'Hare J, Diggs-Andrews K, Schweiger M, Cheng B, Lindtner C, Zielinski E, Vempati P, Su K, Dighe S *et al*: Brain Insulin Controls Adipose Tissue Lipolysis and Lipogenesis. *Cell Metabolism* 2011, 13(2):183-194.
131. Mielke JG, Taghibiglou C, Liu L, Zhang Y, Jia Z, Adeli K, Wang YT: A biochemical and functional characterization of diet-induced brain insulin resistance. *Journal of Neurochemistry* 2005, 93(6):1568-1578.
132. de la Monte SM, Wands JR: Alzheimer's Disease is Type 3 Diabetes—Evidence Reviewed. *Journal of Diabetes Science and Technology* 2008, 2(6):1101-1113.
133. Patarrão RS, Wayne Lautt W, Paula Macedo M: Assessment of methods and indexes of insulin sensitivity. *Revista Portuguesa de Endocrinologia, Diabetes e Metabolismo* 2014, 9(1):65-73.
134. Muniyappa R, Lee S, Chen H, Quon MJ: Current approaches for assessing insulin sensitivity and resistance in vivo: advantages, limitations, and appropriate usage. *American Journal of Physiology-Endocrinology and Metabolism* 2008, 294(1):E15-E26.
135. Wallace TM, Levy JC, Matthews DR: Use and Abuse of HOMA Modeling. *Diabetes Care* 2004, 27(6):1487-1495.
136. DeFronzo RA, Tobin JD, Andres R: Glucose clamp technique: a method for

quantifying insulin secretion and resistance. *American Journal of Physiology-Endocrinology and Metabolism* 1979, 237(3):E214.

137. Tam CS, Xie W, Johnson WD, Cefalu WT, Redman LM, Ravussin E: Defining Insulin Resistance From Hyperinsulinemic-Euglycemic Clamps. *Diabetes Care* 2012, 35(7):1605-1610.

138. Matthews DR, Hosker JP, Rudenski AS, Naylor BA, Treacher DF, Turner RC: Homeostasis model assessment: insulin resistance and β-cell function from fasting plasma glucose and insulin concentrations in man. *Diabetologia* 1985, 28(7):412-419.

139. Katz A, Nambi SS, Mather K, Baron AD, Follmann DA, Sullivan G, Quon MJ: Quantitative Insulin Sensitivity Check Index: A Simple, Accurate Method for Assessing Insulin Sensitivity In Humans. *The Journal of Clinical Endocrinology & Metabolism* 2000, 85(7):2402-2410.

140. Gutt M, Davis CL, Spitzer SB, Llabre MM, Kumar M, Czarnecki EM, Schneiderman N, Skyler JS, Marks JB: Validation of the insulin sensitivity index (ISI0,120): comparison with other measures. *Diabetes Research and Clinical Practice* 2000, 47(3):177-184.

141. Mizuta T, Kawaguchi Y, Eguchi Y, Takahashi H, Ario K, Akiyama T, Oza N, Otsuka T, Kuwashiro T, Yoshimura T *et al*: Whole-Body Insulin Sensitivity Index Is a Highly Specific Predictive Marker for Virological Response to Peginterferon Plus Ribavirin Therapy in Chronic Hepatitis C Patients with Genotype 1b and High Viral Load. *Digestive Diseases and Sciences* 2009, 55(1):183.

142. Borai A, Livingstone C, Ferns GAA: The biochemical assessment of insulin resistance. *Annals of Clinical Biochemistry* 2007, 44(4):324-342.

143. Iozzo P, Jarvisalo MJ, Kiss J, Borra R, Naum GA, Viljanen A, Viljanen T, Gastaldelli A, Buzzigoli E, Guiducci L *et al*: Quantification of Liver Glucose Metabolism by Positron Emission Tomography: Validation Study in Pigs. *Gastroenterology* 2007, 132(2):531-542.

144. Altun Tuzcu S, Cetin FA, Pekkolay Z, Tuzcu AK: 18F-Fluorodeoxyglucose

PET/CT Can Be an Alternative Method to Assessment of Insulin Resistance. *Acta Endocrinologica (Bucharest)* 2019, 15(4):539-543.

145. Nasr G, Sliem H: Silent ischemia in relation to insulin resistance in normotensive prediabetic adults: early detection by single photon emission computed tomography (SPECT). *The International Journal of Cardiovascular Imaging* 2011, 27(3):335-341.
146. Halpenny DF, Burke JP, Lawlor GO, O'Connell M: Role of PET and Combination PET/CT in the Evaluation of Patients with Inflammatory Bowel Disease. *Inflammatory Bowel Diseases* 2009, 15(6):951-958.
147. Magkos F, Mittendorfer B: Stable isotope-labeled tracers for the investigation of fatty acid and triglyceride metabolism in humans in vivo. *Clinical Lipidology* 2009, 4(2):215-230.
148. Choukem SP, Gautier JF: How to measure hepatic insulin resistance? *Diabetes & Metabolism* 2008, 34(6, Part 2):664-673.
149. Miele E, Spinelli GP, Tomao F, Zullo A, De Marinis F, Pasciuti G, Rossi L, Zoratto F, Tomao S: Positron Emission Tomography (PET) radiotracers in oncology – utility of 18F-Fluoro-deoxy-glucose (FDG)-PET in the management of patients with non-small-cell lung cancer (NSCLC). *Journal of Experimental & Clinical Cancer Research* 2008, 27(1):52.
150. MacDonald PE, El-kholy W, Riedel MJ, Salapatek AMF, Light PE, Wheeler MB: The Multiple Actions of GLP-1 on the Process of Glucose-Stimulated Insulin Secretion. *Diabetes* 2002, 51(suppl_3):S434-S442.
151. Ørskov C, Rabenhøj L, Wettergren A, Kofod H, Holst JJ: Tissue and Plasma Concentrations of Amidated and Glycine-Extended Glucagon-Like Peptide I in Humans. *Diabetes* 1994, 43(4):535-539.
152. Müller TD, Finan B, Bloom SR, D'Alessio D, Drucker DJ, Flatt PR, Fritsche A, Gribble F, Grill HJ, Habener JF *et al*: Glucagon-like peptide 1 (GLP-1). *Molecular Metabolism* 2019, 30:72-130.
153. Gallwitz B: Anorexigenic Effects of GLP-1 and Its Analogues. In: *Appetite Control.* Edited by Joost H-G. Berlin, Heidelberg: Springer Berlin Heidelberg;

2012: 185-207.

154. Verspohl EJ: Novel therapeutics for type 2 diabetes: Incretin hormone mimetics (glucagon-like peptide-1 receptor agonists) and dipeptidyl peptidase-4 inhibitors. *Pharmacology & Therapeutics* 2009, 124(1):113-138.

155. Drucker DJ, Nauck MA: The incretin system: glucagon-like peptide-1 receptor agonists and dipeptidyl peptidase-4 inhibitors in type 2 diabetes. *The Lancet* 2006, 368(9548):1696-1705.

156. Sekirov I, Russell SL, Antunes LCM, Finlay BB: Gut Microbiota in Health and Disease. *Physiological Reviews* 2010, 90(3):859-904.

157. Tsabouri S, Priftis KN, Chaliasos N, Siamopoulou A: Modulation of gut microbiota downregulates the development of food allergy in infancy. *Allergologia et Immunopathologia* 2014, 42(1):69-77.

158. Schloss Patrick D, Handelsman J: Status of the Microbial Census. *Microbiology and Molecular Biology Reviews* 2004, 68(4):686-691.

159. Xu J, Gordon JI: Honor thy symbionts. *Proceedings of the National Academy of Sciences* 2003, 100(18):10452-10459.

160. Karlsson FH, Ussery DW, Nielsen J, Nookaew I: A Closer Look at Bacteroides: Phylogenetic Relationship and Genomic Implications of a Life in the Human Gut. *Microbial Ecology* 2011, 61(3):473-485.

161. Fan Y, Pedersen O: Gut microbiota in human metabolic health and disease. *Nature Reviews Microbiology* 2021, 19(1):55-71.

162. Thursby E, Juge N: Introduction to the human gut microbiota. *Biochemical Journal* 2017, 474(11):1823-1836.

163. Simrén M, Barbara G, Flint HJ, Spiegel BMR, Spiller RC, Vanner S, Verdu EF, Whorwell PJ, Zoetendal EG: Intestinal microbiota in functional bowel disorders: a Rome foundation report. *Gut* 2013, 62(1):159.

164. Łuc M, Misiak B, Pawłowski M, Stańczykiewicz B, Zabłocka A, Szcześniak D, Pałęga A, Rymaszewska J: Gut microbiota in dementia. Critical review of novel findings and their potential application. *Progress in Neuro-Psychopharmacology and Biological Psychiatry* 2021, 104:110039.

165. Wozniak H, Beckmann TS, Fröhlich L, Soccorsi T, Le Terrier C, de Watteville A, Schrenzel J, Heidegger C-P: The central and biodynamic role of gut microbiota in critically ill patients. *Critical Care* 2022, 26(1):250.

166. Canfora EE, Jocken JW, Blaak EE: Short-chain fatty acids in control of body weight and insulin sensitivity. *Nature Reviews Endocrinology* 2015, 11(10):577-591.

167. Caricilli AM, Saad MJA: The Role of Gut Microbiota on Insulin Resistance. In: *Nutrients.* vol. 5; 2013: 829-851.

168. Qin J, Li Y, Cai Z, Li S, Zhu J, Zhang F, Liang S, Zhang W, Guan Y, Shen D *et al*: A metagenome-wide association study of gut microbiota in type 2 diabetes. *Nature* 2012, 490(7418):55-60.

169. Gurung M, Li Z, You H, Rodrigues R, Jump DB, Morgun A, Shulzhenko N: Role of gut microbiota in type 2 diabetes pathophysiology. *EBioMedicine* 2020, 51:102590.

170. Sikalidis AK, Maykish A: The Gut Microbiome and Type 2 Diabetes Mellitus: Discussing A Complex Relationship. In: *Biomedicines.* vol. 8; 2020.

171. Jensen AB, Sørensen TIA, Pedersen O, Jess T, Brunak S, Allin KH: Increase in clinically recorded type 2 diabetes after colectomy. *eLife* 2018, 7:e37420.

172. Thaiss CA, Levy M, Grosheva I, Zheng D, Soffer E, Blacher E, Braverman S, Tengeler AC, Barak O, Elazar M *et al*: Hyperglycemia drives intestinal barrier dysfunction and risk for enteric infection. *Science* 2018, 359(6382):1376-1383.

173. Karlsson FH, Tremaroli V, Nookaew I, Bergström G, Behre CJ, Fagerberg B, Nielsen J, Bäckhed F: Gut metagenome in European women with normal, impaired and diabetic glucose control. *Nature* 2013, 498(7452):99-103.

174. Allin KH, Tremaroli V, Caesar R, Jensen BAH, Damgaard MTF, Bahl MI, Licht TR, Hansen TH, Nielsen T, Dantoft TM *et al*: Aberrant intestinal microbiota in individuals with prediabetes. *Diabetologia* 2018, 61(4):810-820.

175. Zhong H, Ren H, Lu Y, Fang C, Hou G, Yang Z, Chen B, Yang F, Zhao Y, Shi Z *et al*: Distinct gut metagenomics and metaproteomics signatures in

prediabetics and treatment-naïve type 2 diabetics. *EBioMedicine* 2019, 47:373-383.

176. Cardiovascular diseases (CVDs) [https://www.who.int/news-room/fact-sheets/detail/cardiovascular-diseases-(cvds)]

177. Severino P, Amato A, Pucci M, Infusino F, Adamo F, Birtolo LI, Netti L, Montefusco G, Chimenti C, Lavalle C *et al*: Ischemic Heart Disease Pathophysiology Paradigms Overview: From Plaque Activation to Microvascular Dysfunction. In: *International Journal of Molecular Sciences.* vol. 21; 2020.

178. Cui X, Ye L, Li J, Jin L, Wang W, Li S, Bao M, Wu S, Li L, Geng B *et al*: Metagenomic and metabolomic analyses unveil dysbiosis of gut microbiota in chronic heart failure patients. *Scientific Reports* 2018, 8(1):635.

179. Jie Z, Xia H, Zhong S-L, Feng Q, Li S, Liang S, Zhong H, Liu Z, Gao Y, Zhao H *et al*: The gut microbiome in atherosclerotic cardiovascular disease. *Nature Communications* 2017, 8(1):845.

180. Padwal R, Straus SE, McAlister FA: Cardiovascular risk factors and their effects on the decision to treat hypertension: evidence based review. *BMJ* 2001, 322(7292):977.

181. Brunt EM, Tiniakos DG: Histopathology of nonalcoholic fatty liver disease. *World journal of gastroenterology* 2010, 16(42):5286–5296.

182. Tiniakos DG: Nonalcoholic fatty liver disease/nonalcoholic steatohepatitis: histological diagnostic criteria and scoring systems. *European Journal of Gastroenterology & Hepatology* 2010, 22(6).

183. Younossi ZM, Koenig AB, Abdelatif D, Fazel Y, Henry L, Wymer M: Global epidemiology of nonalcoholic fatty liver disease—Meta-analytic assessment of prevalence, incidence, and outcomes. *Hepatology* 2016, 64(1):73-84.

184. Tilg H, Moschen AR: Evolution of inflammation in nonalcoholic fatty liver disease: The multiple parallel hits hypothesis. *Hepatology* 2010, 52(5):1836-1846.

185. Abu-Shanab A, Quigley EMM: The role of the gut microbiota in nonalcoholic fatty liver disease. *Nature Reviews Gastroenterology & Hepatology* 2010, 7(12):691-701.

186. Jiang W, Wu N, Wang X, Chi Y, Zhang Y, Qiu X, Hu Y, Li J, Liu Y: Dysbiosis gut microbiota associated with inflammation and impaired mucosal immune function in intestine of humans with non-alcoholic fatty liver disease. *Scientific Reports* 2015, 5(1):8096.

187. Zhu L, Baker SS, Gill C, Liu W, Alkhouri R, Baker RD, Gill SR: Characterization of gut microbiomes in nonalcoholic steatohepatitis (NASH) patients: A connection between endogenous alcohol and NASH. *Hepatology* 2013, 57(2):601-609.

188. Global status report on the public health response to dementia. Geneva: World Health Organization; 2021.

189. Erkkinen MG, Kim M-O, Geschwind MD: Clinical Neurology and Epidemiology of the Major Neurodegenerative Diseases. 2018, 10(4).

190. Mosconi L, Pupi A, De Leon MJ: Brain Glucose Hypometabolism and Oxidative Stress in Preclinical Alzheimer's Disease. *Annals of the New York Academy of Sciences* 2008, 1147(1):180-195.

191. Mosconi L, Mistur R, Switalski R, Tsui WH, Glodzik L, Li Y, Pirraglia E, De Santi S, Reisberg B, Wisniewski T *et al*: FDG-PET changes in brain glucose metabolism from normal cognition to pathologically verified Alzheimer’s disease. *European Journal of Nuclear Medicine and Molecular Imaging* 2009, 36(5):811-822.

192. M. de la Monte S: Brain Insulin Resistance and Deficiency as Therapeutic Targets in Alzheimer's Disease. *Current Alzheimer Research* 2012, 9(1):35-66.

193. Grenham S, Clarke G, Cryan J, Dinan T: Brain–Gut–Microbe Communication in Health and Disease. *Frontiers in Physiology* 2011, 2.

194. Vogt NM, Kerby RL, Dill-McFarland KA, Harding SJ, Merluzzi AP, Johnson SC, Carlsson CM, Asthana S, Zetterberg H, Blennow K *et al*: Gut microbiome alterations in Alzheimer’s disease. *Scientific Reports* 2017, 7(1):13537.

195. Johnson CH, Ivanisevic J, Siuzdak G: Metabolomics: beyond biomarkers and towards mechanisms. *Nature Reviews Molecular Cell Biology* 2016, 17(7):451-459.

196. Palomino-Schätzlein M, Simó R, Hernández C, Ciudin A, Mateos-Gregorio P, Hernández-Mijares A, Pineda-Lucena A, Herance JR: Metabolic fingerprint of insulin resistance in human polymorphonuclear leucocytes. *PLOS ONE* 2018, 13(7):e0199351.

197. Metabolomics [https://www.ebi.ac.uk/training/online/courses/metabolomics-introduction/what-is/]

198. Stringer KA, McKay RT, Karnovsky A, Quémerais B, Lacy P: Metabolomics and Its Application to Acute Lung Diseases. *Frontiers in Immunology* 2016, 7.

199. Wishart DS: Current Progress in computational metabolomics. *Briefings in Bioinformatics* 2007, 8(5):279-293.

200. Wishart DS: Advances in metabolite identification. *Bioanalysis* 2011, 3(15):1769-1782.

201. Psychogios N, Hau DD, Peng J, Guo AC, Mandal R, Bouatra S, Sinelnikov I, Krishnamurthy R, Eisner R, Gautam B *et al*: The Human Serum Metabolome. *PLOS ONE* 2011, 6(2):e16957.

202. Bouatra S, Aziat F, Mandal R, Guo AC, Wilson MR, Knox C, Bjorndahl TC, Krishnamurthy R, Saleem F, Liu P *et al*: The Human Urine Metabolome. *PLOS ONE* 2013, 8(9):e73076.

203. Worley B, Powers R: Multivariate Analysis in Metabolomics. *Current Metabolomics* 2013, 1(1):92-107.

204. Beale DJ, Pinu FR, Kouremenos KA, Poojary MM, Narayana VK, Boughton BA, Kanojia K, Dayalan S, Jones OAH, Dias DA: Review of recent developments in GC–MS approaches to metabolomics-based research. *Metabolomics* 2018, 14(11):152.

205. Liu X, Locasale JW: Metabolomics: A Primer. *Trends in Biochemical Sciences* 2017, 42(4):274-284.

206. Palomino-Schätzlein M, Mayneris-Perxachs J, Caballano-Infantes E, Rodríguez MA, Palomo-Buitrago M-E, Xiao X, Mares R, Ricart W, Simó R, Herance JR *et al*: Combining metabolic profiling of plasma and faeces as a fingerprint of insulin resistance in obesity. *Clinical Nutrition* 2020, 39(7):2292-2300.

207. Claridge TDW: Chapter 1 - Introduction. In: *High-Resolution NMR Techniques in Organic Chemistry (Third Edition)*. Edited by Claridge TDW. Boston: Elsevier; 2016: 1-10.

208. Moco S: Studying Metabolism by NMR-Based Metabolomics. *Frontiers in Molecular Biosciences* 2022, 9.

209. Wilson DM, Burlingame AL, Cronholm T, Sjövall J: Deuterium and carbon-13 tracer studies of ethanol metabolism in the rat by 2H, 1H-decoupled 13C nuclear magnetic resonance. *Biochemical and Biophysical Research Communications* 1974, 56(3):828-835.

210. Sahoo NK, Tejaswini G, Sahu M, Muralikrishna K: An overview on NMR spectroscopy based metabolomics. *International Journal of Pharmaceutical Sciences and Developmental Research* 2020, 6(1):016-020.

211. Brennan L: NMR-based metabolomics: From sample preparation to applications in nutrition research. *Progress in Nuclear Magnetic Resonance Spectroscopy* 2014, 83:42-49.

212. Cacciatore S, Loda M: Innovation in metabolomics to improve personalized healthcare. *Annals of the New York Academy of Sciences* 2015, 1346(1):57-62.

213. Beckonert O, Keun HC, Ebbels TMD, Bundy J, Holmes E, Lindon JC, Nicholson JK: Metabolic profiling, metabolomic and metabonomic procedures for NMR spectroscopy of urine, plasma, serum and tissue extracts. *Nature Protocols* 2007, 2(11):2692-2703.

214. Pinto J, Domingues MRM, Galhano E, Pita C, Almeida MdC, Carreira IM, Gil AM: Human plasma stability during handling and storage: impact on NMR metabolomics. *Analyst* 2014, 139(5):1168-1177.

215. Zhao J, Evans CR, Carmody LA, LiPuma JJ: Impact of storage conditions on

metabolite profiles of sputum samples from persons with cystic fibrosis. *Journal of Cystic Fibrosis* 2015, 14(4):468-473.

216. Emwas A-H, Roy R, McKay RT, Tenori L, Saccenti E, Gowda GAN, Raftery D, Alahmari F, Jaremko L, Jaremko M *et al*: NMR Spectroscopy for Metabolomics Research. In: *Metabolites.* vol. 9; 2019.
217. Keun HC, Beckonert O, Griffin JL, Richter C, Moskau D, Lindon JC, Nicholson JK: Cryogenic Probe 13C NMR Spectroscopy of Urine for Metabonomic Studies. *Analytical Chemistry* 2002, 74(17):4588-4593.
218. Bharti SK, Roy R: Quantitative 1H NMR spectroscopy. *TrAC Trends in Analytical Chemistry* 2012, 35:5-26.
219. Wishart DS, Feunang YD, Marcu A, Guo AC, Liang K, Vázquez-Fresno R, Sajed T, Johnson D, Li C, Karu N *et al*: HMDB 4.0: the human metabolome database for 2018. *Nucleic Acids Research* 2017, 46(D1):D608-D617.
220. Ulrich EL, Akutsu H, Doreleijers JF, Harano Y, Ioannidis YE, Lin J, Livny M, Mading S, Maziuk D, Miller Z *et al*: BioMagResBank. *Nucleic Acids Research* 2008, 36(suppl_1):D402-D408.
221. De Castro F, Benedetti M, Del Coco L, Fanizzi FP: NMR-Based Metabolomics in Metal-Based Drug Research. In: *Molecules.* vol. 24; 2019.
222. De Meyer T, Sinnaeve D, Van Gasse B, Tsiporkova E, Rietzschel ER, De Buyzere ML, Gillebert TC, Bekaert S, Martins JC, Van Criekinge W: NMR-Based Characterization of Metabolic Alterations in Hypertension Using an Adaptive, Intelligent Binning Algorithm. *Analytical Chemistry* 2008, 80(10):3783-3790.
223. Triba MN, Le Moyec L, Amathieu R, Goossens C, Bouchemal N, Nahon P, Rutledge DN, Savarin P: PLS/OPLS models in metabolomics: the impact of permutation of dataset rows on the K-fold cross-validation quality parameters. *Molecular BioSystems* 2015, 11(1):13-19.
224. Zou KH, Tuncali K, Silverman SG: Correlation and Simple Linear Regression. *Radiology* 2003, 227(3):617-628.
225. Putignani L, Del Chierico F, Vernocchi P, Cicala M, Cucchiara S, Dallapiccola

B, Dysbiotrack Study G: Gut Microbiota Dysbiosis as Risk and Premorbid Factors of IBD and IBS Along the Childhood–Adulthood Transition. *Inflammatory Bowel Diseases* 2016, 22(2):487-504.

226. Adachi K, Sugiyama T, Yamaguchi Y, Tamura Y, Izawa S, Hijikata Y, Ebi M, Funaki Y, Ogasawara N, Goto C *et al*: Gut microbiota disorders cause type 2 diabetes mellitus and homeostatic disturbances in gut-related metabolism in Japanese subjects. *Journal of Clinical Biochemistry and Nutrition* 2019, 64(3):231-238.
227. Sato J, Kanazawa A, Ikeda F, Yoshihara T, Goto H, Abe H, Komiya K, Kawaguchi M, Shimizu T, Ogihara T *et al*: Gut Dysbiosis and Detection of "Live Gut Bacteria" in Blood of Japanese Patients With Type 2 Diabetes. *Diabetes Care* 2014, 37(8):2343-2350.
228. Wang TJ, Larson MG, Vasan RS, Cheng S, Rhee EP, McCabe E, Lewis GD, Fox CS, Jacques PF, Fernandez C *et al*: Metabolite profiles and the risk of developing diabetes. *Nature Medicine* 2011, 17(4):448-453.
229. Stančáková A, Civelek M, Saleem NK, Soininen P, Kangas AJ, Cederberg H, Paananen J, Pihlajamäki J, Bonnycastle LL, Morken MA *et al*: Hyperglycemia and a Common Variant of GCKR Are Associated With the Levels of Eight Amino Acids in 9,369 Finnish Men. *Diabetes* 2012, 61(7):1895-1902.
230. Chen S, Akter S, Kuwahara K, Matsushita Y, Nakagawa T, Konishi M, Honda T, Yamamoto S, Hayashi T, Noda M *et al*: Serum amino acid profiles and risk of type 2 diabetes among Japanese adults in the Hitachi Health Study. *Sci Rep* 2019, 9(1):7010.
231. Flores-Guerrero JL, Osté MCJ, Kieneker LM, Gruppen EG, Wolak-Dinsmore J, Otvos JD, Connelly MA, Bakker SJL, Dullaart RPF: Plasma Branched-Chain Amino Acids and Risk of Incident Type 2 Diabetes: Results from the PREVEND Prospective Cohort Study. In: *Journal of Clinical Medicine.* vol. 7; 2018.
232. Ruiz-Canela M, Guasch-Ferré M, Toledo E, Clish CB, Razquin C, Liang L, Wang DD, Corella D, Estruch R, Hernáez Á *et al*: Plasma branched

chain/aromatic amino acids, enriched Mediterranean diet and risk of type 2 diabetes: case-cohort study within the PREDIMED Trial. *Diabetologia* 2018, 61(7):1560-1571.

233. Cariou B, Chetiveaux M, Za ŕ Y, Pouteau E, Disse E, Guyomarc'h-Delasalle B, Laville M, Krempf M: Fasting plasma chenodeoxycholic acid and cholic acid concentrations are inversely correlated with insulin sensitivity in adults. *Nutrition & Metabolism* 2011, 8(1):48.

234. Wang Z, Klipfell E, Bennett BJ, Koeth R, Levison BS, DuGar B, Feldstein AE, Britt EB, Fu X, Chung Y-M *et al*: Gut flora metabolism of phosphatidylcholine promotes cardiovascular disease. *Nature* 2011, 472(7341):57-63.

235. Tang WHW, Wang Z, Levison BS, Koeth RA, Britt EB, Fu X, Wu Y, Hazen SL: Intestinal Microbial Metabolism of Phosphatidylcholine and Cardiovascular Risk. *New England Journal of Medicine* 2013, 368(17):1575-1584.

236. Senthong V, Wang Z, Li XS, Fan Y, Wu Y, Wilson Tang WH, Hazen SL: Intestinal Microbiota-Generated Metabolite Trimethylamine-N-Oxide and 5-Year Mortality Risk in Stable Coronary Artery Disease: The Contributory Role of Intestinal Microbiota in a COURAGE-Like Patient Cohort. *Journal of the American Heart Association*, 5(6):e002816.

237. Bhattacharya S, Granger CB, Craig D, Haynes C, Bain J, Stevens RD, Hauser ER, Newgard CB, Kraus WE, Newby LK *et al*: Validation of the association between a branched chain amino acid metabolite profile and extremes of coronary artery disease in patients referred for cardiac catheterization. *Atherosclerosis* 2014, 232(1):191-196.

238. Kuller L, Arnold A, Tracy R, Otvos J, Burke G, Psaty B, Siscovick D, Freedman DS, Kronmal R: Nuclear Magnetic Resonance Spectroscopy of Lipoproteins and Risk of Coronary Heart Disease in the Cardiovascular Health Study. *Arteriosclerosis, Thrombosis, and Vascular Biology* 2002, 22(7):1175-1180.

239. Mora S, Otvos JD, Rifai N, Rosenson RS, Buring JE, Ridker PM: Lipoprotein Particle Profiles by Nuclear Magnetic Resonance Compared With Standard Lipids and Apolipoproteins in Predicting Incident Cardiovascular Disease in Women. *Circulation* 2009, 119(7):931-939.

240. Tang WHW, Hazen SL: The contributory role of gut microbiota in cardiovascular disease. *The Journal of Clinical Investigation* 2014, 124(10):4204-4211.

241. Zhu W, Gregory JC, Org E, Buffa JA, Gupta N, Wang Z, Li L, Fu X, Wu Y, Mehrabian M *et al*: Gut Microbial Metabolite TMAO Enhances Platelet Hyperreactivity and Thrombosis Risk. *Cell* 2016, 165(1):111-124.

242. Ganna A, Salihovic S, Sundström J, Broeckling CD, Hedman ÅK, Magnusson PKE, Pedersen NL, Larsson A, Siegbahn A, Zilmer M *et al*: Large-scale Metabolomic Profiling Identifies Novel Biomarkers for Incident Coronary Heart Disease. *PLOS Genetics* 2014, 10(12):e1004801.

243. Park JY, Lee S-H, Shin M-J, Hwang G-S: Alteration in Metabolic Signature and Lipid Metabolism in Patients with Angina Pectoris and Myocardial Infarction. *PLOS ONE* 2015, 10(8):e0135228.

244. Wang J, Li Z, Chen J, Zhao H, Luo L, Chen C, Xu X, Zhang W, Gao K, Li B *et al*: Metabolomic identification of diagnostic plasma biomarkers in humans with chronic heart failure. *Molecular BioSystems* 2013, 9(11):2618-2626.

245. Piras C, Noto A, Ibba L, Deidda M, Fanos V, Muntoni S, Leoni VP, Atzori L: Contribution of Metabolomics to the Understanding of NAFLD and NASH Syndromes: A Systematic Review. In: *Metabolites.* vol. 11; 2021.

246. Kalhan SC, Guo L, Edmison J, Dasarathy S, McCullough AJ, Hanson RW, Milburn M: Plasma metabolomic profile in nonalcoholic fatty liver disease. *Metabolism* 2011, 60(3):404-413.

247. Lake AD, Novak P, Shipkova P, Aranibar N, Robertson DG, Reily MD, Lehman-McKeeman LD, Vaillancourt RR, Cherrington NJ: Branched chain amino acid metabolism profiles in progressive human nonalcoholic fatty liver disease. *Amino Acids* 2015, 47(3):603-615.

248. Zhou Y, Orešič M, Leivonen M, Gopalacharyulu P, Hyysalo J, Arola J, Verrijken A, Francque S, Van Gaal L, Hyötyläinen T *et al*: Noninvasive Detection of Nonalcoholic Steatohepatitis Using Clinical Markers and Circulating Levels of Lipids and Metabolites. *Clinical Gastroenterology and Hepatology* 2016, 14(10):1463-1472.e1466.

249. Zhu L, Baker SS, Gill C, Liu W, Alkhouri R, Baker RD, Gill SR: Characterization of gut microbiomes in nonalcoholic steatohepatitis (NASH) patients: a connection between endogenous alcohol and NASH. *Hepatology* 2013, 57(2):601-609.

250. Paglia G, Stocchero M, Cacciatore S, Lai S, Angel P, Alam MT, Keller M, Ralser M, Astarita G: Unbiased Metabolomic Investigation of Alzheimer's Disease Brain Points to Dysregulation of Mitochondrial Aspartate Metabolism. *Journal of Proteome Research* 2016, 15(2):608-618.

251. Snowden SG, Ebshiana AA, Hye A, An Y, Pletnikova O, O'Brien R, Troncoso J, Legido-Quigley C, Thambisetty M: Association between fatty acid metabolism in the brain and Alzheimer disease neuropathology and cognitive performance: A nontargeted metabolomic study. *PLOS Medicine* 2017, 14(3):e1002266.

252. Koal T, Klavins K, Seppi D, Kemmler G, Humpel C: Sphingomyelin SM(d18:1/18:0) is Significantly Enhanced in Cerebrospinal Fluid Samples Dichotomized by Pathological Amyloid-β 42, Tau, and Phospho-Tau-181 Levels. *Journal of Alzheimer's Disease* 2015, 44:1193-1201.

253. Trupp M, Jonsson P, Öhrfelt A, Zetterberg H, Obudulu O, Malm L, Wuolikainen A, Linder J, Moritz T, Blennow K *et al*: Metabolite and Peptide Levels in Plasma and CSF Differentiating Healthy Controls from Patients with Newly Diagnosed Parkinson's Disease. *Journal of Parkinson's Disease* 2014, 4:549-560.

254. Saiki S, Hatano T, Fujimaki M, Ishikawa K-I, Mori A, Oji Y, Okuzumi A, Fukuhara T, Koinuma T, Imamichi Y *et al*: Decreased long-chain acylcarnitines from insufficient β-oxidation as potential early diagnostic

markers for Parkinson's disease. *Scientific Reports* 2017, 7(1):7328.

255. Domingo-Ortí I, Lamas-Domingo R, Ciudin A, Hernández C, Herance JR, Palomino-Schätzlein M, Pineda-Lucena A: Metabolic footprint of aging and obesity in red blood cells. *Aging*, 13(4):4850-4880.

256. Zhu Y, Armstrong JL, Tchkonia T, Kirkland JL: Cellular senescence and the senescent secretory phenotype in age-related chronic diseases. *Current Opinion in Clinical Nutrition & Metabolic Care* 2014, 17(4).

257. Mauvais-Jarvis F, Bairey Merz N, Barnes PJ, Brinton RD, Carrero J-J, DeMeo DL, De Vries GJ, Epperson CN, Govindan R, Klein SL *et al*: Sex and gender: modifiers of health, disease, and medicine. *The Lancet* 2020, 396(10250):565-582.

258. Mackie RI, Sghir A, Gaskins HR: Developmental microbial ecology of the neonatal gastrointestinal tract. *The American Journal of Clinical Nutrition* 1999, 69(5):1035s-1045s.

259. Nagpal R, Mainali R, Ahmadi S, Wang S, Singh R, Kavanagh K, Kitzman DW, Kushugulova A, Marotta F, Yadav H: Gut microbiome and aging: Physiological and mechanistic insights. *Nutrition and Healthy Aging* 2018, 4:267-285.

260. Bian G, Gloor Gregory B, Gong A, Jia C, Zhang W, Hu J, Zhang H, Zhang Y, Zhou Z, Zhang J *et al*: The Gut Microbiota of Healthy Aged Chinese Is Similar to That of the Healthy Young. *mSphere* 2017, 2(5):e00327-00317.

261. Odamaki T, Kato K, Sugahara H, Hashikura N, Takahashi S, Xiao J-z, Abe F, Osawa R: Age-related changes in gut microbiota composition from newborn to centenarian: a cross-sectional study. *BMC Microbiology* 2016, 16(1):90.

262. Claesson MJ, Cusack S, O'Sullivan O, Greene-Diniz R, de Weerd H, Flannery E, Marchesi JR, Falush D, Dinan T, Fitzgerald G *et al*: Composition, variability, and temporal stability of the intestinal microbiota of the elderly. *Proceedings of the National Academy of Sciences* 2011, 108(supplement_1):4586-4591.

263. Trabado S, Al-Salameh A, Croixmarie V, Masson P, Corruble E, Fève B, Colle

R, Ripoll L, Walther B, Boursier-Neyret C *et al*: The human plasma-metabolome: Reference values in 800 French healthy volunteers; impact of cholesterol, gender and age. *PLOS ONE* 2017, 12(3):e0173615.

264. Jové M, Maté I, Naudí A, Mota-Martorell N, Portero-Otín M, De la Fuente M, Pamplona R: Human Aging Is a Metabolome-related Matter of Gender. *The Journals of Gerontology: Series A* 2016, 71(5):578-585.
265. Kovalik J-P, Zhao X, Gao F, Leng S, Chow V, Chew H, Teo LLY, Tan RS, Ewe SH, Tan HC *et al*: Amino acid differences between diabetic older adults and non-diabetic older adults and their associations with cardiovascular function. *Journal of Molecular and Cellular Cardiology* 2021, 158:63-71.
266. Wittenbecher C, Guasch-Ferré M, Haslam DE, Dennis C, Li J, Bhupathiraju SN, Lee C-H, Qi Q, Liang L, Eliassen AH *et al*: Changes in metabolomics profiles over ten years and subsequent risk of developing type 2 diabetes: Results from the Nurses' Health Study. *eBioMedicine* 2022, 75:103799.
267. Cui M, Trimigno A, Aru V, Rasmussen MA, Khakimov B, Engelsen SB: Influence of Age, Sex, and Diet on the Human Fecal Metabolome Investigated by 1H NMR Spectroscopy. *Journal of Proteome Research* 2021, 20(7):3642-3653.
268. Calvani R, Brasili E, Praticò G, Capuani G, Tomassini A, Marini F, Sciubba F, Finamore A, Roselli M, Marzetti E *et al*: Fecal and urinary NMR-based metabolomics unveil an aging signature in mice. *Experimental Gerontology* 2014, 49:5-11.
269. Ryan AS: Insulin Resistance with Aging. *Sports Medicine* 2000, 30(5):327-346.
270. Fink RI, Kolterman OG, Griffin J, Olefsky JM: Mechanisms of Insulin Resistance in Aging. *The Journal of Clinical Investigation* 1983, 71(6):1523-1535.
271. Cowie CC, Casagrande SS, Geiss LS: CHAPTER 3 Prevalence and Incidence of Type 2 Diabetes and Prediabetes. In: *Diabetes in America.* 3rd edn. Bethesda: National Institute of Diabetes and Digestive and Kidney Diseases

(US); 2018.

272. Shou J, Chen P-J, Xiao W-H: Mechanism of increased risk of insulin resistance in aging skeletal muscle. *Diabetology & Metabolic Syndrome* 2020, 12(1):14.

273. Sniderman AD, Holme I, Aastveit A, Furberg C, Walldius G, Jungner I: Relation of Age, the Apolipoprotein B/Apolipoprotein A-I Ratio, and the Risk of Fatal Myocardial Infarction and Implications for the Primary Prevention of Cardiovascular Disease. *The American Journal of Cardiology* 2007, 100(2):217-221.

274. Fryar CD, Chen T-C, Li X: Prevalence of uncontrolled risk factors for cardiovascular disease: United States, 1999-2010. *NCHS Data Brief* 2012(103):1-8.

275. Jousilahti P, Vartiainen E, Tuomilehto J, Puska P: Sex, Age, Cardiovascular Risk Factors, and Coronary Heart Disease. *Circulation* 1999, 99(9):1165-1172.

276. Jousilahti P, Vartiainen E, Tuomilehto J, Puska P: Twenty-Year Dynamics of Serum Cholesterol Levels in the Middle-Aged Population of Eastern Finland. *Annals of Internal Medicine* 1996, 125(9):713-722.

277. Booth GL, Kapral MK, Fung K, Tu JV: Relation between age and cardiovascular disease in men and women with diabetes compared with non-diabetic people: a population-based retrospective cohort study. *The Lancet* 2006, 368(9529):29-36.

278. Viikari J, Rönnemaa T, Seppänen A, Mamiemi J, Porkka K, Räsänen L, Uhari M, Salo MK, Kaprio EA, Nuutinen EM *et al*: Serum Lipids and Lipoproteins in Children, Adolescents and Young Adults in 1980–1986. *Annals of Medicine* 1991, 23(1):53-59.

279. Kim IH, Kisseleva T, Brenner DA: Aging and liver disease. *Current Opinion in Gastroenterology* 2015, 31(3).

280. Le Couteur DG, Warren A, Cogger VC, Smedsrød B, Sørensen KK, De Cabo R, Fraser R, McCuskey RS: Old Age and the Hepatic Sinusoid. *The Anatomical Record* 2008, 291(6):672-683.

281. Tietz NW, Shuey DF, Wekstein DR: Laboratory Values in Fit Aging Individuals--Sexagenarians through Centenarians. *Clinical Chemistry* 1992, 38(6):1167-1185.

282. Jin CJ, Baumann A, Brandt A, Engstler AJ, Nier A, Hege M, Schmeer C, Kehm R, Höhn A, Grune T *et al*: Aging-related liver degeneration is associated with increased bacterial endotoxin and lipopolysaccharide binding protein levels. *American Journal of Physiology-Gastrointestinal and Liver Physiology* 2020, 318(4):G736-G747.

283. Amarapurkar D, Kamani P, Patel N, Gupte P, Kumar P, Agal S, Baijal R, Lala S, Chaudhary D, Deshpande A: Prevalence of non-alcoholic fatty liver disease: population based study. *Annals of Hepatology* 2007, 6(3):161-163.

284. Park SH, Jeon WK, Kim SH, Kim HJ, Park DI, Cho YK, Sung IK, Sohn CI, Keum DK, Kim BI: Prevalence and risk factors of non-alcoholic fatty liver disease among Korean adults. *Journal of Gastroenterology and Hepatology* 2006, 21(1):138-143.

285. Noureddin M, Yates KP, Vaughn IA, Neuschwander-Tetri BA, Sanyal AJ, McCullough A, Merriman R, Hameed B, Doo E, Kleiner DE *et al*: Clinical and histological determinants of nonalcoholic steatohepatitis and advanced fibrosis in elderly patients. *Hepatology* 2013, 58(5):1644-1654.

286. Targher G, Corey KE, Byrne CD, Roden M: The complex link between NAFLD and type 2 diabetes mellitus — mechanisms and treatments. *Nature Reviews Gastroenterology & Hepatology* 2021, 18(9):599-612.

287. Leite NC, Salles GF, Araujo ALE, Villela-Nogueira CA, Cardoso CRL: Prevalence and associated factors of non-alcoholic fatty liver disease in patients with type-2 diabetes mellitus. *Liver International* 2009, 29(1):113-119.

288. Prashanth M, Ganesh H, Vima M, John M, Bandgar T, Joshi SR, Shah S, Rathi P, Joshi A, Thakkar H *et al*: Prevalence of nonalcoholic fatty liver disease in patients with type 2 diabetes mellitus. *Journal of The Association of Physicians of India* 2009, 57(3):205-210.

289. Clegg DJ, Mauvais-Jarvis F: An integrated view of sex differences in metabolic physiology and disease. *Molecular Metabolism* 2018, 15:1-2.

290. Mauvais-Jarvis F: Sex differences in metabolic homeostasis, diabetes, and obesity. *Biology of Sex Differences* 2015, 6(1):14.

291. IDF Diabetes Atlas Ninth edition 2019, 9th edn. Brussels: International Diabetes Federation; 2019.

292. Kautzky-Willer A, Harreiter J, Pacini G: Sex and Gender Differences in Risk, Pathophysiology and Complications of Type 2 Diabetes Mellitus. *Endocrine Reviews* 2016, 37(3):278-316.

293. Haro C, Rangel-Zúñiga OA, Alcalá-Díaz JF, Gómez-Delgado F, Pérez-Martínez P, Delgado-Lista J, Quintana-Navarro GM, Landa BB, Navas-Cortés JA, Tena-Sempere M *et al*: Intestinal Microbiota Is Influenced by Gender and Body Mass Index. *PLOS ONE* 2016, 11(5):e0154090.

294. Yoon K, Kim N: Roles of Sex Hormones and Gender in the Gut Microbiota. *J Neurogastroenterol Motil* 2021, 27(3):314-325.

295. Flak MB, Neves JF, Blumberg RS: Welcome to the Microgenderome. *Science* 2013, 339(6123):1044-1045.

296. Takagi T, Naito Y, Inoue R, Kashiwagi S, Uchiyama K, Mizushima K, Tsuchiya S, Dohi O, Yoshida N, Kamada K *et al*: Differences in gut microbiota associated with age, sex, and stool consistency in healthy Japanese subjects. *Journal of Gastroenterology* 2019, 54(1):53-63.

297. Sinha T, Vich Vila A, Garmaeva S, Jankipersadsing SA, Imhann F, Collij V, Bonder MJ, Jiang X, Gurry T, Alm EJ *et al*: Analysis of 1135 gut metagenomes identifies sex-specific resistome profiles. *Gut Microbes* 2019, 10(3):358-366.

298. IDF Diabetes Atlas 10TH edition, 10th edn. Brussels: International Diabetes Federation; 2021.

299. Bellamy L, Casas J-P, Hingorani AD, Williams D: Type 2 diabetes mellitus after gestational diabetes: a systematic review and meta-analysis. *The Lancet* 2009, 373(9677):1773-1779.

300. Tarnopolsky MA, Ruby BC: Sex differences in carbohydrate metabolism. *Current Opinion in Clinical Nutrition & Metabolic Care* 2001, 4(6).

301. Blaak E: Gender differences in fat metabolism. *Current Opinion in Clinical Nutrition & Metabolic Care* 2001, 4(6).

302. Krumsiek J, Mittelstrass K, Do KT, Stückler F, Ried J, Adamski J, Peters A, Illig T, Kronenberg F, Friedrich N *et al*: Gender-specific pathway differences in the human serum metabolome. *Metabolomics* 2015, 11(6):1815-1833.

303. Guasch-Ferré M, Hruby A, Toledo E, Clish CB, Martínez-González MA, Salas-Salvadó J, Hu FB: Metabolomics in Prediabetes and Diabetes: A Systematic Review and Meta-analysis. *Diabetes Care* 2016, 39(5):833-846.

304. Zhao L, Lou H, Peng Y, Chen S, Zhang Y, Li X: Comprehensive relationships between gut microbiome and faecal metabolome in individuals with type 2 diabetes and its complications. *Endocrine* 2019, 66(3):526-537.

305. Van Doorn M, Vogels J, Tas A, Van Hoogdalem EJ, Burggraaf J, Cohen A, Van Der Greef J: Evaluation of metabolite profiles as biomarkers for the pharmacological effects of thiazolidinediones in Type 2 diabetes mellitus patients and healthy volunteers. *British Journal of Clinical Pharmacology* 2007, 63(5):562-574.

306. Nuutila P, Knuuti MJ, Mäki M, Laine H, Ruotsalainen U, Teräs M, Haaparanta M, Solin O, Yki-Järvinen H: Gender and Insulin Sensitivity in the Heart and in Skeletal Muscles: Studies Using Positron Emission Tomography. *Diabetes* 1995, 44(1):31-36.

307. Geer EB, Shen W: Gender differences in insulin resistance, body composition, and energy balance. *Gender Medicine* 2009, 6:60-75.

308. Moghetti P, Tosi F, Castello R, Magnani CM, Negri C, Brun E, Furlani L, Caputo M, Muggeo M: The insulin resistance in women with hyperandrogenism is partially reversed by antiandrogen treatment: evidence that androgens impair insulin action in women. *The Journal of Clinical Endocrinology & Metabolism* 1996, 81(3):952-960.

309. Polderman KH, Gooren LJ, Asscheman H, Bakker A, Heine RJ: Induction of

insulin resistance by androgens and estrogens. *The Journal of Clinical Endocrinology & Metabolism* 1994, 79(1):265-271.

310. Louet J-F, LeMay C, Mauvais-Jarvis F: Antidiabetic actions of estrogen: Insight from human and genetic mouse models. *Current Atherosclerosis Reports* 2004, 6(3):180-185.
311. Cnop M, Havel PJ, Utzschneider KM, Carr DB, Sinha MK, Boyko EJ, Retzlaff BM, Knopp RH, Brunzell JD, Kahn SE: Relationship of adiponectin to body fat distribution, insulin sensitivity and plasma lipoproteins: evidence for independent roles of age and sex. *Diabetologia* 2003, 46(4):459-469.
312. Salas-Salvadó J, Granada M, Bulló M, Corominas A, Casas P, Foz M: Plasma adiponectin distribution in a Mediterranean population and its association with cardiovascular risk factors and metabolic syndrome. *Metabolism* 2007, 56(11):1486-1492.
313. Yamauchi T, Kamon J, Waki H, Terauchi Y, Kubota N, Hara K, Mori Y, Ide T, Murakami K, Tsuboyama-Kasaoka N *et al*: The fat-derived hormone adiponectin reverses insulin resistance associated with both lipoatrophy and obesity. *Nature Medicine* 2001, 7(8):941-946.
314. Roy AK, Chatterjee B: Sexual Dimorphism in the Liver. *Annual Review of Physiology* 1983, 45(1):37-50.
315. Kur P, Kolasa-Wołosiuk A, Misiakiewicz-Has K, Wiszniewska B: Sex Hormone-Dependent Physiology and Diseases of Liver. In: *International Journal of Environmental Research and Public Health.* vol. 17; 2020.
316. Riazi K, Azhari H, Charette JH, Underwood FE, King JA, Afshar EE, Swain MG, Congly SE, Kaplan GG, Shaheen A-A: The prevalence and incidence of NAFLD worldwide: a systematic review and meta-analysis. *The Lancet Gastroenterology & Hepatology* 2022, 7(9):851-861.
317. Eguchi Y, Hyogo H, Ono M, Mizuta T, Ono N, Fujimoto K, Chayama K, Saibara T, Jsg N: Prevalence and associated metabolic factors of nonalcoholic fatty liver disease in the general population from 2009 to 2010 in Japan: a multicenter large retrospective study. *Journal of Gastroenterology* 2012,

47(5):586-595.

318. Kirsch R, Clarkson V, Shephard EG, Marais DA, Jaffer MA, Woodburne VE, Kirsch RE, Hall PDLM: Rodent nutritional model of non-alcoholic steatohepatitis: Species, strain and sex difference studies. *Journal of Gastroenterology and Hepatology* 2003, 18(11):1272-1282.

319. Du T, Sun X, Yuan G, Zhou X, Lu H, Lin X, Yu X: Sex differences in the impact of nonalcoholic fatty liver disease on cardiovascular risk factors. *Nutrition, Metabolism and Cardiovascular Diseases* 2017, 27(1):63-69.

320. Dai W, Ye L, Liu A, Wen SW, Deng J, Wu X, Lai Z: Prevalence of nonalcoholic fatty liver disease in patients with type 2 diabetes mellitus: A meta-analysis. *Medicine* 2017, 96(39).

321. Yi M, Chen RP, Yang R, Chen H: Increased prevalence and risk of non-alcoholic fatty liver disease in overweight and obese patients with Type 2 diabetes in South China. *Diabetic Medicine* 2017, 34(4):505-513.

322. Vali Y, Lee J, Boursier J, Spijker R, Loffler J, Verheij J, Brosnan MJ, Bocskei Z, Anstee QM, Bossuyt PM *et al*: Enhanced liver fibrosis test for the non-invasive diagnosis of fibrosis in patients with NAFLD: A systematic review and meta-analysis. *Journal of Hepatology* 2020, 73(2):252-262.

323. Peytremann-Bridevaux I, Faeh D, Santos-Eggimann B: Prevalence of overweight and obesity in rural and urban settings of 10 European countries. *Preventive Medicine* 2007, 44(5):442-446.

324. Qu H-Q, Li Q, Rentfro AR, Fisher-Hoch SP, McCormick JB: The Definition of Insulin Resistance Using HOMA-IR for Americans of Mexican Descent Using Machine Learning. *PLOS ONE* 2011, 6(6):e21041.

325. Kong J, Nam SO, Ko A, Byun SY, Lim TJ, Kim YM, Yeon GM, Cho JW, Lee Y-J: Longitudinal changes in insulin resistance in children with epilepsy on ketogenic diet: Prevalence and risk factors. *Epilepsy & Behavior* 2020, 112:107393.

326. Carmina E, Lobo RA: Use of fasting blood to assess the prevalence of insulin resistance in women with polycystic ovary syndrome. *Fertility and Sterility*

2004, 82(3):661-665.

327. Unger G, Benozzi SF, Perruzza F, Pennacchiotti GL: Triglycerides and glucose index: A useful indicator of insulin resistance. *Endocrinología y Nutrición (English Edition)* 2014, 61(10):533-540.

328. Dobiášová M: AIP--atherogenic index of plasma as a significant predictor of cardiovascular risk: from research to practice. *Vnitrni lekarstvi* 2006, 52(1):64-71.

329. Dobiášová M, Frohlich J: The plasma parameter log (TG/HDL-C) as an atherogenic index: correlation with lipoprotein particle size and esterification rate inapob-lipoprotein-depleted plasma (FERHDL). *Clinical Biochemistry* 2001, 34(7):583-588.

330. Kotronen A, Peltonen M, Hakkarainen A, Sevastianova K, Bergholm R, Johansson LM, Lundbom N, Rissanen A, Ridderstråle M, Groop L *et al*: Prediction of Non-Alcoholic Fatty Liver Disease and Liver Fat Using Metabolic and Genetic Factors. *Gastroenterology* 2009, 137(3):865-872.

331. Lee J-H, Kim D, Kim HJ, Lee C-H, Yang JI, Kim W, Kim YJ, Yoon J-H, Cho S-H, Sung M-W *et al*: Hepatic steatosis index: A simple screening tool reflecting nonalcoholic fatty liver disease. *Digestive and Liver Disease* 2010, 42(7):503-508.

332. Bedogni G, Bellentani S, Miglioli L, Masutti F, Passalacqua M, Castiglione A, Tiribelli C: The Fatty Liver Index: a simple and accurate predictor of hepatic steatosis in the general population. *BMC Gastroenterology* 2006, 6(1):33.

333. Sterling RK, Lissen E, Clumeck N, Sola R, Correa MC, Montaner J, M SS, Torriani FJ, Dieterich DT, Thomas DL *et al*: Development of a simple noninvasive index to predict significant fibrosis in patients with HIV/HCV coinfection. *Hepatology* 2006, 43(6):1317-1325.

334. Angulo P, Hui JM, Marchesini G, Bugianesi E, George J, Farrell GC, Enders F, Saksena S, Burt AD, Bida JP *et al*: The NAFLD fibrosis score: A noninvasive system that identifies liver fibrosis in patients with NAFLD. *Hepatology* 2007, 45(4):846-854.

335. Herance JR, Martín-Saladich Q, Velásquez MA, Hernandez C, Aparicio C, Ramirez-Serra C, Ferrer R, Giralt-Arnaiz M, González-Ballester MÁ, Pericàs JM *et al*: Identification of Myocardial Insulin Resistance by Using Liver Tests: A Simple Approach for Clinical Practice. In: *International Journal of Molecular Sciences.* vol. 23; 2022.

336. Yu Z, Morrison M: Improved extraction of PCR-quality community DNA from digesta and fecal samples. 2004, 36(5):808-812.

337. Cardona S, Eck A, Cassellas M, Gallart M, Alastrue C, Dore J, Azpiroz F, Roca J, Guarner F, Manichanh C: Storage conditions of intestinal microbiota matter in metagenomic analysis. *BMC Microbiology* 2012, 12(1):158.

338. Palkova L, Tomova A, Repiska G, Babinska K, Bokor B, Mikula I, Minarik G, Ostatnikova D, Soltys K: Evaluation of 16S rRNA primer sets for characterisation of microbiota in paediatric patients with autism spectrum disorder. *Scientific Reports* 2021, 11(1):6781.

339. Caporaso JG, Lauber CL, Walters WA, Berg-Lyons D, Lozupone CA, Turnbaugh PJ, Fierer N, Knight R: Global patterns of 16S rRNA diversity at a depth of millions of sequences per sample. *Proc Natl Acad Sci U S A* 2011, 108 Suppl 1:4516-4522.

340. Bolyen E, Rideout JR, Dillon MR, Bokulich NA, Abnet CC, Al-Ghalith GA, Alexander H, Alm EJ, Arumugam M, Asnicar F *et al*: Reproducible, interactive, scalable and extensible microbiome data science using QIIME 2. *Nature Biotechnology* 2019, 37(8):852-857.

341. Bokulich NA, Kaehler BD, Rideout JR, Dillon M, Bolyen E, Knight R, Huttley GA, Gregory Caporaso J: Optimizing taxonomic classification of marker-gene amplicon sequences with QIIME 2's q2-feature-classifier plugin. *Microbiome* 2018, 6(1):90.

342. Moreno-Navarrete JM, Novelle MG, Catalán V, Ortega F, Moreno M, Gomez-Ambrosi J, Xifra G, Serrano M, Guerra E, Ricart W *et al*: Insulin Resistance Modulates Iron-Related Proteins in Adipose Tissue. *Diabetes Care* 2014, 37(4):1092-1100.

343. Mosteller RD: Simplified Calculation of Body-Surface Area. *New England Journal of Medicine* 1987, 317(17):1098-1098.

344. Rinninella E, Raoul P, Cintoni M, Franceschi F, Miggiano GA, Gasbarrini A, Mele MC: What is the Healthy Gut Microbiota Composition? A Changing Ecosystem across Age, Environment, Diet, and Diseases. In: *Microorganisms.* vol. 7; 2019.

345. Stojanov S, Berlec A, Štrukelj B: The Influence of Probiotics on the Firmicutes/Bacteroidetes Ratio in the Treatment of Obesity and Inflammatory Bowel disease. In: *Microorganisms.* vol. 8; 2020.

346. Liu X, Zheng Y, Guasch-Ferré M, Ruiz-Canela M, Toledo E, Clish C, Liang L, Razquin C, Corella D, Estruch R *et al*: High plasma glutamate and low glutamine-to-glutamate ratio are associated with type 2 diabetes: Case-cohort study within the PREDIMED trial. *Nutrition, Metabolism and Cardiovascular Diseases* 2019, 29(10):1040-1049.

347. Maggio CA, Pi-Sunyer FX: Obesity and type 2 diabetes. *Endocrinology and Metabolism Clinics* 2003, 32(4):805-822.

348. Larsen N, Vogensen FK, van den Berg FW, Nielsen DS, Andreasen AS, Pedersen BK, Al-Soud WA, Sorensen SJ, Hansen LH, Jakobsen M: Gut microbiota in human adults with type 2 diabetes differs from non-diabetic adults. *PLoS One* 2010, 5(2):e9085.

349. Xu J, Lian F, Zhao L, Zhao Y, Chen X, Zhang X, Guo Y, Zhang C, Zhou Q, Xue Z *et al*: Structural modulation of gut microbiota during alleviation of type 2 diabetes with a Chinese herbal formula. *ISME J* 2015, 9(3):552-562.

350. Bostanciklioğlu M: The role of gut microbiota in pathogenesis of Alzheimer's disease. *Journal of Applied Microbiology* 2019, 127(4):954-967.

351. Fikri AM, Smyth R, Kumar V, Al-Abadla Z, Abusnana S, Munday MR: Pre-diagnostic biomarkers of type 2 diabetes identified in the UAE's obese national population using targeted metabolomics. *Scientific Reports* 2020, 10(1):17616.

352. Prag HA, Aksentijevic D, Dannhorn A, Giles AV, Mulvey JF, Sauchanka O,

Du L, Bates G, Reinhold J, Kula-Alwar D *et al*: Ischemia-Selective Cardioprotection by Malonate for Ischemia/Reperfusion Injury. *Circulation Research* 2022, 131(6):528-541.

353. Garvey WT, Kwon S, Zheng D, Shaughnessy S, Wallace P, Hutto A, Pugh K, Jenkins AJ, Klein RL, Liao Y: Effects of Insulin Resistance and Type 2 Diabetes on Lipoprotein Subclass Particle Size and Concentration Determined by Nuclear Magnetic Resonance. *Diabetes* 2003, 52(2):453-462.
354. Mora S, Otvos JD, Rosenson RS, Pradhan A, Buring JE, Ridker PM: Lipoprotein Particle Size and Concentration by Nuclear Magnetic Resonance and Incident Type 2 Diabetes in Women. *Diabetes* 2010, 59(5):1153-1160.
355. Festa A, Williams K, Hanley AJG, Otvos JD, Goff DC, Wagenknecht LE, Haffner SM: Nuclear Magnetic Resonance Lipoprotein Abnormalities in Prediabetic Subjects in the Insulin Resistance Atherosclerosis Study. *Circulation* 2005, 111(25):3465-3472.
356. Andersson-Hall U, Gustavsson C, Pedersen A, Malmodin D, Joelsson L, Holmäng A: Higher Concentrations of BCAAs and 3-HIB Are Associated with Insulin Resistance in the Transition from Gestational Diabetes to Type 2 Diabetes. *Journal of Diabetes Research* 2018, 2018:4207067.
357. Abdul Kadir A, Clarke K, Evans RD: Cardiac ketone body metabolism. *Biochimica et Biophysica Acta (BBA) - Molecular Basis of Disease* 2020, 1866(6):165739.
358. Wu X-J, Shu Q-Q, Wang B, Dong L, Hao B: Acetoacetate Improves Memory in Alzheimer's Mice via Promoting Brain-Derived Neurotrophic Factor and Inhibiting Inflammation. *American Journal of Alzheimer's Disease & Other Dementias®* 2022, 37:15333175221124949.
359. Newsholme P, Procopio J, Lima MMR, Pithon-Curi TC, Curi R: Glutamine and glutamate—their central role in cell metabolism and function. *Cell Biochemistry and Function* 2003, 21(1):1-9.
360. Cheng S, Rhee EP, Larson MG, Lewis GD, McCabe EL, Shen D, Palma MJ, Roberts LD, Dejam A, Souza AL *et al*: Metabolite profiling identifies

pathways associated with metabolic risk in humans. *Circulation* 2012, 125(18):2222-2231.

361. Leylabadlo HE, Ghotaslou R, Feizabadi MM, Farajnia S, Moaddab SY, Ganbarov K, Khodadadi E, Tanomand A, Sheykhsaran E, Yousefi B *et al*: The critical role of Faecalibacterium prausnitzii in human health: An overview. *Microbial Pathogenesis* 2020, 149:104344.
362. Koliada A, Syzenko G, Moseiko V, Budovska L, Puchkov K, Perederiy V, Gavalko Y, Dorofeyev A, Romanenko M, Tkach S *et al*: Association between body mass index and Firmicutes/Bacteroidetes ratio in an adult Ukrainian population. *BMC Microbiol* 2017, 17(1):120.
363. Moran-Ramos S, Macias-Kauffer L, López-Contreras BE, Villamil-Ramírez H, Ocampo-Medina E, León-Mimila P, del Rio-Navarro BE, Granados-Portillo O, Ibarra-Gonzalez I, Vela-Amieva M *et al*: A higher bacterial inward BCAA transport driven by Faecalibacterium prausnitzii is associated with lower serum levels of BCAA in early adolescents. *Molecular Medicine* 2021, 27(1):108.
364. Ganesan K, Chung SK, Vanamala J, Xu B: Causal Relationship between Diet-Induced Gut Microbiota Changes and Diabetes: A Novel Strategy to Transplant Faecalibacterium prausnitzii in Preventing Diabetes. In: *International Journal of Molecular Sciences*. vol. 19; 2018.
365. Zambom de Souza AZ, Zambom AZ, Abboud KY, Reis SK, Tannihão F, Guadagnini D, Saad MJA, Prada PO: Oral supplementation with l-glutamine alters gut microbiota of obese and overweight adults: A pilot study. *Nutrition* 2015, 31(6):884-889.
366. Lim E, Lee M-J: Optimal cut-off value of high-sensitivity troponin I in diagnosing myocardial infarction in patients with end-stage renal disease. *Medicine* 2020, 99(5).
367. Webster AC, Nagler EV, Morton RL, Masson P: Chronic Kidney Disease. *The Lancet* 2017, 389(10075):1238-1252.
368. Pfennig N, Trüper HG: The Family Chromatiaceae. In: *The Prokaryotes: A*

Handbook on the Biology of Bacteria: Ecophysiology, Isolation, Identification, Applications. Edited by Balows A, Trüper HG, Dworkin M, Harder W, Schleifer K-H. New York, NY: Springer New York; 1992: 3200-3221.

369. Michail S, Lin M, Frey MR, Fanter R, Paliy O, Hilbush B, Reo NV: Altered gut microbial energy and metabolism in children with non-alcoholic fatty liver disease. *FEMS Microbiology Ecology* 2015, 91(2):1-9.
370. Sookoian S, Salatino A, Castaño GO, Landa MS, Fijalkowky C, Garaycoechea M, Pirola CJ: Intrahepatic bacterial metataxonomic signature in non-alcoholic fatty liver disease. *Gut* 2020, 69(8):1483.
371. Clerc P, Polster BM: Investigation of Mitochondrial Dysfunction by Sequential Microplate-Based Respiration Measurements from Intact and Permeabilized Neurons. *PLOS ONE* 2012, 7(4):e34465.
372. Shippy DC, Wilhelm C, Viharkumar PA, Raife TJ, Ulland TK: β-Hydroxybutyrate inhibits inflammasome activation to attenuate Alzheimer's disease pathology. *Journal of Neuroinflammation* 2020, 17(1):280.
373. Haam J-H, Lee YK, Suh E, Kim Y-S: Characteristics of Urine Organic Acid Metabolites in Nonalcoholic Fatty Liver Disease Assessed Using Magnetic Resonance Imaging with Elastography in Korean Adults. In: *Diagnostics*. vol. 12; 2022.
374. Sattar N: Gender aspects in type 2 diabetes mellitus and cardiometabolic risk. *Best Practice & Research Clinical Endocrinology & Metabolism* 2013, 27(4):501-507.
375. Gijón-Conde T, Graciani A, Guallar-Castillón P, Aguilera MT, Rodríguez-Artalejo F, Banegas JR: Leptin Reference Values and Cutoffs for Identifying Cardiometabolic Abnormalities in the Spanish Population. *Revista Española de Cardiología (English Edition)* 2015, 68(8):672-679.
376. Silbiger SR, Neugarten J: The Role of Gender in the Progression of Renal Disease. *Advances in Renal Replacement Therapy* 2003, 10(1):3-14.
377. Balakrishnan M, Patel P, Dunn-Valadez S, Dao C, Khan V, Ali H, El-Serag L, Hernaez R, Sisson A, Thrift AP *et al*: Women Have a Lower Risk of

Nonalcoholic Fatty Liver Disease but a Higher Risk of Progression vs Men: A Systematic Review and Meta-analysis. *Clinical Gastroenterology and Hepatology* 2021, 19(1):61-71.e15.

378. Lopetuso LR, Scaldaferri F, Petito V, Gasbarrini A: Commensal Clostridia: leading players in the maintenance of gut homeostasis. *Gut Pathogens* 2013, 5(1):23.
379. Hu T, Wu Q, Yao Q, Jiang K, Yu J, Tang Q: Short-chain fatty acid metabolism and multiple effects on cardiovascular diseases. *Ageing Research Reviews* 2022, 81:101706.
380. Chen H, Meng L, Shen L: Multiple roles of short-chain fatty acids in Alzheimer disease. *Nutrition* 2022, 93:111499.
381. Canfora EE, Meex RCR, Venema K, Blaak EE: Gut microbial metabolites in obesity, NAFLD and T2DM. *Nature Reviews Endocrinology* 2019, 15(5):261-273.
382. Ikeyama N, Murakami T, Toyoda A, Mori H, Iino T, Ohkuma M, Sakamoto M: Microbial interaction between the succinate-utilizing bacterium Phascolarctobacterium faecium and the gut commensal Bacteroides thetaiotaomicron. *MicrobiologyOpen* 2020, 9(10):e1111.
383. Cho S-H, Cho Y-J, Park J-H: The human symbiont Bacteroides thetaiotaomicron promotes diet-induced obesity by regulating host lipid metabolism. *Journal of Microbiology* 2022, 60(1):118-127.
384. Coppola S, Avagliano C, Calignano A, Berni Canani R: The Protective Role of Butyrate against Obesity and Obesity-Related Diseases. In: *Molecules.* vol. 26; 2021.
385. Dudzinska W: Purine nucleotides and their metabolites in patients with type 1 and 2 diabetes mellitus %J Journal of Biomedical Science and Engineering. 2014, Vol.07No.01:7.
386. Serena C, Ceperuelo-Mallafre V, Keiran N, Queipo-Ortuno MI, Bernal R, Gomez-Huelgas R, Urpi-Sarda M, Sabater M, Perez-Brocal V, Andres-Lacueva C *et al*: Elevated circulating levels of succinate in human

obesity are linked to specific gut microbiota. *ISME J* 2018, 12(7):1642-1657.

387. Wakita Y, Shimomura Y, Kitada Y, Yamamoto H, Ohashi Y, Matsumoto M: Taxonomic classification for microbiome analysis, which correlates well with the metabolite milieu of the gut. *BMC Microbiology* 2018, 18(1):188.

388. Aujoulat F, Mazuet C, Criscuolo A, Popoff MR, Enault C, Diancourt L, Jumas-Bilak E, Lavigne J-P, Marchandin H: Peptoniphilus nemausensis sp. nov. A new Gram-positive anaerobic coccus isolated from human clinical samples, an emendated description of the genus Peptoniphilus and an evaluation of the taxonomic status of Peptoniphilus species with not validly published names. *Systematic and Applied Microbiology* 2021, 44(5):126235.

389. Herance JR, Simó R, Velasquez MA, Paun B, Garcı́a-Leon D, Aparicio C, Marés R, Simó-Servat O, Castell-Conesa J, Hernández C *et al*: Phenotyping Type 2 Diabetes in Terms of Myocardial Insulin Resistance and Its Potential Cardiovascular Consequences: A New Strategy Based on 18F-FDG PET/CT. *Journal of Personalized Medicine* 2022, 12(1).

390. Blüher M, Michael MD, Peroni OD, Ueki K, Carter N, Kahn BB, Kahn CR: Adipose Tissue Selective Insulin Receptor Knockout Protects against Obesity and Obesity-Related Glucose Intolerance. *Developmental Cell* 2002, 3(1):25-38.

391. Saad MJA, Santos A, Prada PO: Linking Gut Microbiota and Inflammation to Obesity and Insulin Resistance. *Physiology* 2016, 31(4):283-293.

392. Chen Z, Radjabzadeh D, Chen L, Kurilshikov A, Kavousi M, Ahmadizar F, Ikram MA, Uitterlinden AG, Zhernakova A, Fu J *et al*: Association of Insulin Resistance and Type 2 Diabetes With Gut Microbial Diversity: A Microbiome-Wide Analysis From Population Studies. *JAMA Network Open* 2021, 4(7):e2118811-e2118811.

393. Kim JK, Fillmore JJ, Chen Y, Yu C, Moore IK, Pypaert M, Lutz EP, Kako Y, Velez-Carrasco W, Goldberg IJ *et al*: Tissue-specific overexpression of lipoprotein lipase causes tissue-specific insulin resistance. *Proceedings of the National Academy of Sciences* 2001, 98(13):7522-7527.

394. van der Kolk BW, Vogelzangs N, Jocken JWE, Valsesia A, Hankemeier T, Astrup A, Saris WHM, Arts ICW, van Greevenbroek MMJ, Blaak EE *et al*: Plasma lipid profiling of tissue-specific insulin resistance in human obesity. *International Journal of Obesity* 2019, 43(5):989-998.

395. Vogelzangs N, van der Kallen CJH, van Greevenbroek MMJ, van der Kolk BW, Jocken JWE, Goossens GH, Schaper NC, Henry RMA, Eussen SJPM, Valsesia A *et al*: Metabolic profiling of tissue-specific insulin resistance in human obesity: results from the Diogenes study and the Maastricht Study. *International Journal of Obesity* 2020, 44(6):1376-1386.

396. FízeI'ová M, Cederberg H, Stančáková A, Jauhiainen R, Vangipurapu J, Kuusisto J, Laakso M: Markers of Tissue-Specific Insulin Resistance Predict the Worsening of Hyperglycemia, Incident Type 2 Diabetes and Cardiovascular Disease. *PLOS ONE* 2014, 9(10):e109772.

397. Fedorov A, Beichel R, Kalpathy-Cramer J, Finet J, Fillion-Robin JC, Pujol S, Bauer C, Jennings D, Fennessy F, Sonka M *et al*: 3D Slicer as an image computing platform for the Quantitative Imaging Network. *Magn Reson Imaging* 2012, 30(9):1323-1341.

398. Fedorov A, Clunie D, Ulrich E, Bauer C, Wahle A, Brown B, Onken M, Riesmeier J, Pieper S, Kikinis R *et al*: DICOM for quantitative imaging biomarker development: a standards based approach to sharing clinical data and structured PET/CT analysis results in head and neck cancer research. *PeerJ* 2016, 4:e2057.

399. Kitagawa T, Nakamoto Y, Fujii Y, Sasaki K, Tatsugami F, Awai K, Hirokawa Y, Kihara Y: Relationship between coronary arterial 18F-sodium fluoride uptake and epicardial adipose tissue analyzed using computed tomography. *European Journal of Nuclear Medicine and Molecular Imaging* 2020, 47(7):1746-1756.

400. Rothman DL, Shulman RG, Shulman GI: 31P nuclear magnetic resonance measurements of muscle glucose-6-phosphate. Evidence for reduced insulin-dependent muscle glucose transport or phosphorylation activity in non-insulin-dependent diabetes mellitus. *The Journal of Clinical Investigation*

1992, 89(4):1069-1075.

401. Kataoka H: Vascular expansion during worsening of heart failure: Effects on clinical features and its determinants. *International Journal of Cardiology* 2017, 230:556-561.

402. Kataoka H: Biochemical Determinants of Changes in Plasma Volume After Decongestion Therapy for Worsening Heart Failure. *Journal of Cardiac Failure* 2019, 25(3):213-217.

403. Afdhal NH: Fibroscan (transient elastography) for the measurement of liver fibrosis. *Gastroenterology & hepatology* 2012, 8(9):605-607.

404. Lichtinghagen R, Pietsch D, Bantel H, Manns MP, Brand K, Bahr MJ: The Enhanced Liver Fibrosis (ELF) score: Normal values, influence factors and proposed cut-off values. *Journal of Hepatology* 2013, 59(2):236-242.

405. Wade WG: The Genus Eubacterium and Related Genera. In: *The Prokaryotes: Volume 4: Bacteria: Firmicutes, Cyanobacteria.* Edited by Dworkin M, Falkow S, Rosenberg E, Schleifer K-H, Stackebrandt E. New York, NY: Springer US; 2006: 823-835.

406. Mountfort DO, Grant WD, Clarke R, Asher RA: Eubacterium callanderi sp. nov. That Demethoxylates O-Methoxylated Aromatic Acids to Volatile Fatty Acids. 1988, 38(3):254-258.

407. Thiolas A, Bollet C, Gasmi M, Drancourt M, Raoult D: Eubacterium callanderi Bacteremia: Report of the First Case. *Journal of Clinical Microbiology* 2003, 41(5):2235-2236.

408. Coelho AI, Berry GT, Rubio-Gozalbo ME: Galactose metabolism and health. *Current Opinion in Clinical Nutrition & Metabolic Care* 2015, 18(4).

409. Roser M, Josic D, Kontou M, Mosetter K, Maurer P, Reutter W: Metabolism of galactose in the brain and liver of rats and its conversion into glutamate and other amino acids. *Journal of Neural Transmission* 2009, 116(2):131-139.

410. Salkovic-Petrisic M, Osmanovic-Barilar J, Knezovic A, Hoyer S, Mosetter K, Reutter W: Long-term oral galactose treatment prevents cognitive deficits in male Wistar rats treated intracerebroventricularly with streptozotocin.

Neuropharmacology 2014, 77:68-80.

411. Zhang Z-M, Chen M-J, Zou J-F, Jiang S, Shang E-X, Qian D-W, Duan J-A: UPLC-Q-TOF/MS based fecal metabolomics reveals the potential anti-diabetic effect of Xiexin Decoction on T2DM rats. *Journal of Chromatography B* 2021, 1173:122683.
412. Fiehn O, Garvey WT, Newman JW, Lok KH, Hoppel CL, Adams SH: Plasma Metabolomic Profiles Reflective of Glucose Homeostasis in Non-Diabetic and Type 2 Diabetic Obese African-American Women. *PLOS ONE* 2010, 5(12):e15234.
413. Li X, Xu Z, Lu X, Yang X, Yin P, Kong H, Yu Y, Xu G: Comprehensive two-dimensional gas chromatography/time-of-flight mass spectrometry for metabonomics: Biomarker discovery for diabetes mellitus. *Analytica Chimica Acta* 2009, 633(2):257-262.
414. Vangipurapu J, Fernandes Silva L, Kuulasmaa T, Smith U, Laakso M: Microbiota-Related Metabolites and the Risk of Type 2 Diabetes. *Diabetes Care* 2020, 43(6):1319-1325.
415. Hodge AM, Jenkins AJ, English DR, O'Dea K, Giles GG: NMR-determined lipoprotein subclass profile predicts type 2 diabetes. *Diabetes Research and Clinical Practice* 2009, 83(1):132-139.
416. Jiang R, Schulze MB, Li T, Rifai N, Stampfer MJ, Rimm EB, Hu FB: Non-HDL Cholesterol and Apolipoprotein B Predict Cardiovascular Disease Events Among Men With Type 2 Diabetes. *Diabetes Care* 2004, 27(8):1991-1997.
417. Croze ML, Gélo en A, Soulage CO: Abnormalities in myo-inositol metabolism associated with type 2 diabetes in mice fed a high-fat diet: benefits of a dietary myo-inositol supplementation. *British Journal of Nutrition* 2015, 113(12):1862-1875.
418. Zeisel SH, da Costa K-A: Choline: an essential nutrient for public health. *Nutrition Reviews* 2009, 67(11):615-623.
419. Koeth RA, Wang Z, Levison BS, Buffa JA, Org E, Sheehy BT, Britt EB, Fu X,

Wu Y, Li L *et al*: Intestinal microbiota metabolism of l-carnitine, a nutrient in red meat, promotes atherosclerosis. *Nature Medicine* 2013, 19(5):576-585.

420. Shan Z, Sun T, Huang H, Chen S, Chen L, Luo C, Yang W, Yang X, Yao P, Cheng J *et al*: Association between microbiota-dependent metabolite trimethylamine-N-oxide and type 2 diabetes. *The American Journal of Clinical Nutrition* 2017, 106(3):888-894.

421. Lemaitre RN, Jensen PN, Wang Z, Fretts AM, McKnight B, Nemet I, Biggs ML, Sotoodehnia N, de Oliveira Otto MC, Psaty BM *et al*: Association of Trimethylamine N-Oxide and Related Metabolites in Plasma and Incident Type 2 Diabetes: The Cardiovascular Health Study. *JAMA Network Open* 2021, 4(8):e2122844-e2122844.

422. Mahendran Y, Cederberg H, Vangipurapu J, Kangas AJ, Soininen P, Kuusisto J, Uusitupa M, Ala-Korpela M, Laakso M: Glycerol and Fatty Acids in Serum Predict the Development of Hyperglycemia and Type 2 Diabetes in Finnish Men. *Diabetes Care* 2013, 36(11):3732-3738.

423. Ahola-Olli AV, Mustelin L, Kalimeri M, Kettunen J, Jokelainen J, Auvinen J, Puukka K, Havulinna AS, Lehtimäki T, Kähönen M *et al*: Circulating metabolites and the risk of type 2 diabetes: a prospective study of 11,896 young adults from four Finnish cohorts. *Diabetologia* 2019, 62(12):2298-2309.

424. Lee G, You HJ, Bajaj JS, Joo SK, Yu J, Park S, Kang H, Park JH, Kim JH, Lee DH *et al*: Distinct signatures of gut microbiome and metabolites associated with significant fibrosis in non-obese NAFLD. *Nature Communications* 2020, 11(1):4982.

425. Cheng J, Xue F, Zhang M, Cheng C, Qiao L, Ma J, Sui W, Xu X, Gao C, Hao P *et al*: TRIM31 Deficiency Is Associated with Impaired Glucose Metabolism and Disrupted Gut Microbiota in Mice. *Front Physiol* 2018, 9:24.

426. Mardanov AV, Panova IA, Beletsky AV, Avakyan MR, Kadnikov VV, Antsiferov DV, Banks D, Frank YA, Pimenov NV, Ravin NV *et al*: Genomic insights into a new acidophilic, copper-resistant Desulfosporosinus isolate

from the oxidized tailings area of an abandoned gold mine. *FEMS Microbiology Ecology* 2016, 92(8):fiw111.

427. Krueger ES, Lloyd TS, Tessem JS: The Accumulation and Molecular Effects of Trimethylamine N-Oxide on Metabolic Tissues: It's Not All Bad. In: *Nutrients.* vol. 13; 2021.

428. Krueger SK, Williams DE: Mammalian flavin-containing monooxygenases: structure/function, genetic polymorphisms and role in drug metabolism. *Pharmacology & Therapeutics* 2005, 106(3):357-387.

429. Firestein S: How the olfactory system makes sense of scents. *Nature* 2001, 413(6852):211-218.

430. Borsook D, Maleki N, Burstein R: Chapter 42 - Migraine. In: *Neurobiology of Brain Disorders.* Edited by Zigmond MJ, Rowland LP, Coyle JT. San Diego: Academic Press; 2015: 693-708.

431. Wang Y, Ye X, Ding D, Lu Y: Characteristics of the intestinal flora in patients with peripheral neuropathy associated with type 2 diabetes. *Journal of International Medical Research* 2020, 48(9):0300060520936806.

432. Svingen G, Ueland PM, Schartum-Hansen H, Pedersen ER, Seifert R, Nygard OK: Metabolites in the choline oxidation pathway in relation to diabetes, glycemic control and insulin sensitivity among patients with angina pectoris. *Atherosclerosis* 2014, 235(2):e51.

433. Gill JMR, Brown JC, Bedford D, Wright DM, Cooney J, Hughes DA, Packard CJ, Caslake MJ: Hepatic production of VLDL1 but not VLDL2 is related to insulin resistance in normoglycaemic middle-aged subjects. *Atherosclerosis* 2004, 176(1):49-56.

434. Mackey RH, Mora S, Bertoni AG, Wassel CL, Carnethon MR, Sibley CT, Goff DC, Jr.: Lipoprotein Particles and Incident Type 2 Diabetes in the Multi-Ethnic Study of Atherosclerosis. *Diabetes Care* 2015, 38(4):628-636.

435. Sekizkardes H, Chung ST, Chacko S, Haymond MW, Startzell M, Walter M, Walter PJ, Lightbourne M, Brown RJ: Free fatty acid processing diverges in human pathologic insulin resistance conditions. *The Journal of Clinical*

Investigation 2020, 130(7):3592-3602.

436. Xia F, Xu X, Zhai H, Meng Y, Zhang H, Du S, Xu H, Wu H, Lu Y: Castration-induced testosterone deficiency increases fasting glucose associated with hepatic and extra-hepatic insulin resistance in adult male rats. *Reproductive Biology and Endocrinology* 2013, 11(1):106.

437. Kawanaka M, Nishino K, Oka T, Urata N, Nakamura J, Suehiro M, Kawamoto H, Chiba Y, Yamada G: Tyrosine levels are associated with insulin resistance in patients with nonalcoholic fatty liver disease. *Hepatic Medicine : Evidence and Research* 2015, 7:29–35.

438. Blancquaert L, Everaert I, Missinne M, Baguet A, Stegen S, Volkaert A, Petrovic M, Vervaet C, Achten E, De Maeyer M *et al*: Effects of Histidine and β-alanine Supplementation on Human Muscle Carnosine Storage. *Medicine & Science in Sports & Exercise* 2017, 49(3).

439. Feng RN, Niu YC, Sun XW, Li Q, Zhao C, Wang C, Guo FC, Sun CH, Li Y: Histidine supplementation improves insulin resistance through suppressed inflammation in obese women with the metabolic syndrome: a randomised controlled trial. *Diabetologia* 2013, 56(5):985-994.

440. Jeppesen, Facchini, Reaven: Individuals with high total cholesterol/hdl cholesterol ratios are insulin resistant. *Journal of Internal Medicine* 1998, 243(4):293-298.

441. Bugianesi E, Moscatiello S, Ciaravella MF, Marchesini G: Insulin Resistance in Nonalcoholic Fatty Liver Disease. *Current Pharmaceutical Design* 2010, 16(17):1941-1951.

442. Perry IJ, Wannamethee SG, Shaper AG: Prospective Study of Serum γ-Glutamyltransferase and Risk of NIDDM. *Diabetes Care* 1998, 21(5):732-737.

443. Merchante N, Rivero A, de los Santos-Gil I, Merino D, Márquez M, López-Ruz MÁ, Rodríguez-Baño J, del Valle J, Camacho Á, Sanz-Sanz J *et al*: Insulin resistance is associated with liver stiffness in HIV/HCV co-infected patients. *Gut* 2009, 58(12):1654.

444. Stefan N, Vozarova B, Funahashi T, Matsuzawa Y, Weyer C, Lindsay RS, Youngren JF, Havel PJ, Pratley RE, Bogardus C *et al*: Plasma Adiponectin Concentration Is Associated With Skeletal Muscle Insulin Receptor Tyrosine Phosphorylation, and Low Plasma Concentration Precedes a Decrease in Whole-Body Insulin Sensitivity in Humans. *Diabetes* 2002, 51(6):1884-1888.

445. Burgert TS, Taksali SE, Dziura J, Goodman TR, Yeckel CW, Papademetris X, Constable RT, Weiss R, Tamborlane WV, Savoye M *et al*: Alanine Aminotransferase Levels and Fatty Liver in Childhood Obesity: Associations with Insulin Resistance, Adiponectin, and Visceral Fat. *The Journal of Clinical Endocrinology & Metabolism* 2006, 91(11):4287-4294.

446. Kato K-i, Takeshita Y, Misu H, Zen Y, Kaneko S, Takamura T: Liver steatosis is associated with insulin resistance in skeletal muscle rather than in the liver in Japanese patients with non-alcoholic fatty liver disease. *Journal of Diabetes Investigation* 2015, 6(2):158-163.

447. Ng RC-L, Cheng O-Y, Jian M, Kwan JS-C, Ho PW-L, Cheng KK-Y, Yeung PKK, Zhou LL, Hoo RL-C, Chung SK *et al*: Chronic adiponectin deficiency leads to Alzheimer's disease-like cognitive impairments and pathologies through AMPK inactivation and cerebral insulin resistance in aged mice. *Molecular Neurodegeneration* 2016, 11(1):71.

448. Gerber Y, VanWagner LB, Yaffe K, Terry JG, Rana JS, Reis JP, Sidney S: Non-alcoholic fatty liver disease and cognitive function in middle-aged adults: the CARDIA study. *BMC Gastroenterology* 2021, 21(1):96.

449. Weinstein G, Davis-Plourde K, Himali JJ, Zelber-Sagi S, Beiser AS, Seshadri S: Non-alcoholic fatty liver disease, liver fibrosis score and cognitive function in middle-aged adults: The Framingham Study. *Liver International* 2019, 39(9):1713-1721.

450. Budoff Matthew J, Raggi P, Beller George A, Berman Daniel S, Druz Regina S, Malik S, Rigolin Vera H, Weigold Wm G, Soman P, null n: Noninvasive Cardiovascular Risk Assessment of the Asymptomatic Diabetic Patient. *JACC: Cardiovascular Imaging* 2016, 9(2):176-192.

451. Rodgers JL, Jones J, Bolleddu SI, Vanthenapalli S, Rodgers LE, Shah K, Karia K, Panguluri SK: Cardiovascular Risks Associated with Gender and Aging. In: *Journal of Cardiovascular Development and Disease*. vol. 6; 2019.

452. Pracon R, Kruk M, Kepka C, Pregowski J, Opolski MP, Dzielinska Z, Michalowska I, Chmielak Z, Demkow M, Ruzyllo W: Epicardial Adipose Tissue Radiodensity Is Independently Related to Coronary Atherosclerosis. *Circulation Journal* 2011, 75(2):391-397.

453. Shimabukuro M, Hirata Y, Tabata M, Dagvasumberel M, Sato H, Kurobe H, Fukuda D, Soeki T, Kitagawa T, Takanashi S *et al*: Epicardial Adipose Tissue Volume and Adipocytokine Imbalance Are Strongly Linked to Human Coronary Atherosclerosis. *Arteriosclerosis, Thrombosis, and Vascular Biology* 2013, 33(5):1077-1084.

8. Annexes

All supplementary figures were included here.

8.1 Studies between T2DM and healthy controls

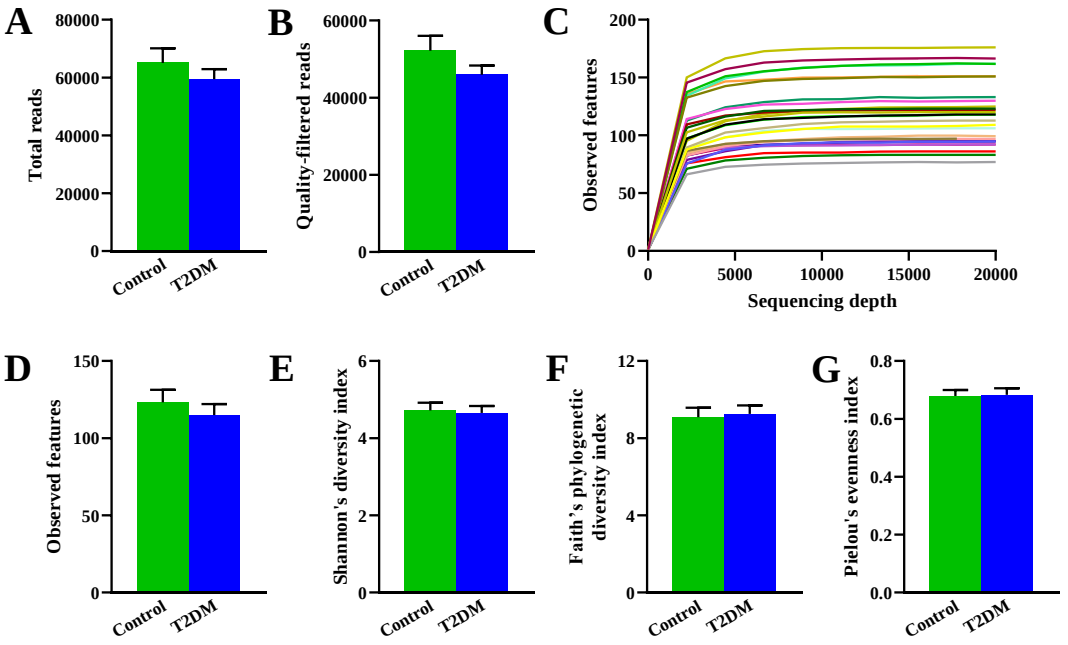

Supplementary Figure 2.1 Sequencing and alpha diversity analyses. A) and B) were bar plots of sequencing reads. C) was a rarefaction curve. D), E) and F) were different indicators reflecting the species richness when the sequencing depth was 20000. G) was Pielou's evenness index which presented the species evenness of a community. Data were shown as mean ± SEM in A, B, and D to F. Data were shown as the median and interquartile range in G.

8.2 Studies between middle-aged and old-aged T2DM patients

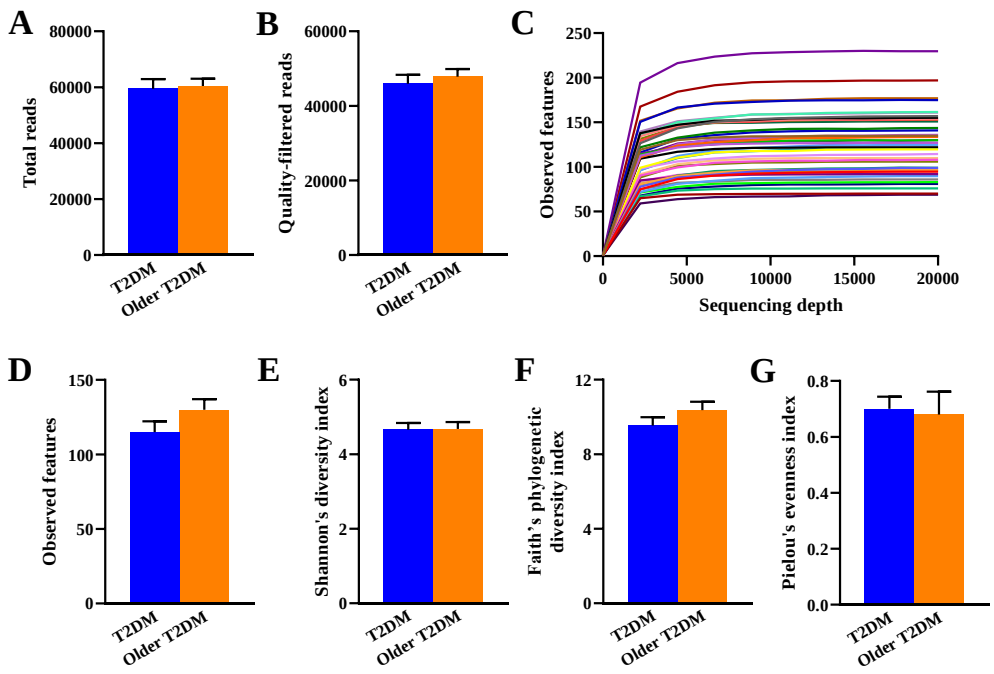

Supplementary Figure 2.2 Basic sequencing and alpha diversity analyses between middle-aged and old-aged T2DM patients. A) and B) showed the bar plots of sequencing reads. C) displayed rarefaction curve. D) to F) showed the different indicators reflecting the species richness when the sequencing depth was 20000. G) exhibited Pielou's evenness index which presented the species evenness of a community. Data were shown as mean ± SEM in A), B) and D) to F). Data were shown as the median and interquartile range in G).

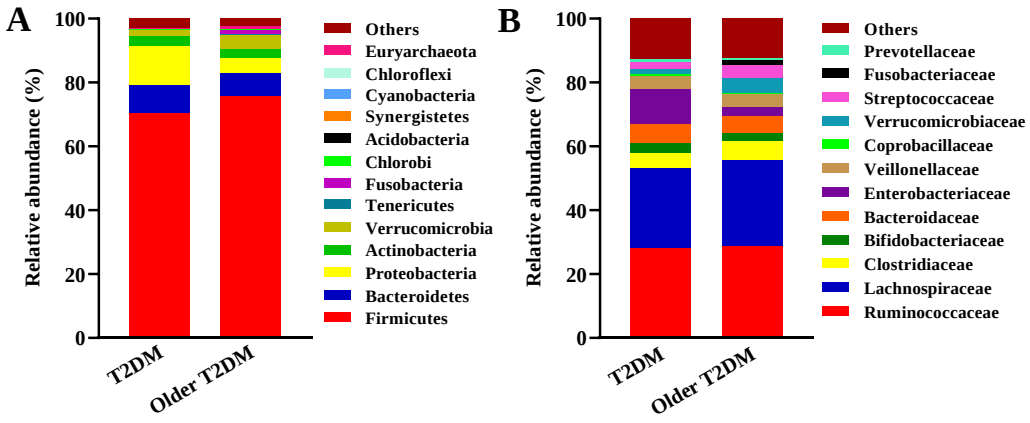

Supplementary Figure 2.3 Composition of gut microbiota in middle-aged and old-aged T2DM individuals. A) and B) showed the relative abundance of gut bacteria at the phylum and family levels respectively.

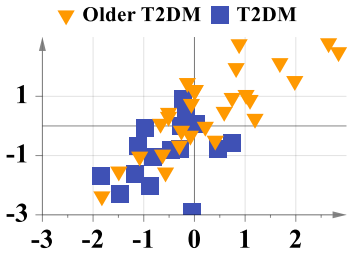

Supplementary Figure 2.4 PLS regression analysis of fecal metabolic profiles versus NAFLD fibrosis score in middle-aged and old-aged T2DM groups. The model's parameters were: UV scaling, R2Y(cum)= 0.589, Q2(cum)= 0.262. Permutation test: R2=(0.0, 0.479), Q2=(0.0, -0.099), p from CV-Anova = 0.013.

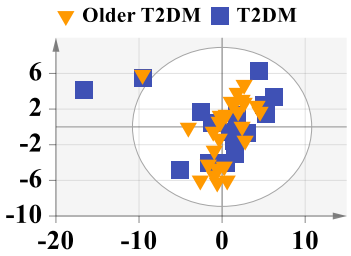

Supplementary Figure 2.5 Principal component analysis of plasma metabolites between middle-aged and old-aged T2DM subjects. The model's parameters were: UV scaling, R2X(cum)= 0.841, Q2(cum)= 0.679.

8.3 Studies between female and male T2DM patients

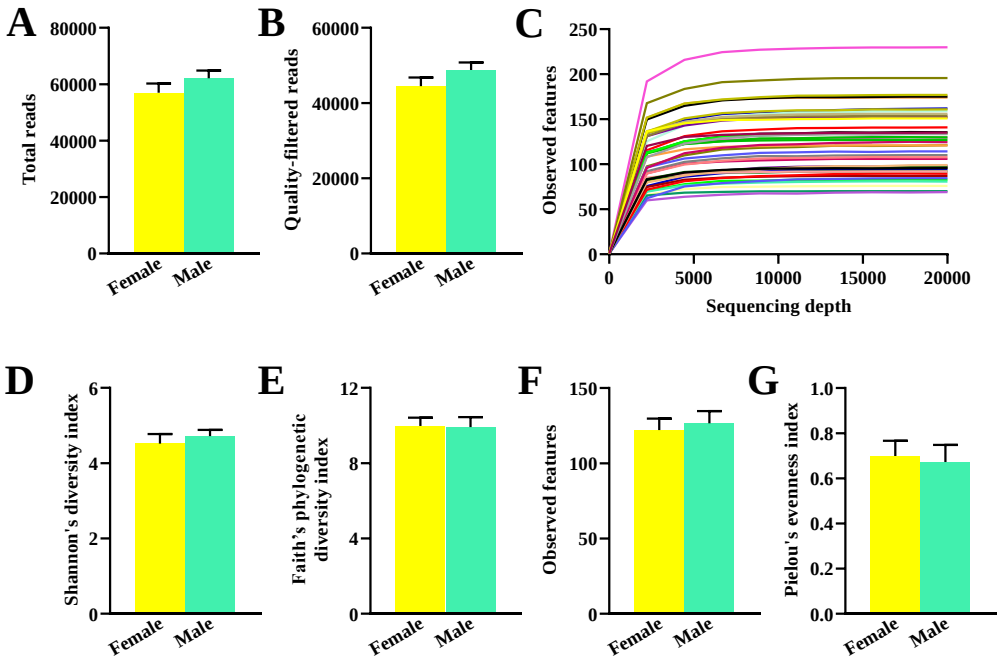

Supplementary Figure 2.6 Sequencing and alpha diversity analyses between female and male T2DM patients. A) and B) showed the bar plots of sequencing reads. C) displayed the rarefaction curve. D) to F) showed the different indicators reflecting the species richness when the sequencing depth was 20000. G) showed Pielou's evenness index which presented the species evenness of a community. Data were shown as mean ± SEM in A), B) and D) to F). Data were shown as the median and interquartile range in G).

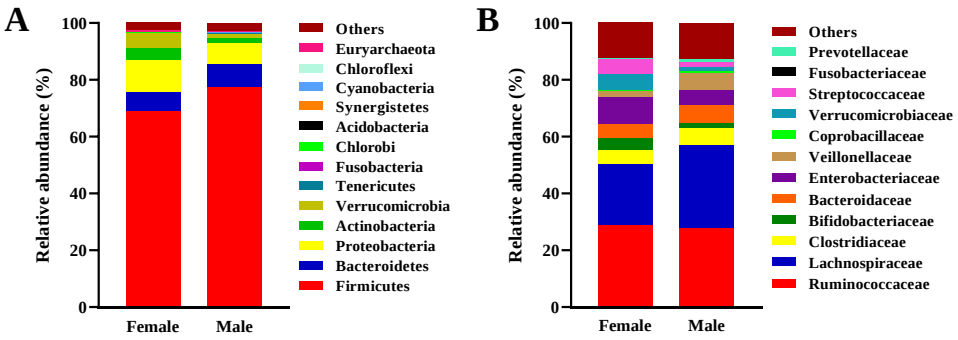

Supplementary Figure 2.7 Composition of gut microbiota in female and male patients. A) and B) showed the relative abundance of gut bacteria at the phylum and family levels respectively.

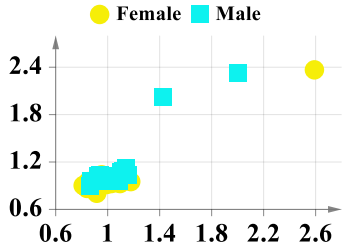

Supplementary Figure 2.8 PLS regression analysis of gut microbiota versus the waist/hip ratio in female and male T2DM groups. The model parameters were: UV scaling, R2Y(cum)= 0.830, Q2(cum)= 0.199. Permutation test: R2=(0.0, 0.812), Q2=(0.0, -0.124), p from CV-Anova = 0.111.

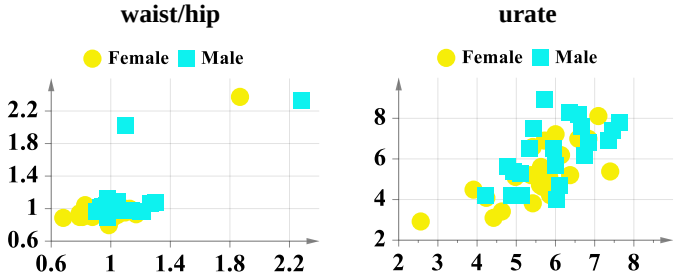

Supplementary Figure 2.9 PLS regression analysis of fecal metabolic profiles with anthropometric and biochemical variables in female and male T2DM. The models' parameters were: **waist/hip**, UV scaling, R2Y(cum)= 0.619, Q2(cum)= 0.241. Permutation test: R2=(0.0, 0.459), Q2=(0.0, -0.120), p from CV-Anova = 0.137. **Urate**, UV scaling, R2Y(cum)= 0.456, Q2(cum)= 0.073. Permutation test: R2=(0.0, 0.252), Q2=(0.0, -0.067), p from CV-Anova = 0.211.

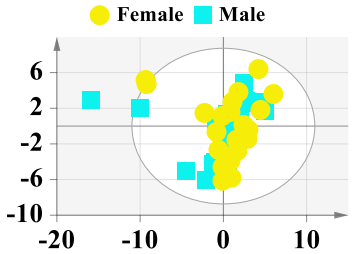

Supplementary Figure 2.10 PCA analysis of plasma metabolomic profiles between female and male T2DM subjects. The model's parameters were: UV scaling, R2X(cum)= 0.846, Q2(cum)= 0.704.

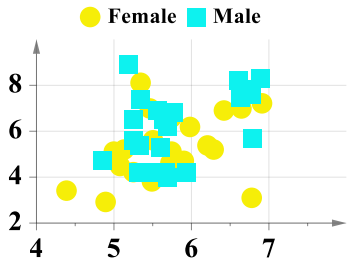

Supplementary Figure 2.11 PLS regression analysis of plasma metabolomics versus blood urate in female and male T2DM groups. The model's parameters were: UV scaling, R2Y(cum)= 0.172, Q2(cum)= 0.078. Permutation test: R2=(0.0, 0.081), Q2=(0.0, -0.077), p from CV-Anova = 0.197.

8.4 Studies between mIS and mIR patients

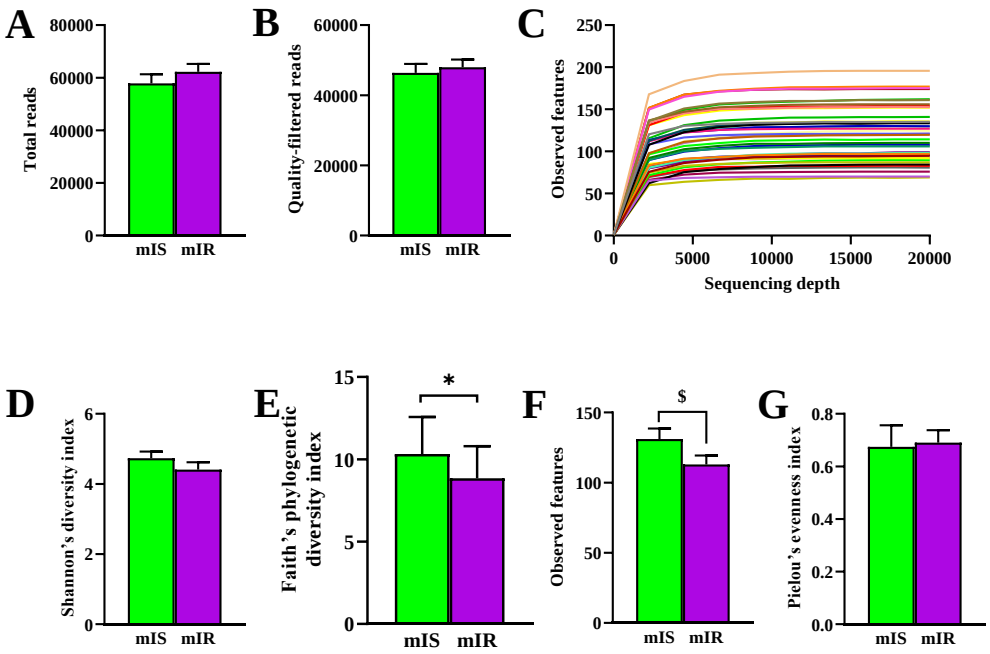

Supplementary Figure 3.1 Sequencing and alpha diversity analyses between mIS and mIR. A) and B) showed the bar plots of sequencing reads. C) displayed the rarefaction curve. D) to F) showed the different indicators reflecting the species richness when the sequencing depth was 20000. G) showed Pielou's evenness index which presented the species evenness of a community. Data were shown as mean ± SEM in A), B) and D) to F). Data were shown as the median and interquartile range in G). * and $ mean $p<0.05$, $0.05<p<0.1$, respectively.

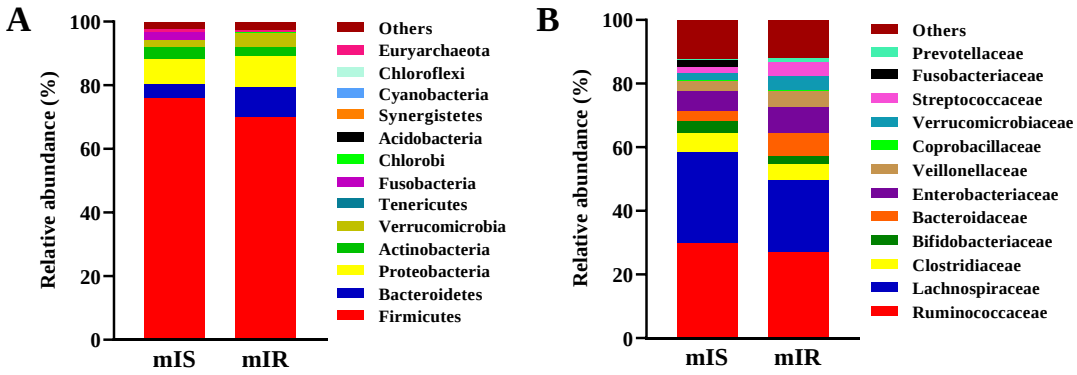

Supplementary Figure 3.2 Composition of gut microbiota in the mIS and mIR groups. A) and B) showed the relative abundance of major gut bacteria at the phylum and family levels respectively.

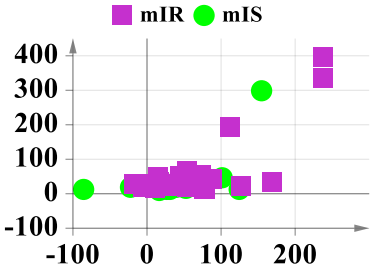

Supplementary Figure 3.3 PLS regression analysis of fecal metabolic profiles versus hepatic enzyme GGT in mIS and mIR. The models' parameters were: UV scaling, R2Y(cum)= 0.537, Q2(cum)= 0.147. Permutation test: R2=(0.0, 0.271), Q2=(0.0, -0.100), p from CV-Anova = 0.045.

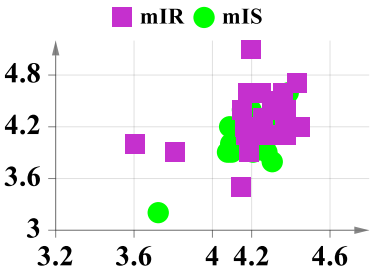

Supplementary Figure 3.4 PLS regression analysis of plasma metabolic profiles versus blood albumin in mIS and mIR. The models' parameters were: UV scaling, R2Y(cum)= 0.261, Q2(cum)= 0.193. Permutation test: R2=(0.0, 0.074), Q2=(0.0, -0.087), p from CV-Anova = 0.017.

8.5 Studies between L-IS and L-IR patients

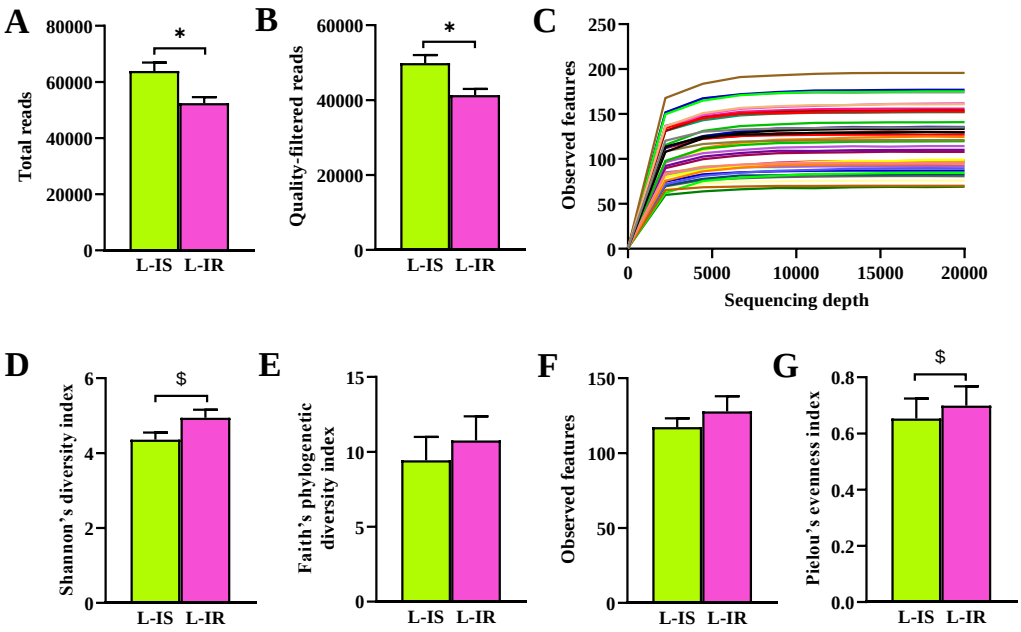

Supplementary Figure 3.5 Sequencing and alpha diversity analyses in L-IS and L-IR. A) Bar plots of total sequencing reads, B) Bar plots of quality filtered sequencing reads. C) Rarefaction curve. D) to F) Graphical representation reflecting the species richness when the sequencing depth was 20000 determined with different methods reflecting the species richness when the sequencing depth was 20000. G) Pielou's evenness index which presented the species evenness of a community. * and $ mean $p<0.05$, $0.05<p<0.1$, respectively.

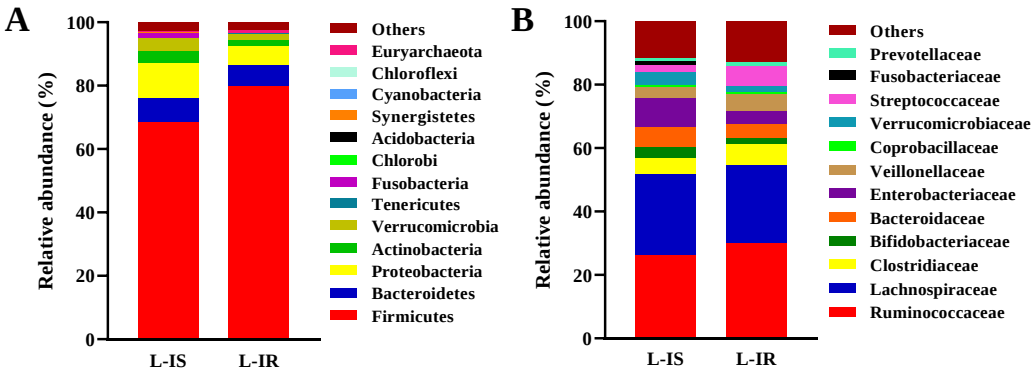

Supplementary Figure 3.6 Bacterial composition in L-IS and L-IR at A) phylum and B) family level.

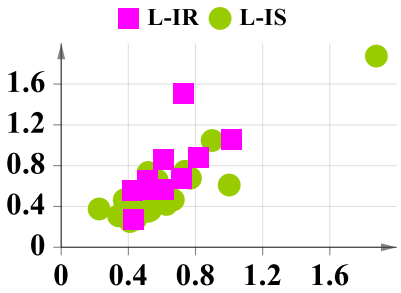

Supplementary Figure 3.7 PLS regression analysis of fecal metabolic profiles versus total bilirubin in L-IS and L-IR. The model's parameters were: UV scaling, R2Y(cum)= 0.682, Q2(cum)= 0.280. Permutation test: R2=(0.0, 0.556), Q2=(0.0, -0.114), p from CV-Anova = 0.076.

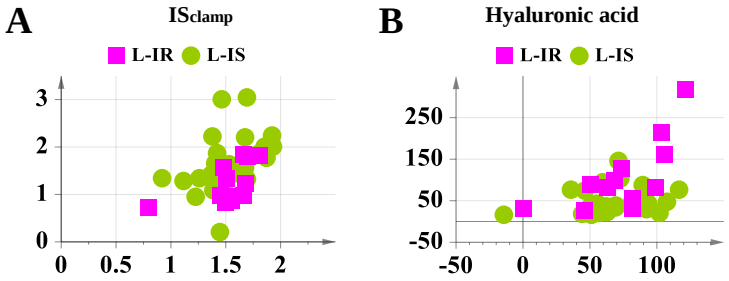

Supplementary Figure 3.8 PLS regression analysis of plasma metabolic profiles versus significant biochemical parameters in L-IS and L-IR. The parameters of models were: A) **IS_{clamp}**, R2Y(cum)= 0.187, Q2(cum)= 0.109. Permutation test: R2=(0.0, 0.107), Q2=(0.0, -0.076), p from CV-Anova = 0.125. B) **Hyaluronic acid**, R2Y(cum)= 0.220, Q2(cum)= 0.100. Permutation test: R2=(0.0, 0.103), Q2=(0.0, -0.074), p from CV-Anova = 0.168. All PLS models were obtained by using UV scaling.